

AD 740175

IIT RESEARCH INSTITUTE

VOLUME II

CIVIL DEFENSE SHELTER OPTIONS DELIBERATE SHELTERS

Final Report

OCD Contract DAHC-68-C-0126
OCD Work Unit 1614D

December 1971

DDC
RECEIVED
APR 17 1972
RECEIVED
B

Approved for public release;
distribution unlimited.

ORIGINAL COPY WAS OF POOR QUALITY.
BEST POSSIBLE REPRODUCTION FROM
COPY FURNISHED

IITRI

see AD 740 174

Reproduced by
NATIONAL TECHNICAL
INFORMATION SERVICE
Springfield, Va. 22151

330 R

UNCLASSIFIED

Security Classification

DOCUMENT CONTROL DATA - R & D

(Security classification of title, body of abstract and indexing annotation must be entered when the overall report is classified)

1. ORIGINATING ACTIVITY (Corporate author)

IIT Research Institute
10 West 35th Street
Chicago, Illinois 60616

2a. REPORT SECURITY CLASSIFICATION

2b. GROUP

3. REPORT TITLE

CIVIL DEFENSE SHELTER OPTIONS: DELIBERATE SHELTERS VOLUME II

4. DESCRIPTIVE NOTES (Type of report and inclusive dates)

Final Report

5. AUTHOR(S) (First name, middle initial, last name)

A. Longinow C. A. Kot
J. Kalinowski F. Salzberg

6. REPORT DATE

December 1971

7a. TOTAL NO. OF PAGES

379

7b. NO. OF REFS

72

8a. CONTRACT OR GRANT NO.

DAHC-68-C-0126

8b. PROJECT NO.

OCD Work Unit 1614D

9a. ORIGINATOR'S REPORT NUMBER(S)

J6144

9b. OTHER REPORT NO(S) (Any other numbers that may be assigned this report)

10. DISTRIBUTION STATEMENT

Approved for public release; distribution unlimited.

11. SUPPLEMENTARY NOTES

12. SPONSORING MILITARY ACTIVITY

Office of Civil Defense
Office of Secretary of Army
Washington, D.C. 20310

13. ABSTRACT

The ability of specific shelter structures to provide protection for personnel subjected to nuclear weapon environments is investigated and respective sheltering costs are estimated. Specific structures considered and costs for several defined sheltering options are given, and the capability of these shelters in providing protection relative to a range of weapon environments is presented. The bases for these predictions are described.

VOLUME II

CIVIL DEFENSE SHELTER OPTIONS:
DELIBERATE SHELTERS

OCD Contract DAHC-68-C-0126
OCD Work Unit 1614D

Final Report

by

A. Longinow
J. Kalinowski
C. A. Kot
F. Salzberg

for

Office of Civil Defense
Office of the Secretary of the Army
Washington, D.C. 20310

December 1971

Approved for public release;
distribution unlimited.

OCD Review Notice

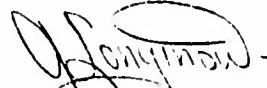
This report has been reviewed in the Office of Civil Defense and approved for publication. Approval does not signify that the contents necessarily reflect the views and policies of the Office of Civil Defense.

ORIGINAL COPY WAS OF POOR QUALITY.
BEST POSSIBLE REPRODUCTION FROM
COPY SUPPLIED.

FOREWORD

This final report on IIT Research Institute Project J6144, Contract DAHC-68-C-0126, OCD Work Unit 1614D, entitled "Civil Defense Shelter Options: Deliberate Shelters," is presented in two volumes. The work was performed in the Structural Analysis Section, Engineering Mechanics Division of IITRI by A. Longinow, A. J. Kalinowski, C. A. Kot and F. Salzberg. It was monitored by Mr. C. D. Kepple of the Shelter Research Division, Office of Civil Defense.

Respectfully submitted,
IIT RESEARCH INSTITUTE



A. Longinow
Manager
Structural Analysis Section

APPROVED:



M. R. Johnson
Assistant Director
Engineering Mechanics Division

ABSTRACT

The ability of specific shelter structures to provide protection for personnel subjected to nuclear weapon environments is investigated and respective sheltering costs are estimated. Specific structures considered and costs for several defined sheltering options are given, and the capability of these shelters in providing protection relative to a range of weapon environments is presented. The bases for these predictions are described.

VOLUME II - CONTENTS

<u>Chapter</u>		<u>Page</u>
TWO	ANALYSIS OF STRUCTURAL BEHAVIOR	65
	2.1 Analysis of Rectangular Shelters	71
	2.1.1 Analytical Model	73
	2.1.2 Loading (Closed Shelter)	76
	2.1.3 Loading (Open Shelter)	77
	2.1.4 Definition of Structural Failure	80
	2.1.4.1 Incipient Failure Criterion for Slabs	81
	2.1.4.2 Catastrophic Collapse Criterion for Slabs	85
	2.2 Analysis of Arch Shelters	95
	2.2.1 Definitions of Structural Failure	97
	2.2.2 Analytical Model	100
	2.2.3 Loading (Closed Shelter)	100
	2.2.4 Loading (Open Shelter)	101
	2.2.5 Incipient Failure Determination for Concrete Arches	101
	2.2.6 Incipient Failure Determination for Steel Arches	109
	2.2.7 Catastrophic Failure Determination (Concrete and Steel Arches)	109
THREE	BLAST FILLING OF PERSONNEL SHELTERS	111
	3.1 Blast Wave Propagation into Shelters	111
	3.2 Internal Pressures and Temperatures	118
	3.3 Jet Velocity and Momentum	131
FOUR	VULNERABILITY OF DUAL-PURPOSE SHELTERS TO FIRES	142
	4.1 Debris Fires	143
	4.1.1 Debris Fire Experiments	144
	4.1.2 Heat Flow Analysis	145
	4.2 Fire Storm	146
	4.3 Fire Vulnerability of Selected Shelters	153
	4.4 Remedial Action	158
	4.5 Evaluation of Fire Vulnerability of Shelters Selected by Bechtel Corporation	158
FIVE	SURVIVABILITY AGAINST BLAST-INDUCED AIRFLOW	161
	5.1 Governing Equations of Motion for a Tumbling Man	163
	5.1.1 Governing Equations	163
	5.1.2 Integration of Governing Equations	174

CONTENTS (Contd)

<u>Chapter</u>	<u>Page</u>
5.2 Determination of Shelteree Aerodynamic Body Forces and Point of Application	175
5.2.1 Load Determination	176
5.2.2 Determination of Point of Application	185
5.3 Tumbling Man Survivability Results	186
5.4 Interpretation of Results for Survivability Determination	190
5.4.1 Impact Criterion	190
5.4.2 Construction of Survivability Curves	201
APPENDIX A -- DESCRIPTION AND COST OF SHELTERS	205
A.1 Single-Purpose Shelters	205
A.1.1 Arch Structures	205
A.1.2 Rectangular Structures	214
A.1.3 Entranceways for Arch and Triangular Structures	219
A.1.3.1 Low Level Weapon Effects Designs	219
A.1.3.2 High Level Weapon Effects Designs	219
A.2 Cost of Single-Purpose Shelters	225
A.3 Dual-Purpose Shelters	228
A.3.1 School Basements	228
A.3.2 Parking Garages	237
A.3.3 Expressway Grade Separation Shelters	247
A.3.4 Subway Passenger Station Shelter	252
A.4 Cost of Dual-Purpose Shelters	258
A.4.1 Schools and Parking Garages	258
A.4.2 Grade Separation Shelters	268
APPENDIX B -- BREAKDOWN OF SHELTER COSTS	273
B.1 Single-Purpose Shelters	273
B.2 Dual-Purpose Shelters	279
APPENDIX C -- DESCRIPTION AND DOCUMENTATION OF COMPUTER PROGRAMS	295
C.1 Rectangular Reinforced Concrete Slab Analysis Program	295
C.1.1 MAIN PROGRAM	297
C.1.2 Slab Analysis Program User Instructions	300
C.1.3 Subroutines INTG and FUN	308
C.1.4 Subroutine FINT and STEPIT	312

CONTENTS (Concl)

<u>Chapter</u>	<u>Page</u>
C.1.5 Subroutine CRIT	315
C.1.6 Subroutine PRESSI	317
C.2 Buried Arch Shelter Analysis Program	326
APPENDIX D -- SLAB COEFFICIENTS	328
APPENDIX E -- DESCRIPTION OF TUMBLING MAN COMPUTER PROGRAM	334
E.1 Computer Program Description	334
E.2 MAIN Program Input	335
E.3 Program Output	338
E.4 Program Listings and Descriptions	340
E.5 MAIN Program Listing	340
E.5.1 Subroutines FORCE and INPUT Listings	344
E.5.2 Subroutine INTGV1 Listing	348
E.5.3 Subroutine FUN Listing	350
E.5.4 Subroutines FUN1 and FUN7 Listings	354
E.5.5 Subroutine CRIT Listing	357
E.5.6 Subroutine PLOTS Listing	363
E.5.7 Subroutine MAXVEC Listing	366
E.5.8 Function SGN Listing	366
REFERENCES	367
DISTRIBUTION LIST	373

VOLUME II - ILLUSTRATIONS

<u>Figure</u>	<u>Page</u>
2.1 Characteristics of an Idealized Shelter Structure with Loading	67
2.2 Typical Survivability Function for a Simple Structure	70
2.3 Rectangular, Single-Purpose Shelter (Ref. 14)	72
2.4 Section through Typical School Shelter	74
2.5 Section through Typical Parking Garage Shelter	75
2.6 External Wall Loading	78
2.7 Characterization of Resistance Functions	82
2.8 Large Deflection of a Two-Way Simply-Supported RC Slab (Ref. 4)	86
2.9 Membrane-Large Deflection Action of a Two-Way Slab (Ref. 60)	88
2.10 Cracked Surface of Two-Way RC Slab (Ref. 60)	89
2.11 Slab Reinforcement Matrix and Equivalent Analytical Model	90
2.12 Membrane Failure Curves	91
2.13 Membrane Failure Curves	92
2.14 Membrane Failure Curves	93
2.15 Cross Section of Basic Arch Shelter	95
2.16 Nonlinear Resistance Function	98
2.17 Finite Element Representation of Concrete Arch and Soil	103
2.18 Concrete Arch Resistance Function	104
2.19 Comparison of Two Arch Analysis Methods	106
2.20 Definition of Arch Structure Failure	110
3.1 Blast Wave Behavior at an Opening	114
3.2 Shock Configurations in a Shelter	116
3.3 Average Pressure-Time Variation for Basement School Shelter	119
3.4 Average Temperature-Time Variation for Basement School Shelter	120
3.5 Variation of Peak Average Internal Shelter Pressure with ϕ	125
3.6 Variation of Peak Average Internal Shelter Temperature with ϕ	126
3.7 Peak Average Internal Shelter Overpressure for a Basement School Shelter (Ref. 15)	128

ILLUSTRATIONS (Contd)

<u>Figure</u>		<u>Page</u>
3.8	Peak Internal Shelter Temperature for a Basement School Shelter (Ref. 15)	129
3.9	Tolerance Times for Unprotected Subjects Abruptly Exposed to High Wall Temperatures (Ref. 28)	132
3.10	Jet Velocity Distribution	134
3.11	Arch Shelter Plan Showing Jet Boundaries (Ref. 14)	139
3.12	Variation of Internal Particle Velocities	140
3.13	Variation of Particle Velocity at the Entrance	141
4.1	Heat Flow from Debris Fire into the Shelter per Square Foot of Exposed Ceiling as a Function of Fuel Load	147
4.2	Heat Flow from Debris Fire into the Shelter per Square Foot of Exposed Ceiling as a Function of Fuel Load	148
4.3	Heat Flow from a Debris Fire into the Shelter per Square Foot of Exposed Ceiling as a Function of Fuel Load	149
4.4	Heat Flow from a Debris Fire into the Shelter per Square Foot of Exposed Ceiling as a Function of Fuel Load	150
4.5	Heat Flow from a Debris Fire into the Shelter per Square Foot of Exposed Ceiling as a Function of Fuel Load	151
4.6	Heat Flow from a Debris Fire under Collapsed Roof into Shelter per Square Foot of Exposed Ceiling	152
4.7	Heat Flow into the Shelters Exposed to a Fire Storm	154
4.8	Ventilation Rates Required per Occupant for Various Heat Flow from Debris Fires to Maintain $ET = 82^{\circ}F$ within the Shelter	157
5.1	Tumbling Man Notation, Standing Configuration	164
5.2	Tumbling Man Notation, Prone Configuration	165
5.3	Tumbling Man Notation, Sitting Configuration	166
5.4	Generalized Tumbling Man Notation	167
5.5	Six Possible Modes of Motion	168
5.6	Jet Profile	178
5.7	Loading Diagram	182
5.8	Tumbling Man Centerline (A-B) Spatial Trajectory (Problem 30-U-M)	191
5.9	Tumbling Man Time Trajectory (Problem 30-U-M)	192
5.10	Tumbling Man Time Trajectory (Problem 30-P-M)	193

ILLUSTRATIONS (Contd)

<u>Figure</u>	<u>Page</u>
5.11 Tumbling Man Centerline (A-B) Spacial Trajectory (Problem 30-S-M)	194
5.12 Tumbling Man Trajectory (Problem 30-S-M)	195
5.13 Tumbling Man Centerline (A-B) Spacial Trajectory (Problem 10-U-M)	196
5.14 Tumbling Man Time Trajectory (Problem 10-U-M)	197
5.15 Tumbling Man Trajectory (Problem 10-P-M)	198
5.16 Tumbling Man Centerline (A-B) Spacial Trajectory (Problem 10-S-M)	199
5.17 Tumbling Man Time Trajectory (Problem 10-S-M)	200
5.18 Survivability of Tumbling Man Against Entrance Jet Velocity	203
A.1 Site Plans for 1000-Man Peripheral Shelter Complexes	207
A.2 General Configuration of Basic 500-Man Arch Shelter	209
A.3 Arch Shelter Location Relative to Ground Surface	210
A.4 Basic Dimensions of Arch Shelter	210
A.5 Construction Details of RC Arch	212
A.6 General Configuration of Basic 500-Man Rectangular RC Shelter	215
A.7 Basic Dimensions of RC Rectangular Shelter	216
A.8 Construction Details of RC Rectangular Shelter	218
A.9 Rectangular Shelter Location Relative to Ground Surface	218
A.10 Entranceway Details for Single-Purpose Arch and Triangular Shelters	220
A.11 Entranceway for 100 and 150 psi Design Shelters	222
A.12 Entranceway Tunnel Plan	223
A.13 Entranceway Cross Section	224
A.14 Classroom Shelter for 550 Persons, 5 psi	231
A.15 Classroom Shelter for 550 Persons, 25 and 50 psi	232
A.16 Classroom Shelter for 1100 Persons, 5 psi	233
A.17 Classroom Shelter for 1100 Persons, 25 and 50 psi	234
A.18 Parking Garage Shelter for 5000 Persons, 5 psi	239
A.19 Parking Garage Shelter for 5000 Persons, 25 and 50 psi	241
A.20 Parking Garage Shelter for 5000 Persons, 25 and 50 psi	243

ILLUSTRATIONS (Concl)

<u>Figure</u>	<u>Page</u>
A.21 Cutaway View of an Expressway Grade Separation Shelter	248
A.22 Upper Level Floor Plan	249
A.23 Lower Level Floor Plan	250
A.24 General Construction Site Plan	253
A.25 Judiciary Square Passenger Station, General Plan and Elevation	254
A.26 Judiciary Square Passenger Station, Roof Plan	255
A.27 Judiciary Square Passenger Station Arch	256
A.28 Cost of Structure and Equipment Shelter Components as Percent of Total Shelter Cost	266
A.29 Cost of Structure and Equipment Shelter Components as Percent of Total Shelter Cost	267
C.1 General Flowchart for Slab Analysis Computer Program	296
C.2 Approximate Analytic Form for Overpressure vs Time for Nuclear Blast Wave in Terms of Peak Overpressure	318
C.3 Idealization of Shock Parameter b Curve	319
C.4 Subroutine Press Flow Chart	322
E.1 Tumbling Man Computer Program Flow Chart	337

VOLUME II - TABLES

		<u>Page</u>
2.1	Basic Properties of Arch Shells and End Walls	96
3.1	Average Internal Pressure and Temperature Data	122
3.2	Inlet Areas and Volumes of Subject Shelters	123
3.3	Peak Average Temperatures and Pressures in Subject Shelters	127
4.1	Composition of Debris Fires in the IITRI Experiments	145
4.2	Vulnerability of Dual-Purpose Shelters to Debris and Fire Storm Type Fires	155
4.3	Estimated Combustible and Noncombustible Components of Several Typical Structures	159
4.4	Fire Vulnerability of Shelters in Detroit, Michigan, Zone 7 of Bechtel Study	160
5.1	Summary of Parametric Study	189
A.1	Subject Shelters	206
A.2	Basic Dimensions of Arch Shelter	211
A.3	Percent Reinforcement for Indicated Structural Members	213
A.4	Basic Dimensions of RC Rectangular Shelter	217
A.5	Percent Reinforcement for Indicated Structural Members	217
A.6	Entranceway Dimensions	221
A.7	Sheltering Cost Options for Single-Purpose Shelters	227
A.8	Summary of Single-Purpose Shelter Costs per Square Foot of Shelter Area	229
A.9	Summary of Shelter Costs per sq ft of Shelter Area	230
A.10	Basic Characteristics of School Basement Shelters	230
A.11	Member Size and Percent Reinforcement	236
A.12	Basic Characteristics of Parking Garage Shelters	238
A.13	Sizes of Structural Members in Parking Garage Shelters	238
A.14	Percent Reinforcement for Indicated Structural Members of Parking Garage Shelters	246
A.15	Structural Component Thicknesses for Three Shelters	251
A.16	Openings Leading into the Passenger Station	257
A.17	Summary of Total Costs for School Basement Shelters, Cost Option 1	261
A.18	Summary of Total Costs for School Basement Shelters, Cost Option 2	262

TABLES (Contd)

		<u>Page</u>
A.19	Summary of Total Costs for School Basement Shelters, Cost Option 3	263
A.20	Summary of Total Costs for Parking Garage Shelters, Structure I, for Various Cost Options	264
A.21	Summary of Total Costs for Parking Garage Shelters, Structure II, for Various Cost Options	265
A.22	Summary of Costs, Expressway Grade Separation Shelters, Cost Option 1	271
A.23	Summary of Costs, Expressway Grade Separation Shelters, Cost Option 2	271
A.24	Architectural, Electrical and Mechanical Costs	272
B.1	Sheltering Cost Options	274
B.2	Shelter Site Data	275
B.3	Cost of Specific OCD Shelter Habitability Items Using Cost Options 2 and 5	275
B.4	Cost of Mechanical Equipment for 500-Man Shelter Using Cost Options 3 and 6	276
B.5	Cost of Electrical Items for 500-Man Shelter Using Cost Options 3 and 6	277
B.6	Cost of Specific Architectural Items Using Cost Options 3 and 6	278
B.7	Entranceway Costs for 500-Man Capacity Arch and Rectangular Shelters	280
B.8	Total Costs for Single-Purpose Shelters	281
B.9	Total Costs for Single-Purpose Shelters	283
B.10	Definition of Sheltering Cost Options for Dual-Purpose Shelters	284
B.11	Structural Construction Cost and Quantity Breakdown for School Shelters	285
B.12	Estimated Architectural Construction Cost and Quantity Breakdown	286
B.13	Estimated Mechanical and Electrical Construction Cost and Quantity Breakdown for Cost Option 1	287
B.14	Estimated Structural Construction Cost and Quantity Breakdown for Parking Garage Shelters	288
B.15	Estimated Architectural Construction Cost and Quantity Breakdown for Parking Garage Shelters	289
B.16	Estimated Mechanical and Electrical Construction Cost and Quantity Breakdown for Parking Garage Shelters, Cost Option 1	290

TABLES (Concl)

		<u>Page</u>
B.17	Estimated Construction Cost and Quantity Breakdown for Conventional School Basement Shelters	291
B.18	Mechanical and Electrical Items for Conventional Basement Shelters	292
B.19	Estimated Construction Cost and Quantity Breakdown for Conventional Parking Garage Shelters	293
B.20	Mechanical and Electrical Items for Conventional Parking Garage Shelters	294
C.1	Input Data Format	301
C.2	Shock Parameter Idealization	321
D.1	Coefficients for Two-Way Slab Fixed on Four Sides with Uniform Load	329
D.2	Coefficients for Two-Way Slab with Simple Supports on Two Long Sides, Fixed Supports on Two Short Sides and Uniform Load	330
D.3	Coefficients for Two-Way Slab with Simple Supports on Four Sides and Uniform Load	331
D.4	Column Supported Slab with Square Interior Uniform Load	332
D.5	Two-Way Slab with Simple Supports on Two Short Sides, Fixed Supports on Two Long Sides and Uniform Load	333

CHAPTER TWO

ANALYSIS OF STRUCTURAL BEHAVIOR

An exact solution for the response of a structure to dynamic loads is a practical possibility only when the structure in question is sufficiently simple and when the overpressure loading-time variation is a known mathematical function. Actual structures and loadings ordinarily do not satisfy these conditions. For this reason, it is necessary in such cases to idealize both the structure and the loading. Structural idealization is performed by considering only the dominant modes of response. Very often only the first mode need be considered and the structure may then be represented by an equivalent single degree-of-freedom system.

In the analysis of blast resistant structures we are ordinarily interested in deflections and their relationship to the primary stresses in the structure. It is necessary thus to select the equivalent system such that the deflections of the concentrated masses are identical with those of certain points on the actual structure. The resulting deflections may then be related to stresses. The magnitude of error in such an analysis is in the amount which would have been contributed by the neglected modes. For most cases of practical interest, one mode predominates and reasonably accurate results may be obtained by considering only this mode.

In idealizing dynamic loads two simplifications are ordinarily considered. The first involves the geometric distribution of the load on the structure; the second involves the load time variation. If in the idealized structure, the mass of the system is concentrated only at certain points, then modified load magnitudes need to be applied at these points. The general form of the dynamic analysis (Ref.13) performed on the subject shelters is described in relation to a rectangular shelter, however, the formulation is general enough to be applicable to any reasonable structural system.

The shelter shown in Fig. 2.1a is a buried structure subject to uniform, time dependent loading (Fig. 2.1b) over the surface of the ground. The static load deflection relationship (resistance function) for the point at the center of the roof slab is shown in Fig. 2.1c. Such a relationship is a function of the spacial distribution of load over the surface of the ground, the type of soil, depth of burial, and geometric, material and structural properties of the shelter. The equivalent structural system is shown in Fig. 2.1d and is selected such that the concentrated mass deflection is at all times equal to the midspan deflection of the slab. This may be accomplished (neglecting higher modes) by obtaining a relationship between equivalent structure parameters p_e (load), m_e (mass) and k_e (stiffness) for a single degree-of-freedom and the actual structure parameters $p(t)$, m and k (Ref. 13).

The procedure used involves an assumed deflected shape corresponding to the dominant mode. This establishes a relationship between the deflections of all points on the structural element which is constant with time and makes possible the representation of the structural element by an equivalent system having one degree-of-freedom. Factors which transform the actual parameters $p(t)$, m and k to the equivalent ones (p_e , m_e , k_e) are related and obtained as described herein.

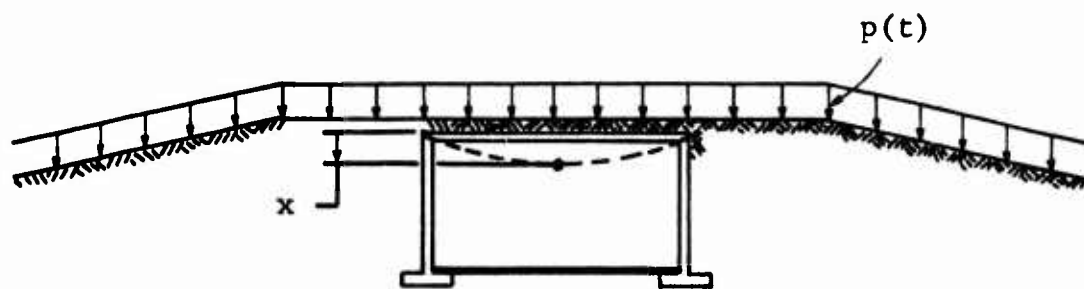
$$p_e(t) = K_L p(t) \quad (2.1)$$

The load transformation factor K_L is determined by equating the external work done by $p_e(t)$ on the equivalent system to that done by $p(t)$ on the actual system. The time variation in both cases is the same.

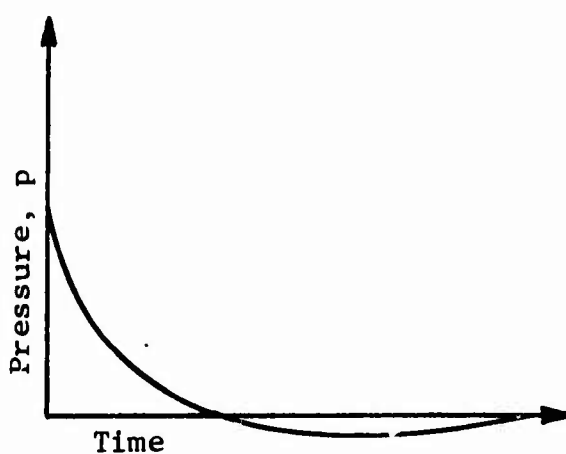
$$m_e = K_m m \quad (2.2)$$

The mass transformation factor K_m is determined by equating the kinetic energies of the real and equivalent systems.

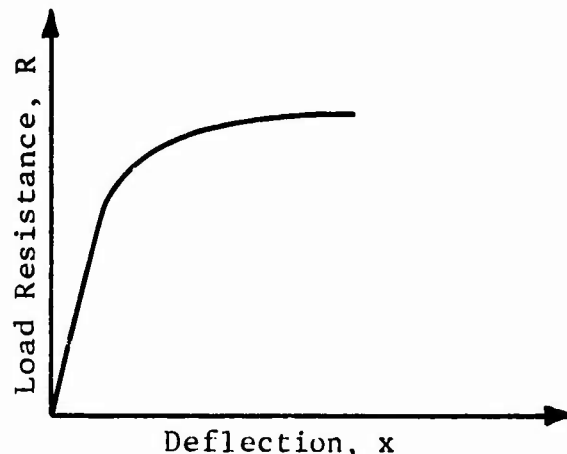
$$R_e = K_r R \quad (2.3)$$



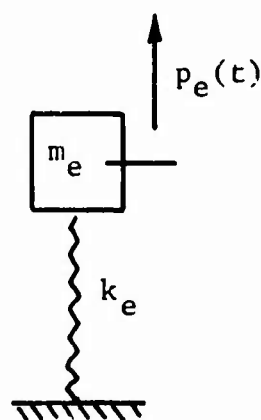
(a) Actual Structure



(b) Load Function



(c) Resistance Function



(d) Equivalent Structure and Loading

Fig. 2.1 CHARACTERISTICS OF AN IDEALIZED SHELTER STRUCTURE WITH LOADING

The resistance, R , of an element is the internal force tending to restore the element to its equilibrium position (Fig. 2.1c). At a given deflection the resistance is defined as being numerically equal to the static load required to produce the same deflection. The maximum resistance then is the maximum load that the element can carry and is computed using ultimate strength criteria. The resistance transformation factor, K_r , is obtained by equating the internal energies of the two systems. On this basis $K_L = K_r$.

The spring constant of the actual system is defined as the static load required to produce a unit deflection. Deflections of the actual and equivalent system are equal. The spring constant of the equivalent system is obtained from

$$k_e = K_r k \quad (2.4)$$

where k is the stiffness (spring constant) of the actual system.

Having defined the transformation factors, the equivalent system may be analyzed. This is done by solving the corresponding equation of motion using the transformed parameters. The basic equation of motion of the equivalent single degree-of-freedom system is

$$m_e \frac{d^2 x}{dt^2} = p_e(t) - R_e(x). \quad (2.5)$$

Replacing the equivalent terms m_e , p_e , R_e with Eqs. (2.1) through (2.3) we obtain

$$\frac{K_m}{K_L} m \frac{d^2 x}{dt^2} = p(t) - R(x). \quad (2.6)$$

Thus given a structural element, its characteristic resistance function, a loading function and appropriate transformation parameters K_L and K_m , the solution of Eq. (2.6) enables us to predict deflection (and consequently stress and strain) at any time during the loading history. Further, this information allows us to make judgments as to the physical state of the structural member in question by means of comparisons with existing experimental data.

The analysis approach described was programmed for electronic computation and used to analyze the subject shelters. Essentially this is a numerical procedure which is capable of solving Eq. (2.6) for any given loading and arbitrary resistance function. Since this equation is basic to numerous structures which may be represented by a single degree-of-freedom, the procedure developed is capable of analyzing any such structure provided the resistance function is known. Full range resistance functions for structures more complex than a beam, a plate or an arch are not readily available. For this reason each shelter was analyzed using a step-by-step process which first determines the response (physical state) of individual key components. Judgments as to the physical state of the structure as a whole are then based on the relative physical states of such components.

The objective of the analyses performed was to establish for each shelter considered:

- the overpressure level at which the shelter is in a state of incipient failure, and
- the overpressure level at which the structure has lost its entire sheltering capability (catastrophic collapse).

Physical states prior to the state of incipient failure, overpressure level P_A (Fig. 2.2), are of no interest since relevant injury producing mechanisms are not expected to be manifest within the shelter. We postulate 100 percent survivors prior to incipient failure. The overpressure level at which the structure has lost its sheltering capability (overpressure level P_B) is defined as the state at which no survivors (both instantaneously and over longer periods of time) are expected.

The range between these two overpressure levels is one of relevant injury producing mechanisms and the transition can take on different forms. We know that survivability (percent survivors) declines between these two points; being maximum at overpressure level P_A and minimum at overpressure level P_B .

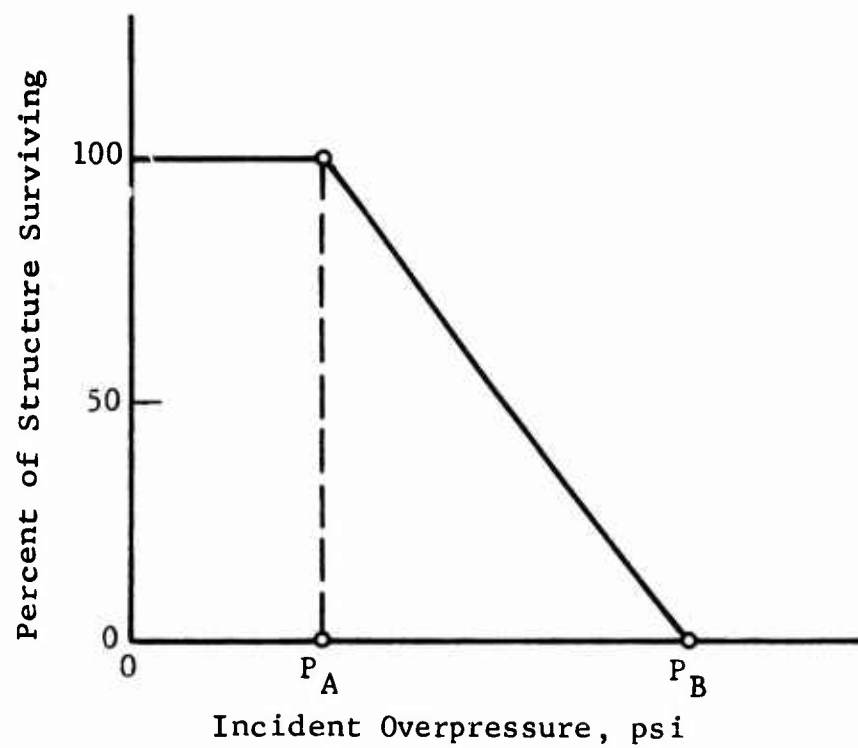


Fig. 2.2 TYPICAL SURVIVABILITY FUNCTION
FOR A SIMPLE STRUCTURE

The manner of transition is not known and does not lend itself to analysis within the current state of the art. We postulate a linear transition between the two points.

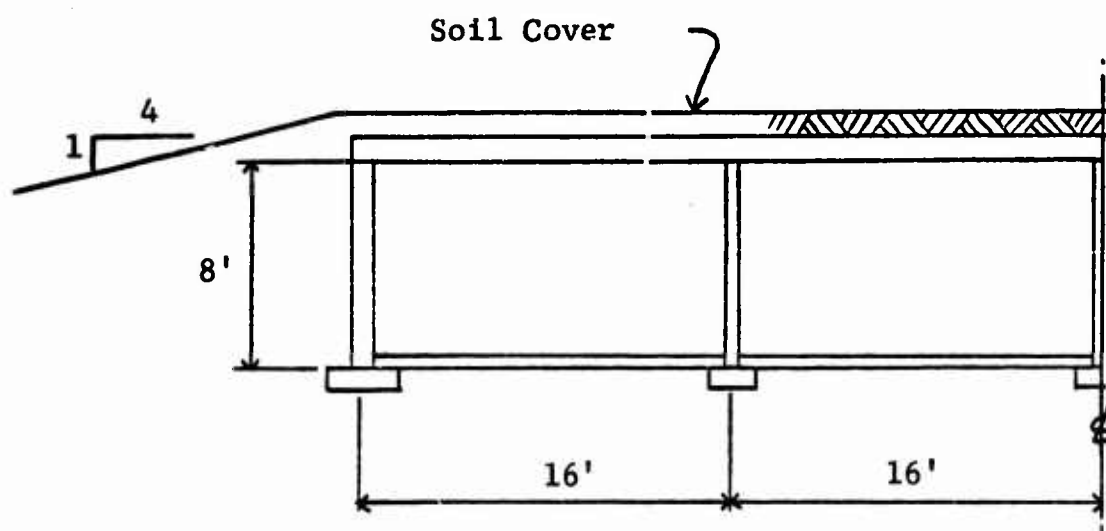
Computational methods used to determine P_A and P_B for the rectangular and arch type shelters are different at the detailed level of analysis. This difference is due to dissimilarities in the structural configurations and the way in which soil-structure interaction takes part in each case. Consequently, the analysis of each structural type is presented separately.

2.1 ANALYSIS OF RECTANGULAR SHELTERS

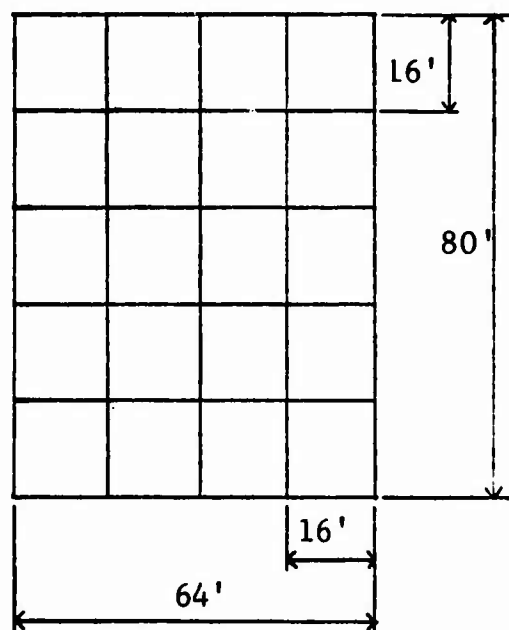
The specific rectangular shelters considered include both single- and dual-purpose types and are described in Appendix A. Single-purpose shelters include four structures with identical structural systems except that each was designed (Ref. 14) to resist a different overpressure level (0^* , 10, 20 and 30 psi) and associated effects resulting from a single megaton range weapon.

These shelters are mounded RC structures whose interior and exterior walls form a rectangular grid when viewed in plan. A typical shelter is illustrated in Fig. 2.3. The roof is a two-way RC slab which is continuous over the interior walls. Exterior and interior walls are one-way RC slabs which rest on wall footings. The floor slab is wire mesh reinforced and is structurally separate from all shelter components. The entranceway (shown in Appendix A) is a corrugated steel tunnel containing bulkheads and blast doors. Shelters are mounded using a 4 to 1 slope which is sufficiently gentle to preclude significant dynamic and reflected pressures acting on the structure.

* This is used to indicate fallout radiation as the primary design weapon environment.



(a) Half-Section Through Shelter



(b) Plan, 500-Man Capacity Shelter

Fig. 2.3 RECTANGULAR, SINGLE-PURPOSE SHELTER (Ref. 14)

Dual-purpose shelters analyzed herein include two use classes, i.e., schools and parking garages. Six school shelters are analyzed which may be divided into two categories with respect to size (5500 and 11000 sq ft of floor area) and three categories with respect to design weapon environments (5, 25 and 50 psi design overpressure levels and associated effects resulting from a single megaton range weapon).

School shelters (Ref.15) are basement structures (see Fig. 2.4) having identical structural systems. The structural system consists of two-way RC roof slabs (at grade) which are continuous over interior partitions. External walls and interior partitions are one-way RC slabs (constructed as tilt-up walls) supported on wall footings. The basement floor slab (wire mesh reinforced) is structurally separate from walls and footings.

Three parking garage shelters (Ref.16) are considered. Each was designed to resist a different weapon environment resulting from a single megaton range weapon. The three design weapon environments consist of 5, 25 and 50 psi overpressure levels and associated effects of thermal and prompt nuclear radiation. Each of the shelters is a below grade structure (see Fig. 2.5) and contains 50,000 sq ft of floor area. The structural system consists of a flat slab supported by columns (with column capitals and drop panels) and peripheral walls. The peripheral walls (constructed as tilt-up walls) are one-way RC slabs supported by wall footings. Columns rest on individual footings. The interior floor slab (wire mesh reinforced) is structurally separate from walls, columns and footings.

2.1.1 Analytical Model

The rectangular structures described consist of an inter-connecting network of slabs in the first case and slabs and columns in the second case. When loaded, the internal force and moment distributions throughout each component in the network are coupled, i.e., statically indeterminate. Although it is possible to solve the complete interaction problem by considering

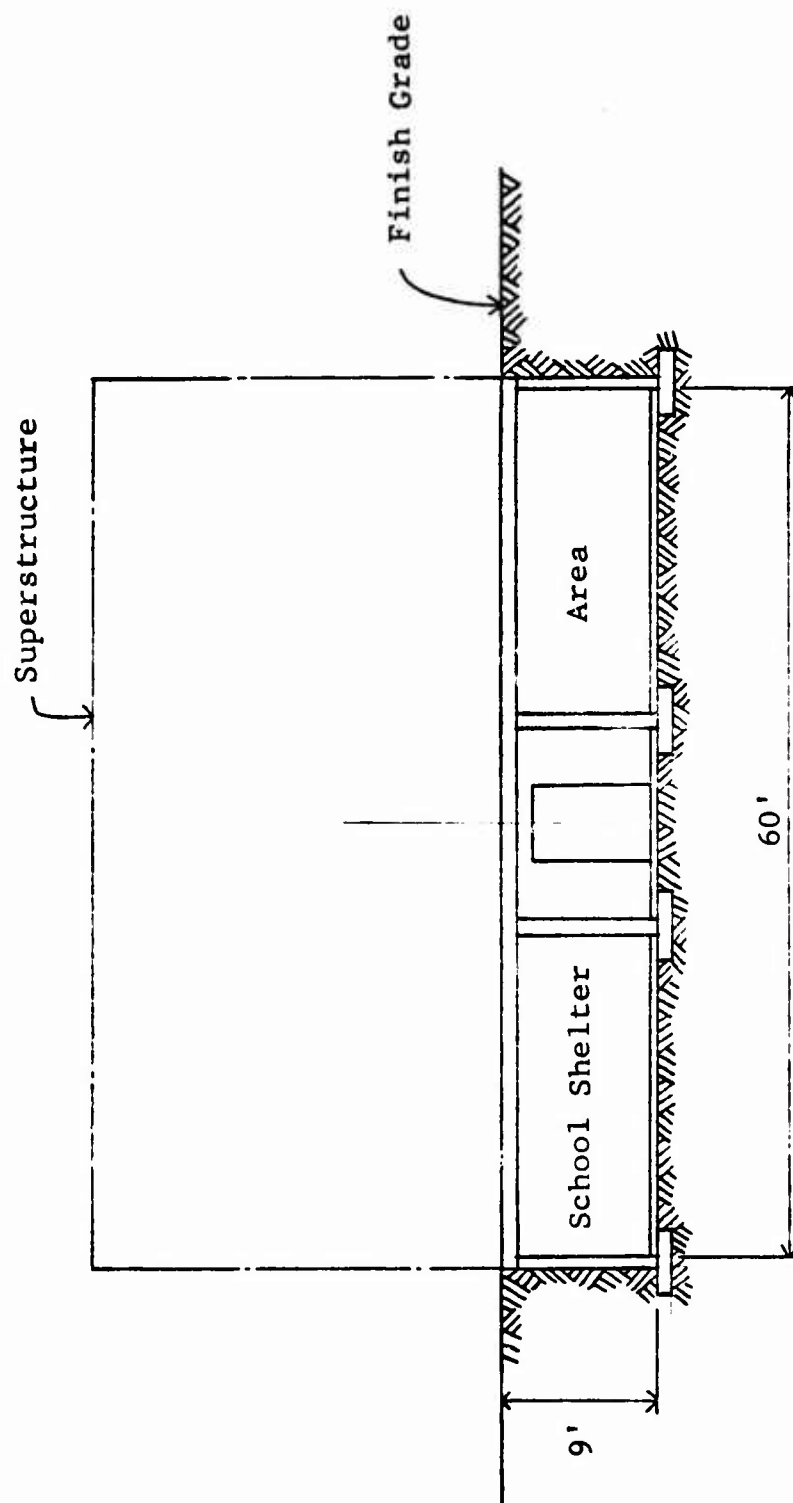


Fig. 2.4 SECTION THROUGH TYPICAL SCHOOL SHELTER

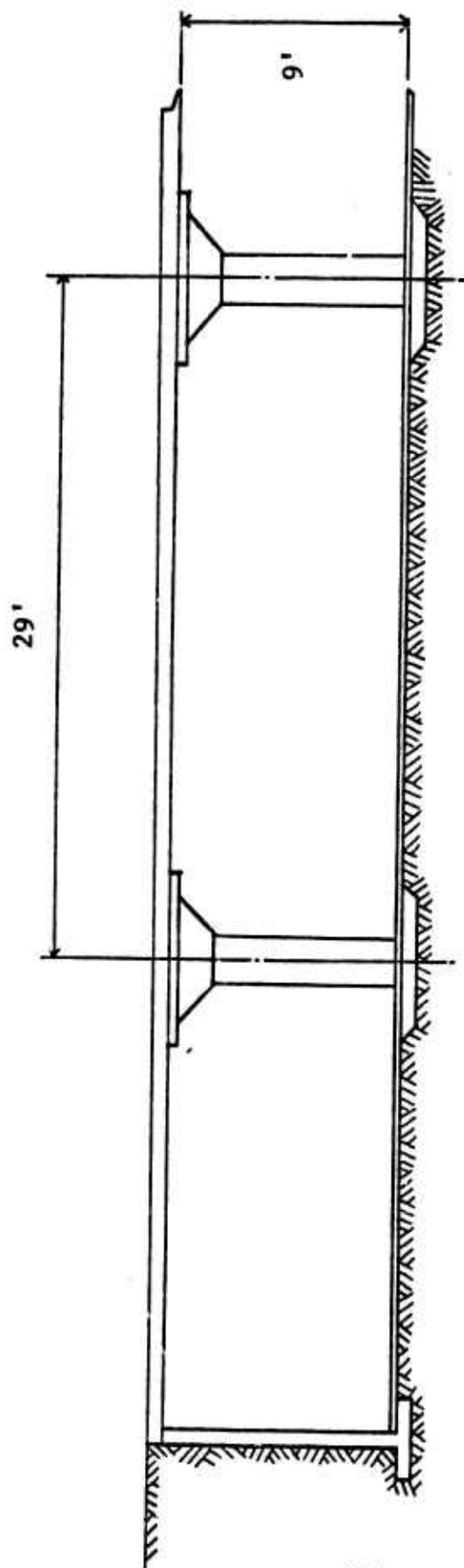


Fig. 2.5 SECTION THROUGH TYPICAL PARKING GARAGE SHELTER

all components in the network simultaneously, the level of effort demanded for this approach is beyond the scope of this study. Instead, we uncouple the network by making certain simplifying assumptions regarding the restraint conditions at the junction points of each component. Upon decomposing the system into a series of smaller systems in the manner described, each component can be analyzed as a separate unit and the weakest link in each chain found.

2.1.2 Loading (Closed Shelter)

Roof Slab.--Rectangular structures considered herein have roof slabs either at grade or slightly below. For those at grade, the overpressure is applied directly to the surface of the roof slab. For those slightly buried, the loading is the same except that the deadweight of the soil contributes to part of the loading. The spacial pressure distribution is assumed to be uniform. This assumption is reasonable when the time it takes the overpressure wave front to engulf the slab is small compared to the period of the lowest natural frequency of the slab. In such a case, the slab does not have sufficient time to respond to the asymmetric loading that it experiences as the wave travels by. Instead, the slab responds to the nearly uniform pressure distribution it experiences, after the wave front has traversed the length of the slab. For the range of weapon sizes considered (0.2, 0.4, 1.0 and 10.0 MT) the decay of overpressure over the particular slab lengths is sufficiently small to make the uniform pressure assumption reasonable.

External Walls.--The loading on the external walls is due to a combination of both the overpressure loading and the lateral side pressure resulting from the deadweight of the soil. The overpressure loading in the lateral direction is difficult to predict due to the complex nature of the actual soil-structure interaction relationship. We take the usual approximating approach (Ref. 10,17) for determining this loading by assuming that it depends on the specific soil and is a fraction of the surface

overpressure. Further, the net mass of the wall slab is taken to be its actual mass plus an additional portion of the neighboring soil mass. The volume of this additional mass is usually assumed (Ref.17) to be equal to the slab area times one-half the slab depth. Wall loading is illustrated in Fig. 2.6.

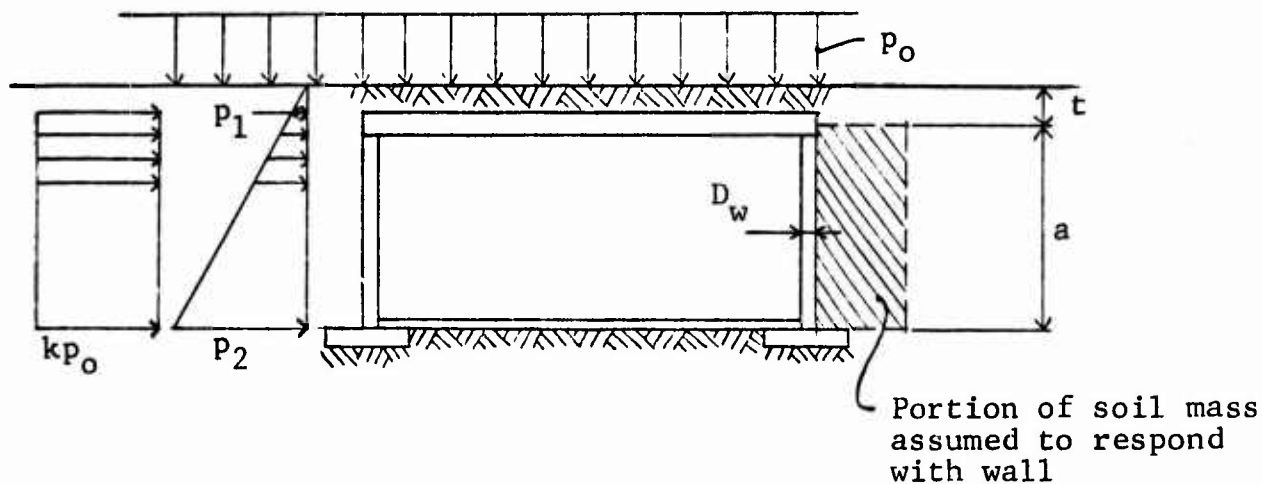
Footings.--Once the solution to the roof slab problem has been established, the resulting vertical shear forces at the slab supports (the walls are actually the supports) are known. These values are then assumed to be transmitted through the walls into the footings.

2.1.3 Loading (Open Shelter)

Roof Slabs and External Walls.--When blast doors are open or left off, the loading of the shelter is considerably different than when blast doors are closed. As the blast pressure wave $P_{in}(t, \bar{x})$ (expressed in terms of time and space) enters the shelter it tends to balance the external pressure $P_{ex}(t, \bar{x})$ acting on the outside surface of the shelter. The net pressure at some point \bar{x} on the surface of an interior wall or roof slabs is therefore given by

$$\Delta P(t, \bar{x}) = P_{ex}(t, \bar{x}) - P_{in}(t, \bar{x}) \quad (2.7)$$

Computations of P_{ex} and P_{in} have been made for a whole range of overpressure levels, time durations and shelter volume to entrance area ratios and are included in Chapter Four. The results of these computations indicate that in all cases of practical importance, the pressure differential, ΔP , is very nearly equal to the external pressure for the early time duration, ΔT_c . The internal fill pressure, P_{in} , is initially very small in the duration ΔT_c ; consequently, for all practical purposes, ΔP can be approximated with P_{ex} over this interval. For the range of structures we are considering in this study, the period of the lowest natural frequency of the roof slab (or external wall), T_n , is of the order or smaller than ΔT_c . Consequently, the slab will fully respond (i.e., reach its maximum stress) to the $\Delta P \approx P_{ex}$ pressure,



$$\left. \begin{aligned} p_1 &= \gamma_s t \\ p_2 &= \gamma_s (t + a) \end{aligned} \right\} \text{ lateral (deadweight) soil pressure on vertical wall } (\gamma_s = \text{soil density})$$

kp_o = lateral blast induced wall pressure

k = coefficient of lateral pressure

$$p_n \text{ (net wall pressure)} = kp_o + p_{av}$$

$$p_{av} = \frac{1}{2}(p_1 + p_2) = \frac{\gamma_s}{2}(a + 2t)$$

$$m_e \text{ (equivalent unit wall mass)} = \frac{A_w}{2g}(a\gamma_s + 2D_w\gamma_c)$$

A_w = wall area

γ_c = wall density

g = acceleration due to gravity

t = average depth of burial

Fig. 2.6 EXTERNAL WALL LOADING

before it has a chance to be relieved by the balancing effect of P_{in} . Hence for the time duration of interest, ΔT_c , the loading on the external walls or roof slabs will be essentially the same regardless of whether the blast doors are open or closed, and consequently the roof or wall slab failure pressure is taken to be the same for either situation.

Internal Walls.--The transverse pressure differential across the internal walls of the basement rooms is the most difficult loading to estimate, mainly because of the complex geometrical path the pressure wave must traverse before coming in contact with the wall. For example, in the basement school shelters (see Fig. A.14, Appendix A) the overpressure wave must first travel down a stairwell, through a blast door, down a narrow passageway, make a 90 deg right turn through another blast door and finally down a narrow hallway before exerting any pressure loading on an internal wall of the structure. At the instant the pressure wave reaches the entrance to the basement room, the pressure differential ΔP_w across the internal wall exposed to the hallway is the difference between the hall pressure P_h and the existing atmospheric pressure P_r within the room. Although this ΔP_w will be rather large initially, the pressure wave will rapidly fill the room and eventually tend to equalize with the hallway pressure ($\Delta P = 0$) in the time, t_{fill} . The determination of the actual pressure differential as a function of time is an extremely difficult problem in gas dynamics. The problem is complicated by the fact that the aboveground overpressure time variation is both reduced in magnitude and distorted in waveform as a result of passing through the mentioned channels and orifices before entering the basement room. In short, we are not able to obtain a reliable estimate of the internal wall pressure differentials within the capabilities of our current analytical techniques.

Because we cannot determine the loading accurately, we of course, cannot define the actual overpressure at which the internal wall will fail. What we can predict however, is the ultimate ΔP_w that will fail the wall based on an assumed flat-top pressure differential pulse shape.

It was found that for the basement shelters treated in this study the failure (initial yielding) overpressure was on the order of 2 to 3 psi. This is for 6-in. RC interior walls (height 9.0 ft, width: 24.0 ft). Experimental studies performed (Ref. 18) indicate that pressure differentials of this order were experienced in room configurations and blast environment conditions similar to the ones existing in shelters considered in this study. It should be emphasized however that the rooms in the experimental shelters were smaller.

It appears that in shelters whose blast doors are left off or open and whose internal walls are not designed to resist overpressures normal to their planes, survivability may be considerably different from the closed door case. The loss of walls' supporting action could cause failure of the roof slab. Injuries and/or fatalities would be produced by debris from walls as well as the roof slab. To what extent the internal wall failure affects the survivability of the shelter cannot be accurately estimated until techniques are developed, analytically or experimentally, which can reliably predict the pressure differentials which develop across the internal wall slabs. Survivability functions developed in this study do not reflect injury/fatality mechanisms produced by the failure of internal walls.

2.1.4 Definition of Structural Failure

For the structures described, incipient failure (overpressure level P_A , Fig. 2.2) refers to the overpressure level at which the classical small deformation theory predicts failure in the weaker of the key components, i.e., roof slab, wall, column, etc. of the structure considered. This refers to the overpressure level at which the load resistance versus deflection function (Fig. 2.1c) of the weakest key component becomes level. This leveling off implies that the component being analyzed cannot sustain any increase in load without experiencing unbounded deformations. At the point of incipient failure, the slab cross section experiences the maximum possible bending moment that can be sustained at various points in the slab.

In some instances it is possible that the slab (roof or wall) may experience a shear failure or bond stress failure at the slab supports at an overpressure value lower than that which causes failure in bending (i.e., the point at which the resistance function becomes flat). In these cases, incipient failure is defined as the overpressure at which a shear or bond failure occurs.

Beyond the point of incipient failure, the concrete is considered inserviceable from the viewpoint of carrying applied loads in flexure; however, the steel reinforcement network still remains intact and is capable of resisting additional loading through membrane action. The overpressure level at which membrane action gives away is defined as the point of catastrophic collapse (point P_B , Fig. 2.2). It is postulated that at this point a roof slab would break away resulting in 0 percent survivors.

2.1.4.1 Incipient Failure Criterion for Slabs

Flexure.--As discussed previously, the overpressure level producing incipient flexural failure in a structural component is a load value beyond which the component is not capable of resisting flexural deformations. This value is determined herein by means of a resistance function which describes the full-range behavior of the component in question. A typical resistance function for a slab capable of developing two sets of plastic moments is shown in Fig. 2.7 and is determined using yield-line theory as described in Ref. 19. Means for constructing resistance functions for slabs of the type that frequently occur in rectangular RC shelters are described below. Referring to Fig. 2.7:

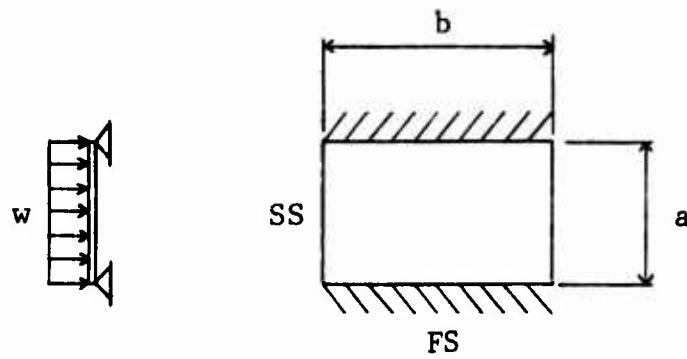
$$R_1 = \phi M_{pa} + \mu M_{pb} \quad \text{limiting resistance in the elastic range, lb} \quad (2.8)$$

$$k_1 = \gamma E_c I_a / a^2 \quad \text{stiffness in the elastic range, lb/in.} \quad (2.9)$$

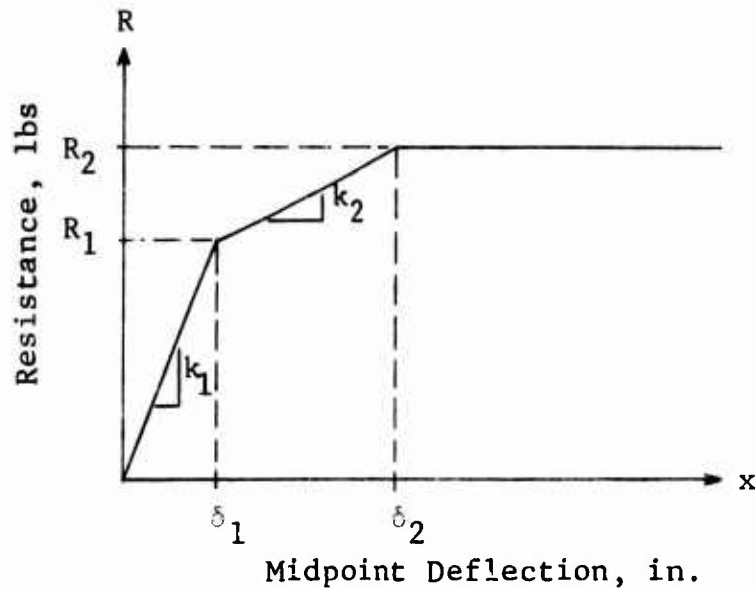
$$R_2 = 2\beta M_{pa} + 2\alpha \frac{b}{a} M_{pb} \quad \text{limiting resistance in the elasto-plastic range, lb} \quad (2.10)$$

$$k_2 = \rho E_c I_a / a^2 \quad \text{stiffness in the elasto-plastic range, lb/in.} \quad (2.11)$$

where M_{pa} and M_{pb} are plastic moments per unit length of side "a" (short side) and side "b" (long side) respectively (see Fig. 2.7). For the condition where tension steel area per unit length (A_s)



a) Loaded Slab



b) Resistance Function

$R(x) = k_1 x$	$0 \leq x \leq \delta_1$	Elastic
$R(x) = k_2(x - \frac{R_1}{k_1}) + R_1$	$\delta_1 \leq x \leq \delta_2$	Elasto-Plastic
$R(x) = R_2$	$\delta_2 \leq x \leq \infty$	Fully Plastic

$$\delta_1 = R/k_1 ; \quad \delta_2 = \frac{R_2 - R_1}{k_2} + \frac{R_1}{k_1}$$

w: Uniformly distributed load

SS: Simple supports

FS: Fixed supports

Fig. 2.7 CHARACTERIZATION OF RESISTANCE FUNCTIONS FOR SLABS

is equal to the compression steel area (A'_s) the values M_{pa} and M_{pb} are expressed as follows:

$$M_{pa} = A'_s f_{dy} d_s = p_s d'_s d_s f_{dy} \quad (2.12)$$

$$M_{pb} = A'_l f_{dy} d_l = p_l d'_l d_l f_{dy} \quad (2.13)$$

Coefficients $\phi, \mu, \gamma, \alpha, \beta$ and ρ characterize the influence of the type of loading, support conditions, geometric ratio a/b and the strain phase and are tabulated in Appendix D. Other parameters appearing in Eqs. (2.8) through (2.13) are defined below.

b = long side of slab, in.

a = short side of slab, in.

E_c = Young's modulus for concrete, psi

I_a = average moment of inertia per unit length of the short and long sides = $(I_s + I_l)$ where I_s is the average of the transformed section modulus, I_{ts} , and the full section modulus I_{gs} for the short side; I_l is a similar quantity for the long side. Thus,

$I_s = [I_{gs} + I_{ts}] / 2$ where $I_{gs} = D^3 / 12$ and

$$I_{ts} = \frac{(k_s d_s)^3}{3} + p_s d_s \left[n(d_s - k_s d_s)^2 + (2n - 1)(k_s d_s - d'_s)^2 \right]$$

Similar formulas can be generated for the long side by replacing the subscript s with l in the above equations.

D = slab thickness, in.

d_s, d_l = short or long side depth measured from the compression face of beam (or slab) to the centroid of the longitudinal tensile reinforcement, in.

n = ratio of steel modulus, E_s , to concrete modulus E_c , for short and long side, respectively.

p_s = percent steel perpendicular to the short side

p_l = percent steel perpendicular to the long side

k_s, k_l = cracked section factor for the short or long side (Table 11, Ref. 71)

A'_s, A'_l = area of reinforcing steel per inch of edge length, in.

f_{dy} = dynamic yield strength of steel, psi

d'_s, d'_l = distance between centroids of compression and tensile steel in doubly reinforced member for short and long side respectively, in.

Shear and Bond.--The incipient failure overpressure for shear or bond failure is the value beyond which the slab is no longer capable of resisting the dynamic shear forces (V_a, V_b) that exist at slab supports. These shear forces (reactions) can be computed directly by the use of the resistance function $R(x)$ (see Fig. 2.7) and the net load $P(t)$, applied to the surface of the slab. The values V_a and V_b are expressed as follows:

$$\begin{aligned} V_a &= \theta_{1s}P + \theta_{2s}R \\ V_b &= \theta_{1l}P + \theta_{2l}R \end{aligned} \quad (2.14)$$

where V_a and V_b are total dynamic shear forces along sides a and b respectively, lb. Coefficients θ_{1s} , θ_{2s} , θ_{1l} and θ_{2l} depend on the type of loading, slab end conditions, the geometric ratio a/b and the strain phase, i.e., elastic, elasto-plastic or plastic. These are tabulated in Appendix D. The slab is at the shear mode of incipient failure (Ref. 20) when the ultimate shear stress $\sigma_u \geq 4(0.85)\sqrt{f'_c}$ unless shear reinforcement is provided.

When shear reinforcement is provided, the slab is at the shear mode of incipient failure when the ultimate shear stress $\sigma_u \geq 6(0.85)\sqrt{f'_c}$. See Ref. 20 for criteria on effective shear reinforcement (Sec 1707, para d, p 75). Ultimate shear stress is computed from:

$$\sigma_u = \frac{V_u}{b_o d} \quad (2.15)$$

where

b_o is the critical section along side a and/or b,
 d is the distance from extreme compression fiber to the centroid of tension reinforcement.

The critical section is perpendicular to the plane of the slab and located at a distance $d/2$ from periphery of reaction area along the long or short side of the slab. V_u is computed using Eq.(2.14).

The slab is at the bond mode of incipient failure when the ultimate bond stress u_u is equal to or exceeds the following values for tension bars with sizes conforming to ASTM A305:

$$\frac{6.7\sqrt{f'_c}}{D} \text{ or } 560 \text{ psi for top bars} \quad (2.16)$$

$$\frac{9.5\sqrt{f'_c}}{D} \text{ or } 800 \text{ psi for other than top bars}$$

The ultimate bond stress u_u is computed from

$$u_o = \frac{V_u}{0.85 \sum o_j d}$$

where $\sum o$ is the sum of perimeters of all effective bars crossing the section on the tension side, if of uniform size; for mixed sizes, substitute $4 A_s / \bar{D}$, where A_s is the total steel area and \bar{D} is the largest bar diameter. For bundled bars, use the sum of the exposed portions of the perimeters. D is the nominal diameter of bar, inches.

Appendix C contains recommendations for the construction of resistance functions for slabs where tension and compression steel exists in different amounts. This appendix also contains a computer program for the analysis of R/C slabs.

2.1.4.2 Catastrophic Collapse Criterion for Slabs

When a slab experiences a loading which corresponds to the point of incipient failure, it cannot resist additional loading in the flexure mode. At the point of incipient failure the resistance function shown in Fig. 2.7 implies that for load magnitudes equal to or greater than the maximum flexural resistance of the slab, deformations will grow without bound. In reality the true resistance function does not remain horizontal indefinitely. The small deformation theory upon which the flexural resistance function was based does not consider membrane action which significantly enters the picture as deformations get large. The two-way slab (Ref. 4) shown in Fig. 2.8 illustrates the membrane large deflection action that can develop during a dynamic loading situation. The major error introduced by employing small deformation theory is due to the fact that the dynamic equilibrium equations used in the derivation of the resistance function, refer to the undeformed (flat) shape of the plate which precludes any supporting action from membrane forces.

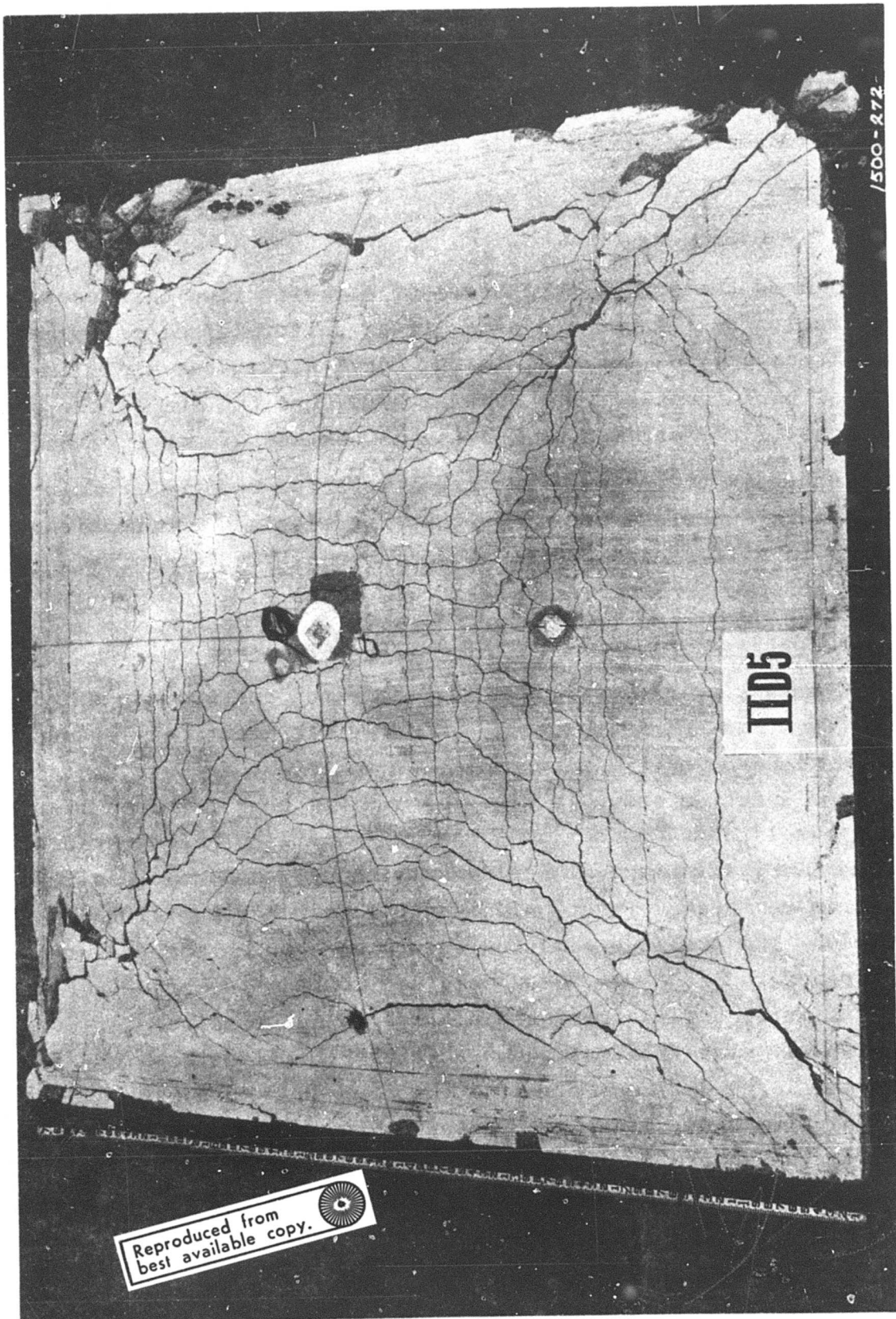


Fig. 2.8 LARGE DEFLECTION OF A TWO-WAY SIMPLY-SUPPORTED RC SLAB (Ref. 4)

Large deformation theory however, accounts for membrane forces by considering equilibrium of the deformed (dished) shape. Employing large deformation theory allows us to account for the reserve strength a slab has in its dished configuration.

The approximate load carrying capacity of a slab in its dished configuration may be determined by first converting the reinforcement network into an equivalent constant thickness membrane having the same length and width as the actual slab. In this model it is assumed that the concrete has lost its load resisting capacity and instead serves as a matrix for keeping the reinforcement rods separate and as an agent for transmitting the applied pressure load to the steel rods. For example, the plates tested under dynamic loading and illustrated in Figs. 2.8 through 2.10 support these assumptions. It will be noted that the severe cracking experienced precludes any significant membrane resistance of concrete. It is further assumed that reinforcing rods are securely anchored (in tension) around the periphery of the slab. This anchoring may be realized when either the rods are cast into a supporting edge (e.g., an external wall) or the rod tension is counterbalanced by tension that exists in a similarly loaded neighboring slab. An actual reinforcing steel network and an equivalent constant thickness membrane (analytical model) are illustrated in Fig. 2.11.

The thickness, t_e , of the equivalent membrane is determined such that the cross-sectional area of a unit strip in the equivalent membrane is equal to that of a unit strip in the steel network. Thus, $t_e = \bar{A}_s$ where \bar{A}_s is the steel area per unit length. If \bar{A}_s is not the same for both sides of a two-way slab, then \bar{A}_s is taken to be the average of both sides. The equivalent membrane must be able to transmit tensile forces across the entire span of the slab, therefore \bar{A}_s must only be representative of the continuous bars which span the full length.

Resistance functions (pressure load versus midspan deflection curves) for membranes rigidly supported at their periphery are shown (Ref. 21) in Figs. 2.12 through 2.14 for several a/b ratio values.

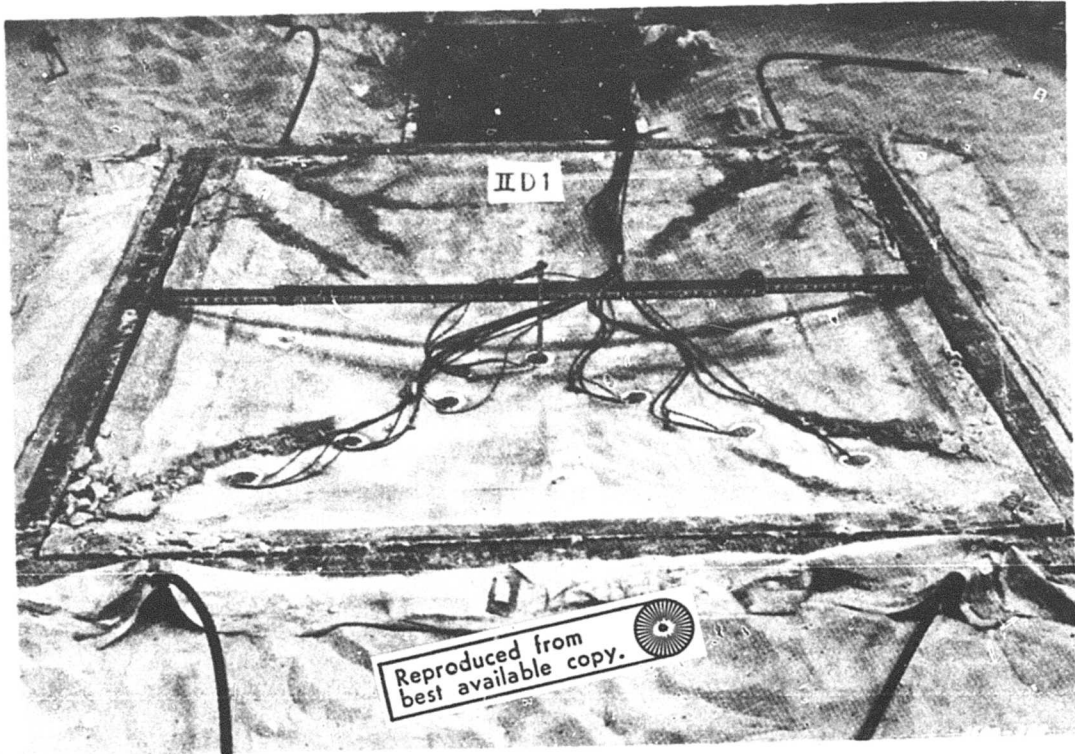


Fig. 2.9 MEMBRANE - LARGE DEFLECTION ACTION
OF A TWO-WAY RC SLAB (Ref. 4)



Note: Test condition: fixed edge, uniformly-dynamically loaded RC slab (101 psi peak pressure load).

Fig. 2.10 CRACKED SURFACE OF TWO-WAY RC SLAB (Ref. 60)

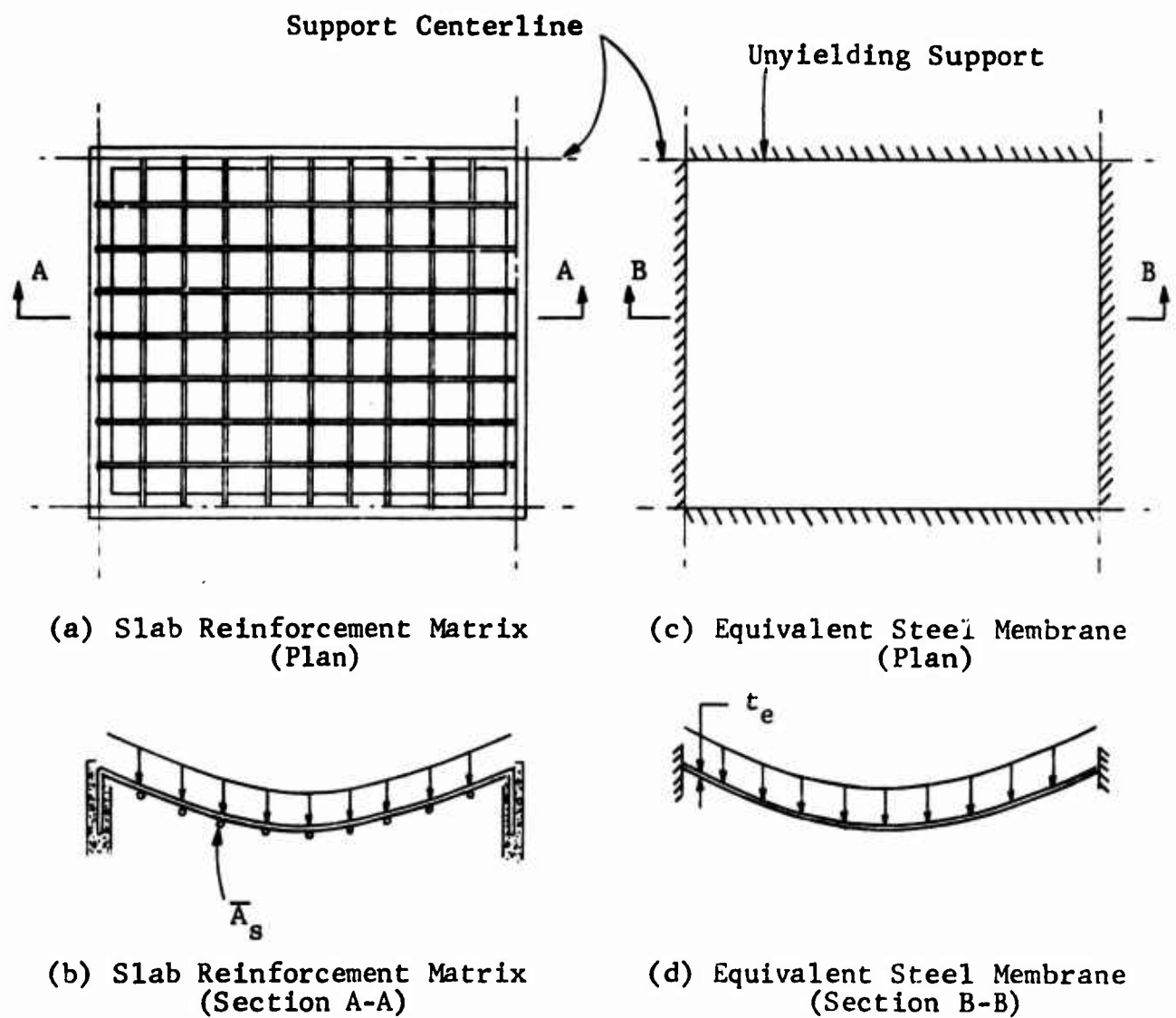


Fig. 2.11 SLAB REINFORCEMENT MATRIX
AND (EQUIVALENT) ANALYTICAL MODEL

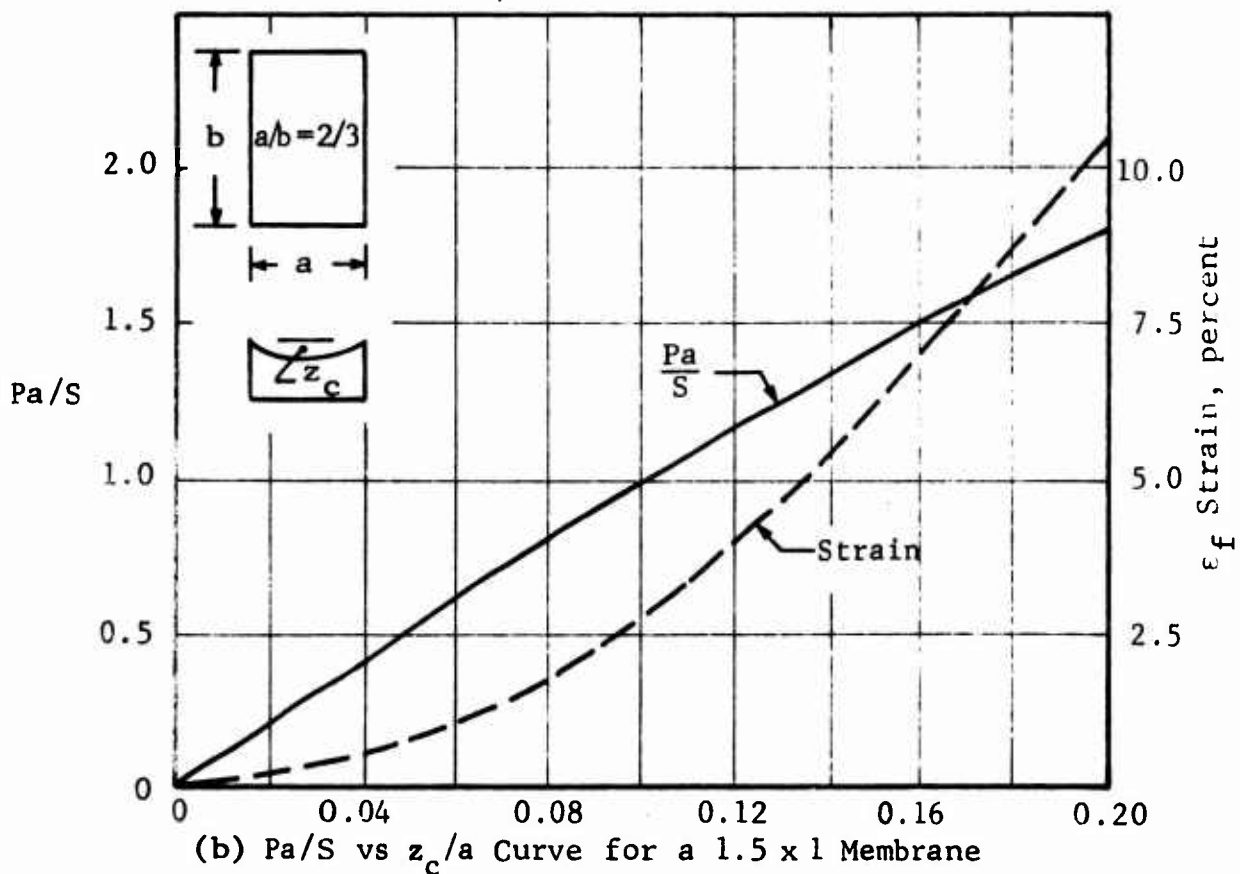
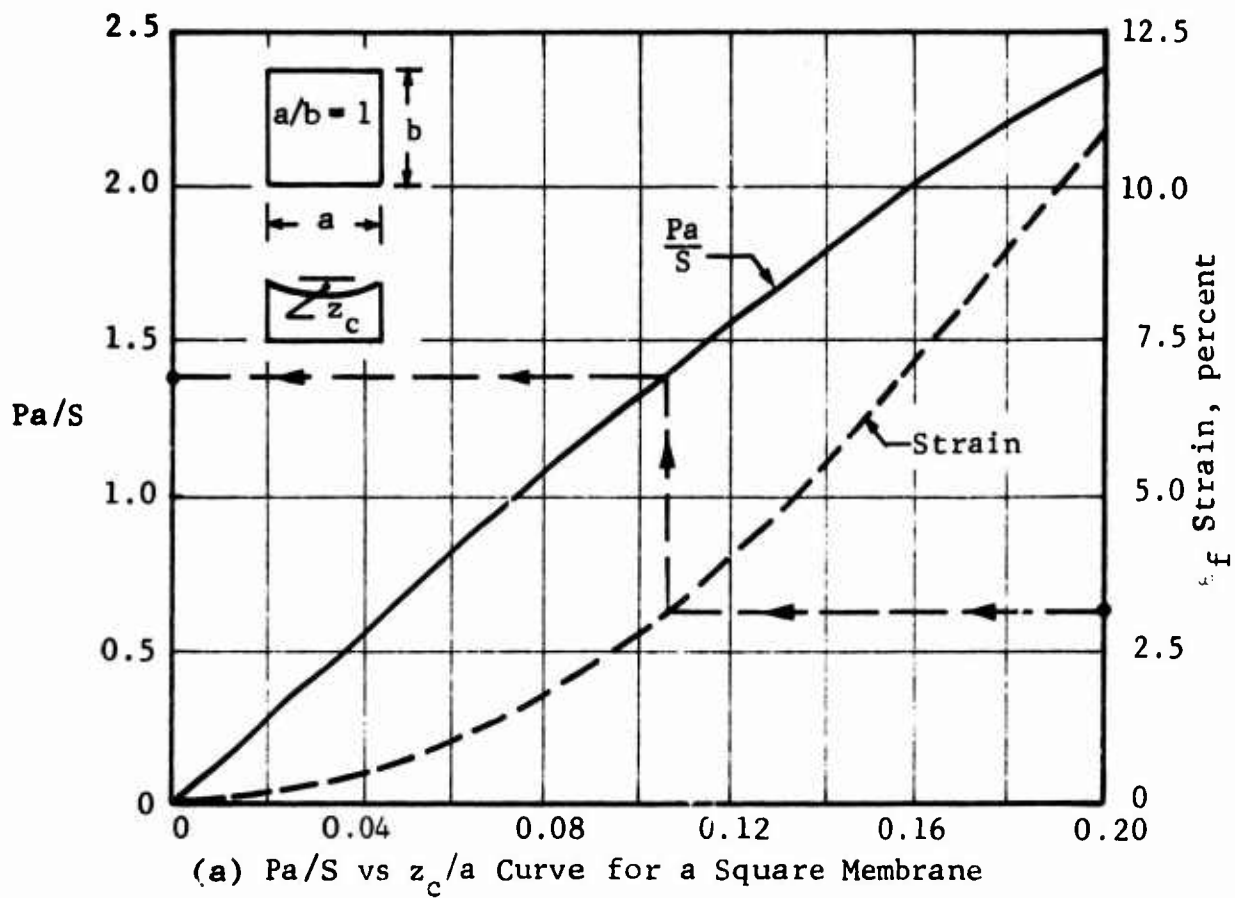


Fig. 2.12 MEMBRANE FAILURE CURVES

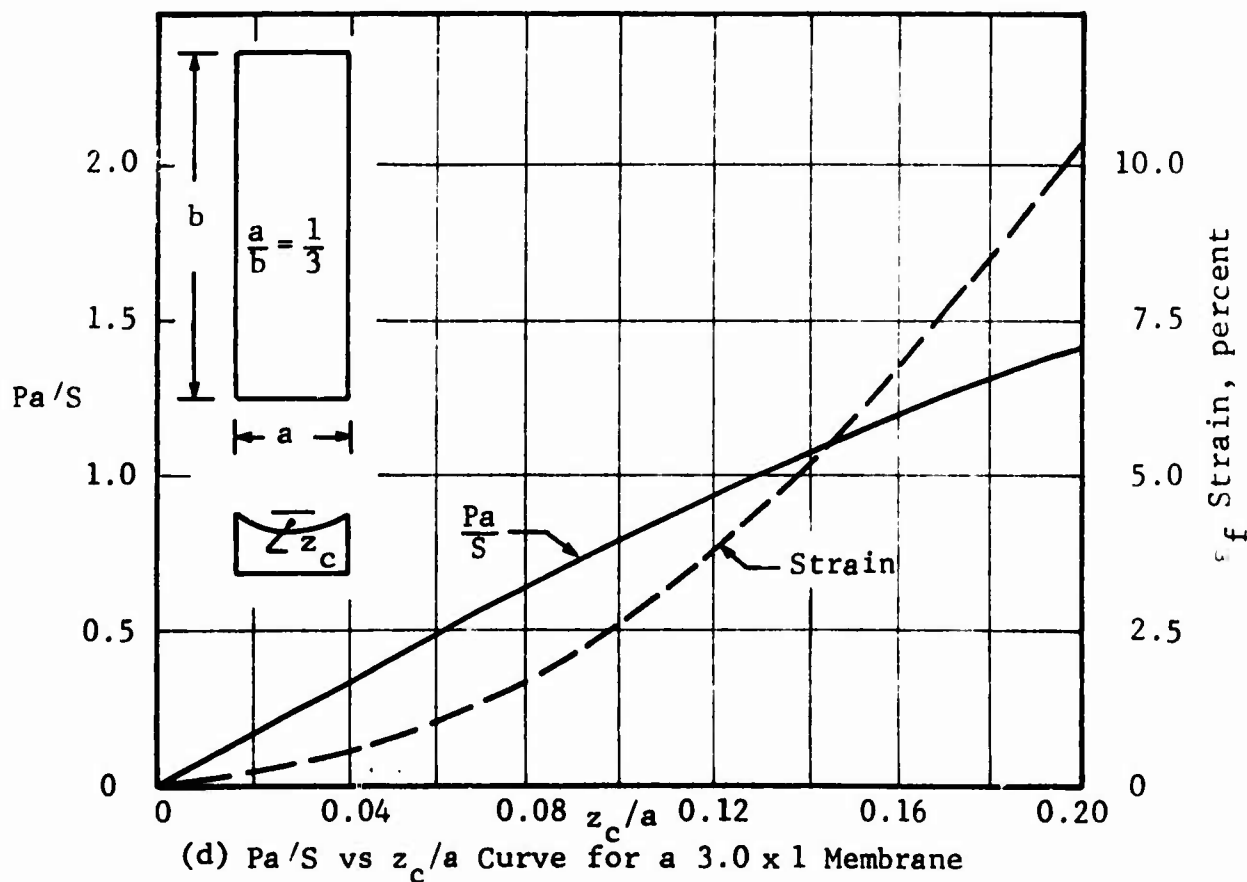
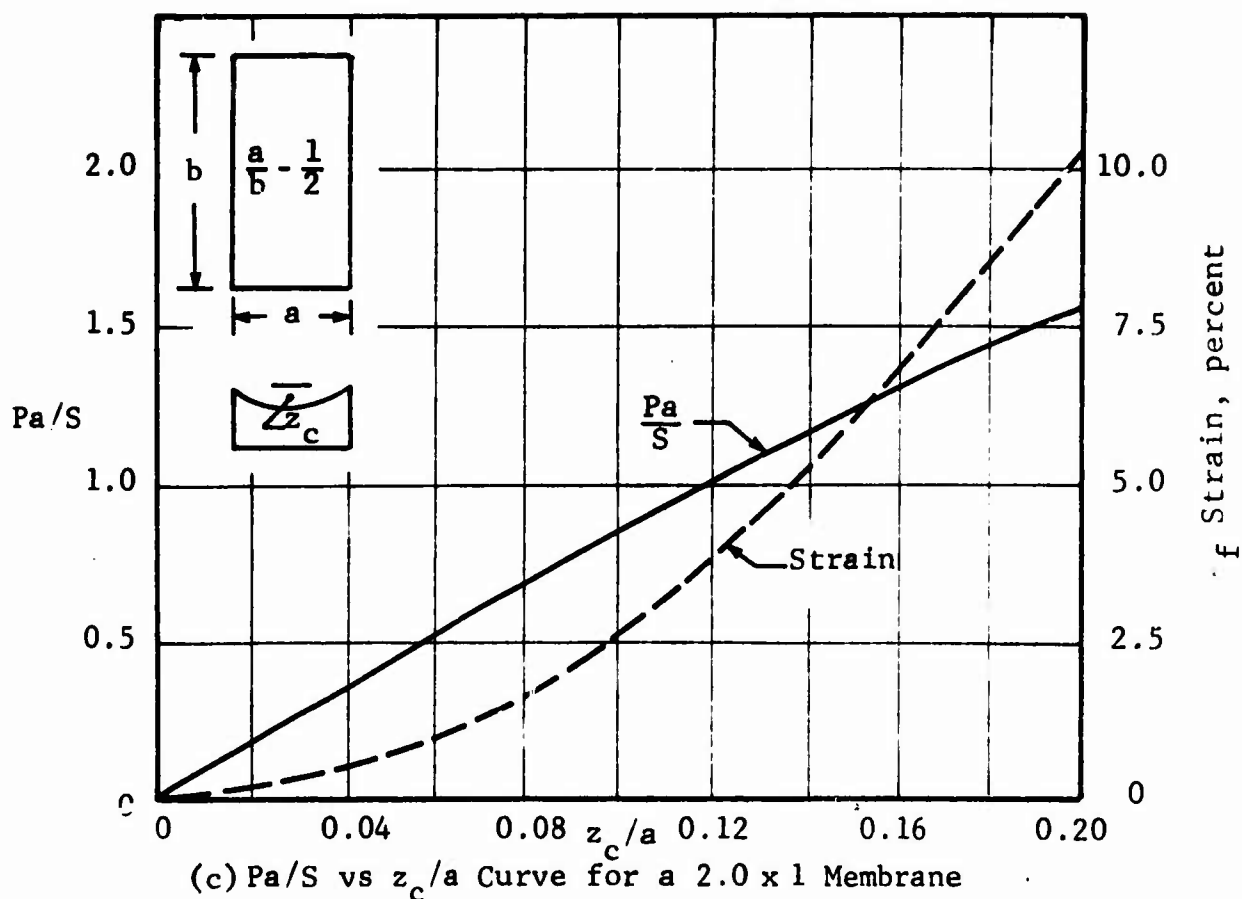


Fig. 2.13 MEMBRANE FAILURE CURVES

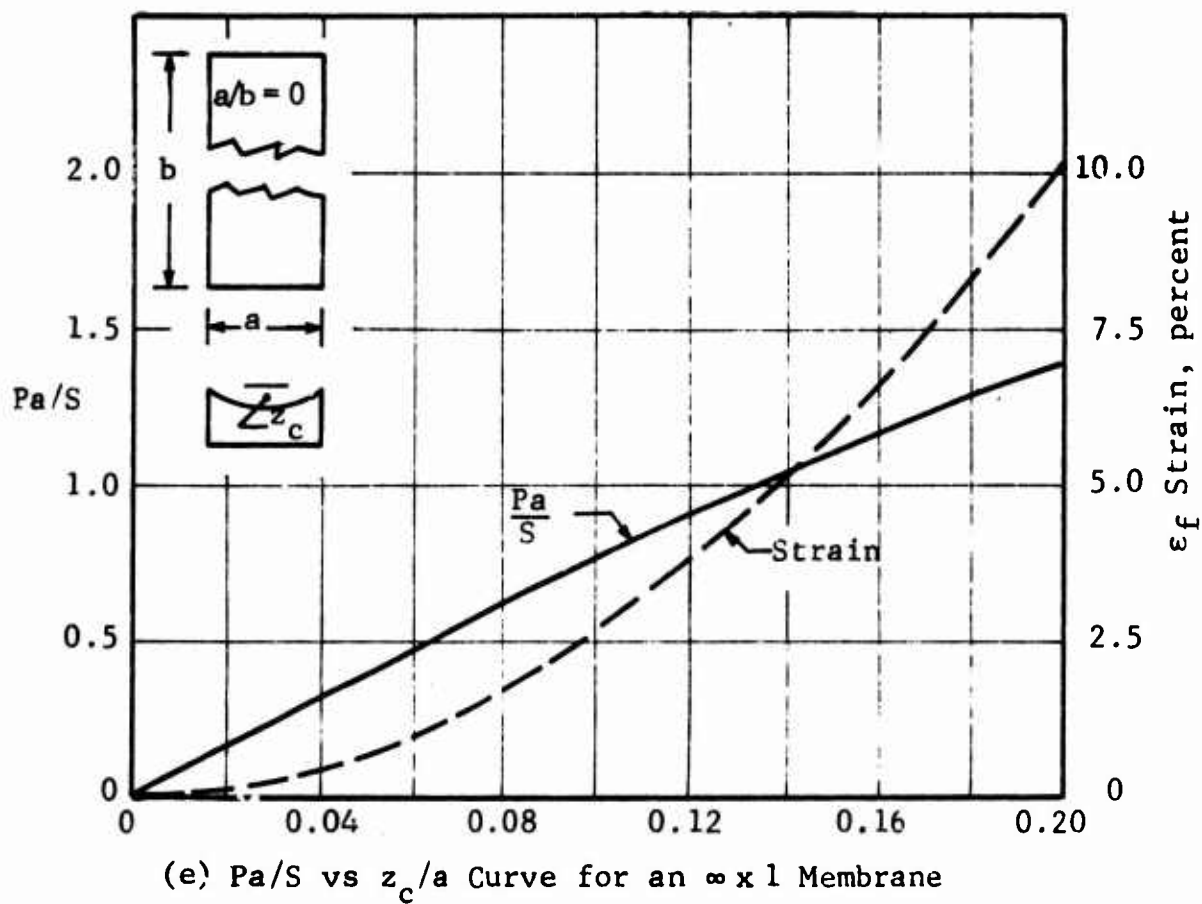


Fig. 2.14 MEMBRANE FAILURE CURVES

The nomenclature used in these graphs is defined as follows:

- a = length of short side, in.
- b = length of long side, in.
- P = total load (uniformly distributed) supported by membrane, psi
- z_c = midspan deflection, in.
- $S = t_e \sigma_u = \bar{A} \sigma_u$ = ultimate tensile force per unit length of membrane, lb/in.
- σ_u = dynamic ultimate strength of membrane material, psi
- ϵ_f = dynamic ultimate strain of membrane material, percent

In order to determine the overpressure magnitude producing membrane failure we proceed as follows:

To find: P_{of} = overpressure producing membrane failure

Required data: a/b , t_e , σ_u , ϵ_f

Procedure:

1. Select the appropriate figure (Fig. 2.12 through 2.14) whose a/b ratio is closest to the actual ratio.
2. Using the value of ϵ_f , determine the $P_a/S = k^*$ ratio in the manner indicated in Fig. 2.12a.
3. Determine P_{of} by the use of the following equation:

$$P_{of} = \frac{k^* t_e \sigma_u}{D_{lf} a} - Q_{dl} \quad (2.17)$$

where

- t_e = equivalent membrane thickness, in.
- Q_{dl} = dead load per unit area of membrane, psi
- D_{lf} = dynamic load factor

Since for problems of interest the positive phase duration of the blast pulse is large when compared to the natural period of vibration of the membrane, and since the variation of P_a/S (Figs. 2.12 through 2.14) is very nearly linear, the dynamic load factor (D_{lf}) was taken as 2.0 in this study for computational purposes.

2.2 ANALYSIS OF ARCH SHELTERS

Arch shelters considered belong in the single-purpose category and are described in detail (including costs) in Appendix A. Two categories are included, i.e., low level blast effects shelters (up to 30 psi design overpressure) and high level blast effects shelters (100 and 150 psi design overpressure).

Low level blast effects shelters include two sets of four structures each. In the first set the arch shell is of RC, while in the second set a steel shell is used. In each of the two sets the four arches are similar except that each is designed to resist a different overpressure level (weapon environment) resulting from a single megaton range weapon. The four design overpressure levels are 0*, 10, 20 and 30 psi. All structures are semicircular arches having a 17.5-ft inside radius and an 80-ft inside length. A typical cross section showing common (basic) dimensions and the position of the soil cover relative to the structure is shown in Fig. 2.15.

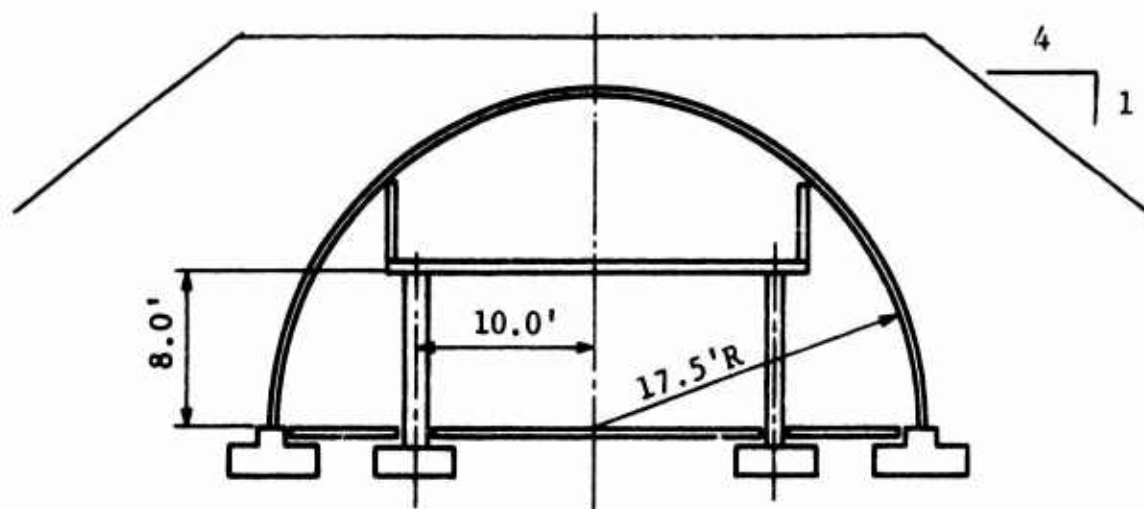


Fig. 2.15 CROSS SECTION OF BASIC ARCH SHELTER

*This is used to indicate fallout radiation as the primary design weapon environment.

The slope of the mound (4 to 1) is sufficiently gentle to preclude significant dynamic and reflected pressures acting on the structure. The end walls (see Fig. A.2, Appendix A) are RC slabs in every case. Entranceways consist of corrugated steel tunnels containing bulkheads and blast doors.

High level blast effects shelters include two structures. One was designed to resist 100 psi, the second 150 psi. They are RC structures and are similar to the one described above except that the entranceways also consist of RC instead of corrugated steel. Basic properties are summarized in Table 2.1.

TABLE 2.1
BASIC PROPERTIES OF ARCH SHELLS AND END WALLS

Steel Arches				
Design Weapon Environment (psi)	Section Type	Moment of Inertia per Unit Axial Length (in. ⁴ /in.)	Cross-Sectional Area per Unit Axial Length (in. ² /in.)	
Fallout	12 gage corrugated steel	0.0604	0.129	
10	1 gage corrugated steel	0.1659	0.343	
20	3/8 in. corrugated steel	0.2380	0.487	
30	1/2 in. tee-flange steel	0.2920	0.583	

Concrete Arches		
Design Weapon Environment	Arch Thickness (in.)	Endwall Thickness (in.)
Fallout	4	8
10	4	8
20	4	9
30	4	10
100	8	35
150	13.5	41

2.2.1 Definitions of Structural Failure

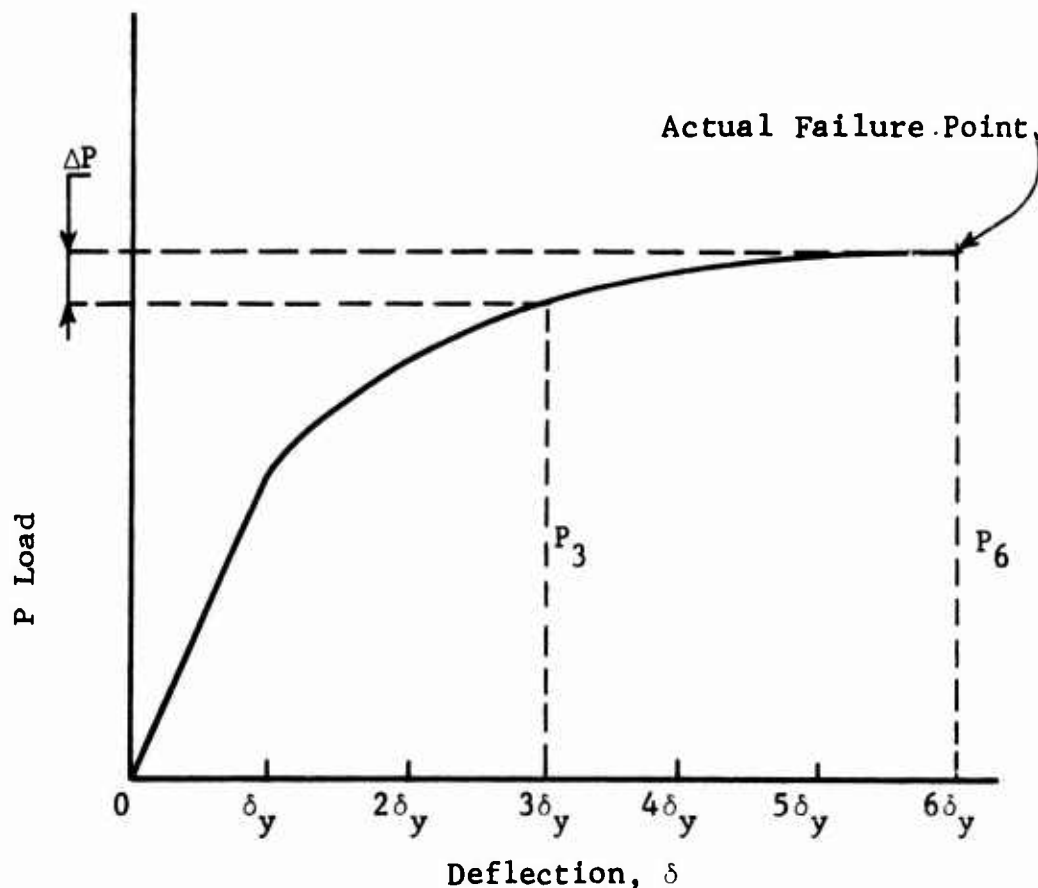
Arch structures are normally designed to carry transverse pressure loads in membrane compression, whereas slabs (prior to yielding) carry pressure loads in bending. This basic difference in the load carrying mechanism leads us to redefine our previous definitions for the incipient failure pressure P_A and the catastrophic failure pressure P_B .

Incipient Failure Definition for Buried Concrete Arches.-- For concrete arches, incipient failure is defined as the overpressure which results in the strain through an entire cross section of the arch shell to exceed the ultimate failure strain of concrete in compression (0.0024 in./in.). When this state of strain is reached, the arch is assumed to collapse in the neighborhood of its center portion (i.e., away from the supporting end walls). The external overpressure which results in this midspan state of strain is termed the incipient failure pressure P_A .

Incipient Failure Definition for Buried Steel Arches.-- In steel arches the ductility of the steel does not permit the arch material to fracture apart as with concrete, thus we need a different definition for incipient failure pressure. The steel arch will continue to support pressure loads at strains beyond the yield strain, however this is at the expense of suffering midspan deflections which grow increasingly out of proportion with each unit increase in external load. For sufficiently large loads the midspan deflection growth will continue, thus allowing yield hinges to form. This permits the deformation characteristics of the arch to resemble a mechanism and the arch collapses. What is sometimes done, is to define collapse as the external load which results in a prescribed number of yield deflections (Ref. 22). If we use the allowable yield deflection approach, the problem we are confronted with is that the deflection just prior to the mechanism formation is usually many yield deflections. This is ordinarily well into the large deformation range and consequently out of range of most computational techniques (including the one used here).

The problem can be overcome if we first recognize that a plot of the actual applied load versus midspan deflection would be nonlinear in that it would rise linearly up to a point (δ_y) and then nonlinearly level off, as in Fig. 2.16.

Let P_b be the actual failure load and $\delta_c = 6\delta_y$ be the corresponding failure deflection (i.e., 6 yield deflections). Suppose we did not know the precise number of yield deflections which defined failure; or, we purposely defined δ_c lower than the collapse value to keep the structural computations within their range of accuracy (within the small deformation limit).



Note: $\delta_y \equiv$ one yield deflection

Fig. 2.16 NONLINEAR RESISTANCE FUNCTION

For either of these two reasons, suppose that $\delta_c = 3\delta_y$ was selected as the critical number of yield deflections to failure. From Fig. 2.16 we see that although the erroneous failure criterion ($3\delta_y$) is 50 percent in error with respect to the actual failure deflection, the corresponding failure load (P_3) is only off by about 8 percent (on the conservative side) from the actual failure load P_b . In other words the predicted failure pressure is fairly insensitive to the number of yield deflections chosen for the failure criterion. The failure criteria used for the steel arches in this study corresponded to $4\delta_y$ (i.e., four yield deflections). Although this is still probably less than the actual number of yield deflections at failure, (Ref. 22 used yield deflections anywhere from 2 to 5), it is still sufficiently accurate to predict failure in view of the sensitivity argument given. In summary, incipient failure pressure P_a for steel arches is defined as the external overpressure which results in the midspan deflection exceeding four yield deflections.

Catastrophic Failure Definition (Steel and Concrete Arches).--

Once the incipient failure pressure is reached, the arch (steel or concrete) is assumed to collapse in the vicinity of its center portion, i.e., away from the end walls. The portion of the arch in the vicinity of the end walls receives partial support from these walls, consequently the arch shell in this region is stronger than at midspan. Thus failure at midspan does not imply that total collapse of the shelter will occur. What may actually happen, at external pressures greater than P_a , is that the arch deforms into two "lean-to" type compartments.

The volume (or survival space) of the postulated lean-to compartments would be bounded by the end wall and the collapsed portions of the arch. It is postulated that end walls remain essentially vertical for pressures in the vicinity of P_a . The catastrophic failure pressure P_b is defined as that pressure which will ultimately fail the end walls in a bending failure,

bond failure or shear failure. When this occurs the bounding surface of the wall fails causing the lean-to voids to collapse and thus bury or crush the occupants.

2.2.2 Analytical Model

As mentioned previously, an arch shelter consists of a semi-circular cylindrical shell bounded by two end walls. The end walls are RC slabs and the arch shell consists either of steel or concrete.

As with the box-type structure described earlier, the internal moment and force distributions throughout each main component of the structure (shell, end wall, footing, etc.) are coupled (i.e., they are statically indeterminate). Here too, the coupled problem is simplified by making certain assumptions regarding the restraint conditions (clamped or pinned) involving the junction between adjacent members. Upon decomposing the total structural problem into a series of smaller uncoupled problems, each component is then analyzed as a separate unit and the weakest link in each chain is found.

2.2.3 Loading (Closed Shelter)

Arch Shell.--Arch shelters under consideration are buried as indicated in Fig. 2.15. The spacial pressure distribution on the soil surface is assumed to be uniform and its time variation is taken to be the same as the free field overpressure loading. Analogous to the box-type structures, the uniform spacial distribution is reasonable so long as the time it takes the overpressure wave front to engulf the structure is small compared to the lowest natural period of vibration of the soil-arch structural system.

End-Walls.--The loading on the end walls is due to a combination of both the overpressure loading and the lateral side pressure of the soil. The specific loading assumptions are the same as those discussed for the box-type structures and thus will not be repeated here (see Subsection 2.1.2).

Footings.--Once the solution to the arch structure has been established, the resulting vertical shear forces at the arch supports are known. These shear values must in turn be supported by the footings, thus establishing the sought loading.

2.2.4 Loading (Open Shelter)

When the blast doors are open, the differential pressure loading on the structure is only slightly different from the closed shelter case discussed. Briefly, the internal pressure cannot build up fast enough to substantially reduce the net differential pressure loading across the roof arch or end wall. By the term "fast enough" we mean that if structural failure is to occur, it will have occurred by the time any significant reduction in pressure differential has been produced. Consequently, the loading is assumed to be the same as in that of the closed shelter.

2.2.5 Incipient Failure Determination for Concrete Arches

The method of solution closely follows, in principle, that discussed in connection with slab failure. Briefly, the method consists of first finding the static resistance function, $R(w)$, for the midspan deflection of the arch. Appropriate mass and load factors are determined through energy considerations. Next the equivalent first mode, single degree-of-freedom differential equation analogous to Eq. (2.6) is constructed. For a prescribed weapon size and trial overpressure, the equation of motion is integrated to determine if the failure deflection has been reached, or exceeded. (Recall that for concrete arches, we defined the failure midspan deflection as that value which results in a concrete cross section to be at a strain level of 0.0024 in./in., and for steel arches the failure deflection was defined as four yield deflections.) The above process is repeated (the overpressure is incremented) until an overpressure (the incipient failure overpressure, P_A) is found which results in the timewise peak midspan deflection which equals the failure deflection.

Determination of Concrete Arch Resistance Curve.--A finite element model representing the soil-arch configuration was constructed as illustrated in Fig. 2.17. The uniformly distributed overpressure, P_o , was converted into concentrated nodal forces acting normal to the soil surface. The resulting load-deflection curve should of course depend on the physical properties of the soil surrounding the arch. For a structure located in a stiff soil, the soil will behave somewhat like an arch in that it carries a portion of the load applied at the surface (active arching action). At the other extreme, a soft soil will transmit most of the surface pressure directly to the buried structure (passive arching action). The extent to which surface pressure is transmitted to a buried structure depends on the surface loading, type of soil, stiffness of the structure and depth at which it is buried.

For the arch-soil analysis, an intermediate stiff soil is chosen with a modulus (E_s) of 5000 psi, compressive yield strength (σ_o) of 65 psi and Poisson's ratio of 0.4. The resistance versus crown deflection curve is shown in Fig. 2.18.

In the analysis performed, the influence of soil yielding under the arch footings was neglected. This omission would tend to make the evaluation of survivability somewhat conservative. The yielding of footings would allow the arch to carry more load before failure occurs.

Referring to Fig. 2.18, the fact that nonlinearities in the material stress strain law are admitted into the analysis accounts for the leveling off of the load-deflection (resistance) curve. Most of the leveling off is a result of the plastic flow experienced within the soil. To illustrate this fact the resistance curve was run a second time with all parameters the same except that the compressive yield strength of the soil was assumed to be 200 psi. The result was that the flattening of the resistance curve (Fig. 2.18) was postponed in that yielding of the soil did not take place until larger values of the external load were applied.

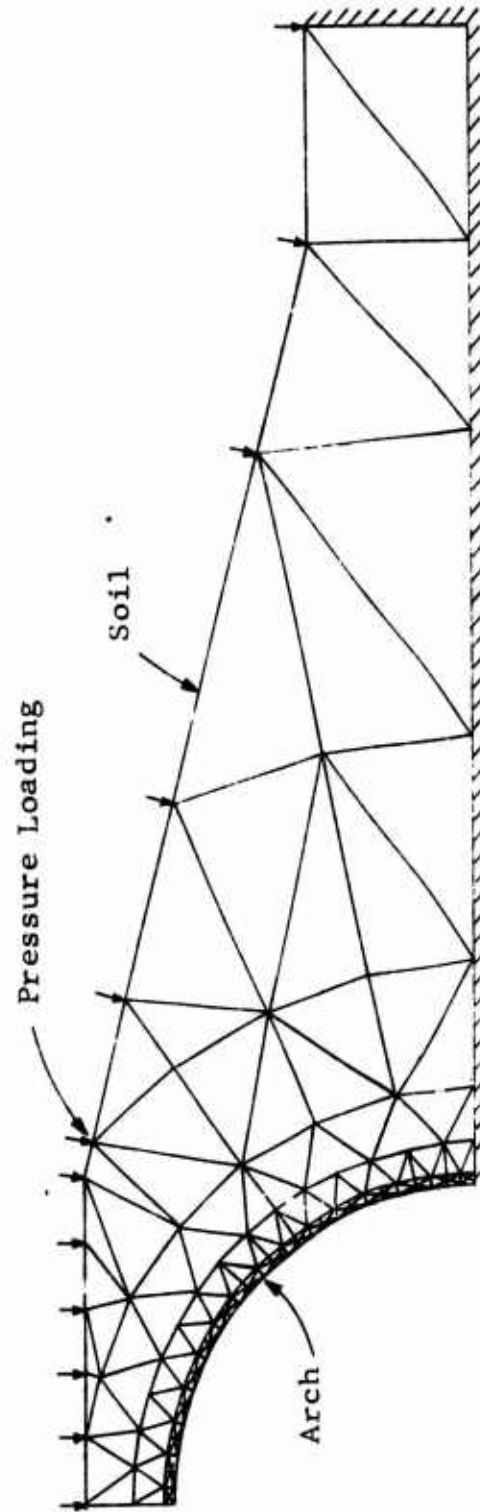


Fig. 2.17 FINITE ELEMENT REPRESENTATION OF CONCRETE ARCH AND SOIL

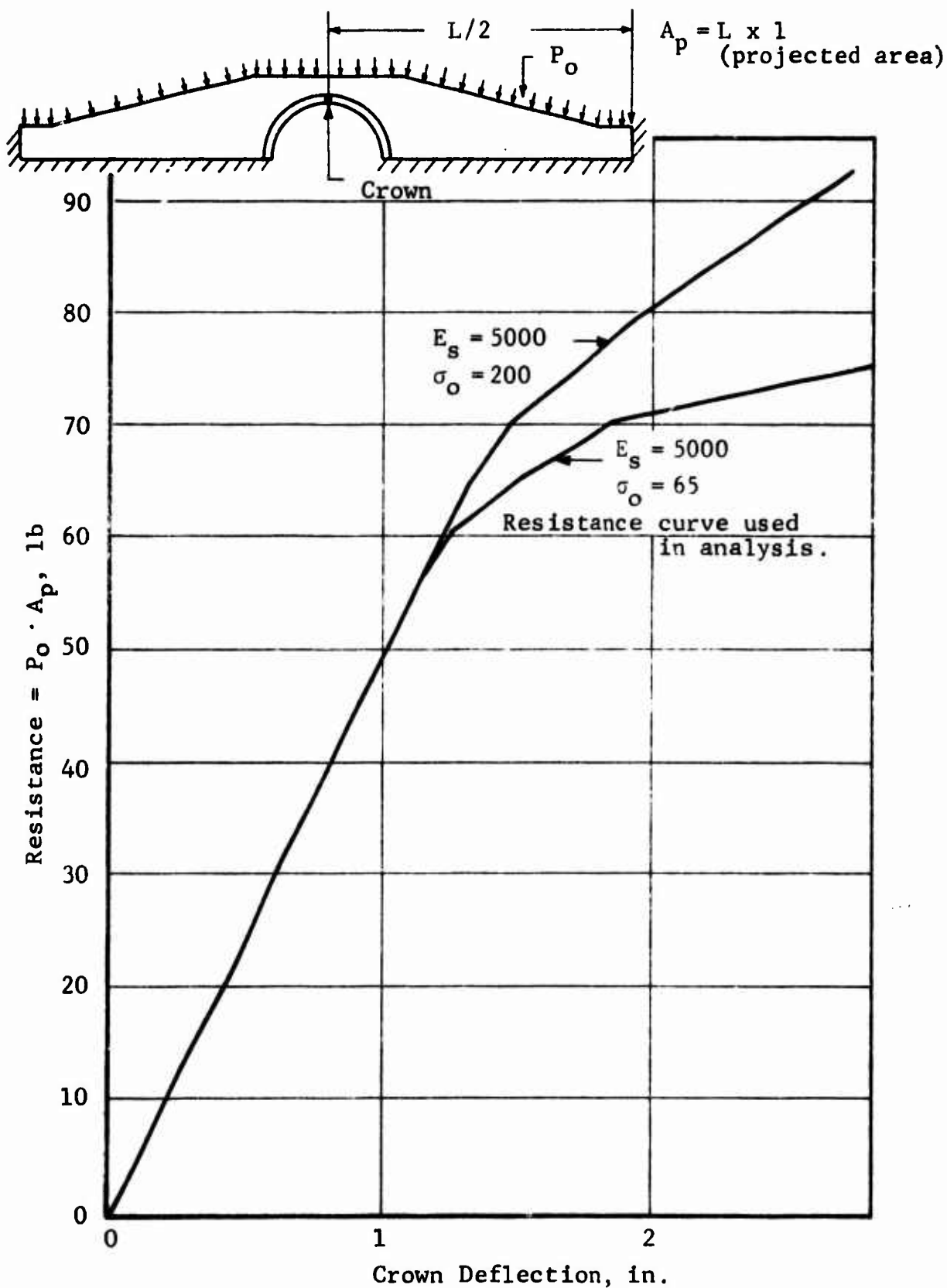


Fig. 2.18 CONCRETE ARCH RESISTANCE FUNCTION

What is often done in the analysis of buried arches of the type considered here is to assume a priori a pressure loading on the arch, perhaps the most popular being the uniform compression mode loading assumption (Ref. 23). Briefly, the uniform compression mode corresponds to a purely radial pressure distribution whose magnitude is equal to the pressure at the soil surface. It is of interest to compare the soil-arch loading (i.e., the load the soil imparts to the arch resulting from the free surface loading) with the uniform compression mode. Since the finite element computer program used herein (Ref. 24) operates in terms of applied nodal forces rather than applied pressures, it was necessary to convert the uniform compression pressure loading into an equivalent distribution concentrated force in order to make an appropriate comparison. A comparison of the two types of loading is illustrated in Fig. 2.19 and corresponds to the concrete arch case represented in Figs. 2.17 and 2.18. With the exception of the vertical loading component in the midhaunch-to-support region, the interaction solution loading is somewhat lower. This implies that the soil itself is behaving as an arch wherein a portion of the surface load is taken by the soil.

Determination of Load Transformation Factor K_L .--The external work, W_a , done on the actual arch-soil (unit depth) configuration shown in Fig. 2.17 by the externally applied pressure is given by the expression

$$W_a = \sum_i (F_x^i w_x^i + F_y^i w_y^i) \quad (2.18)$$

where F_x^i , F_y^i are respectively the horizontal and vertical external forces applied to each surface node of the arch-soil model; w_x^i , w_y^i are respectively the corresponding horizontal and vertical surface displacements; and the summation is made over all surface nodes.

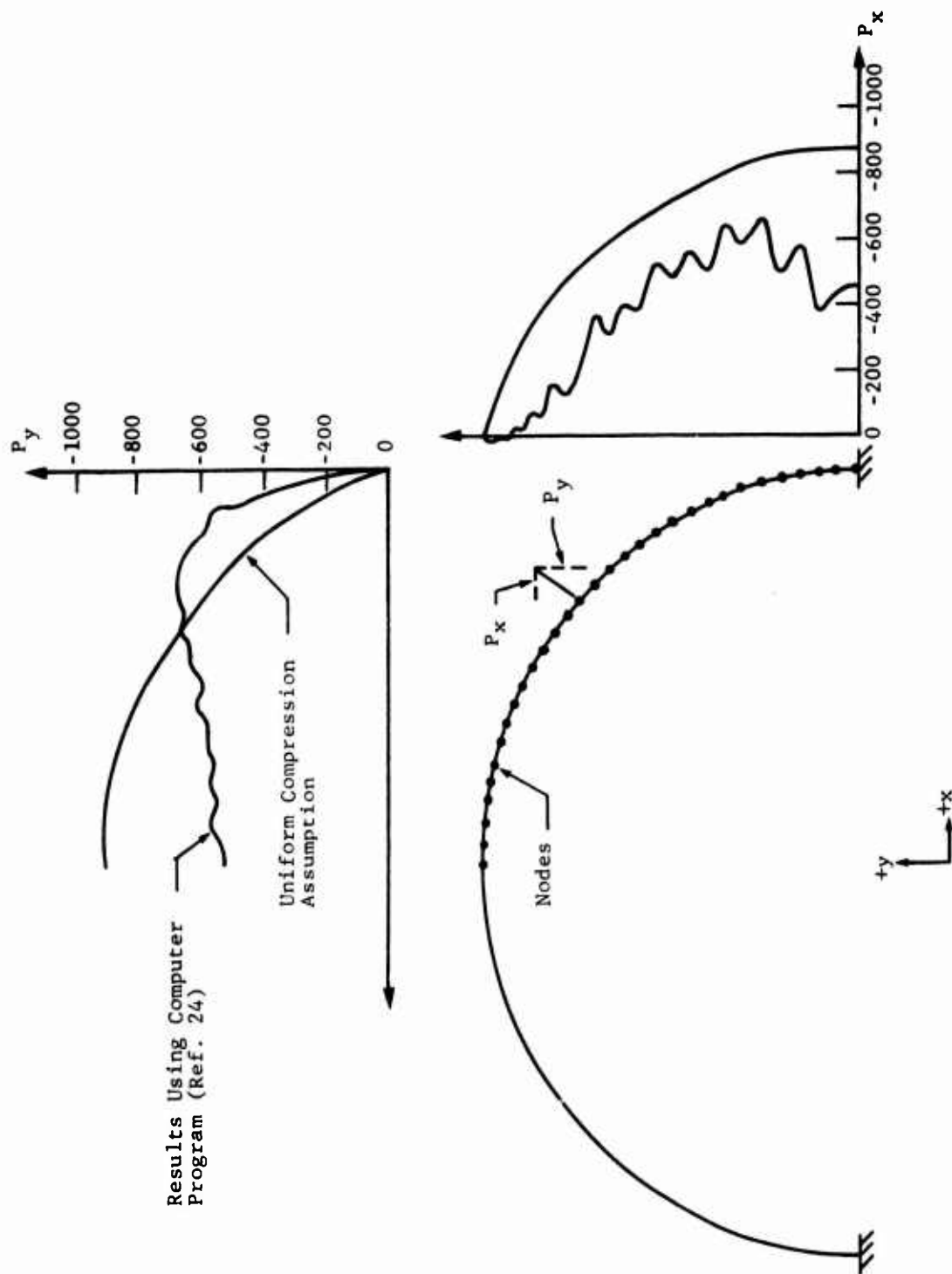


Fig. 2.19 COMPARISON OF TWO ARCH ANALYSIS METHODS

The external work, W_e , of the equivalent single degree-of-freedom model (e.g., Fig. 2.1d) is given by

$$W_e = \frac{1}{2} P_e w_e \quad (2.19)$$

where P_e is the net external force on the spring model and w_e is the spring deflection.

Equating the actual and equivalent work expressions and noting that the total vertical force P acting on the actual arch-soil configuration is equal to $\sum_i F_y^i$ we arrive at the expression

$$P_e = P \left[\frac{\sum_i (F_x^i w_x^i + F_y^i w_y^i)}{w_e \underbrace{\sum_i F_y^i}_{K_L}} \right] \quad (2.20)$$

Setting w_e equal to the midspan deflection of the arch, the term in brackets (according to the definition given by Eq. (2.1)) is the load factor, K_L . The load factor expression (in brackets) is computed automatically in the arch-soil interaction finite element computer program.

Determination of Mass Transformation Factor K_m .--To establish the mass factor, we need an approximate relation for the nodal velocity distributions. As a crude approximation, we assume the ratio of the nodal to midspan velocity distribution is proportional to the ratio of the nodal to midspan deflection. Or mathematically,

$$\frac{\dot{w}_y^i}{\dot{w}_m} = \frac{w_y^i}{w_m} ; \quad \frac{\dot{w}_x^i}{\dot{w}_m} = \frac{w_x^i}{w_m} \quad (2.21)$$

where (w_y^i, w_x^i) are the vertical and horizontal nodal displacements due to a static unit surface pressure load, w^m is the mid-span deflection and the dotted quantities are the corresponding velocities.

The kinetic energy of the actual arch-soil configuration is thus given by the expression

$$KE_a = \frac{1}{2} \sum_i m^i \left[(\dot{w}_y^i)^2 + (\dot{w}_x^i)^2 \right] \quad (2.22)$$

where m^i is the mass of each lumped nodal mass. Or, upon inserting the velocity ratios we can rewrite the above expression as

$$KE_a = \frac{(\dot{w}^m)^2}{2} \sum_i m^i \frac{[(w_y^i)^2 + (w_x^i)^2]}{(w^m)^2} \quad (2.23)$$

The kinetic energy of the equivalent single degree-of-freedom system is given by

$$KE_e = \frac{1}{2} M_e V_e^2. \quad (2.24)$$

Equating KE_a and KE_e and setting V_e equal to the midspan velocity \dot{w}^m we obtain

$$M_e = M_t \left[\frac{\sum_i m_i [(w_y^i)^2 + (w_x^i)^2]}{(w^m)^2 \sum_i m_i} \right] \quad (2.25)$$

$\underbrace{\hspace{10em}}_{K_m}$

where M_t is defined as the total nodal mass summation (i.e., $M_t = \sum_i m_i$). By comparing this last expression to Eq. (2.2) we see that the expression in brackets is the mass transformation factor K_m .

2.2.6 Incipient Failure Determination for Steel Arches

The method herein closely follows that discussed in connection with concrete arches and hence only the differences will be highlighted. The first step is to determine the static resistance function, $R(w)$, for the midspan deflection of the arch. The determination of the resistance function for the steel arch is the same as that for the concrete arch except for one detail. The steel arches are actually corrugated. The corrugations are perpendicular to the plane of Fig. 2.17 and therefore do not appear in the drawing. The corrugations are not physically modeled; instead, an equivalent constant thickness steel arch is used whose cross-sectional moment of inertia and area are equal to that of the corrugated arch. In this way the important stiffness properties of the corrugated arch are preserved.

The next step is to determine the mass and load transformation factors K_L , K_m . This is accomplished by the use of Eqs. (2.20) and (2.25). Once we have $R(w)$, K_L , K_m , the equivalent single degree-of-freedom differential equation analogous to Eq. (2.6) is constructed.

For a prescribed weapon size, and trial overpressure, the equation of motion is integrated to determine if the failure deflection has been reached or exceeded (recall that for steel arches, we defined the failure midspan deflection as that value which equals four yield deflections). The above process is repeated (the overpressure is incremented) until an overpressure (the incipient failure overpressure, P_a) is found which results in the timewise peak midspan deflection which just equals the four yield deflections.

2.2.7 Catastrophic Failure Determination (Concrete and Steel Arches)

Catastrophic failure (100 percent fatality) for arch structures is assumed to occur at an overpressure level which produces the failure mode illustrated in Fig. 2.20.

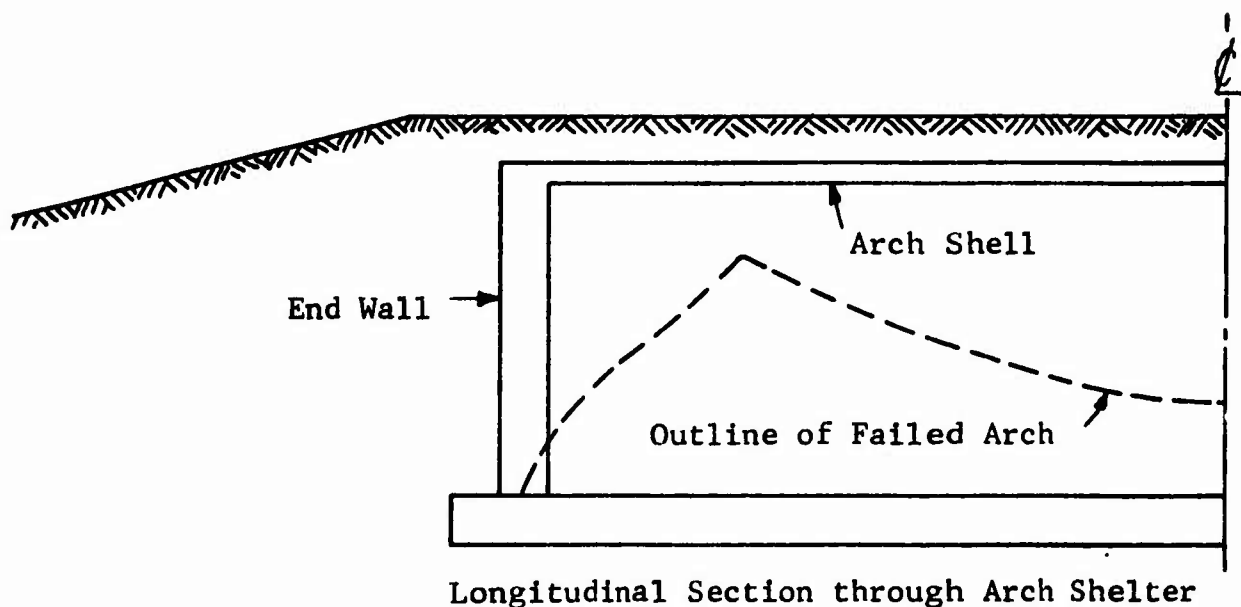


Fig. 2.20 DEFINITION OF ARCH STRUCTURE FAILURE

The principal structural components of arches (single-purpose shelters) considered in this study are the arch shell and the end-walls. In all cases studied it was found that the arch shell is the weaker of the two. For this reason incipient failure is based on the overpressure which will produce failure in the arch shell alone. Catastrophic failure is assumed to occur at an overpressure level which in addition to failing the shell, also produces failure of the end-walls in the manner indicated in Fig. 2.20.

CHAPTER THREE

BLAST FILLING OF PERSONNEL SHELTERS

3.1 BLAST WAVE PROPAGATION INTO SHELTERS

In order to estimate the effects of an air blast wave upon people or equipment inside of shelter spaces, it is necessary to consider the aerodynamic phenomena occurring during the propagation of the blast wave into such spaces. The magnitude of the effects is obviously a function of the blast wave characteristics, the geometry of the chamber, and its entrance configuration.

A typical blast wave generated by a large-scale nuclear weapon is characterized by a propagating shock front, at which the pressure jumps nearly instantaneously to a peak value, followed by an exponential decay in pressure over a period of a few seconds. The sudden increase in pressure is matched by a corresponding particle velocity increase. The pressure in the blast wave continues to decay below the value of the ambient pressure. During the so-called negative phase of the blast wave the local particle velocity reverses direction, thus the flow direction at this time is opposite to that of shock propagation.

The interaction of such a blast wave with a shelter space depends on the geometry of the latter and upon the blast orientation relative to the chamber entrance. Possible variations are above or below ground location, chambers connected to the atmosphere by direct entrance or through tunnels, etc. Similarly the blast wave propagation may be normal, oblique or parallel to the plane of the entranceway. Even for the case of normal orientation one must distinguish between the cases where the surface containing the entrance is large or infinite such as the ground surface, or is small such as the face of a building. In either case normal reflection takes place at the surface, the pressure being increased at least by a factor of two over the incident shock front pressure. However, if the reflecting surface is

small the high reflected pressure is rapidly eroded as rarefaction waves generated at the wall edges move across the wall.

For typical chamber geometries, where the largest chamber dimensions are of the order of 100 ft the blast wave interaction process may be conveniently divided into two phases. The first of these with a typical duration of couple hundred milliseconds is the shock diffraction phase during which the predominating phenomena are expansions, reflections, and interactions of shock and rarefaction waves at the chamber entrance and in its interior. This is followed by a phase in which the primary phenomenon is the rapid inflow of gases from the outside or free field region into the chamber. This latter phase continues until pressure equalization between the inside and outside occurs, then the gradual outflow of air from the chamber commences. Obviously it is assumed that the chamber retains its structural integrity.

It is during the shock diffraction phase that the geometric variables of the chamber and its entrance and also the blast orientation are of greatest importance. To discuss the problem qualitatively, consider the case of a blast wave with normal incidence to the plane of the chamber entrance. It is assumed that the surface containing the entrance opening is infinite in extent. The properties behind the incident shock wave can be obtained from Rankine Hugoniot equations. These for the case of air with an assumed perfect gas equation of state are conveniently expressed as:

$$\frac{\rho_s}{\rho_o} = \frac{1 + \mu\xi}{\mu + \xi} \quad (3.1)$$

$$\frac{c_s}{c_o} = \sqrt{\frac{\xi(\mu + \xi)}{1 + \mu\xi}} \quad (3.2)$$

$$\frac{u_s}{c_o} = \frac{(\mu - 1)(\xi - 1)}{\sqrt{(\mu + 1)(1 + \mu\xi)}} \quad (3.3)$$

$$\frac{U}{c} = \sqrt{\frac{1 + \mu\xi}{1 + \mu}} \quad (3.4)$$

Here subscripts o and s designate ambient and shock conditions respectively. The variables are:

- ρ = density
- c = sound velocity,
- u = particle velocity,
- U = shock velocity, and
- $\xi = P_s/P_o$ is the ratio of shock pressure to ambient pressure.

The parameter μ is defined by

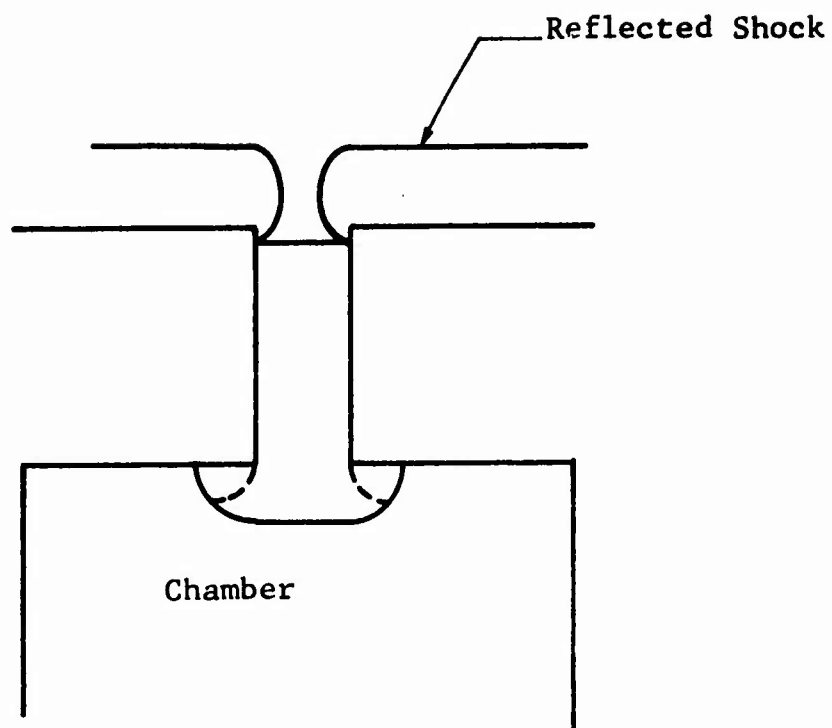
$$\mu = \frac{\gamma + 1}{\gamma - 1} \quad (3.5)$$

where γ is ratio of specific heats of a perfect gas. Thus for any given shock pressure Eq. (3.5) permits the computation of all the variables in the incident shock front. Upon incidence on the wall, the shock wave undergoes a normal reflection and the reflected shock propagates away from the wall. The pressure ratio of the reflected shock is given by

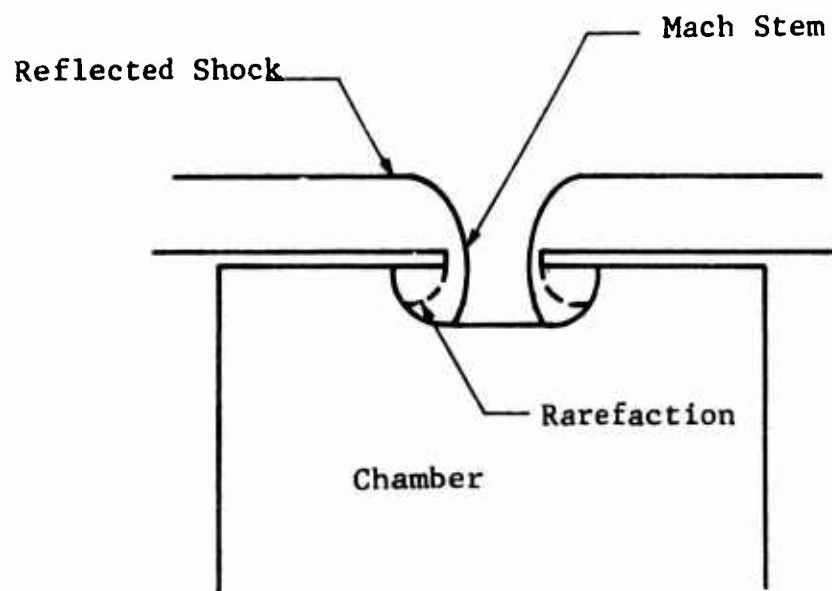
$$\xi_r = \frac{p_r}{p_s} = \frac{(\mu + 2)\xi - 1}{\mu + \xi} \quad (3.6)$$

Here p_r is the reflected pressure, p_s the pressure behind the incident shock and $\xi = p_s/p_o$. Coincident with the shock reflection on the exterior the incident shock is transmitted toward the interior of the chamber. The wave phenomena at the opening during the shock entrance depend on the entrance geometry. Typical behaviors are illustrated in Fig. 3.1.

If the room is connected to the atmosphere by a relatively long tunnel then the wave configuration is as shown in Fig. 3.1a. The shock transmission causes the formation of a Mach stem configuration in order to match the conditions in the reflected region to those behind the transmitted shock. For openings with little depth, again a Mach stem reflection takes place (Fig. 3.1b). However, in addition to this a centered rarefaction wave is formed at the interior corners as the transmitted shock attaches itself



(a)



(b)

Fig. 3.1 BLAST WAVE BEHAVIOR AT AN OPENING

to the interior walls and causes the flow to bend around the 90 deg corner. A similar phenomenon occurs when the shock reaches the end of the tunnel and enters the chamber as shown in Fig. 3.1a. The Mach and rarefaction waves move across the entrance and interact. Once this interaction occurs one has essentially an adiabatic inflow from the high-pressure reflected region to the region behind the transmitted shock wave. The interactions at the entranceway of the chamber are quite complex, and again geometry dependent. Thus the rarefaction waves may actually interact with the Mach waves before these meet at the central plane of the entrance. After the shock enters the chamber (and assuming normal incidence) it has a tendency to spread in a circular fashion. The shock is thus sustained by the inflow from the high-pressure outside region. It finally interacts with the side walls of the chamber in regular reflection, as shown in Fig. 3.2. This shock wave is of very short duration and for most practical Civil Defense purposes is not considered to be an important phenomenon.

The flow expansion around the corners of the entrance produces vortices which in turn cause a low pressure region in this area. Upon normal reflection from the back wall the shock propagates back toward the entrance of the room. However this shock interacts with the incoming high speed flow coming from the entrance. Since this inflow takes on the form of a strong jet, the reflected shock wave is destroyed by this interaction (see Ref. 25). From this point on, the phenomena in the chamber are governed by the jet inflow, wave interactions becoming insignificant. The flow behavior is essentially that of a chamber being filled from a high pressure reservoir. In the case of the blast wave flow, the reservoir pressure continuously decreases while the pressure in the chamber increases. The filling process continues until the inside and outside pressures equalize. At this time flow reversal occurs and outflow from the chamber commences.

The chamber filling phenomena are primarily governed by the pressure difference between the chamber and the outside blast field. The filling is a relatively slow process and may in a first approximation be described by a quasi-steady behavior.

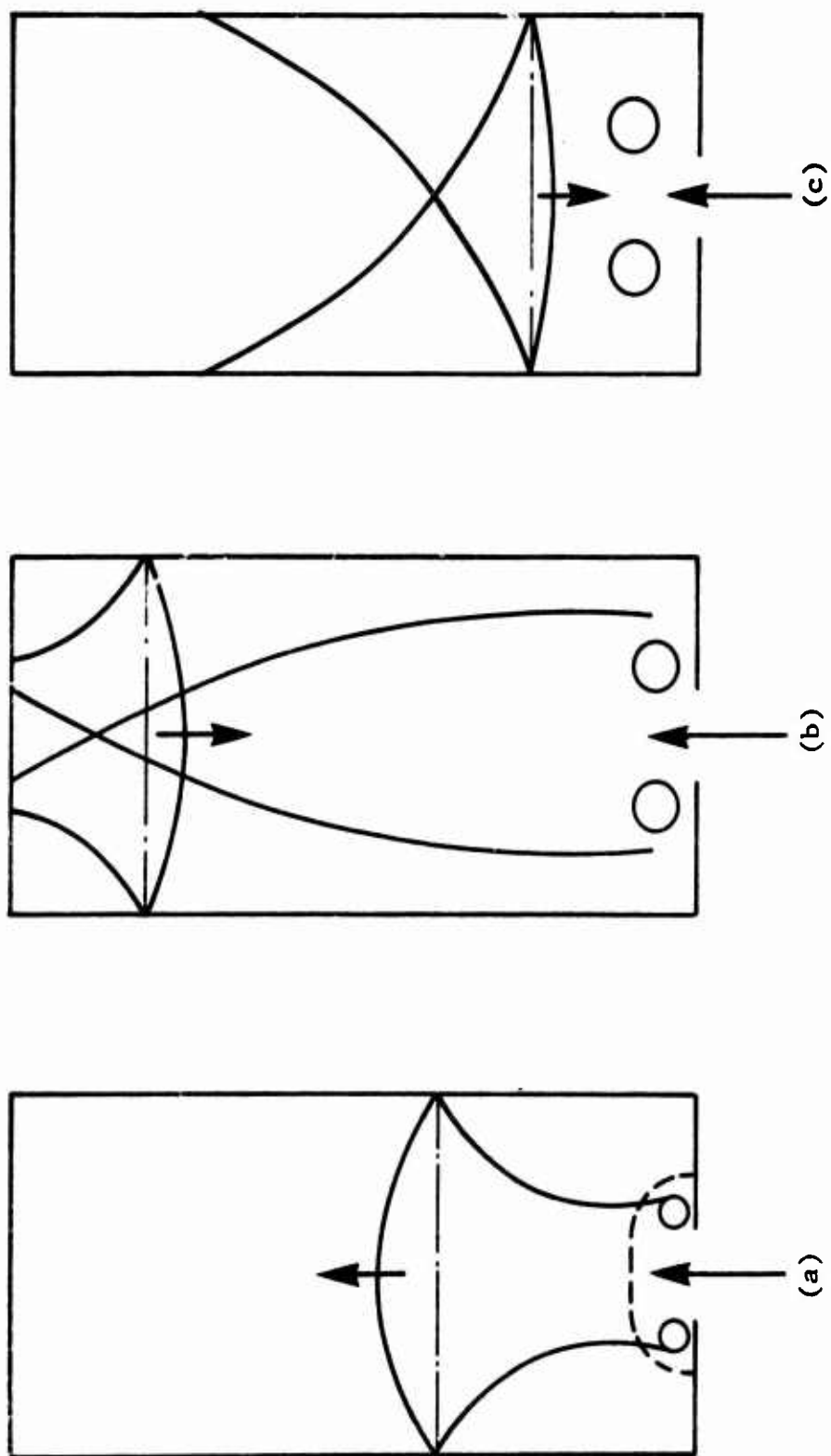


Fig. 3.2 SHOCK CONFIGURATIONS IN A SHELTER

For pressure ratios smaller than the critical value ($p_{\text{chamber}}/p_{\text{blast}} \cong 0.528$ for air) the mass flow rate is independent of the chamber pressure and the flow is choked at the entrance aperture. This implies a flow velocity equal to the sonic velocity at this cross section.

Since in general the entrance configuration is not of a smooth converging-diverging shape no acceleration to supersonic speeds of the jet should be expected. Even if a local contraction should cause the flow to accelerate to supersonic speed in the immediate vicinity of the entrance, these velocities would quickly be reduced (within one or two entrance diameters) to subsonic speeds by the appearance of shock waves which will adjust the pressure in the jet to the surrounding chamber pressure. Thus maximum velocities in the jet flow entering the chamber are subsonic for all pressure ratios across the entrance opening.

At pressure ratios larger than the critical value the mass flow rate depends both on the outside and the chamber pressure. Thus the mass flow rate reduces not only because of pressure decay in the blast wave field but also because of the pressure increase in the chamber.

During the filling process the flow entering the chamber behaves somewhat as a free jet expansion. However since both upstream and downstream conditions are changing continuously, the velocities in the jet and its geometry (spreading) are also adjusting continuously. Again these phenomena in a first approximation may be considered as quasi-static. Obviously the flow picture inside a cavity is further complicated by the jet impinging on the back wall. This causes the flow to turn 90 deg and to spread along the back wall. Encountering the side walls of the chamber the flow undergoes an additional 90 deg turn. Thus a general circulation is set up throughout the room. The actual pattern of the circulation depends on the room geometry. Highest velocities should be expected in the center of the inflowing jet. In fact these velocities may be considerably higher than the

particle velocities behind the shock which initially spreads throughout the chamber. Thus when considering vulnerability of equipment or shelterees, it should be remembered that the severest drag loading conditions may occur during the filling process rather than during passage of the shock wave.

An accurate analytical description of the shock and cavity filling phenomena discussed is not feasible since the flow processes are three-dimensional and nonsteady. Reasonable approximations of the shock and flow behavior in shelters should result for two-dimensional numerical calculations. First order estimates of the loads expected on shelters can be made by simple one-dimensional quasi-steady analysis. Since the load prediction is but a minor task of the current project, the latter approach was used.

3.2 INTERNAL PRESSURES AND TEMPERATURES

Pressures and temperatures that may be expected to occur within personnel shelters as a result of nuclear weapon-produced blast when shelter doors are left off, open, or when their capacity is exceeded are considered. These transient phenomena are examined to determine the extent of their influence on the survivability of shelter occupants.

Internal pressure and temperature-time histories were calculated using an existing electronic computer program (Ref.25) which permits the computation of average values of these phenomena in chambers as a function of time. Calculations were performed for all gross shelter geometries described in Appendix A for a free-field blast overpressure range from 5 to 50 psi resulting from KT and MT size weapons. Typical pressure and temperature-time variations are shown in Figs. 3.3 and 3.4 respectively. Since we are dealing with average values of these two phenomena over the entire interior of a given shelter, the influence of partitions as well as other obstructions does not enter into the calculations.

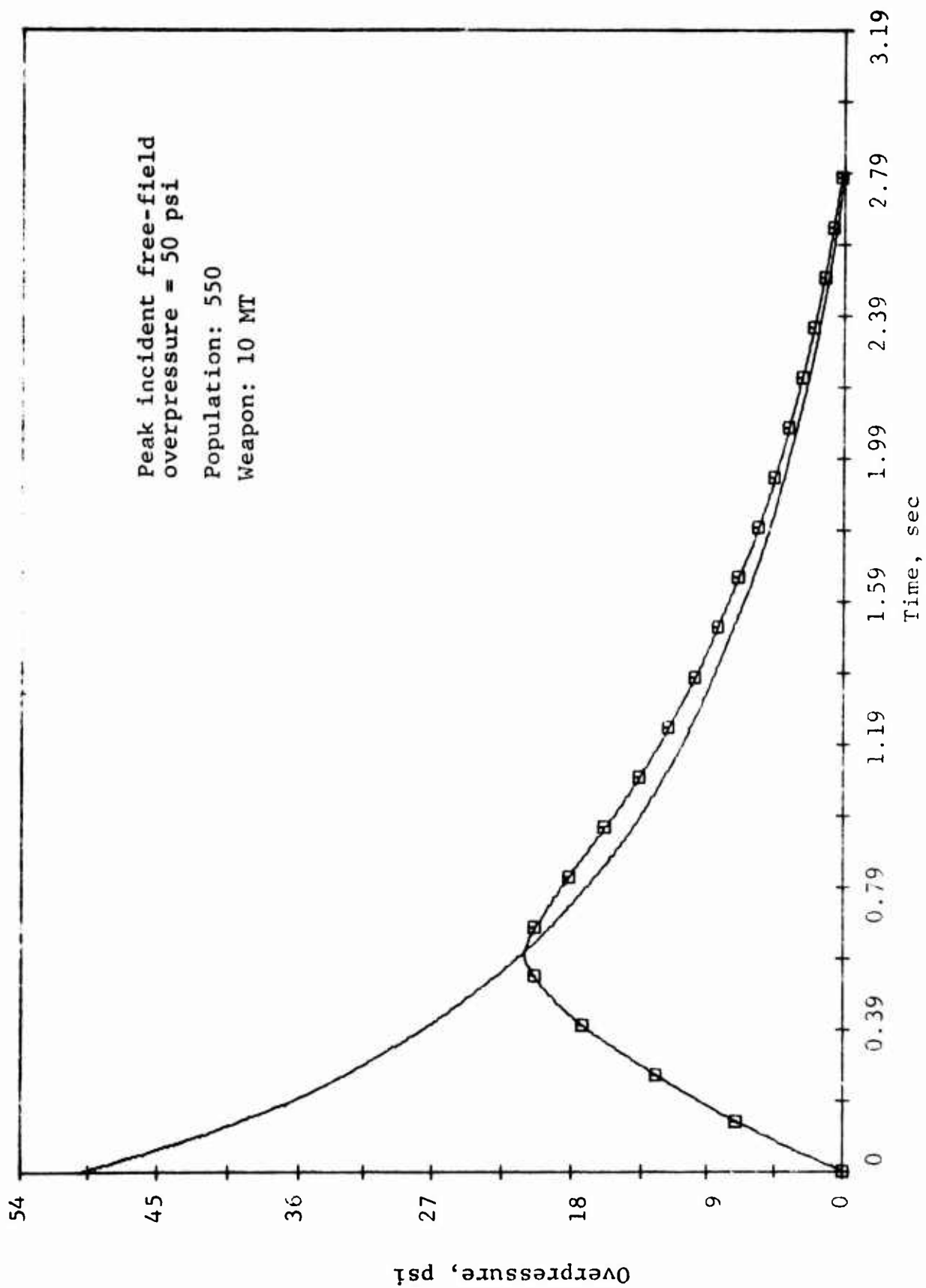


Fig. 3.3 AVERAGE PRESSURE-TIME VARIATION FOR BASEMENT SCHOOL SHELTER

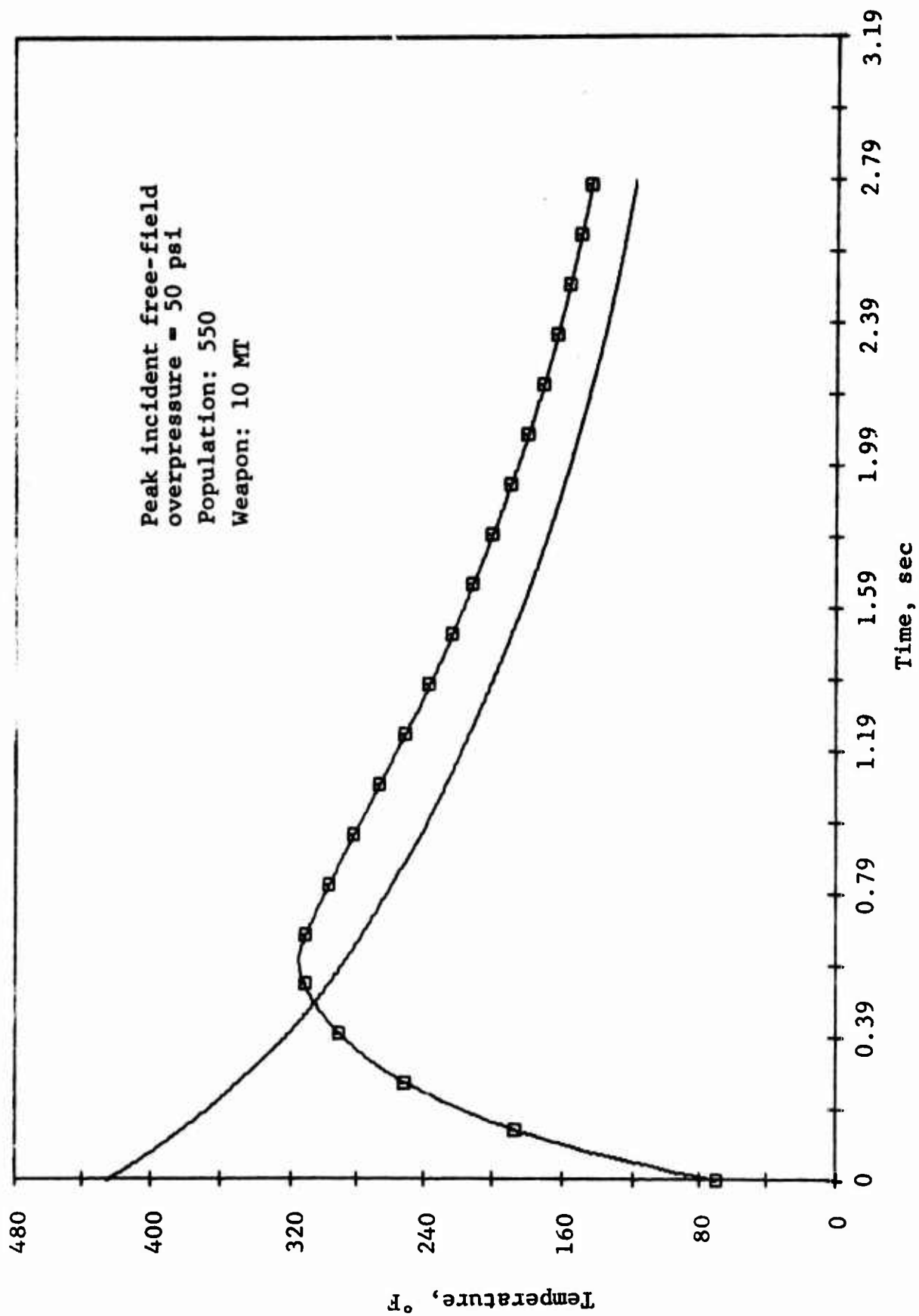


Fig. 3.4 AVERAGE TEMPERATURE-TIME VARIATION FOR BASEMENT SCHOOL SHELTER

The primary parameters are the shelter volume and the area of the inlet. The inlet, consisting of the entranceway and air intake shaft openings, was assumed to be a constant area duct.

For the purpose of evaluating the responses of both the structure and the inhabitants to the pressure and temperature buildup within, we require the following set of information:

- Peak average pressure
- Time to peak average pressure
- Initial pressure rise rate
- Peak average temperature
- Time to peak average temperature
- Temperature at the end of the positive phase.

This information, encompassing the specific range of free-field blast overpressure levels and shelter volume to inlet area ratios, is quantified in Table 3.1 in terms of the nondimensional parameter ϕ . This parameter is defined as

$$\phi = \frac{V}{A c_o t_+} \quad (3.7)$$

where

V is the gross shelter volume excluding partitions, stairwells, etc.,

A is the total unprotected inlet area which may include entranceways, fresh air intake and exhaust shaft openings, etc.,

c_o is the ambient sound velocity (1129 fps) which makes ϕ nondimensional,

t_+ is the duration of the positive phase.

Data presented are restricted to the range of shelter volume to inlet area (V/A) ratios indicated in Table 3.2 and to the peak incident overpressure levels indicated in Table 3.1. The data are independent of weapon size. An additional restriction is that temperature values given are based on an initial shelter temperature of 70°F.

TABLE 3.1
AVERAGE INTERNAL PRESSURE AND TEMPERATURE DATA

Shelter (Cavity) Response	φ = V/A c _o t ₊														
	Peak Incident Overpressure, 5 psi					Peak Incident Overpressure, 10 psi					Peak Incident Overpressure, 20 psi				
	0.10	0.25	0.70	2.00	5.00	0.10	0.25	0.70	2.00	5.00	0.10	0.25	0.70	2.00	5.00
Peak Average Pressure (psi)	4.28	3.63	2.62	1.55	0.83	8.01	6.46	4.34	2.38	1.21	14.76	11.25	7.02	3.59	1.74
Time to Peak Pressure and Temperature (sec)	0.210	0.437	0.883	1.530	2.114	0.211	0.429	0.837	1.393	1.864	0.195	0.387	0.739	1.196	1.562
Initial Pressure Rise Rate (psi/sec)	33.87	13.55	4.84	1.69	0.68	58.38	23.35	8.34	2.92	1.17	107.90	43.15	15.41	5.39	2.16
Peak Average Temperature (°F)	114.11	107.98	98.08	87.02	79.28	152.23	138.51	118.21	97.65	84.44	220.00	191.70	152.44	115.31	92.92
Temperature at t ₊ (°F) (end of positive phase)	73.71	73.39	73.25	76.99	77.02	80.69	79.58	79.17	85.20	81.95	97.59	94.53	94.09	100.16	90.13
Shelter (Cavity) Response	φ = V/A c _o t ₊														
	Peak Incident Overpressure, 30 psi					Peak Incident Overpressure, 40 psi					Peak Incident Overpressure, 50 psi				
	0.10	0.25	0.70	2.00	5.00	0.10	0.25	0.70	2.00	5.00	0.10	0.25	0.70	2.00	5.00
Peak Average Pressure (psi)	21.00	15.48	9.28	4.56	2.16	26.96	19.43	11.34	5.44	2.54	32.75	23.21	13.29	6.28	2.90
Time to Peak Pressure and Temperature (sec)	0.174	0.344	0.653	1.047	1.357	0.151	0.298	0.564	0.903	1.168	0.127	0.250	0.474	0.758	0.981
Initial Pressure Rise Rate (psi/sec)	169.04	67.61	24.15	8.45	3.38	250.27	100.11	35.76	12.51	5.01	364.39	145.75	52.06	18.22	7.29
Peak Average Temperature (°F)	282.20	240.40	183.85	131.60	100.78	341.60	287.22	214.41	147.67	130.92	399.61	333.18	244.74	163.83	116.57
Temperature at t ₊ (°F) (end of positive phase)	116.10	111.04	110.86	114.37	97.73	135.42	128.42	128.52	128.48	105.27	155.19	146.33	146.65	142.67	112.92

TABLE 3.2
INLET AREAS AND VOLUMES OF SUBJECT SHELTERS

Shelter Type	Description	Inlet Area (A) (sq ft)	Shelter Volume (V) (sq ft)	$\frac{V}{A c_o}$ (sec) *
Dual-purpose	School Shelter (population - 550)	48.0	46,690.0	0.862
	School Shelter (population - 1100)	74.7	88,885.0	1.054
	Parking Garage Shelter (population - 5000)	382.2	443,329.0	1.196
Single-purpose	Arch Shelter (population - 500)	11.0	38,946.0	3.136
	Rectangular Shelter (population - 500)	11.0	40,960.0	3.298
	Rectangular Shelter (population - 1000)	22.0	81,920.0	3.298

* c_o (ambient sound velocity) was taken as 1129 fps.

Variations of peak internal pressure and temperature with ϕ are shown in Fig. 3.5 and 3.6 respectively. These are plots of data given in Table 3.1. Peak average pressures and temperatures decrease with increasing values of the parameter ϕ . For a given peak incident pressure level and weapon size (identified by t_+), ϕ increases with increasing values of V/A . Therefore for a given inlet area, the larger the shelter volume, the smaller the peak average internal pressure, temperature, initial pressure rise rate and the larger the time to peak average pressure and temperature.

Shelters considered (see Appendix A) are identified in Table 3.2 in terms of their respective volumes and inlet areas. Gross volumes were used in every case. Inlet areas include entranceways as well as other inlets such as air intake and exhaust shaft openings. For example, in the case of basement school shelters (Table 3.2) the inlet area (Fig. A.11) consists of the following:

- Two personnel blast door openings, 3 ft by 6 ft 8 in. each
- Fresh air intake and exhaust opening, 2 ft by 4 ft

Therefore in every case considered we assume that all shelter openings are unprotected.

Peak average pressures and temperatures within each of the shelters described, were determined using data given in Fig. 3.5 and 3.6. Results are listed in Table 3.3 and represent four weapon sizes (10, 1.0, 0.5 and 0.2 MT) and six incident peak overpressure levels (50, 40, 30, 20, 10 and 5 psi). In order to emphasize variations, a portion of the results given in Table 3.3 are also presented graphically in Fig. 3.7 and 3.8. As expected the largest peak overpressures and temperatures occur in the shelter having the least V/A ratio, namely the school basement shelter with a capacity for 550 persons (Table 3.2).

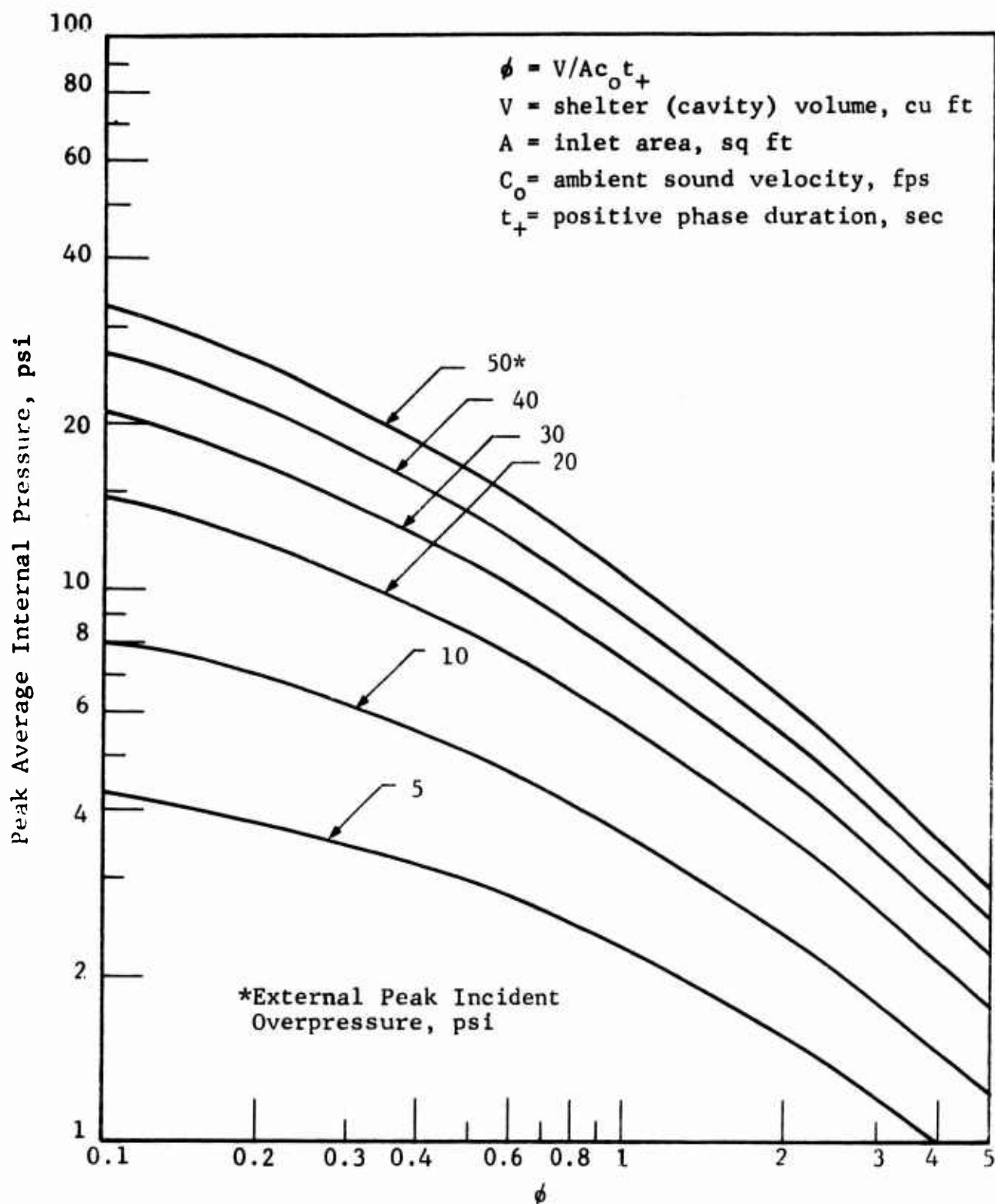


Fig. 3.5 VARIATION OF PEAK AVERAGE INTERNAL SHELTER PRESSURE WITH ϕ

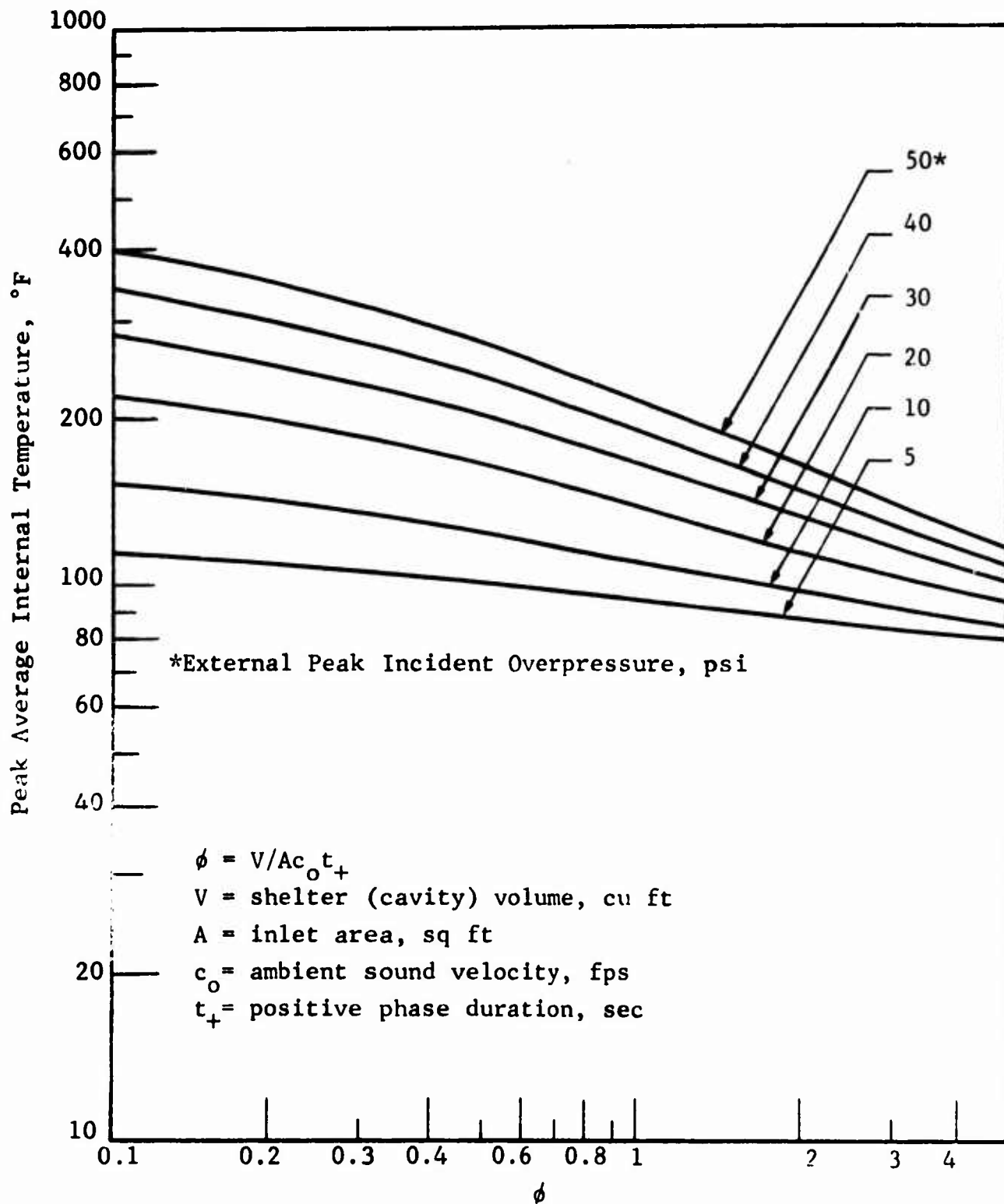


Fig. 3.6 VARIATION OF PEAK AVERAGE INTERNAL SHELTER TEMPERATURE WITH ϕ

TABLE 3.3
PEAK AVERAGE TEMPERATURES AND PRESSURES IN SUBJECT SHELTERS

Yield Overpressure (psi)	Below Grade School Shelter (Population 550) (MT)				Below Grade School Shelter (Population 1100) (MT)				Parking Garage (Population 5000) (MT)				Arch Shelter (Population 500) (MT)				Rectangular Shelter (Population 500,1000) (MT)			
	10	1	0.5	0.2	10	1	0.5	0.2	10	1	0.5	0.2	10	1	0.5	0.2	10	1	0.5	0.2
50	°F	290	224	206	181	272	209	190	170	260	200	180	160	182	138	126	180	136	125	<120
	psi	18.2	11.4	9.7	7.6	16.2	9.9	8.3	6.6	15.0	9.0	7.6	6.1	7.8	4.3	3.4	7.5	4.0	3.3	2.5
40	°F	258	204	188	167	228	188	172	154	230	180	166	148	164	124	118	164	126	116	<110
	psi	16.0	10.2	8.8	7.0	14.4	9.0	7.6	6.1	13.5	8.2	7.0	5.5	7.2	3.9	3.3	6.9	3.8	3.1	2.4
30	°F	224	182	170	154	212	170	158	145	205	165	152	139	152	120	111	150	118	112	100
	psi	13.4	8.8	7.7	6.3	12.1	7.8	6.7	5.5	11.2	7.2	6.2	5.0	4.9	2.8	2.4	6.0	3.4	2.8	2.2
20	°F	188	158	148	138	180	150	140	128	175	145	135	125	138	110	105	136	110	102	98
	psi	10.6	7.6	6.6	5.5	9.9	6.8	5.9	4.9	9.3	6.3	5.5	4.5	5.6	3.3	2.8	5.7	3.2	2.7	2.1
10	°F	142	128	121	115	139	121	118	110	135	120	115	108	105	100	97	117	100	96	90
	psi	6.8	5.3	4.8	4.1	6.4	4.8	4.4	3.7	6.1	4.6	4.1	3.5	4.2	2.7	2.3	4.0	2.6	2.2	1.8
5	°F	110	104	102	99	109	102	100	97	108	100	99	96	99	92	89	98	91	88	85
	psi	4.0	3.6	3.2	2.8	3.8	3.2	2.9	2.6	3.7	3.0	2.8	2.4	2.8	2.0	1.7	2.7	1.9	1.7	1.4

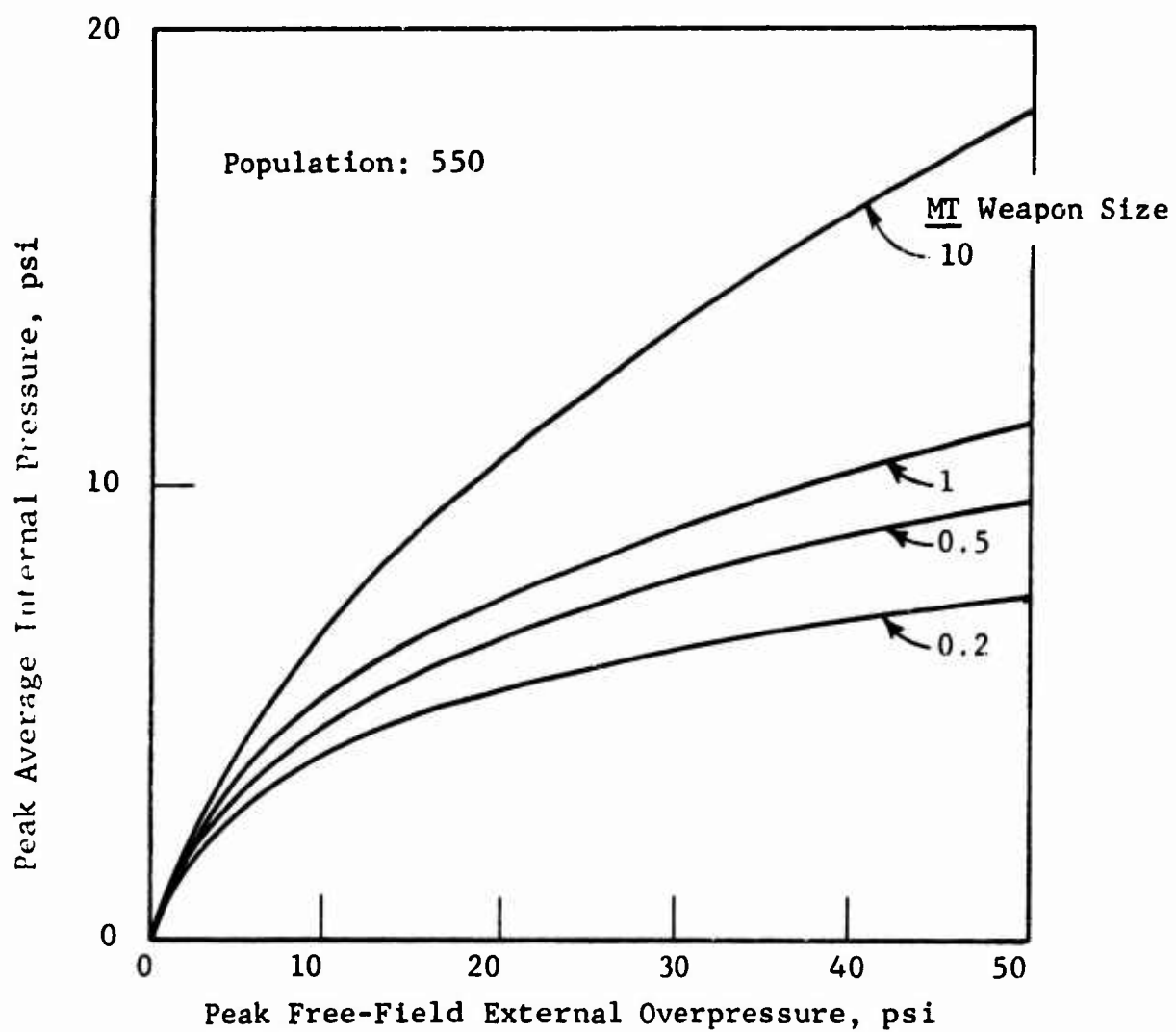


Fig. 3.7 PEAK AVERAGE INTERNAL SHELTER OVERPRESSURE FOR A BASEMENT SCHOOL SHELTER(Ref. 15)

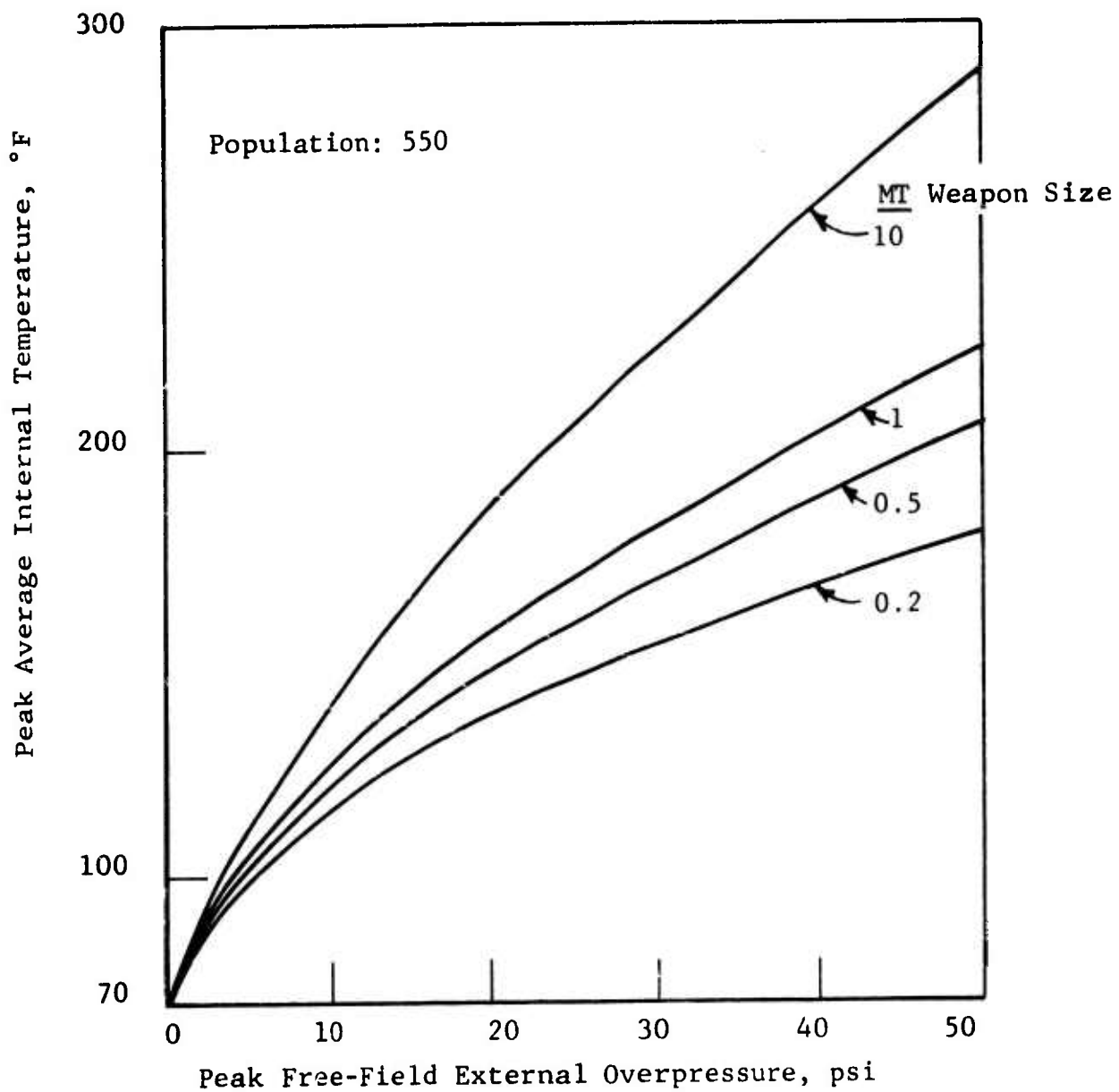


Fig. 3.8 PEAK INTERNAL SHELTER TEMPERATURE FOR A BASEMENT SCHOOL SHELTER (Ref. 15)

Directly applicable biological data dealing with the response of mammals to increased overpressure levels is currently limited primarily to small animal species. According to Ref. 26 such animals can tolerate high overpressures (86 to 170 psi) provided the pressure rises smoothly and the time to peak overpressure is in excess of a few tenths of a millisecond (gradual rise). Extrapolation of such data indicates that for a 70 kg (154.3 lb) mammal the 50 percent mortality point due to gradually rising overpressures is at 75 psi.

Pressure-time histories computed for the subject shelters (see Fig. 3.3 and Table 3.1) fall well within the gradual rise and time to peak overpressure limitations given. The maximum value of peak average overpressure calculated for this set of shelters is 18.2 psi (see Table 3.3) which is well below the 75 psi level for 50 percent mortality. It is concluded that for the specific range of weapon sizes and external peak overpressure levels considered, fatalities resulting from overpressure buildup within this set of shelters are not expected to occur.

Referring now to air temperatures inherent in the blast wave, it will be noted (see Fig. 3.4 and Table 3.1) that even though high values are achieved, the duration is relatively short. Average air temperature within a shelter achieves its peak in a time period of 0.127 to 2.114 sec (depending on overpressure level and weapon size), and drops off to initial shelter temperature (70°F) within a time period of about two positive phase durations. Most of the drop-off is achieved at the end of the positive phase.

For shelters considered herein, the maximum air temperature achieved is 290°F (Table 3.3) and occurs in the smaller of the two school basement shelters (Table 3.2) at the 50 psi overpressure level resulting from a 10 MT weapon. This is the highest peak temperature achieved for the class of shelters considered. It constitutes a 220° increase lasting less than 2.07 sec

Transient air temperatures described should not in themselves constitute a serious hazard to sheltered personnel (Refs. 27

through 32). According to Ref. 28 tolerance to air temperatures between 122 to 140°F runs into hours, since sweating response is usually sufficient to keep storage of heat low, and body temperature limits are not exceeded for a prolonged period of time. The temperature range of 158 to 248°F is physiologically noncompensating, and rapid rates of heat storage in the body give tolerance times in the range of 20 to 80 min. In the temperature range in excess of 248°F, tolerance is predominantly limited by pain. A series of experiments to establish tolerance levels for temperatures in excess of 200°F are described in Ref. 28. The subjects were male adults aged 21 to 48, and in good physical health. Chambers used in producing pain limited heat exposures were sufficiently small so that the heated aluminum walls were close to the subject. The walls were heated by multiple radiant sources capable of producing rapid rates of temperature increase in the neighborhood of 100°F/min. Two forms of applying heat to the subject were used. The one of interest here is referred to as the "abrupt form"; the chamber was preheated and rolled over the subject so as to surround him in a period of about 2 sec. The end point in each experiment was set by the subject when he reached a level of intolerable pain from heat exposure. Results are reproduced in Fig. 3.9.

As far as inhalation of hot air is concerned, it may be stated that air which is hot enough to cause internal injuries as a result of inhalation would probably cause lethal external burns much more rapidly (Ref. 31). Temperatures reached in subject shelters (see Table 3.3) are not sufficiently high or lasting to be significantly hazardous.

3.3 JET VELOCITY AND MOMENTUM

In order to establish an upper bound on the velocities and drag forces that may be expected inside a shelter space the values of these quantities are computed, based on the theory of free jet expansion. The velocity profiles obtained in incompressible flow are nearly identical with compressible flow profiles, see

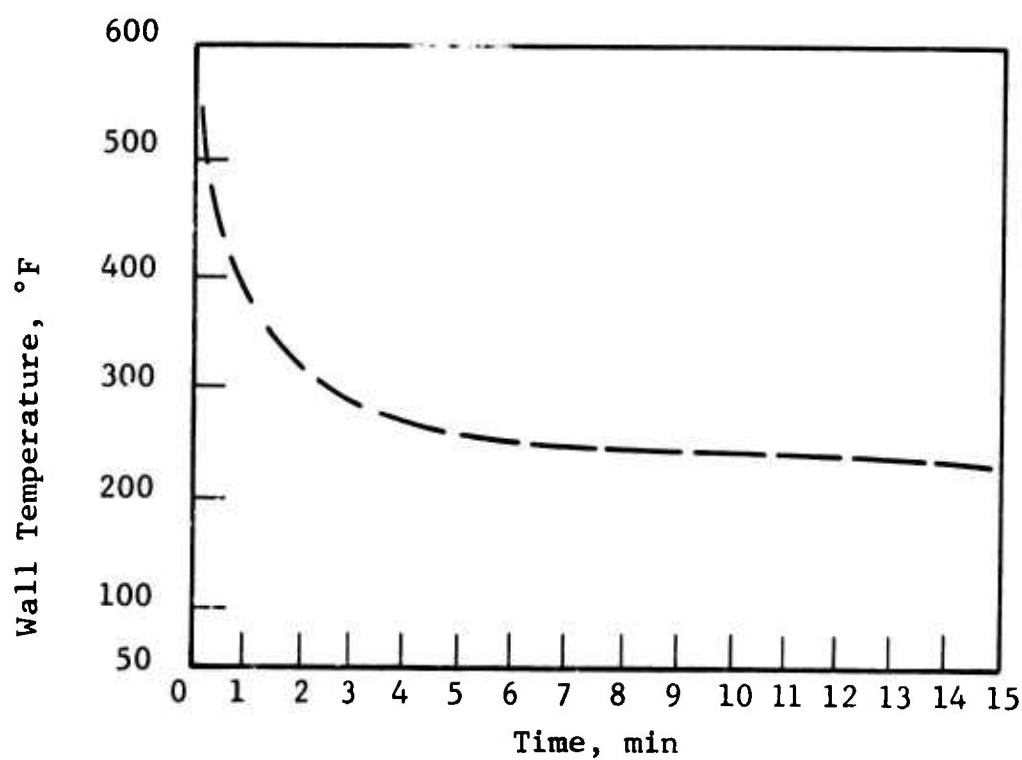


Fig. 3.9 TOLERANCE TIME FOR UNPROTECTED SUBJECTS
ABRUPTLY EXPOSED TO HIGH WALL TEMPERATURES
(Ref. 28)

Refs. 33, 34, and 35, the former will therefore be used since they can be defined by simple mathematical expressions. In general, a free jet issuing from a small opening has a bell-shaped axial velocity distribution as shown schematically in Fig. 3.10.

The velocity is a maximum at the centerline. The maximum velocity which occurs in the opening from which the jet originates, persists for some distance into the free jet in a cone-shaped region. Maximum penetration occurs again at the centerline and is equal to approximately four diameters for an axisymmetric jet and about five orifice widths for the plane two-dimensional jet.

Beyond this initial region of the jet, the flow spreads in a linear fashion. For practical purposes, the behavior of axisymmetric and plane jets is the same and the half-width, or radius b , of the jet is given by Ref. 35

$$b = 0.22 \quad x + b_0. \quad (3.8)$$

Here x is the distance from the opening, and b_0 is the half-width or radius of the opening. The centerline velocity of the plane jet varies inversely with the square root of the distance from the entrance. For the axisymmetric case, it varies inversely with the distance. For turbulent jets the relationships are (Ref. 35)

Plane Jet

$$\frac{U_c}{U_0} \cong 3.8 \sqrt{\frac{n}{\bar{X} - \bar{X}_0}} \quad (3.9)$$

Axisymmetric Jet

$$\frac{U_c}{U_0} \cong \frac{12.4 \sqrt{n}}{\bar{X} - \bar{X}_0} \quad (3.10)$$

Here $\bar{X} = X/b_0$ and b_0 is the opening half-width or radius, X is the axial distance from the entrance, U_0 is the entrance velocity, U_c the centerline velocity at distance X , and n and \bar{X}_0 are

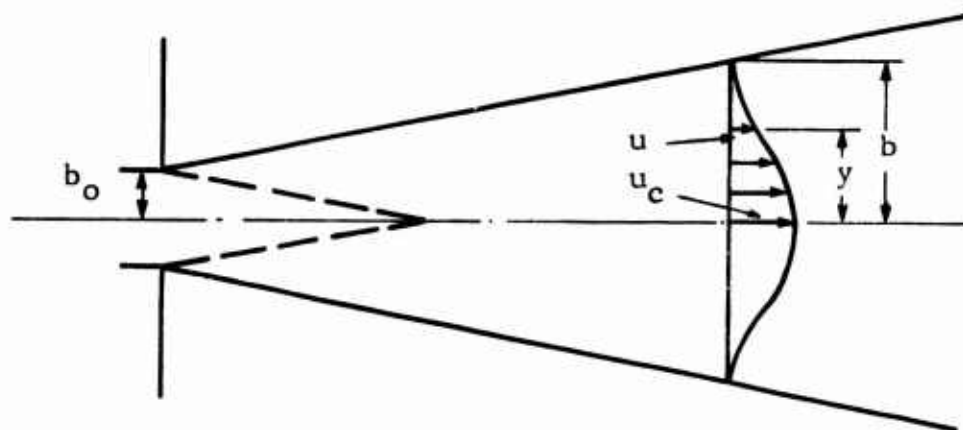


Fig. 3.10 JET VELOCITY DISTRIBUTION

parameters which depend on the flow coefficient, i.e., on how much of the actual area of the opening is occupied by the jet. For flow coefficients of $K = 0.70$ (used in the cavity filling computations) we find from the graphs in Ref. 35 that \bar{X}_0 is -4 for the plane jet and -3 for the axisymmetric jet. Similarly, we find that the values of n are 0.81 and 0.71 for the plane and axisymmetric jets, respectively. Hence, we rewrite the equations for the centerline velocities as

Plane Jet

$$U_c = 3.8 U_o \sqrt{\frac{0.81}{\frac{X}{b_o} + 4}} = \frac{3.42 U_o}{\sqrt{\frac{X}{b_o} + 4}} \quad (3.11)$$

Axisymmetric Jet

$$U_c = \frac{12.4 \sqrt{0.71}}{\frac{X}{b_o} - 3} = \frac{10.45 U_o}{\frac{X}{b_o} + 3} \quad (3.12)$$

It is possible to give the exact bell-shaped velocity distribution in the main part of the jet as a function of distance from the entrance (see Refs. 33 and 35). However, for the purpose of estimating the effect on shelters, it should suffice if an average velocity in the jet is determined. From Ref. 35 an approximate formula for the volumetric rate-of-flow in the jet is

Plane Jet

$$q = \frac{Q}{Q_o} \cong 0.375 \sqrt{\frac{X}{b_o}} \quad (3.13)$$

Axisymmetric Jet

$$q = \frac{Q}{Q_o} \cong 0.155 \frac{X}{b_o} \quad (3.14)$$

Here Q_o is the discharge rate at the entrance. Since the velocity is given by the discharge rate divided by the area, we can easily compute the average velocity,

$$U_{\text{average}} = Q/A.$$

In the case of the plane jet, $A = b$, Q is the discharge rate, and A is the rate per unit height of the opening. Here

$$\frac{U_{\text{average}} b}{U_o b_o} = 0.375 \sqrt{\frac{X}{b_o}} \quad \text{or} \quad U_{\text{average}} \cong \frac{0.375}{b} \sqrt{X b_o} U_o \quad (3.15)$$

For the axisymmetric jet

$$Q = \pi b^2 U_{\text{average}},$$

and

$$Q_o = \pi b_o^2 U_o. \quad (3.16)$$

Hence

$$\frac{b^2 U_{\text{average}}}{b_o^2 U_o} = 0.155 \frac{X}{b_o} \quad \text{or} \quad U_{\text{average}} \cong 0.155 U_o \frac{b_o X}{b^2}. \quad (3.17)$$

Another average velocity can be defined by means of the velocity distribution profile, thus, for the plane jet

$$\bar{U} = U_c \int_0^1 (1 - \xi^{1.5})^2 d\xi = 0.45 U_c \quad (3.18)$$

and for axisymmetric jets:

$$\bar{U} = U_c 2 \int_0^1 (1 - \xi^{1.5}) \xi d\xi = 0.258 U_c \quad (3.19)$$

Here U_c is the centerline velocity, \bar{U} the average velocity, and $\xi = y/b$, i.e., the variable defining the velocity profiles.

It should be noted that all the above formulas are only applicable in the main portion of the jet, that is, not in the immediate vicinity of the entrance. Further, the expressions for average velocity based on volumetric discharge give the same results as those obtained from the velocity profile. To estimate the momentum flux ρU^2 it is sufficient to use the cavity density ρ with the appropriate velocity.

To obtain the variations in velocity and jet width at a particular location as a function of time, it is assumed that the process is quasi-steady. We then simply determine the entrance velocity from the quasi-steady cavity filling calculations. When the pressure ratio exceeds the critical, the flow at the entrance will be sonic and the entrance velocity is then simply

$$U_o = \left[\frac{2\gamma}{\gamma+1} \frac{p_s}{\rho_s} \right]^{1/2} \quad (3.20)$$

where p_s and ρ_s are the blast wave pressure and density, respectively.

For subsonic entrance flow, we get

$$U_o = \left\{ \frac{2\gamma}{\gamma-1} \frac{p_s}{\rho_s} \left[1 - \left(\frac{p_c}{p_s} \right)^{\frac{\gamma-1}{\gamma}} \right] \right\}^{1/2} \quad (3.21)$$

These expressions together with the preceding equations can then be used to estimate velocities and momentum in the shelter during the filling process. Obviously, if precise information on discharge coefficients for the inlet ducting is available, then the entrance velocities can be better estimated by multiplying the given equations by the appropriate coefficients. The expressions as stated provide an upper limit of the entrance velocity.

Using the cavity filling results discussed and the theory given herein, computations were performed to determine the behavior of the jet within a shelter from the time of blast arrival to approximately the time when maximum cavity pressures are reached. Computations were performed for a single shelter type, the buried arch, described in Appendix A. This shelter contains the least quantity of internal obstructions (internal walls, partitions, etc.) of the group of shelters considered, and is thus most adaptable to analysis for blast filling effects using the one-dimensional theory.

The entrance, centerline, and average velocities at a number of locations within the shelter were computed in addition to momentum flux. Such calculations were made using assumptions based on a plane and a circular jet. The latter results in a lower velocity. A flow coefficient of 0.7 was used. This value was determined during cavity filling experiments (Ref. 25). Some representative results are illustrated and discussed.

Figure 3.11 shows the plan area of the subject shelter. Jet boundaries and positions along the centerline at which velocities were calculated are indicated. For the shelter considered, 56.2 percent of the floor area is affected by the jet when a plane jet assumption is used, while 60 percent is affected when a circular jet assumption is considered. This is a substantial portion of the shelter area. Wind (particle) velocity magnitudes within the affected area are indicated in Fig. 3.12 using the plane jet assumption. Duration is between 1.1 and 1.4 sec. Corresponding velocities at the entrance are shown in Fig. 3.13. These are directly at the entrance (minimum duct area) and represent an extreme condition for this shelter.

The data described were used for the purpose of analyzing the translation of shelter occupants when located along the shelter centerline. The formulation of the problem together with results is presented in Chapter Five.

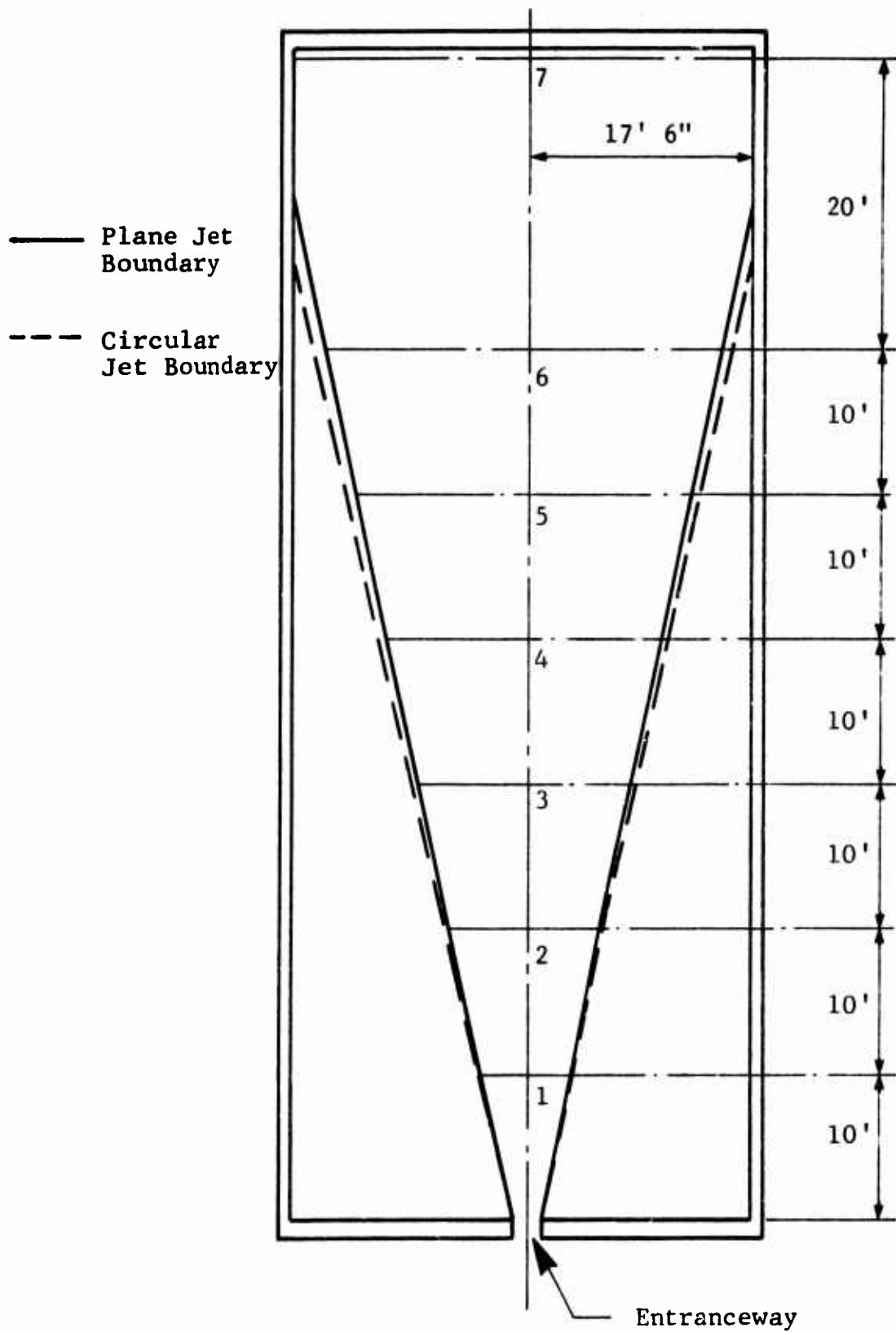


Fig. 3.11 ARCH SHELTER PLAN SHOWING JET BOUNDARIES (Ref. 14)

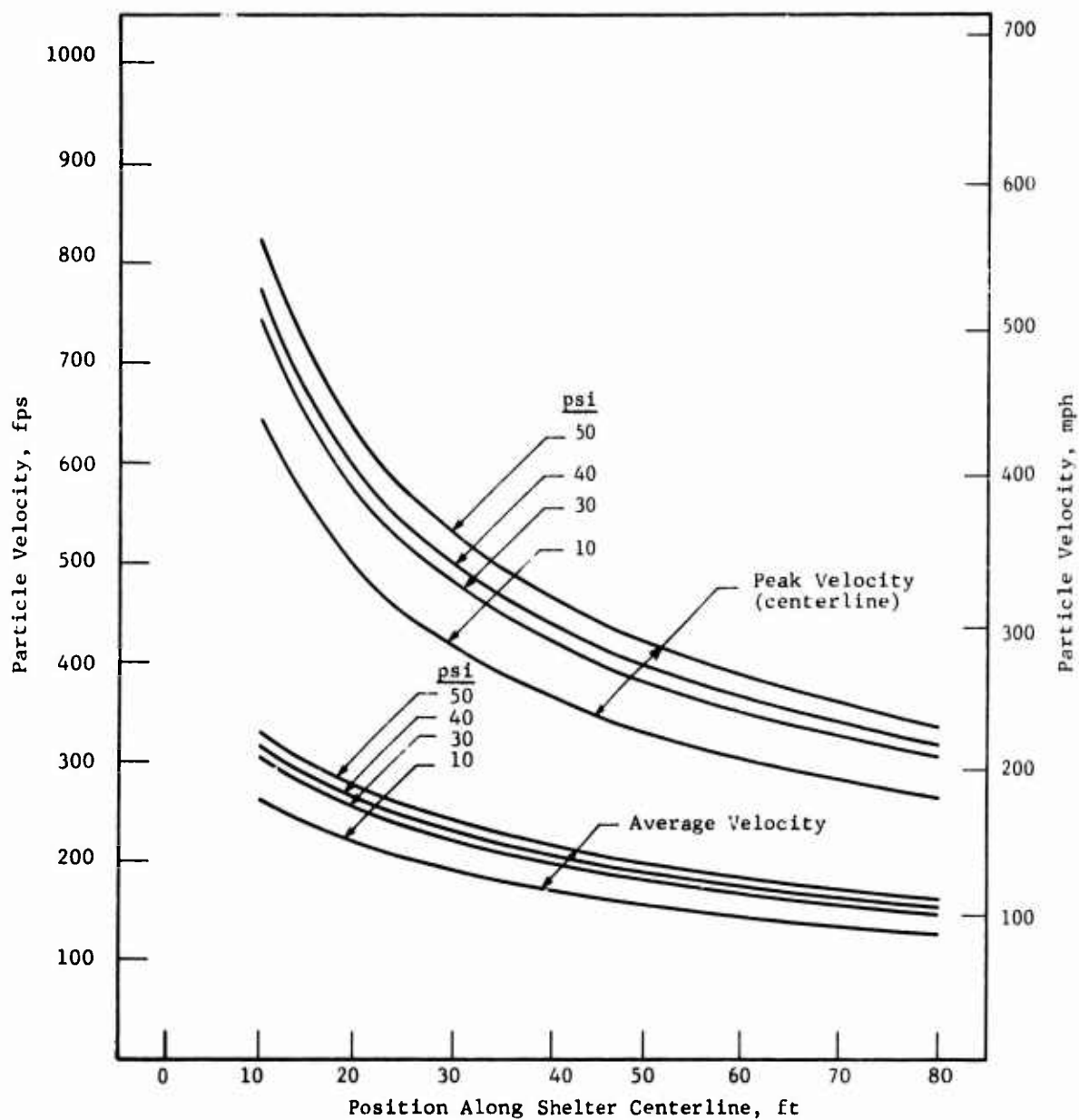


Fig. 3.12 VARIATION OF INTERNAL PARTICLE VELOCITIES

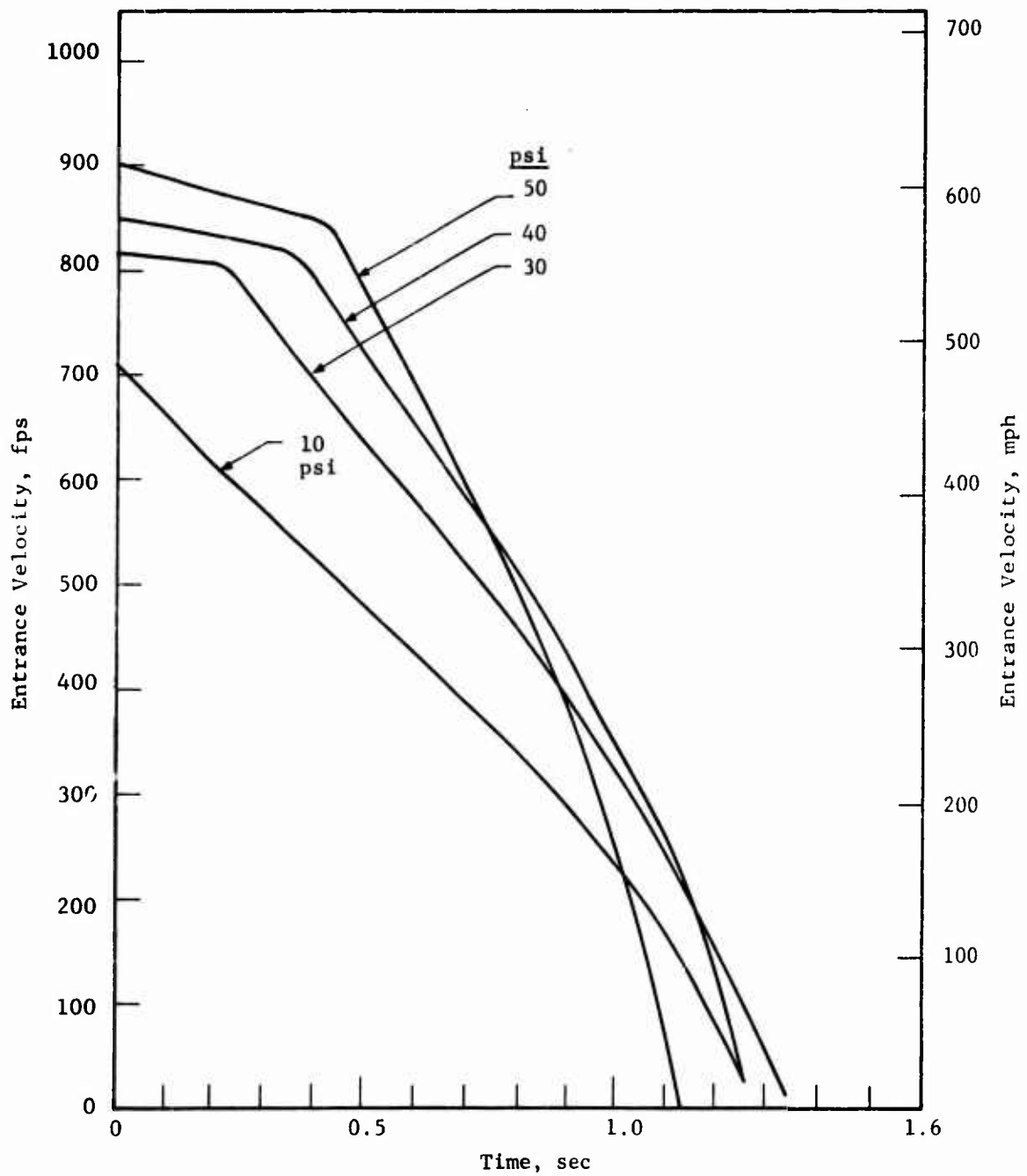


Fig. 3.13 VARIATION OF PARTICLE VELOCITY AT THE ENTRANCE

CHAPTER FOUR

VULNERABILITY OF DUAL-PURPOSE SHELTERS TO FIRES

The evaluation of subject shelters (see Appendix A) regarding their vulnerability to fires initiated by a nuclear detonation is considered. Rather than limit the analysis to the selected shelters, we have developed general relationships which are applicable to a variety of situations. This approach provides better insight into the problem. Methodologies used to evaluate the effects of debris and mass fires on subject shelters are described and the information developed is applied to the consideration of specific examples. Finally, a few dual-purpose shelter sites selected in the city of Detroit by the Bechtel Corporation (Ref.36) are evaluated.

The events of the last war and numerous studies during recent years, have demonstrated that a nuclear detonation can produce a serious fire situation in an urban area. There is concern as to whether or not dual-purpose shelters can adequately protect occupants against fire effects. In particular, this question was brought into focus by the experiences with the Hamburg fire storm (Ref. 37). There is little disagreement about the severity of the resulting destruction and the fact that large percentages of the population originally from the fire storm area were able to survive; there is some uncertainty about whether most people escaped the area before the fire storm developed or were protected by shelters. Even though such uncertainty exists, the Hamburg experience cannot be dismissed out of hand. The Hamburg experience constitutes an extreme case if it is remembered that very few U.S. cities are as densely built up. The phenomenon of free burning fires is highly environment-dependent; thus, a shelter structure may be safe in one situation and vulnerable in another. For this reason, it is impossible to assign a degree of fire safety to a structure without considering its surroundings.

This is especially true with fires produced by a nuclear detonation in which a dual-purpose shelter may be exposed to a variety

of fire effects (mass fires, debris fires, structural fires, etc.). It can be expected that the sites for such shelters will be selected with fire safety in mind, isolated from other structures by at least 40 ft, so that in the absence of mass fires the thermal effects of nearby burning structures on the shelter will be of little significance. On the other hand, it is not always possible to provide situations which protect dual-purpose structures against the effects of debris or mass fires. The studies described herein concern these threats. Consideration is given only to thermal effects since the state-of-the-art is not sufficiently advanced to evaluate the movement of combustion products into the shelter area from externally burning fires. Available information is limited primarily to the effects of fire gases on people which is treated extensively in the existing literature (Ref. 38).

4.1 DEBRIS FIRES

The blast effects from a nuclear detonation produce debris containing both incombustible and combustible material. The latter may have been ignited by the thermal pulse and continue to burn although displaced by the blast from its original location. This then results in what is commonly called a debris fire.

There are many uncertainties connected with evaluating the effects of debris fires on dual-purpose shelters. These pertain to the distribution of the debris, and the amount and nature of combustible material concerned. Past studies of debris distribution dealt predominately with incombustible material. Existing information is either of a very detailed nature or uses a simplified approach of uniformly distributing the estimated amount of structural material over some preassigned area. The latter method is certainly more readily usable, and may be fairly accurate in homogeneously built-up areas. This is probably not the case with the sites of many dual-purpose shelters in nonhomogeneous areas. Nevertheless, the methodology of uniform debris distribution seems the most appropriate at this time and by judiciously selecting areas of possible debris deposition, conservatively probable results can be produced. This approach has been chosen for evaluating

the effects of debris fires on dual-purpose shelters selected by Bechtel Corporation (Ref. 36) and discussed in Subsection 4.5.

The amount of combustibles contained in debris is a function of the combustibles contained in the structures from which the debris has been produced. This encompasses contents as well as structural members. Both can be fairly well evaluated for given structural characteristics and occupancies. Calculations of this sort for a number of structures are presented.

Another uncertainty connected with the consideration of debris fires, is the characteristics of fuel. It can be speculated that the nature of heat release by the debris fires is a function of (1) the amount of contained fuel, (2) the fineness of the fuel, and (3) the amount of incombustible materials. At this time insufficient information is available to account for the effects of these factors on the heat output from the debris fires. At best, one can select some suitable parameter for characterizing the heat release from such fires. In the analysis presented, the total amount of fuel is selected for this purpose.

4.1.1 Debris Fire Experiments

Until recently most of the information pertaining to heat fluxes from debris fires was of a qualitative nature, based on highly idealized assumptions. Some described temperature levels found in smoldering debris, others attempted to show that under conditions of sufficient thermal resistance, the heat output from debris fires is insufficient to affect the shelter environment. Although these data provide insight into the characteristics of debris fires, they do not lend themselves to calculation of heat fluxes.

Information suitable for this purpose was derived from experimental studies conducted by IITRI which were designed to determine the temperature levels of surfaces of concrete slabs exposed to debris fires (Ref. 39). One full-scale and four laboratory experiments were conducted. The laboratory experiments involved 3-1/2 in. thick, 8 x 8 ft concrete slabs, subjected to four

types of debris fires. Combustible and incombustible materials contained in these fires are listed in Table 4.1. The full-scale experiment involved an 8-1/2 in. composite concrete floor exposed to a 6 psf debris fire with very little incombustible material present. It corresponds to the situation of a combustible structure with contents burning in the top of the shelter. The collapse of the building roof onto the debris during the experiment prevented heat release and increased the severity of heat flow into the shelter. Because of these characteristics the full-scale experiment is treated by itself, separately from the laboratory fires.

TABLE 4.1
COMPOSITION OF DEBRIS FIRES IN THE IITRI EXPERIMENTS

Experiments	Combustibles(psf)	Incombustibles(psf)
1	6.5	8.6
2	16.5	93.0
3	18.5	16.0
4	38.6	113.0

4.1.2 Heat Flow Analysis

The heat flow rates into the shelter are calculated utilizing the experimentally determined temperatures of exposed and unexposed surfaces of the concrete slab and floor, described in Subsection 4.1.1, subjected to the debris fires. A computer code was developed which calculates the heat conduction through a slab with radiative and convective heat flow at its surfaces. Were the physical properties of the concrete used in the experiments known, the code could readily predict, from measured temperatures of the exposed surface, the heat fluxes produced by the debris fires. Since the physical properties were unknown, it was necessary to use a trial and error method.

This is accomplished by performing the calculations with assumed properties and comparing the computed temperature of the unexposed surface with the experimentally determined ones.

Calculations are repeated with various property values until satisfactory agreement is obtained. Properties which provide the best agreement are then used to calculate the gradient at the exposed surface corresponding to the net heat flux into the concrete slab.

The information thus determined on time-dependent heat fluxes produced in the debris fire experiments is subsequently extended to cover other fuel load cases and used to calculate the heat flow through concrete slabs of various thicknesses. The calculation assumes that debris fires burn only for 13 hr. After this period the ashes act as an insulator for the exposed surface which cools by heat loss into the shelter environment only.

The results of the analysis are presented in Figs. 4.1 through 4.5. Heat fluxes into the shelter produced by the full-scale debris fire (~ 100 percent fuel) under the collapsed roof are given in Fig. 4.6. The results given in these figures should be considered as tentative until more information pertaining to other factors affecting debris fires is obtained.

4.2 FIRE STORM

In spite of valuable information provided by various studies concerned with the phenomenon of the fire storm, it cannot be described in sufficient detail to enable calculation of the heat flux into a shelter. The available knowledge indicates that maximum air temperatures within the fire storm region may be in excess of 2000°F, accompanied by air velocities over 50 mph. If one considers average conditions, these may correspond to air temperatures on the order of 400°F. The temperature which may prevail in the vicinity of a shelter cannot be predicted from existing information.

Consequently, calculations are performed for both the peak (2000°F) and the average (400°F) expected temperatures. The fluxes into the shelter are computed for radiative and convective heating of the exposed surface, using an emittance of 0.9 Btu/hr sq ft, since past experience has shown that the air within the fire storm region contains considerable quantities of solids. A 50 mph air velocity is used to evaluate the heat transfer coefficient.

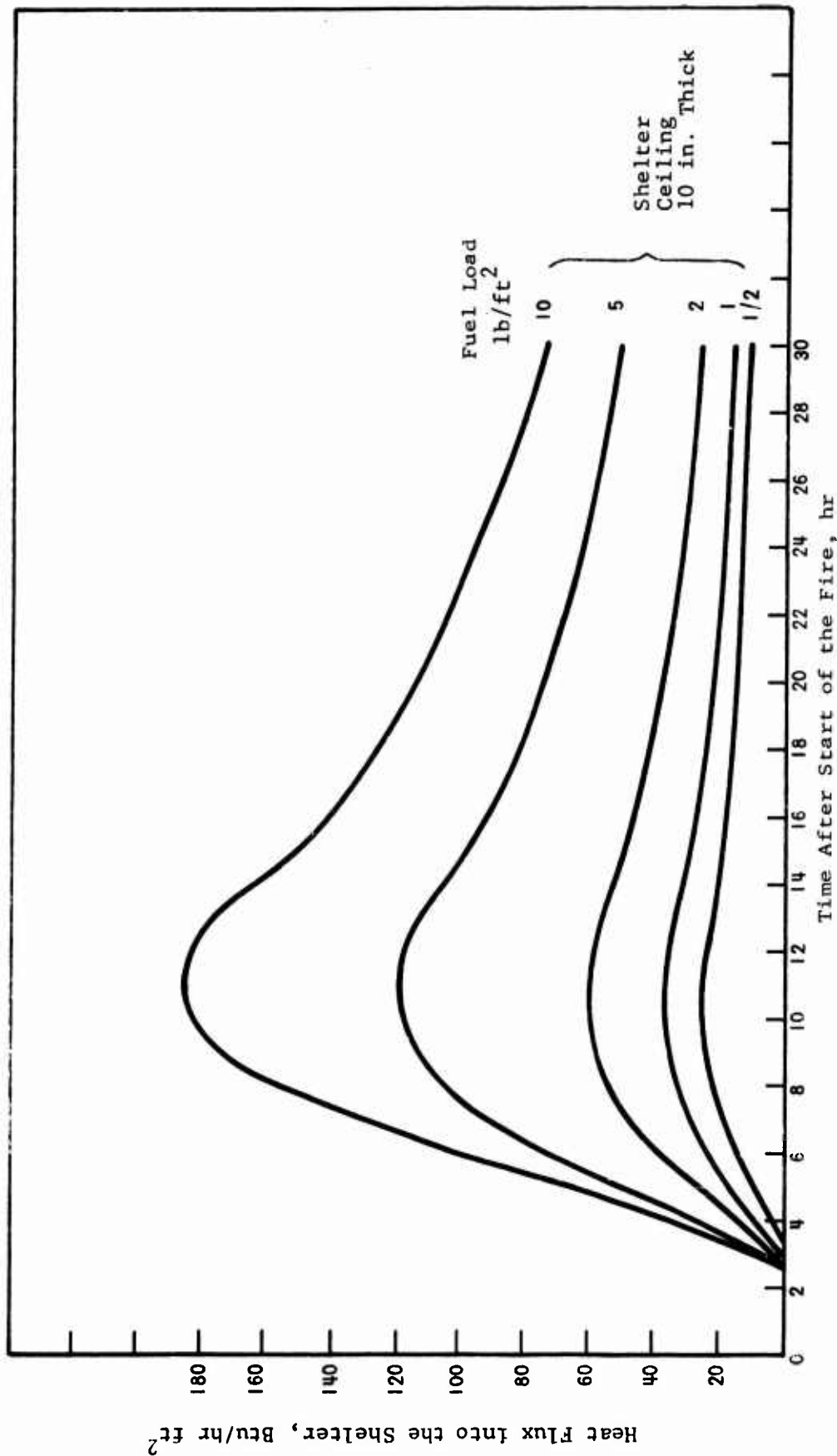


Fig. 4.1.1 HEAT FLOW FROM DEBRIS FIRE INTO THE SHELTER PER SQUARE FOOT OF EXPOSED CEILING AS A FUNCTION OF FUEL LOAD

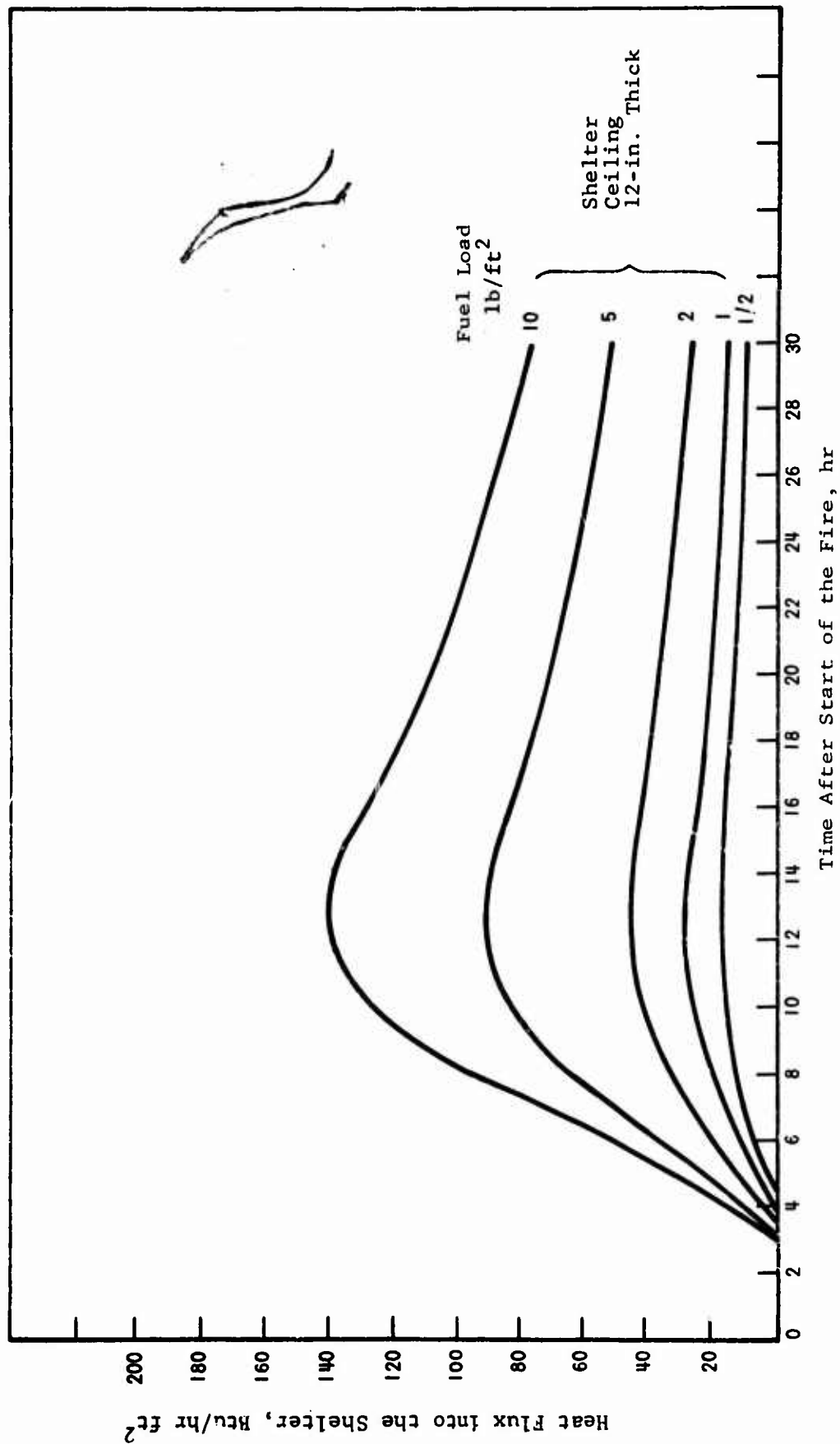


Fig. 4.2 HEAT FLOW FROM DEBRIS FIRE INTO THE SHELTER PER SQUARE FOOT OF EXPOSED CEILING AS A FUNCTION OF FUEL LOAD

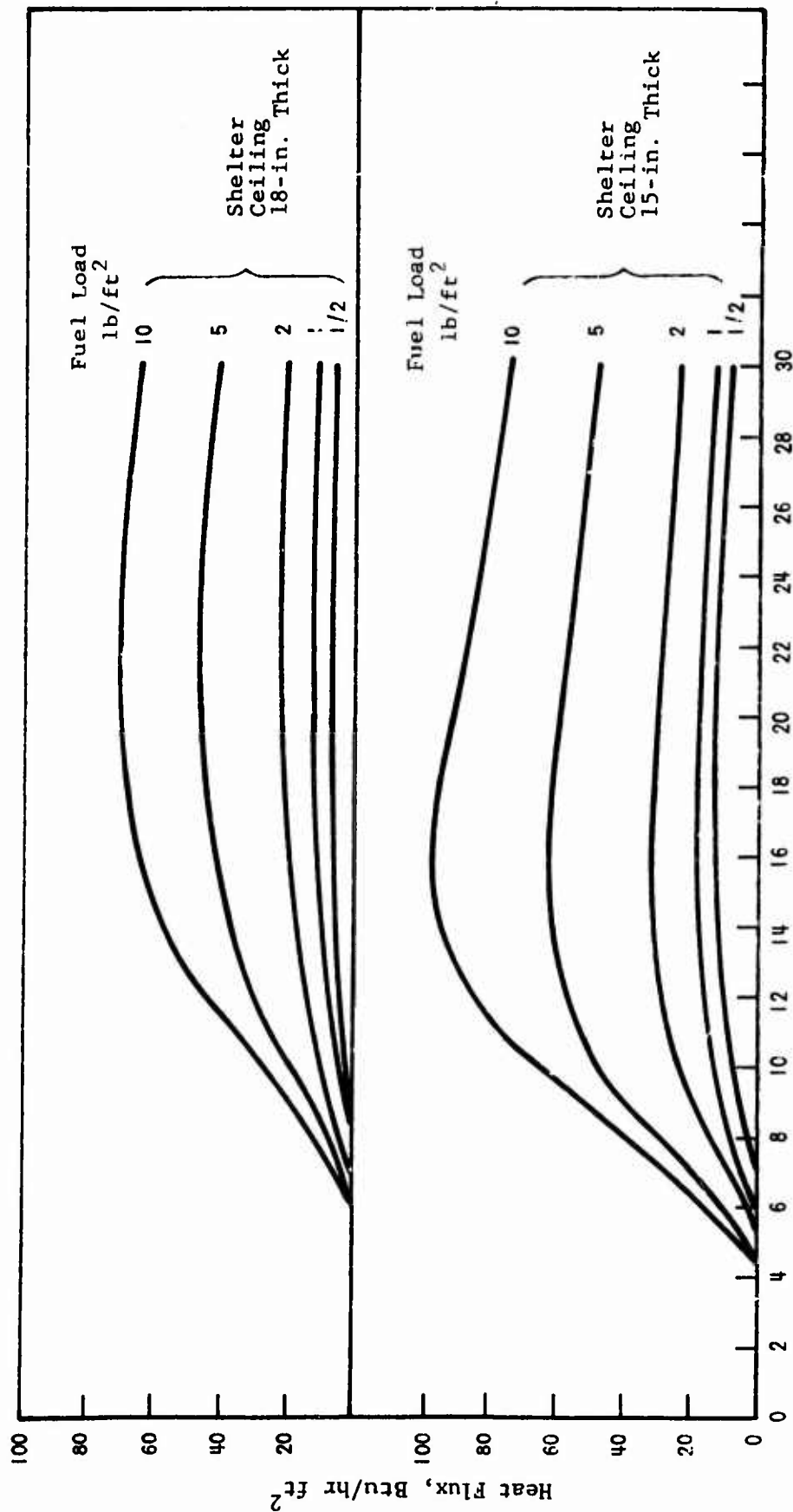


Fig. 4.3 HEAT FLOW FROM A DEBRIS FIRE INTO THE SHELTER PER SQUARE FOOT OF EXPOSED CEILING AS A FUNCTION OF FUEL LOAD

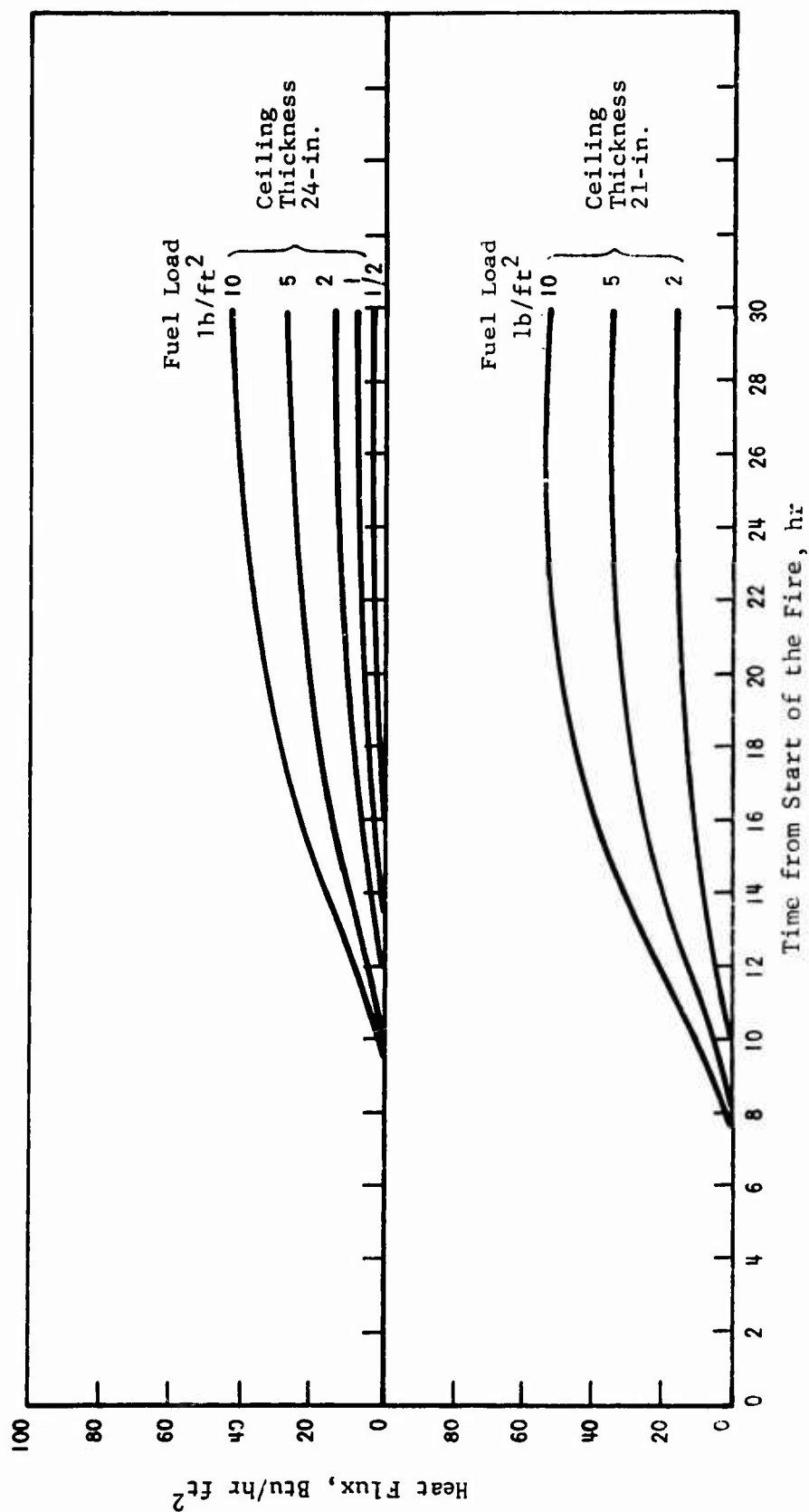


Fig. 4.4 HEAT FLOW FROM A DEBRIS FIRE INTO THE SHELTER PER SQUARE FOOT OF EXPOSED CEILING AS A FUNCTION OF FUEL LOAD

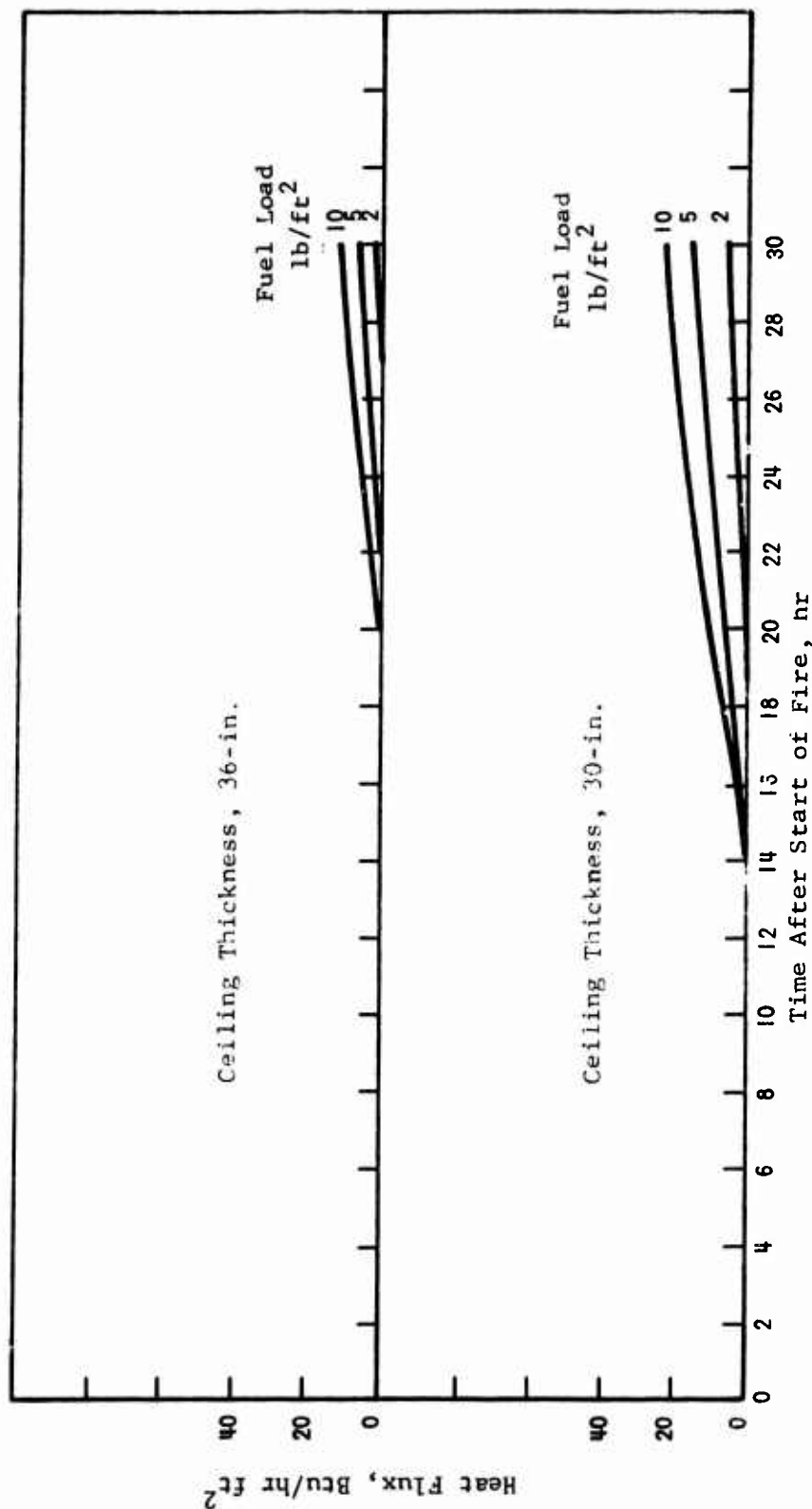


Fig. 4.5 HEAT FLOW FROM DEBRIS FIRES INTO THE SHELTER PER SQUARE FOOT OF EXPOSED CEILING AS A FUNCTION OF FUEL LOAD

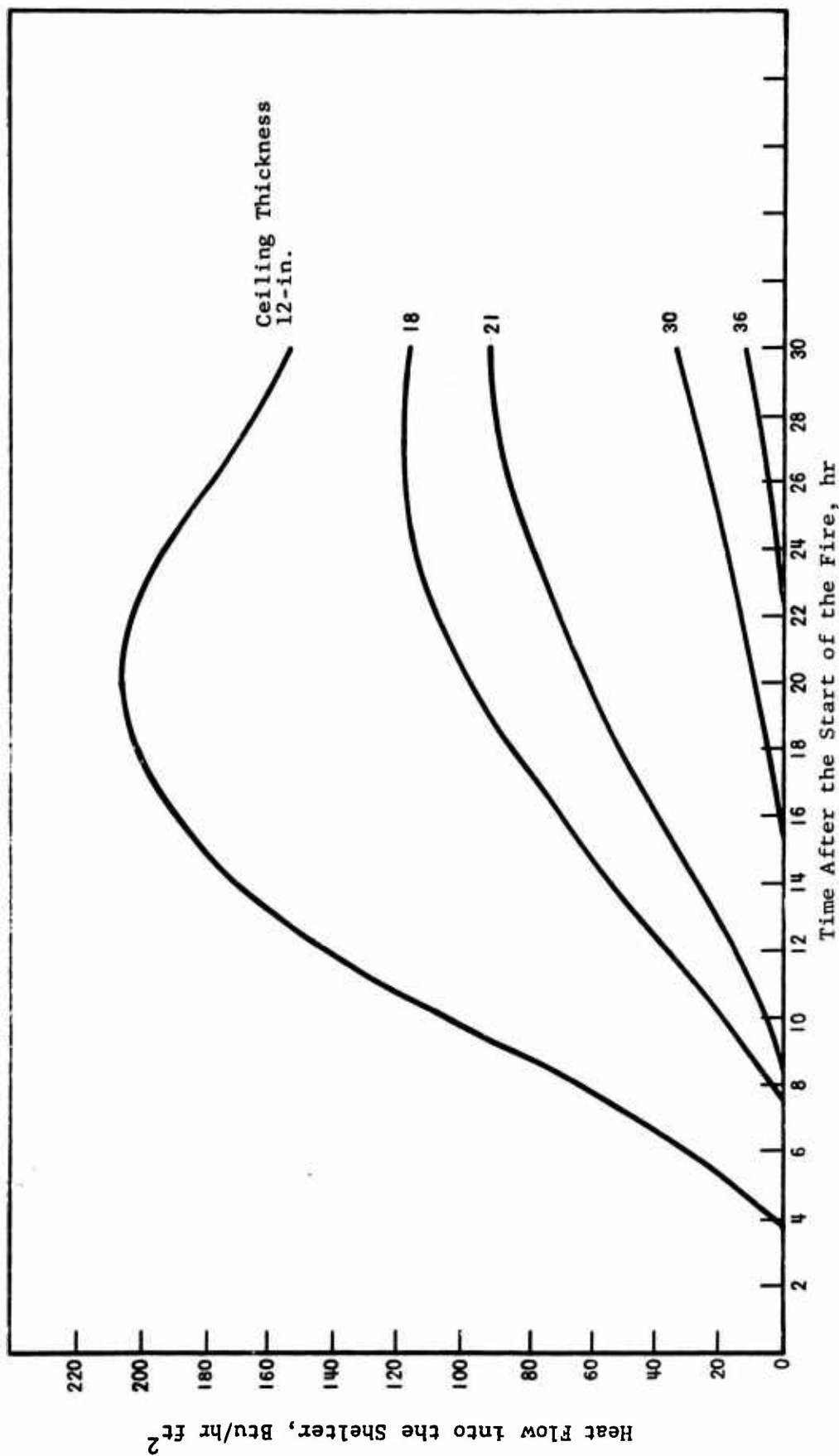


Fig. 4.6 HEAT FLOW FROM A DEBRIS FIRE UNDER COLLAPSED ROOF INTO SHELTER PER SQUARE FOOT OF EXPOSED CEILING

A 2 hr duration of fire storm is assumed, after which time the exposed surface is cooled by a 70°F wind moving at 15 mph. Results of the calculated fluxes for various concrete thicknesses are given in Fig. 4.7.

4.3 FIRE VULNERABILITY OF SELECTED SHELTERS

As mentioned, the shelter site selection contributes to maximum protection from certain types of fires but debris and mass fires remain as threats. The effects of these can readily be determined from the relationships given in Figs. 4.1 to 4.7. The graphs were calculated assuming that sufficient ventilation is provided under all conditions to maintain a constant shelter temperature of 80°F. The heat fluxes into the shelter shown in these figures are due to temperature rise of the under surface of the ceiling causing convective and radiative heat flow. The convective coefficient used is 0.1 Btu/hr sq ft as recommended by the ASHRAE Guide (Ref. 40) for downward-facing heated surfaces.

In order to use the graphs of Figs. 4.1 to 4.7, the thickness of the shelter ceiling and the expected amount of debris fuel must be known. The former is a function of the design overpressure and has been prescribed for the shelters considered. The amount of fuel in the expected debris fires depends on whether it arises from initial content or deposits from other structures. In the first case, the fuel density can be inferred from knowing the occupancy of the structure housing the dual-purpose shelter. The latter requires knowledge of occupancy and structural characteristics of the debris-producing structures affecting the shelter. For the purpose of this study the Blast Resistant School and Community Shelter (Ref. 15) is assumed to contain 1 psf of fuel. A fuel loading of 5 psf is selected for the other shelters which are presumed to be covered by debris from nearby structures. Of course this value may vary depending on the situation encountered, however, 5 psf seems to be on the conservative side.

Based on these assumptions the heat fluxes into the selected shelters are summarized in Table 4.2. The values given are British

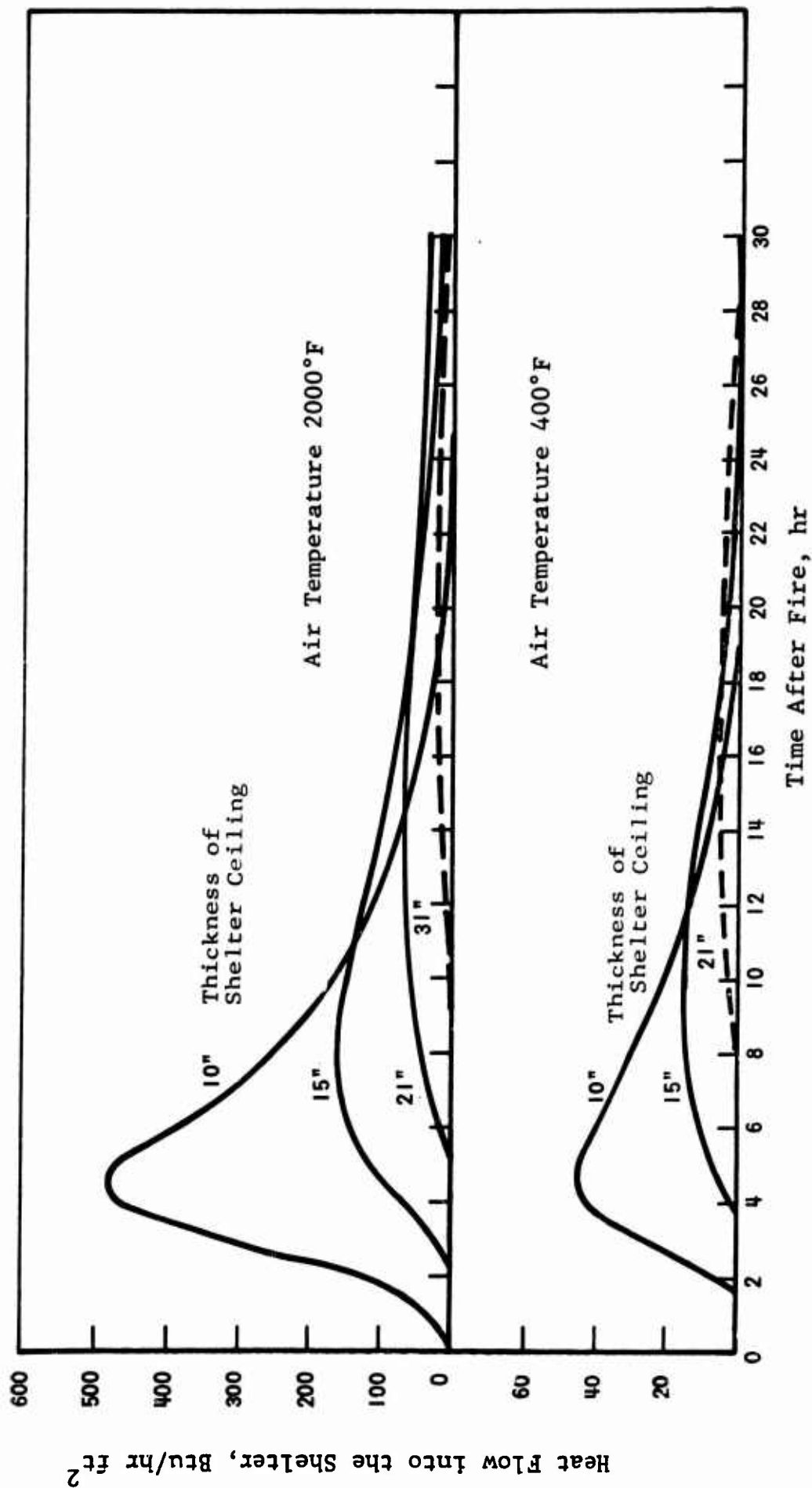


Fig. 4.7 HEAT FLOW INTO THE SHELTERS EXPOSED TO A FIRE STORM

TABLE 4.2
VULNERABILITY OF DUAL-PURPOSE SHELTERS TO DEBRIS AND FIRE STORM TYPE FIRES

Description	Ceiling Thickness (in.)	Fuel Load (lb/sq ft)	Debris Fire	Maximum Heat Flux per sq ft of Ceiling	
				Fire Storm	
				2000°F Peak Air Temperature	400°F Average Air Temperature
Dual-Purpose Blast Resistant School and Community Shelter (Ref. 15)	10	1	36	570	460
	21	1	18	70	5
	30	1	5	40	5
Parking Garage and Community Shelter (Ref. 16)					
Structure I	12	5	90	70	16
	21	5	35	70	5
Structure II	36	5	5	40	5
	42	5	5	40	5

thermal units per hour per square foot of ceiling area and can be used to calculate the ventilation requirements to maintain the desired levels of shelter temperatures. For example, a 10-in. thick ceiling in the Blast Resistant School may permit 36 Btu/hr sq ft heat or 360 Btu/hr per occupant assuming a 10 sq ft area allocation for each occupant from debris fire.

For any prescribed condition of air supply and effective temperature of the shelter air, the ventilation rate (V_R) required to remove the additional heat flow (Q_E) can be readily determined by satisfying the following equations:

$$t_{DBS} = t_{DBO} + \frac{Q_S + Q_E}{14.4 \rho V_R} \quad (4.1)$$

$$W_S = W_O + \frac{0.000016 Q_L}{V_R \rho} \quad (4.2)$$

where t_{DBS} and t_{DBO} are the dry bulb temperatures of the shelter air and additionally supplied air ($^{\circ}\text{F}$), respectively; Q_S and Q_L are sensible and latent heats, respectively, produced by each occupant (Btu/hr); Q_E is the heat flow into the shelter from debris fire (Btu/hr -10 sq ft); V_R is the ventilation rate (cu ft/min); ρ is the air density (pcf); and W_S and W_O are specific humidities of shelter and supply air (lb water/lb dry air), respectively. It is noted that Eq. (4.1) gives only approximate ventilation rates. However, the error introduced is small and well within the accuracy of the heat conduction analysis.

Equations (4.1) and (4.2) are used to perform sample calculations of ventilation rates per occupant required to maintain the effective temperature of $\sim 82^{\circ}\text{F}$ within the shelter when the shelter is subjected to various heat fluxes from debris fires. The dry and wet bulb temperatures of the additionally supplied air are assumed to be 75° and 67°F , respectively. The barometric pressure is taken to be 29.92 in. of mercury. Results of the calculations are shown in Fig. 4.8. Similar relationships can be developed for other conditions of air supply and effective temperatures of the shelter.

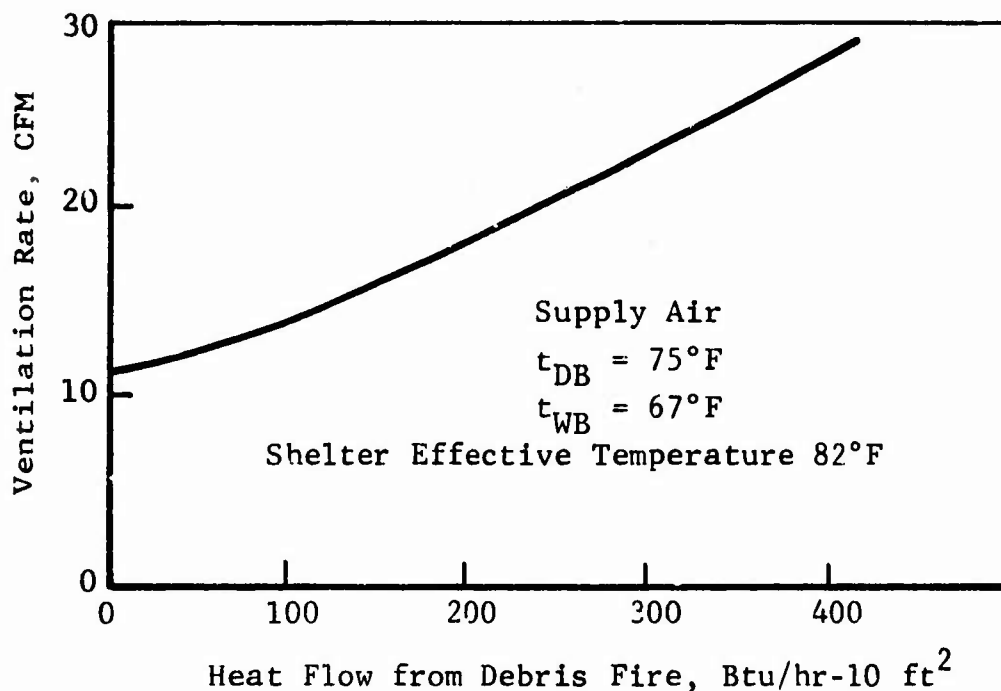


Fig. 4.8 VENTILATION RATES REQUIRED PER OCCUPANT FOR VARIOUS HEAT FLOW FROM DEBRIS FIRES TO MAINTAIN $ET = 82^{\circ}\text{F}$ WITHIN THE SHELTER

The results of Table 4.2 show that, except for high fuel loading accompanied by the collapse of the roof, doubling the ventilation with a 21-in.-thick ceiling is sufficient to maintain a functional shelter environment for most debris fires. Because ventilation may not be possible during the fire storm period, even the assumed 400°F average air temperature may produce an untenable shelter environment. It must be emphasized however that this level of temperature represents an upper bound of practical experiences.

The ventilation estimates based on the results of Table 4.2 neglect any addition of moisture driven from the heated concrete. Tests with concrete floors (Ref. 41) and IITRI experiments (Ref. 39) demonstrate that concrete when heated, emits moisture. The complexity of the moisture problem does not allow its treatment within the scope of the present effort. This type of moisture emission should not constitute a serious problem in the vast majority of practical Civil Defense shelters.

4.4 REMEDIAL ACTION

Various steps can be taken by the designer and the occupants of dual-purpose shelters to protect the shelter against thermal effects. The designer can use thick ceilings. In situations in which this is impractical, radiation shields can be incorporated to substantially reduce the heat flow into the shelter area. The shields also serve as moisture barriers which may be of considerable significance for maintaining a successful shelter environment.

Required activities of the occupants are obviously those which reduce fire hazards; these steps could be taken both before and after detonation. Steps taken before involve removal of fuel situated over the shelter ceiling or its placement in positions shielded from the thermal pulse. Suppression of all incipient fires immediately following the detonation and removal of any debris deposited over the shelter eliminate the fire hazard to the shelter. This suggests that dual-purpose shelters should contain equipment suitable for debris removal.

4.5 EVALUATION OF FIRE VULNERABILITY OF SHELTERS SELECTED BY BECHTEL CORPORATION (Ref. 36)

As mentioned, the sites for dual-purpose shelters are selected to provide maximum protection from possible fire effects. With this in mind, the Bechtel Corporation selected numerous locations in Detroit, Michigan, as possible sites. A pilot fire vulnerability study was conducted using Zone 7 of the Bechtel study (Ref. 36) to evaluate how well these sites are protected against fire effects. The possible effects of nearby burning structures and debris fires are the prime concern in this respect. A quick review of the selected shelter sites reveals that the choice of Zone 7 is good, and burning nearby structures will have little thermal effect on the shelters. However, the debris problem requires more careful examination.

The existing literature does not detail the effect of blast on striated structural materials, such as wood, which has greatly differing properties in transverse and longitudinal directions.

Nor is information available on the trajectory differences of materials of differing densities and thicknesses. The fire problem is further clouded by differences in philosophies for prediction of debris formation and trajectories. Thus, Ahlers and Feinstein (Ref. 42 and 43) have frangible particles flying farther; and Rotz (Ref. 44) presumes that the debris will fill empty spaces (lots, alleys and streets) to a uniform depth.

The approach used is to estimate the combustible components as well as the incombustible ones in typical structures and to distribute these components over a predetermined area. Table 4.3 expresses the cubic feet of debris produced per square foot of original house area for several typical house structures. For calculation purposes a basic house size of 1200 sq ft is assumed. In actual practice, smaller structures, being less efficient in space utilization, contain somewhat more wall material per unit area.

TABLE 4.3
ESTIMATED COMBUSTIBLE AND NONCOMBUSTIBLE COMPONENTS
OF SEVERAL TYPICAL STRUCTURES

Structural Type	Noncombustible Debris (cu ft/sq ft)	Combustible Debris(cu ft/sq ft)	
		Structural	Contents
One-Story Frame Garage	0.10	0.25	0 - 0.03
One-Story Frame Dwelling	0.15	0.80	0.15
One-Story Brick Dwelling	1.30	0.55	0.15
Two-Story Frame Residence	0.25	1.10	0.20
Two-Story Brick Veneer Residence	1.75	1.00	0.20
Two-Story Brick Residence	2.10	0.80	0.20
Three-Story Brick Flat or Apartment	3.90	1.26	0.27
School House - Noncombustibles calculated as 10 cu ft debris/ story ft of perimeter plus 5 cu ft/story ft for corridors (estimated classroom size 30 x 30 ft). - Combustible estimated at 38 lb/pupil.			

Because the structures are in an old area of the city, they are assumed to be one- and two-story dwellings, and three-story apartments or flats. This assumption increases the combustible content of the two-story structures above the average. However, offsetting this is the probably heavier loading in some of the stores which are marked but not identified as to type in the Sanborn maps used in the study.

The original assumption of uniform distribution of debris from any structure within a 200 ft radius results in very low debris depths, particularly of the combustible debris. However, if the radius is increased, the debris depth and amount of combustible debris increase. Therefore the original 200 ft radius was increased to 300 ft.

The results of the analysis of those shelters studied, are summarized in Table 4.4. The most serious result is Site 7-8, where a predicted debris depth of 1.7 ft with a potential fuel load of 7 psf would produce a heat flow of 40 Btu/hr sq ft into the shelter (according to Figs. 4.1 through 4.5). For this heat flux, conditions within the shelter would be intolerable unless the ventilation requirements are doubled or countermeasures instituted.

TABLE 4.4
FIRE VULNERABILITY OF SHELTERS IN DETROIT, MICHIGAN,
ZONE 7 OF BECHTEL STUDY (Ref.36)

Shelter Area	Debris Depth (ft)	Voids	Debris Composition Percent		Maximum Heat Flux into Shelter (Btu/hr sq ft)	Radius of Debris Scatter (ft)
			Rubble	Combustibles		
7-1	0.24	50	38.0	12.0	9	200
7-2	1.00	50	38.0	12.0	26	300
7-3	0.54	50	38.5	11.5	16	200
7-3	0.58	50	37.6	12.4	17	300
7-4	0.91	50	33.8	16.2	32	300
7-5	0.50	50	34.6	15.4	20	200
7-5	1.20	50	37.5	12.5	32	300
7-8	1.70	50	35.9	14.1	40	300

CHAPTER FIVE

SURVIVABILITY AGAINST BLAST-INDUCED AIRFLOW

This chapter is concerned with the survivability of shelter occupants when subjected to blast-induced airflow if the blast doors are left off or open. Specifically, we are concerned with overpressures which will cause fatalities to personnel as a result of impacting a rigid object.

When a shelteree impacts with a rigid object such as an RC wall or floor, fatalities may be produced at relatively low velocities (in the range of 10 to 15 fps). Considering the density of shelterees in any given shelter (10 sq ft per person), it seems likely that numerous persons undergoing translation will collide with other shelterees before encountering a rigid object. In addition, those shelterees who are close to a wall will not be accelerated to high speeds before impacting the wall. For these reasons, the impact criteria given in Ref. 50 is more appropriate for shelters considered herein than the 10 to 15 fps range given above. Data given in Ref. 50 and reworked in Ref. 61 is reproduced below. Strictly speaking, these values are applicable to a 70 kg animal but are here assumed to be applicable to the general shelter population.

<u>Mortality versus Impact Speed, v_{imp}</u>	
Threshold	20.9 fps
10%	24.7
50%	26.2
90%	27.7
95%	27.9

In this study we are specifically concerned with overpressure which will produce fatality to personnel at the 95 percent level. Shelteree acceleration hazards other than impact are not considered in this study though their probable occurrence is recognized as discussed. The effects of acceleration of short duration with respect to ejection from jet aircraft are discussed in Ref. 62 and briefly summarized herein.

When a pilot is ejected from an aircraft, the airstream encountered exerts on him an aerodynamic pressure referred to as windblast, ram pressure or "q". The effects can be divided into those

produced by direct pressure on the body, and those produced by flailing of the head and other extremities. The results of the study (Ref. 62) indicate that the threshold of injury in ejection seats with little or no restraint appears to lie in the region of a q of about 4.5 psi while fatal injury probably occurs at a q of 8.5 psi or more under similar conditions. In 20 U.S. Air Force ejections at speeds between 550 and 650 knots where q loads of between 7 and 10 psi were involved, nine fatalities and eight major injury cases occurred, all largely attributable to wind-blast. It is postulated herein that when a shelteree is located in a portion of a shelter that is subject to the onslaught of a jet, the resultant acceleration may be likened to that experienced by a pilot who is ejected from an aircraft at high speed.

The hydrodynamic computational methods available are limited to a one-dimensional, timewise description of the flow field inside a shelter; obviously, shelters containing many partitions could not be properly analyzed for the resulting internal airflows. Consequently, the study is limited to the single room arch type shelters (Fig. 3.11). The flow field resulting from the blast wave entering the room is assumed not to be affected by the presence of the shelter occupants. To actually account for the effect of the occupants on the flow field would require at least a two-dimensional computational procedure.

Briefly, there are two phases in the one-dimensional flow field used, namely, the shock diffraction phase (SDP) and the drag phase (DP). As the names imply, the SDP phase is a result of the initial shock which enters the shelter and the DP phase is a result of the large particle velocities which exist behind the shock. The SDP phase exerts primarily horizontal forces on the man, whereas the DP phase can produce both horizontal (drag) and vertical (lift) forces. The lift forces are present if the body tilts from its initially vertical position. The inclined body behaves as an airfoil wherein the lift may be either positive or negative depending on whether the tilt is toward or away from the direction of flow.

5.1 GOVERNING EQUATIONS OF MOTION FOR A TUMBLING MAN

The development and integration of the governing equations of motion for the tumbling man model are presented. The man is assumed to be a single rigid body of mass acted upon by two position and time dependent forces $D(x,y,\theta,t)$ and $L(x,y,\theta,t)$, the drag and lift forces respectively. The response motion is considered to be planar, thus only three-degrees-of-freedom are necessary to describe the position of the man at any given instant of time; namely, the two horizontal and vertical coordinates of the center of gravity and the angular center of gravity rotation $(x(t), y(t), \theta(t))$ respectively.

The man is initially assumed to be either standing (Fig. 5.1), prone (Fig. 5.2) or sitting (Fig. 5.3). A generalized orientation model is shown in Fig. 5.4. By appropriately defining the parameters h , S_1 , S_2 and d_1 , all three tumbling man configurations can be made a special case of the generalized model. Consequently, we need only develop the equations of motion for this one case.

5.1.1 Governing Equations

Six possibly distinct modes of motion are considered in the tumbling man analysis and are summarized below:

Mode

- 1 Free-Free
- 2 Sliding only
- 3 Tipping only (right end)
- 4 Tipping only (left end)
- 5 Tipping (right end) and sliding
- 6 Tipping (left end) and sliding

The forces acting in each of these six cases are represented in Fig. 5.5. In each case the equations of motion for the center of gravity coordinate (x,y,θ) are given by the equations,

$$\Sigma F_x = m \frac{d^2x}{dt^2} \quad , \quad \Sigma F_y = m \frac{d^2y}{dt^2} \quad , \quad \Sigma M = I \frac{d^2\theta}{dt^2} \quad (5.1)$$

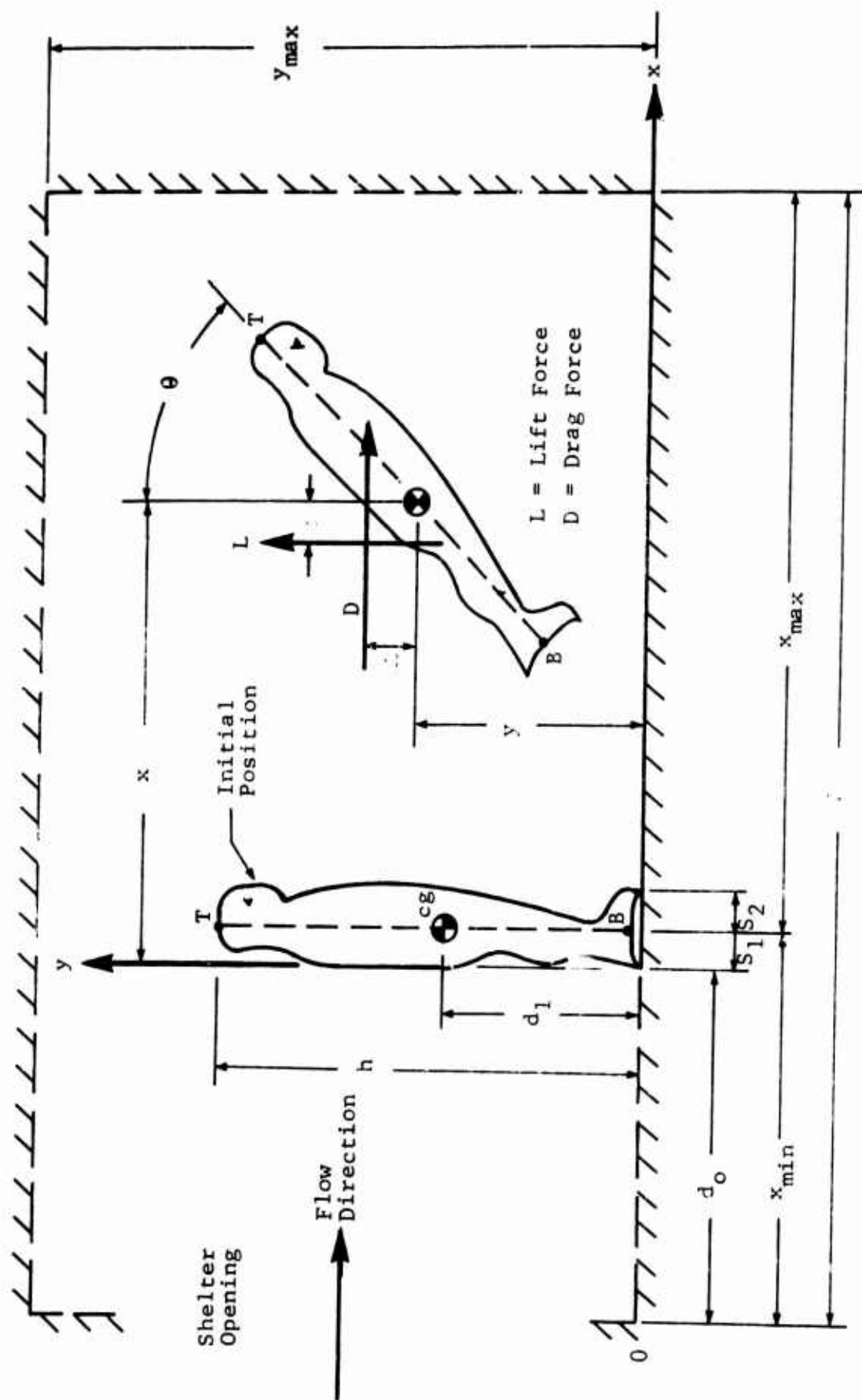


Fig. 5.1 TUMBLING MAN NOTATION, STANDING CONFIGURATION

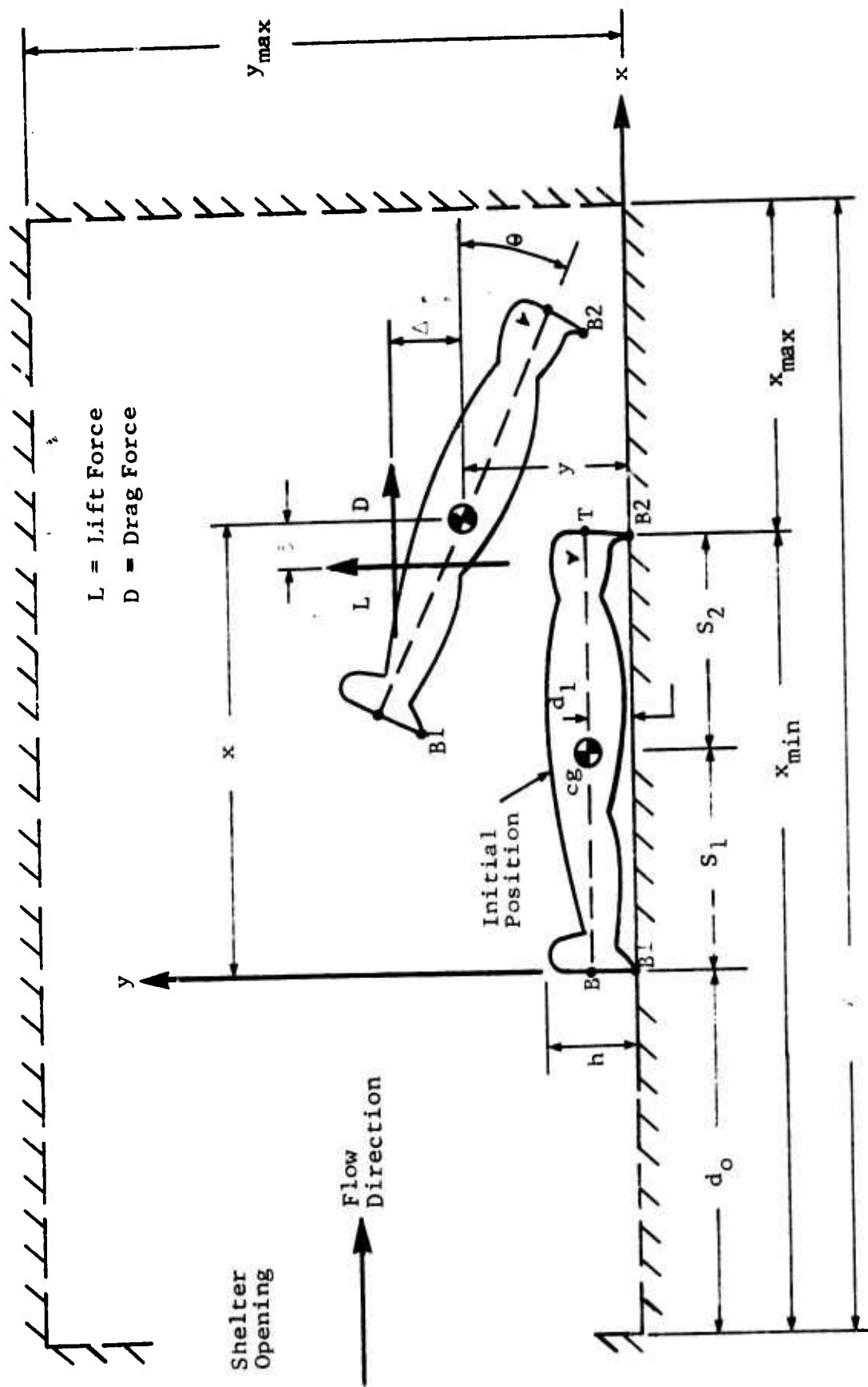


Fig. 5.2 TUMBLING MAN NOTATION, PRONE CONFIGURATION

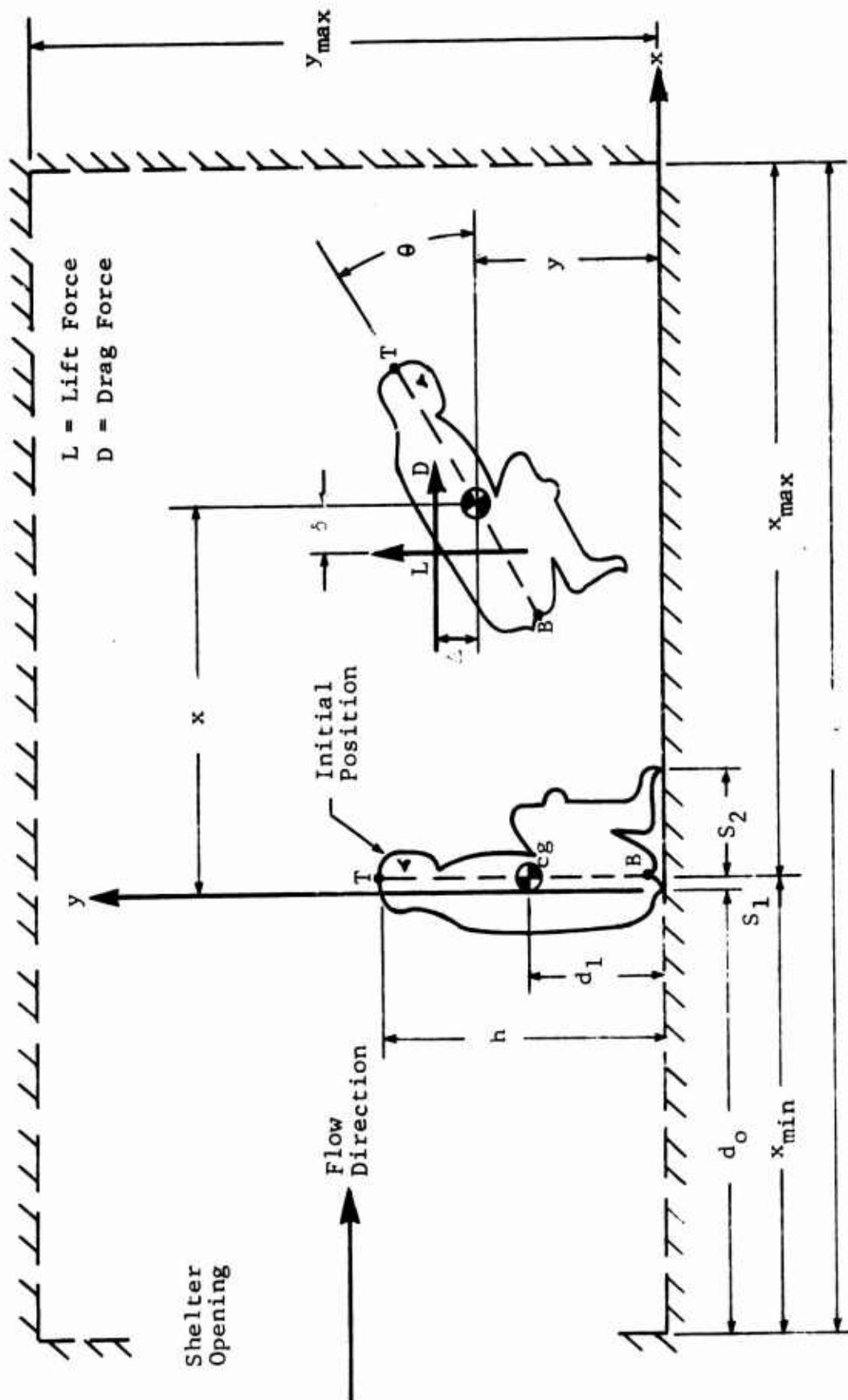


Fig. 5.3 TUMBLING MAN NOTATION, SITTING CONFIGURATION

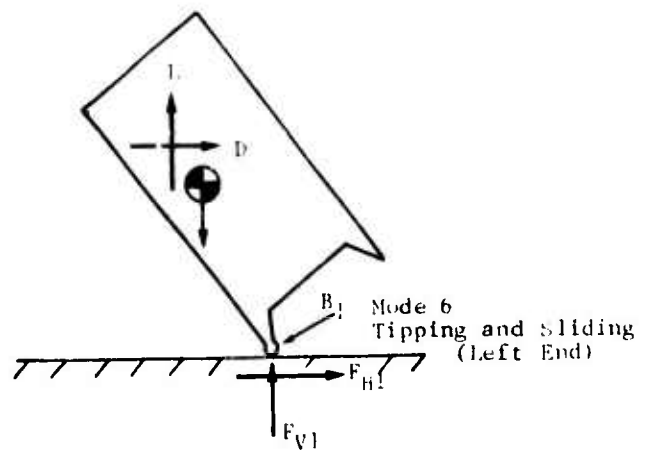
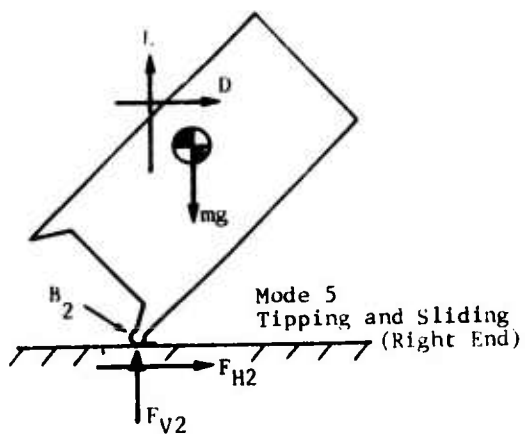
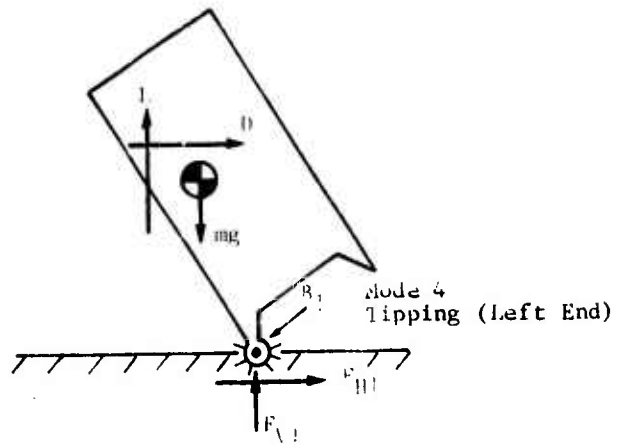
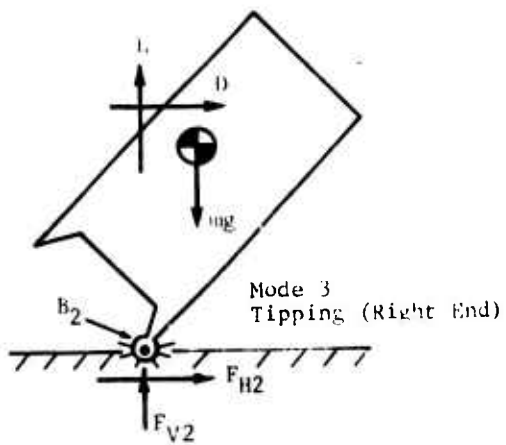
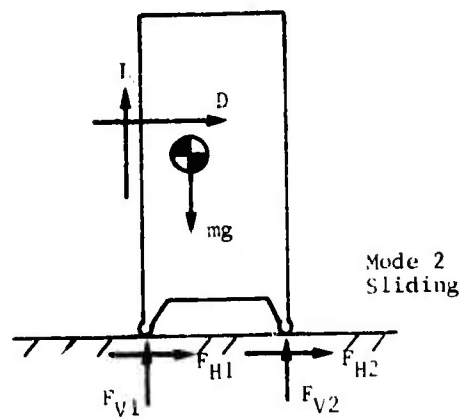
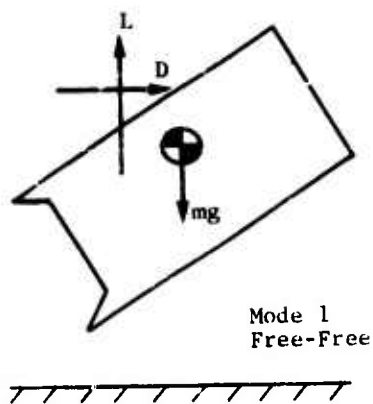


Fig. 5.5 SIX POSSIBLE MODES OF MOTION

subject to constraints $F_i(x, y, \theta, \dot{x}, \dot{y}, \dot{\theta}, t) = 0$

$$i = 1, 2, \dots, I$$

The terms ΣF_x , ΣF_y , ΣM refer to the summation of the horizontal forces, vertical forces and moments, each taken about the center of gravity. This expression differs of course, according to which of the six modes of Fig. 5.5 we refer. The $i = 1, 2, \dots, I$ functions refer to geometrical constraints relating to any dependence between the variables θ, x, y (e.g., the pivot in mode 3 implies that $y = r_2 \cos(\phi_2 - \theta)$ and $x = r_0 - r_2 \sin(\phi_2 - \theta)$ where r_2, ϕ_2 and x_0 are known constraints). There will always be enough constraint equations available so that the unknowns in the problem ($x, y, \theta, F_{v1}, F_{v2}, F_{H1}, F_{H2}$) balance the number of equations they must satisfy (three equations of motion (5.1) and one constraint). In general, the final form of the governing equations will be nonlinear and thus must be numerically integrated. The nonlinearity arises from the nonlinear constraints and the fact that the lift force (L), drag force (D) and center of gravity distances (Δ, δ) are prescribed nonlinear functions of x, y and θ . The functional dependence of the quantities of x, y and θ are discussed in detail in Subsection 5.2.

For the purpose of setting up the numerical integration, we represent the governing equations in terms of a set of six simultaneous first order equations with $x, y, \theta, \frac{dx}{dt}, \frac{dy}{dt}, \frac{d\theta}{dt}$ as the unknowns to be determined. All the reaction forces can be eliminated from the equations of motion via the constraint relations. The resulting first order form of the governing equations for each of the six modes shown in Fig. 5.5 are given. The unknowns are relabeled accordingly,

$$\begin{aligned} x_1 &\equiv \theta \\ x_2 &\equiv d\theta/dt \\ x_3 &\equiv x \\ x_4 &\equiv dx/dt \\ x_5 &\equiv y \\ x_6 &\equiv dy/dt \end{aligned} \tag{5.2}$$

Mode 1: (free-free).--This mode prevails whenever the vertical reactions require a negative value (since the ground can only provide an upward resistance, the body will lift off whenever $F_{V1} < 0$ and $F_{V2} < 0$),

$$\begin{bmatrix} \frac{dx_1}{dt} \\ \frac{dx_2}{dt} \\ \frac{dx_3}{dt} \\ \frac{dx_4}{dt} \\ \frac{dx_5}{dt} \\ \frac{dx_6}{dt} \end{bmatrix} = \begin{bmatrix} x_2 \\ (D\Delta + L\phi)/\bar{I} \\ x_4 \\ D/m \\ x_6 \\ (-mg + L)/m \end{bmatrix} \quad (5.3)$$

where

$$F_{V1} = F_{V2} = F_{H1} = F_{H2} = 0.$$

Mode 2: sliding only.--This mode prevails if the vertical reactions are both positive, $F_{V1} \geq F_{V2} \geq 0$, and $x_4 \neq 0$,

$$\begin{bmatrix} \frac{dx_1}{dt} \\ \frac{dx_2}{dt} \\ \frac{dx_3}{dt} \\ \frac{dx_4}{dt} \\ \frac{dx_5}{dt} \\ \frac{dx_6}{dt} \end{bmatrix} = \begin{bmatrix} x_2 \\ 0 \\ x_4 \\ (D - \mu \operatorname{Sgn}(x_4)[mg - L])/m \\ x_6 \\ 0 \end{bmatrix} \quad (5.4)$$

where the reactions are determined by

$$F_{V1} = \left[(mg-L)(S_2 - \mu d_1 \operatorname{Sgn}(x_4)) - (D\Delta + L\delta) \right] / [S_1 + S_2]$$

$$F_{V2} = mg - L - F_{V1}$$

$$F_{H1} = -\mu \operatorname{Sgn}(x_4) F_{V1}$$

$$F_{H2} = -\mu \operatorname{Sgn}(x_4) F_{V2}$$

The variable μ is the coefficient of friction for contact between the floor and man. The expression $\operatorname{Sgn}()$ refers to the "sign function" where

$$\begin{aligned} \operatorname{Sgn}() &= +1 \quad \text{for } () > 0 \\ &= -1 \quad \text{for } () < 0 \end{aligned}$$

Mode 3: tipping only (right end).--This mode is in effect if $F_{V2} > 0$, $F_{V1} = 0$ and the horizontal pivot force is locked against sliding, $|F_{H2}| < \mu F_{V2}$. It is notationally convenient to define the variables

$$\psi \equiv \phi_2 - x_1$$

$$A_3 \equiv [L\delta + D\Delta + Dr_2 \cos\psi - (mg-L)r_2 \sin\psi] / [\bar{I} + mr_2^2].$$

Then the governing equations can be written in the form

$$\begin{bmatrix} \frac{dx_1}{dt} \\ \frac{dx_2}{dt} \\ \frac{dx_3}{dt} \\ \frac{dx_4}{dt} \\ \frac{dx_5}{dt} \\ \frac{dx_6}{dt} \end{bmatrix} = \begin{bmatrix} x_2 \\ A_3 \\ x_4 \\ r_2 A_3 \cos\psi + r_2 (x_2)^2 \sin\psi \\ x_6 \\ r_2 A_3 \sin\psi + r_2 (x_2)^2 \cos\psi \end{bmatrix} \quad (5.5)$$

where the reactions are determined from

$$F_{V1} = F_{H1} = 0$$

$$F_{V2} = m[r_2 A_3 \sin\psi - r_2 (x_2)^2 \cos\psi] + mg - L$$

$$F_{H2} = m[r_2 A_3 \cos\psi + r_2 (x_2)^2 \sin\psi] - D$$

Mode 4: tipping only (left end).--This mode is in effect if $F_{V1} > 0$, $F_{V2} = 0$ and the horizontal pivot force is locked against sliding, $|F_{H1}| < \mu F_{V1}$. The variables can be defined,

$$\bar{\psi} \equiv x_1 + \phi_1$$

$$A_4 \equiv [L\delta + D\Delta + Dr_1 \cos\bar{\psi} + (mg-L) r_1 \sin\bar{\psi}] / [\bar{I} + mr_1^2].$$

Then the governing equations can be written in the form:

$$\begin{bmatrix} \frac{dx_1}{dt} \\ \frac{dx_2}{dt} \\ \frac{dx_3}{dt} \\ \frac{dx_4}{dt} \\ \frac{dx_5}{dt} \\ \frac{dx_6}{dt} \end{bmatrix} = \begin{bmatrix} x_2 \\ A_4 \\ x_4 \\ A_4 r_1 \cos\bar{\psi} - r_1 x_2^2 \sin\bar{\psi} \\ x_6 \\ -A_4 r_1 \sin\bar{\psi} - r_1 x_2^2 \cos\bar{\psi} \end{bmatrix} \quad (5.6)$$

where the reactions are determined from

$$F_{V2} = F_{H2} = 0$$

$$F_{V1} = m[-A_4 r_1 \sin\bar{\psi} - r_1 x_2^2 \cos\bar{\psi}] + mg - L$$

$$F_{H1} = m[A_4 r_1 \cos\bar{\psi} - r_1 x_2^2 \sin\bar{\psi}] - D.$$

Mode 5: tipping and sliding (right end).--This mode applies if $F_{V1} = 0$, $F_{V2} > 0$ and the horizontal pivot force does not lock, $F_{H2} = \mu F_{V2} \text{Sgn}(\dot{x}_{B2})$ and $\dot{x}_{B2} \neq 0$, where

$$\dot{x}_{B2} = x_4 - r_2 x_2 \cos(\phi_2 - x_2)$$

is the horizontal velocity of pivot point B_2 in Fig. 5.5. The variables are defined,

$$\psi = \phi_2 - x_1$$

$$A_5 = \left[D\Delta + L\dot{\phi} + m(-r_2 x_2^2 \cos\psi + g - L/m)(r_2 \cos\psi \operatorname{Sgn}(\dot{x}_{B2}) \mu - r_2 \sin\psi) \right] \\ \div \left[\bar{I} - m r_2^2 \sin\psi (\cos\psi \operatorname{Sgn}(\dot{x}_{B2}) \mu - \sin\psi) \right].$$

Then the governing equations can be written in the form:

$$\begin{bmatrix} \frac{dx_1}{dt} \\ \frac{dx_2}{dt} \\ \frac{dx_3}{dt} \\ \frac{dx_4}{dt} \\ \frac{dx_5}{dt} \\ \frac{dx_6}{dt} \end{bmatrix} = \begin{bmatrix} x_2 \\ A_5 \\ x_4 \\ D/m - \operatorname{Sgn}(\dot{x}_{B2}) \mu (-r_2 x_2^2 \cos\psi + r_2 \sin\psi A_5 + g - L/m) \\ x_6 \\ -r_2 x_2^2 \cos\psi + r_2 A_5 \sin\psi \end{bmatrix} \quad (5.7)$$

where the reactions are determined from

$$F_{V1} = F_{H1} = 0$$

$$F_{V2} = m(-r_2 x_2^2 \cos\psi + r_2 A_5 \sin\psi) + mg - L$$

$$F_{H2} = -\operatorname{Sgn}(\dot{x}_{B2}) \mu F_{V2}$$

Mode 6: tipping and sliding (left end).--This mode applies if $F_{V2} = 0$, $F_{V1} > 0$ and the horizontal pivot force does not lock, $F_{H1} = F_{V1} \operatorname{Sgn}(\dot{x}_{B1})$ and $\dot{x}_{B1} \neq 0$, where

$$\dot{x}_{B1} = x_4 - r_1 x_2 \cos\tilde{\psi}$$

is the horizontal velocity of pivot point B_1 in Fig. 5.5. The variables are defined,

$$\tilde{\psi} \equiv \phi_1 + x_1$$

$$A_6 \equiv \left[D\Delta + L\delta + m(-x_2^2 r_1 \cos\tilde{\psi} + g - L/m)(r_1 \cos\tilde{\psi} + r_1 \mu \sin\tilde{\psi} \operatorname{Sgn}(\dot{x}_{B1})) \right] \\ \div \left[I + m r_1^2 \sin\tilde{\psi} (\cos\tilde{\psi} + \mu \sin\tilde{\psi} \operatorname{Sgn}(\dot{x}_{B1})) \right].$$

The governing equation can be written in the form:

$$\begin{bmatrix} \frac{dx_1}{dt} \\ \frac{dx_2}{dt} \\ \frac{dx_3}{dt} \\ \frac{dx_4}{dt} \\ \frac{dx_5}{dt} \\ \frac{dx_6}{dt} \end{bmatrix} = \begin{bmatrix} x_2 \\ A_6 \\ x_4 \\ D/m - \mu \operatorname{Sgn}(\dot{x}_{B1}) \left[-x_2^2 r_1 \cos\tilde{\psi} - A_6 r_1 \sin\tilde{\psi} + g - L/m \right] \\ x_6 \\ -x_2^2 r_1 \cos\tilde{\psi} - A_6 r_1 \sin\tilde{\psi} \end{bmatrix} \quad (5.8)$$

where the reactions are determined from

$$F_{V2} = F_{H2} = 0$$

$$F_{V1} = m(-x_2^2 r_1 \cos\tilde{\psi} - A_6 r_1 \sin\tilde{\psi}) + mg - L$$

$$F_{H1} = -\mu F_{V1} \operatorname{Sgn}(\dot{x}_{B1}).$$

5.1.2 Integration of Governing Equations

At time zero, the pressure loading D begins to act on the rigid mass. The mass is assumed to be initially at rest and to remain stationary until the applied forces are large enough to start the body in motion in one of the six modes shown in Fig. 5.5. A static analysis for the sigma and magnitude reactions F_{V1} , F_{V2} , F_{H1} and F_{H2} is the determining factor as to which of the six modes is first activated. For example, if with an incremental addition of applied force a vertical reaction passes from positive to negative, this implies that the end will lift up since negative reactions cannot be physically experienced.

Once the starting mode is established, the appropriate governing set of equations for that mode are numerically integrated by means of a fourth order Runge Kutta algorithm. The starting mode is assumed to be applicable for all subsequent time increments until either a rigid constraint is encountered (the tumbling man hits a floor, wall or ceiling); or the conditions for which the mode equations are valid are violated. An example of the latter is when the body is in mode 5 (sliding and rotating) at time t with F_{V2} equal to a small positive value. Suppose that at $t + \Delta t$, F_{V2} crosses the origin and is a small negative number, this situation is not physically possible. At this point the body is just starting to lift off (mode 1) and the new appropriate differential equation of motion should be used. The transition from mode-to-mode is performed automatically by the computer program. The reactions (F_{V1} , F_{V2} , F_{H1} , F_{H2}) are monitored at all times and are the key factors which indicate when to switch modes.

It should be pointed out that only mode transitions are allowed which do not result in impacting hard constraints. For example, once the program is in mode 1, it can never return to mode 5. This is because such a transition would involve an impact when the body retouches the floor. To properly carry the problem beyond the impact, a separate problem must be solved for the instants before and after impact. Such an analysis would enable us to properly proceed with the tumbling problem.

5.2 DETERMINATION OF SHELTEREE AERODYNAMIC BODY FORCES AND POINT OF APPLICATION

We are concerned herein with developing the equations for the determination of the aerodynamic body forces (lift $L(x,y,\theta,t)$ and drag $D(x,y,\theta,t)$) and points of application with respect to the mass center of gravity (horizontal distance $\delta(x,y,\theta,t)$ and vertical distance $\Delta(x,y,\theta,t)$). The variables L, D, δ, Δ are shown

in Fig. 5.4. We substitute L , D , δ and Δ in the remainder of this section for the cumbersome argument notation (x,y,θ,t) .

5.2.1 Load Determination

The loads on shelterees are subdivided into the shock diffraction phase and the drag phase (see Ref. 46). One-dimensional quasi-steady analysis is used to estimate both the shock loading and the velocities during the cavity filling process.

Since most shelter geometries are complex, we selected as an example of the expected shock a simple arch shelter illustrated in Fig. 2.15 and 3.11 of Ref. 14. The entrance configuration is given in Fig. 3.11 and the duct and door details are given in Fig. A.10. The overall dimensions of the lower level of this shelter are as follows: length 81 ft, cross-sectional area 307 sq ft, and volume 26,805 cu ft. The cross-sectional area of the doorways at either end of the entrance tunnel is 11 sq ft and the area of the tunnel itself is 31.76 sq ft.

We note that the doorway orientation is such that a blast wave traveling side-on, relative to the ground, will strike the entrance nearly head-on. Since the reflecting surface (bulkhead area) is only about three times larger than the door area, data from Ref. 47 should be used to determine the entering shock wave. However, the doorway really represents an orifice plate since just downstream of it, the tunnel enlarges to the area of the bulkhead; thus, we use those data given for the shock transmission through an orifice (Ref. 25) to estimate the shock entering the tunnel. This, in general, yields slightly higher pressures than would the Ref. 47 data. The shock now propagates with essentially undiminished strength to the end of the tunnel where it encounters a 90 deg turn followed immediately by the second doorway. No data exists to treat this particular situation. Some data are available from simple area restrictions in a channel; however, the current situation is more complex in that the doorway is followed directly by a large area change into the room proper.

Past experience indicates (Ref. 25) that a rough estimate of the change in overpressure at a channel convergence or sudden increase in area can be obtained from the formula

$$\Delta p_2 = \frac{2\Delta p_1}{1 + \frac{A_2}{A_1}} \quad (5.9)$$

Here subscript 2 refers to the downstream part of the channel and subscript 1 refers to the upstream part. Thus, Δp_1 is the overpressure of the incident shock wave and Δp_2 is the overpressure of the transmitted wave at a sudden change in area. The formula is based on acoustic theory but gives reasonable results for fairly strong shocks even in the case of large area changes. We thus employ this equation to estimate the shock which propagates into the doorway. A repeated application of the formula then permits the estimation of the strength of the shock propagating through the shelter space.

However, the ratio of the shelter width (35 ft) to the door width (2 ft) is used rather than the shelter to door area ratio. This is justified on the basis that the lower part of the shelter presents basically a two-dimensional geometry bounded on top and bottom by the roof slab and floor respectively. Thus, little expansion of the shock wave in the vertical direction takes place and the primary expansion is in the horizontal plane. The shock pressure estimates, obtained in this fashion, are believed to be conservative for distances of ten door widths (~ 20 ft) or more into the shelter. Along the door centerline from the doorway proper to the quoted distance, the shock decays in an exponential manner (Ref.45). Thus it is in this region adjacent to the door that the highest velocities and pressures may be expected. The values computed for the entranceway and the inside shelter proper are upper and lower bounds respectively for this region. At distances greater than ten door widths the shock strength estimated should present an upper bound of the shock pressure that may be expected in the shelter.

The shock in the shelter propagates until it reaches the back wall where normal reflections take place. The velocity behind the reflected wave (for assumed normal reflections) is computed to be zero. This, in general, is not quite true since in the real situation, a multiple shock configuration exists which is caused by the reflection from the side walls. However, in any case the velocity behind the reflected shock wave will be considerably less than behind the incident wave. Thus the latter velocity can be used as an upper bound during the shock diffraction phase. Before the reflected shock returns to the entrance, it is broken up by the in rushing jet like flow, thus ending the diffraction phase.

Because the shock diffraction around the human body is of very short duration and since the drag load due to the jet inflow is quite severe, the effect of the reflected shock is neglected in the estimation of net loads. In order to estimate the velocities and drag forces that may be expected inside a shelter space, the values of these quantities are computed, based on the theory of free jet expansion. Since the velocity profiles obtained in incompressible flow are nearly identical with compressible flow profiles (see Ref. 33 through 35) the former are used since they can be defined by simple mathematical expressions. In general, a free jet issuing from a small opening has a bell-shaped axial velocity distribution as shown in Fig. 5.6.

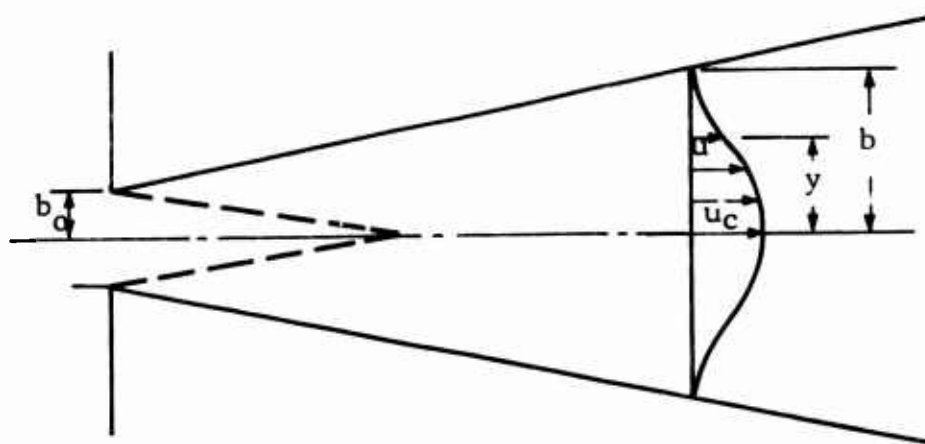


Fig. 5.6 JET PROFILE

The velocity is a maximum at the centerline. The maximum velocity which occurs in the opening from which the jet originates, persists for some distance into the free jet in a cone-shaped region. Maximum penetration occurs again at the centerline and is equal to approximately four diameters for an axisymmetric jet and about five orifice widths for the plane two-dimensional jet.

Beyond this initial region of the jet, the flow spreads in a linear fashion. For practical purposes, the behavior of axisymmetric and plane jets is the same and the half-width, or radius b , of the jet is given by (Ref. 35)

$$b = 0.22 x + b_o . \quad (5.10)$$

Here x is the distance from the opening, and b_o is the half-width or radius of the opening. The door geometry of the shelter under consideration suggests that the plane jet will provide the better approximations. The centerline velocity of the plane jet varies inversely with the square root of the distance from the entrance. For turbulent jets the relationship is (Ref. 35)

$$\frac{U_c}{U_o} \cong 3.8 \sqrt{\frac{n}{\bar{X} - \bar{X}_o}} \quad (5.11)$$

Here $\bar{X} = X/b_o$ and b_o is the opening half-width, X is the axial distance from the entrance, U_o is the entrance velocity, U_c the centerline velocity at distance X , and n and \bar{X}_o are parameters which depend on the flow coefficient, i.e., on how much of the actual area of the opening is occupied by the jet. For flow coefficients of $K=0.70$ (used in the cavity filling computations) we find from the graphs in Ref. 35 that \bar{X}_o is -4 for the plane jet. Similarly, we find that the value of n is 0.81 . Hence, we rewrite the equations for the centerline velocities as

$$U_c = 3.8 U_o \sqrt{\frac{0.81}{\frac{X}{b_o} + 4}} = \frac{3.42 U_o}{\sqrt{\frac{X}{b_o} + 4}} . \quad (5.12)$$

It is possible to give the exact bell-shaped velocity distribution in the main part of the jet as a function of distance from the entrance (Refs. 33 and 35). However, for the purpose of estimating the effect on shelterees, it suffices if an average velocity in the jet is determined. From Ref. 35, an approximate formula for the volumetric rate-of-flow in the jet is

$$q = \frac{Q}{Q_0} \approx 0.375 \sqrt{\frac{x}{b_0}} \quad (5.13)$$

Here Q_0 is the discharge rate at the entrance. Since the velocity is given by the discharge rate divided by the area, we can easily compute the average velocity.

$$U_{\text{average}} = Q/A. \quad (5.14)$$

In the case of the plane jet, $A = b$, Q is the discharge rate, and A is the rate per unit height of the opening. Here

$$\frac{U_{\text{average}} b}{U_0 b_0} = 0.375 \sqrt{\frac{x}{b_0}} \quad \text{or} \quad U_{\text{average}} = \frac{0.375}{b} \sqrt{x b_0}. \quad (5.15)$$

Another average velocity can be defined by means of the velocity distribution profile, thus

$$\bar{U} = U_c \int_0^1 (1 - \xi^{1.5})^2 d\xi = 0.45 U_c. \quad (5.16)$$

Here U_c is the centerline velocity, \bar{U} the average velocity, and $\xi = y/b$, i.e., the variable defining the velocity profiles.

It should be noted that all of these formulas are only applicable in the main portion of the jet, that is, not in the immediate vicinity of the entrance. Further, the expressions for average velocity based on volumetric discharge give the same results as those obtained from the velocity profile. To estimate the momentum flux ρU^2 or the dynamic pressure it is sufficient to use the cavity density ρ with the appropriate velocity.

To obtain the variations in velocity and jet width at a particular location as a function of time, it is assumed that the process is quasi-steady. We then simply determine the entrance velocity from the quasi-steady cavity filling calculations. When the pressure ratio is less than the critical ratio, the flow at the entrance will be sonic and the entrance velocity is then simply

$$U_o = \left[\frac{2\gamma}{\gamma+1} \frac{p_s}{\rho_s} \right]^{1/2} \quad (5.17)$$

where p_s and ρ_s are the blast wave pressure and density, respectively.

For subsonic entrance flow, we get

$$U_o = \left\{ \frac{2\gamma}{\gamma-1} \frac{p_s}{\rho_s} \left[1 - \left(\frac{p_c}{p_s} \right)^{\frac{\gamma-1}{\gamma}} \right] \right\}^{1/2} \quad (5.18)$$

These expressions together with the preceding equations can then be used to estimate velocities and momentum in the shelter during the filling process. Obviously, if precise information on discharge coefficients for the inlet ducting is available, then the entrance velocities can be better estimated by multiplying the given equations by the appropriate coefficients. The expressions as stated herein provide an upper limit of the entrance velocity.

Using the cavity filling results (Ref. 25) for the arch shelter at peak pressures of 50, 30, 20 and 10 psi, we perform computations giving the jet behavior from the time of blast arrival to approximately the time maximum cavity pressures are reached. The entrance velocities, the centerline velocities, the average velocities at a number of locations in the cavity, and the momentum flux are computed. For the plane jet, a flow coefficient of 0.70 was used. This value was established during cavity filling experiments (Ref. 25) and is also used in the filling computations.

The calculated jet flow and the shock wave estimates are used to predict the loading on typical shelterees. During the shock diffraction phase the shock wave strikes the shelteree and diffracts around him; when the shock wave has cleared the person the static pressure equalizes and the remaining load is produced by the flow velocity. Initially this is the particle velocity associated with the shock wave. At later times it is equal to the velocity produced by the quasi-steady jet inflow. The latter velocity varies with the shelteree's location in the shelter and with time. A typical loading diagram is shown qualitatively in Fig. 5.7.

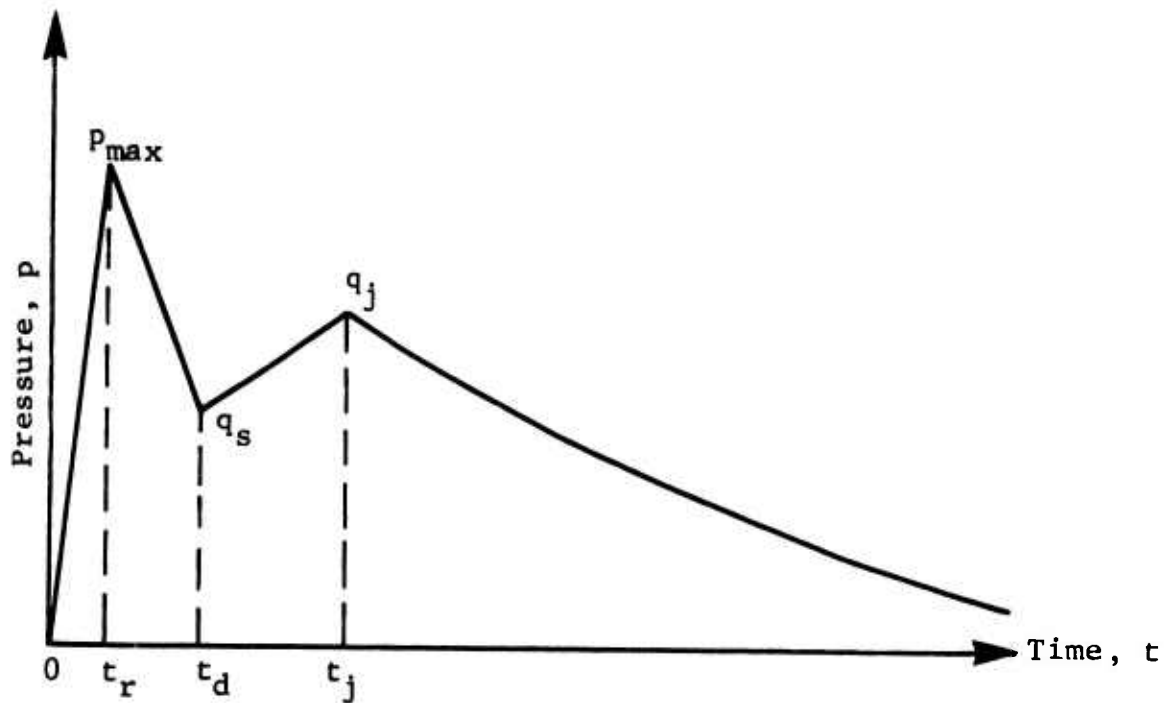


Fig. 5.7 LOADING DIAGRAM (Not to scale)

It is assumed that during the diffraction phase the loading on a person is similar to that on a cylinder in an upright position being struck by a shock normal to its axis. Using the information of Ref. 46 one finds that the rise time t_r to maximum pressure due to shock reflection is

$$t_r = \frac{D}{2U} \quad (5.19)$$

where D is the diameter (estimated at 1 ft for people) and U is the shock velocity. The time of shock clearance or end of the diffraction phase is

$$t_d = \frac{3D}{U} . \quad (5.20)$$

For the pressure range of interest the maximum pressure P_{\max} is obtained by a simple formula based on the data of Ref. 46. For shock overpressure p_s and p_{\max} given in pounds per square inch the equation is

$$p_{\max} = (1.700 + 0.023 p_s) p_s . \quad (5.21)$$

The value of q_s is simply the dynamic pressure of the shock flow,

$$q_s = \frac{1}{2} \rho_s u_s^2 \quad (5.22)$$

where ρ_s and u_s are the shock density and particle velocity respectively. The variation of the load between zero and p_{\max} and also between p_{\max} and q_s is assumed to be linear. Similarly a linear variation of the dynamic pressure is assumed between q_s and q_j where the latter is the dynamic pressure associated with the initial value of the quasi-steady jet flow. The time t_j is estimated from the difference in velocities between the shock front and the jet velocity. Since the latter even in the initial instant varies with distance from the door, we assume for purposes of estimating the time t_j that the jet velocity is the average between the entrance velocity and the jet velocity pertaining to the actual location of the shelteree. Thus t_j is obtained from

$$t_j = \frac{d_o}{U - 0.5 (u_{eo} + u_{jo})} . \quad (5.23)$$

Here d_o is the distance the shelteree is located from the shelter entrance, U is the shock velocity, u_{eo} is the initial entrance velocity as defined by adiabatic inflow conditions, and u_{jo} is the initial jet velocity at the location d_o . The actual loading on

a shelteree also depends on his orientation relative to the flow direction which is always assumed to be horizontal. During the short diffraction phase it is assumed that the load is also horizontal, its magnitude being equal to the product of the pressure times the projected area. A value of 7 sq ft for projected area is used for a typical shelteree in the upright position. During the drag phase of the loading a person experiences both drag (horizontal force) and lift (vertical force). The magnitudes of these loads vary with the orientation. Reference 48 reports data for the drag on people in the upright and prone positions. Also given is the maximum lift that may occur.

Based on these few data points and on the typical aerodynamic behavior expected for cylindrical bodies (Ref. 49) the load variation for shelterees with orientation is constructed. The drag and lift forces are normally defined as

$$D = C_D q A \quad (5.24)$$

$$L = C_L q A .$$

Here $q = \frac{1}{2} \rho u^2$ is the dynamic pressure, A is a representative area for the body under consideration and C_D and C_L are the drag and lift coefficient respectively. An alternate representation is in terms of drag area A_D and lift area A_L , where

$$\begin{aligned} A_D &= D/q \\ A_L &= L/q . \end{aligned} \quad (5.25)$$

It is in this form that the data of Ref. 48 are given. We assume that the lift area varies as the sine of twice the angle of attack 2α having its maximum at $\alpha = 45$ deg and being zero at $\alpha = 0$ deg and $\alpha = 90$ deg. The drag area is assumed to vary as $\sin^2 \alpha$. For calculation purposes these variations are expressed in terms of the angle θ , which is defined by the angle between the vertical and longitudinal axis of the shelteree (see Fig. 5.1).

The angle of attack is defined in terms of θ as

$$\alpha = \theta - \frac{\pi}{2} .$$

The equations for drag and lift are

$$\begin{aligned} A_D &= A_{Dmin} + (A_{Dmax} - A_{Dmin}) \sin^2 \left(\theta - \frac{\pi}{2} \right) \\ A_L &= A_{Lmax} \cdot \sin (2\theta - \pi) \end{aligned} \quad (5.26)$$

The values of the maximums and minimums are given by Ref. 48, based upon a weight of 165 lb and an average height of 4.9 ft.

$$A_{Dmin} = 1.2 \text{ sq ft}$$

$$A_{Dmax} = 9.0 \text{ sq ft}$$

$$A_{Lmax} = 2.5 \text{ sq ft}$$

From this discussion it becomes clear that the earlier presented load diagram (Fig. 5.7) only represents the net load on a shelteree during the diffraction phase. The remainder of the diagram is simply a presentation of dynamic pressure in the shelter. The total load is calculated by combining vectorially the products $D = qA_D$ and $L = qA_L$. Obviously the value of q is a function of the shelteree's position (distance from the entrance) and time, while the values of A_D and A_L are functions of orientation only.

With the currently available data it is possible to calculate loadings for positions from 10 to 80 ft from the entrance and located along the centerline of the entrance opening. Blast wave overpressures between 10 to 50 psig may be considered.

5.2.2 Determination of Point of Application

No aerodynamic information with regard to moment coefficients or what is equivalent the point of force application (center of pressure) is available for shelterees. In the current calculations it was assumed that the drag force is always applied in the center of the projected area normal to the horizontal flow velocity.

Thus

$$\Delta = \left[h/2 - d_1 \right] \cos\theta + \frac{1}{2} \left[S_1 - S_2 \right] \sin\theta \quad (5.27)$$

No point of application for the lift force is specified. This is equivalent to assuming that the lift force L is at all times acting directly through the center of gravity, or that $\delta = 0$ (see Fig. 5.1). Thus the aerodynamic moments computed are based only on the drag component of the load which is normally much larger than the lift.

5.3 TUMBLING MAN SURVIVABILITY RESULTS

The results of the tumbling man analysis are presented. The computer program discussed in Appendix E generated all the results presented here. The loadings on the shelteree are those described in Subsection 5.2, the governing equations of motion are those presented in Subsection 5.1. For prescribed values of the

weapon (MT size),
shelter,
position,
shelteree orientation (standing, prone, sitting),

we first determine the critical overpressure, P_O^C , which will result in a fatal collision of a single shelteree with a hard constraint (floor, end wall, ceiling), when the blast doors are left off or open during an attack. Then, based on the survivability of the individual shelteree located at various positions throughout the shelter, we construct a percent survivability versus overpressure curve based purely on the blast induced airflow.

Because overpressure appears implicitly in the problem solution, we cannot directly solve for the P_O^C value. Instead, we construct a set of parametric computer runs for a range of overpressure values (10 to 50 psi). From these solutions, the results are interpolated to obtain, within the accuracy of the interpolation, the exact overpressure value which produces fatality.

Parametric computations were made for three initial distances from the shelter opening ($d_o = 10, 40, 70$ ft where d_o is defined in Figs. 5.1 through 5.3); three body orientations (standing, prone, sitting); and four external overpressure levels ($P_o = 10, 20, 30$ and 50 psi). Thus a total of 36 combinations of results were determined. Each of these is labeled with a case number (1 through 36) and the case indicates the parameters considered. The notation is as follows:

Orientation Code	{	U ... <u>U</u> pright (standing)
		P ... <u>P</u> rone
		S ... <u>S</u> itting
Initial Position in Shelter Code	{	E ... man near shelter <u>E</u> ntrance
		M ... man <u>M</u> idway into shelter
		W ... man near end <u>W</u> all

The case 50-P-M refers to 50 psi external overpressure with the man lying Prone located Midway into the shelter. The first character denotes the pressure level, the second character-orientation, and the third character the position in the shelter.

The parameters selected for study are listed as follows:

Man Orientation	\bar{I} (lb-sec ² -ft)	m (lb-sec ² /ft)	S_1 (ft)	S_2 (ft)	d_1 (ft)	h (ft)	μ
Standing	8.58	5.16	0.29	0.625	3.200	5.770	0.55
Prone	8.58	5.16	3.20	2.550	0.458	0.916	0.55
Sitting	3.16	5.16	0	1.550	1.030	3.280	0.55

The values for \bar{I} , m and d_1 were selected from data compiled for an "average man" (Ref. 59). The value for μ , the coefficient of friction, was taken from Ref. 61.

The results of the 36 cases are summarized in Table 5.1. The headings in this table require some additional explanation. The "Problem Description" column refers to the coding notation described earlier in this section. The "Mode Path" column refers to the various modes of motion (one through six) experienced by the tumbling man up to the time of impact. The mode numbers correspond to the motion in Fig. 5.5. For example, 3-5-1 indicates that the subject started rotating (mode 3), then rotated and slid (mode 5) and finally lifted off the ground (mode 1). The "Termination Constraint Reached" column identifies the particular constraint the head contacts at impact. The entry name refers to the fact that the man has come to rest before hitting a constraint. The "Terminal u_x , and u_y " columns list the horizontal and vertical coordinates of the head at impact, or the final at-rest position if a constraint is not reached. The reference origin is the same as that used for the measurement of the x,y coordinates of the center of gravity (Fig. 5.4). The "Terminal v_x and v_y " columns contain the horizontal and vertical velocities of the head at impact, or the final at-rest position, if a constraint is not reached. The "Terminal $v_x^2 + v_y^2$ " column refers to the vector magnitude of the head velocity at impact.

Table 5.1 summarizes all the important results of the calculations, however, it is of further importance to display orientation and transient trajectories of several representative cases. The cases we selected to plot are: 30-U-M, 30-P-M, 30-S-M, 10-U-M, 10-P-M, and 10-S-M. These give representative results for a man situated initially midway in the shelter, subject to both a low and high overpressure loading, and for the three different body orientations considered, upright, prone and sitting.

TABLE 5.1
SUMMARY OF PARAMETRIC STUDY

Problem * Description	Mode Path	Termination Time (sec)	Termination Constraint Reached	Terminal u_x (ft)	Terminal u_y (ft)	Terminal v_x (fps)	Terminal v_y (fps)	Terminal $(v_x^2 + v_y^2)^{1/2}$ (fps)	Case No.
50-U-E	3-5-1	0.57	Wall	70.0	1.80	+ 201	+ 11	201.3	1
50-U-M	3-5-1	0.49	Floor	30.1	0	111	- 16.3	112.2	2
50-U-W	3-5-1	0.35	Floor	10.2	2.40	58.4	- 15.5	60.4	3
50-P-E	2-2	3.10	None	42.4	0.45	0	0	0	4
50-P-M	2-2	2.32	None	39.3	0.45	0	0	0	5
50-P-W	2-2	0.57	Wall	10.0	0.45	11.8	0	11.8	6
50-S-E	3-5-1	0.54	Floor	28.1	0	81.0	- 24.9	84.7	7
50-S-M	3-5	0.93	Wall	40.0	1.10	60.2	- 5.4	60.4	8
50-S-W	3-5	0.47	Wall	10.0	0.81	28.4	- 12.7	31.1	9
30-U-E	3-5-1	0.60	Wall	70.0	0.85	184.0	5.2	104.0	10
30-U-M	3-5-1	0.49	Floor	26.2	0	99.7	- 15.7	101.0	11
30-U-W	3-5-1	0.40	Floor	10.0	1.90	55.2	- 16.2	57.5	12
30-P-E	2-2	1.98	None	28.8	0.45	0	0	0	13
30-P-M	2-2	2.10	None	30.6	0.45	0	0	0	14
30-P-W	2-2	0.75	Wall	10.0	0.45	8.05	0	8.05	15
30-S-E	3-5-1	0.55	Floor	26.7	0	65.0	- 22	68.6	16
30-S-M	3-5	0.53	Floor	14.9	0	42.5	- 5.2	42.8	17
30-S-W	3-5	0.54	Wall	10.0	1.30	27.6	- 14.3	31.1	18
20-U-E	3-5-1	0.64	Wall	70.0	0.46	165.0	- 4.7	165.1	19
20-U-M	3-5-1	0.50	Floor	24.7	0	92.3	- 14.1	93.3	20
20-U-W	3-5-1	0.42	Wall	10.0	1.60	51.6	- 17.9	54.6	21
20-P-E	2-2	1.70	None	22.6	0.45	0	0	0	22
20-P-M	2-2	1.76	None	21.0	0.45	0	0	0	23
20-P-W	2-2	1.24	None	9.5	0.45	0	0	0	24
20-S-E	3-5-1	0.57	Floor	26.3	0	52.7	- 17.3	55.4	25
20-S-M	3-5	0.53	Floor	13.4	0	35.4	- 9.8	36.7	26
20-S-W	3-5	0.59	Wall	10.0	1.90	25.8	- 13.8	29.2	27
10-U-E	3-5-1	0.82	Wall	70.0	0.82	103.6	- 3.8	103.6	28
10-U-M	3-5-1	0.48	Floor	15.1	0	62.1	- 18.7	64.8	29
10-U-W	3-5-1	0.52	Floor	9.8	0	39.2	- 21.3	44.6	30
10-P-E	2-2	1.25	None	13.3	0.45	0	0	0	31
10-P-M	2-2	1.12	None	9.1	0.45	0	0	0	32
10-P-W	2-2	1.00	None	6.7	0.45	0	0	0	33
10-S-E	3-5-1	0.46	Floor	15.9	0	40.4	- 9.8	41.5	34
10-S-M	3-5	0.67	Floor	12.1	0	20.1	- 14.5	24.7	35
10-S-W	3-5	0.94	Floor	8.8	0	14.0	- 17.8	22.6	36

*The first entry denotes pressure level; the second, orientation; and the third, the position in the shelter.

Termination Constraint Reached: U ... Upright (standing); P ... Prone; S ... Sitting

Position Code: E ... initial position near Entrance; M ... man initially Midway into shelter; W ... man initially near end Wall

The orientation type plots (Figs. 5.8, 5.11, 5.13, and 5.16) provide a sequential motion account of the man's flight from his at-rest position to the terminal position. The overview is obtained by plotting chronological successive coordinates of the two points A,B which define the end points of a centerline passing through the man's center of gravity. By connecting these points with a line, the orientation history of the centerline distance \overline{AB} can be traced. To curtail cluttering, a limited number of plot points were selected from the total integrated trajectory. The vertical and horizontal scales of the orientation plots (normalized by the model height h) are not in the same proportion. This results in a distortion of the plots in that the line element \overline{AB} appears to stretch or contract as the body rotates into different positions. The prone orientation plots are omitted because the man remains prone throughout the time record.

The transient trajectory type plots (Figs. 5.9, 5.10, 5.12, 5.14, 5.15 and 5.17) provide a time history of the horizontal and vertical velocity and displacements of the man's head (point A in Fig. 5.4). The displacement plots are normalized by the maximum head displacement (peak absolute horizontal or peak absolute vertical component value, whichever is largest). The velocity plots are normalized by the maximum head velocity (peak absolute horizontal or peak absolute vertical component value, whichever is largest). The normalization constants are indicated on each figure.

5.4 INTERPRETATION OF RESULTS FOR SURVIVABILITY DETERMINATION

5.4.1 Impact Criterion

Before converting the parametric results of Table 5.1 into survivability information, we need a fatality definition suitable for the head velocity components just prior to impact with a hard constraint. According to Ref. 50 an impact velocity 27.9 fps has a 95 percent probability of being fatal. This critical impact velocity is for a normal impact in the absence of any substantial tangential velocity (V_x).

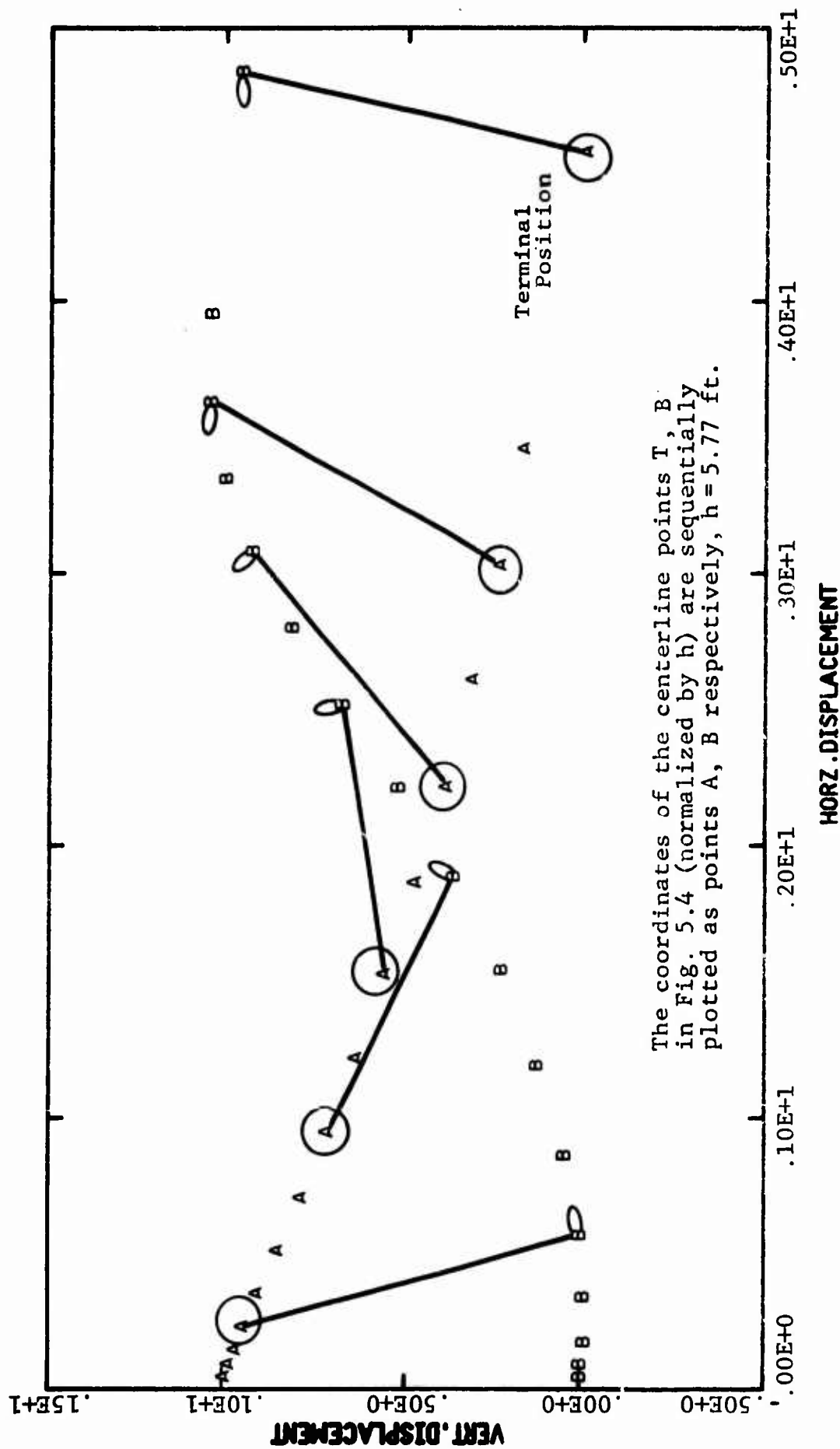


Fig. 5.8 TUMBLING MAN CENTERLINE (A-B) SPACIAL TRAJECTORY
(Problem 30-U-M)

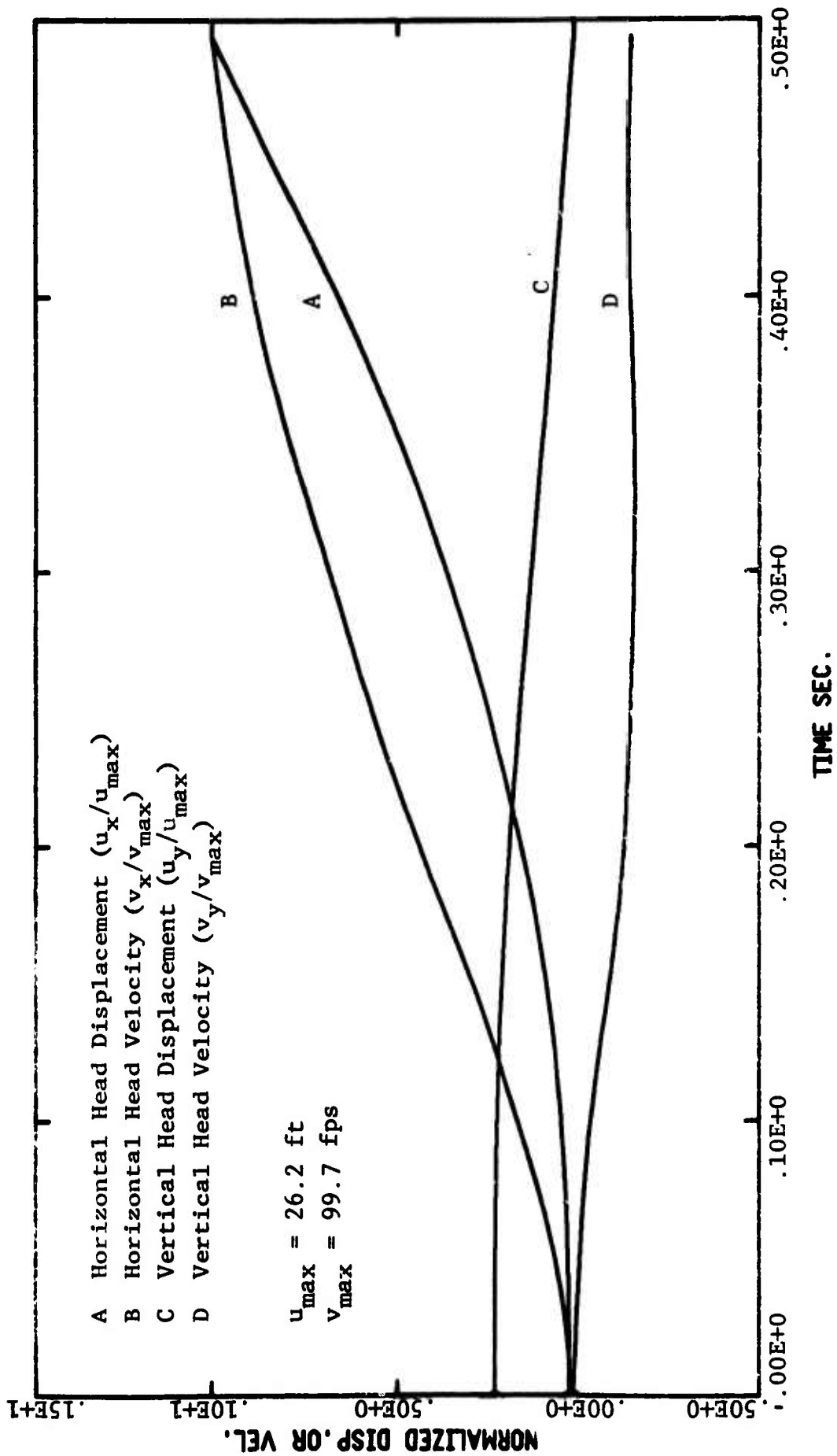


Fig. 5.9 TUMBLING MAN TIME TRAJECTORY
(Problem 30-U-M)

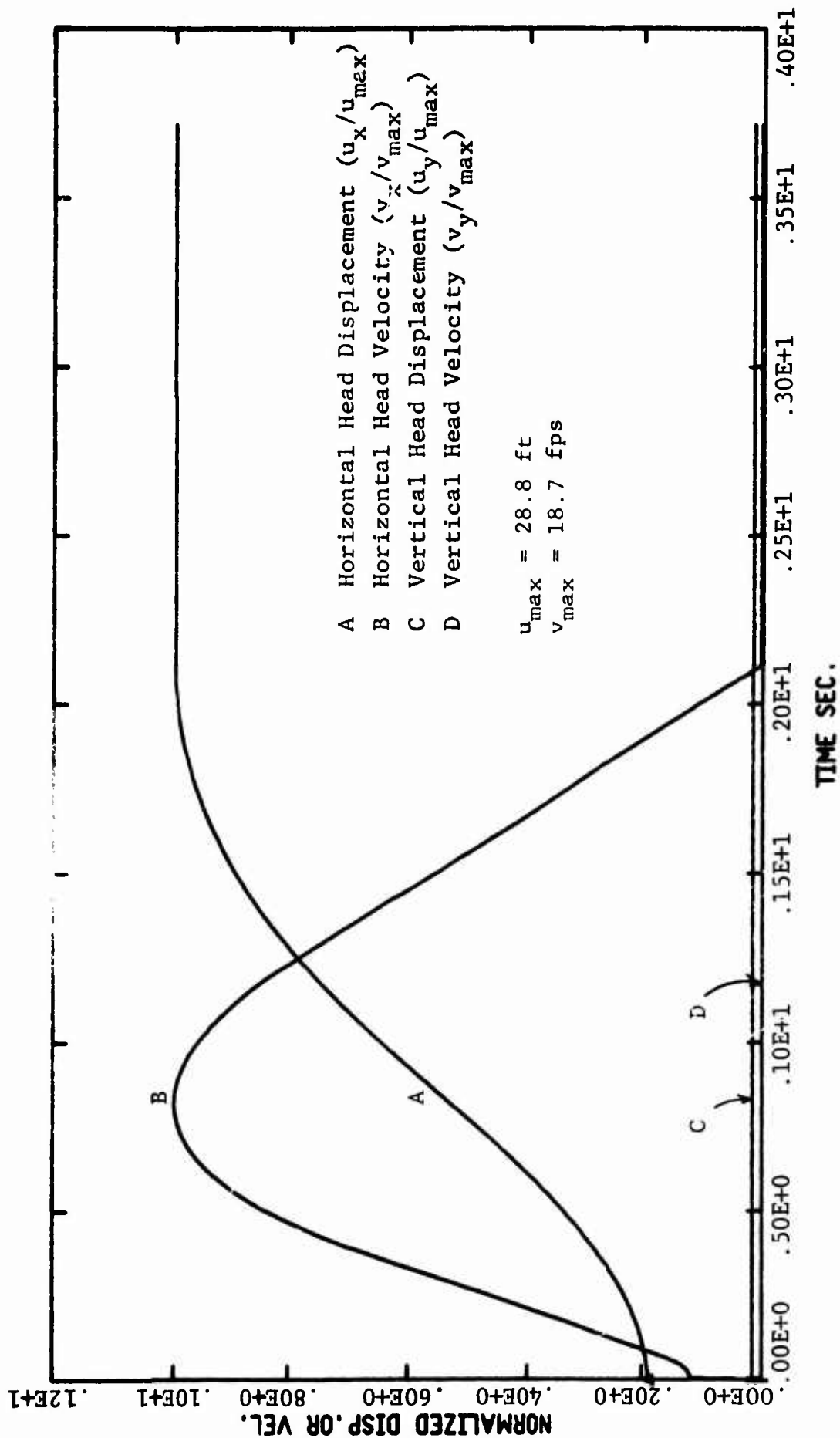


Fig. 5.10 TUMBLING MAN TIME TRAJECTORY
(Problem 30-P-M)

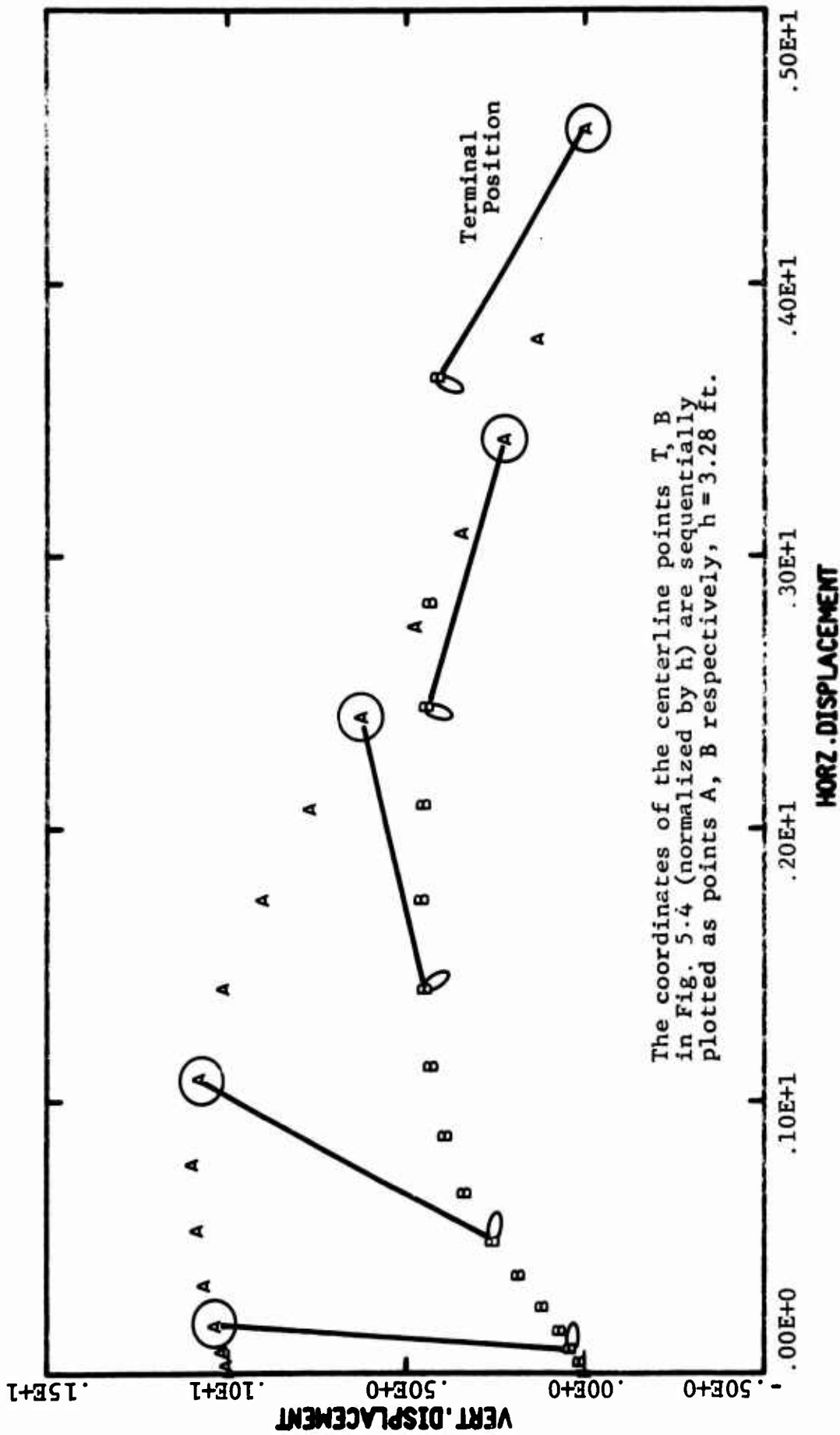


Fig. 5.11 TUMBLING MAN CENTERLINE (A-B) SPACIAL TRAJECTORY
(Problem 30-S-M)

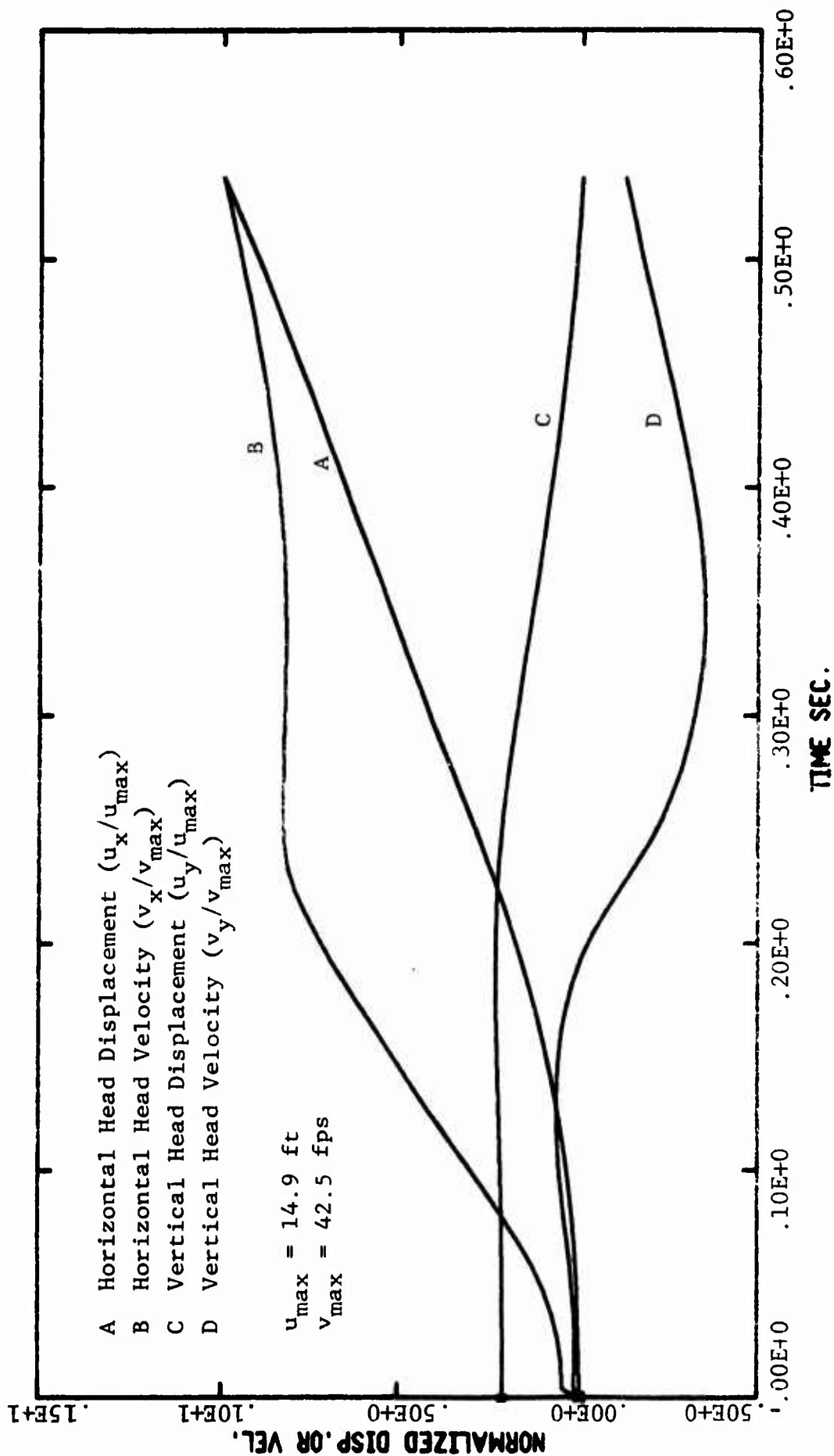


Fig. 5.12 TUMBLING MAN TIME TRAJECTORY
(Problem 30-S-M)

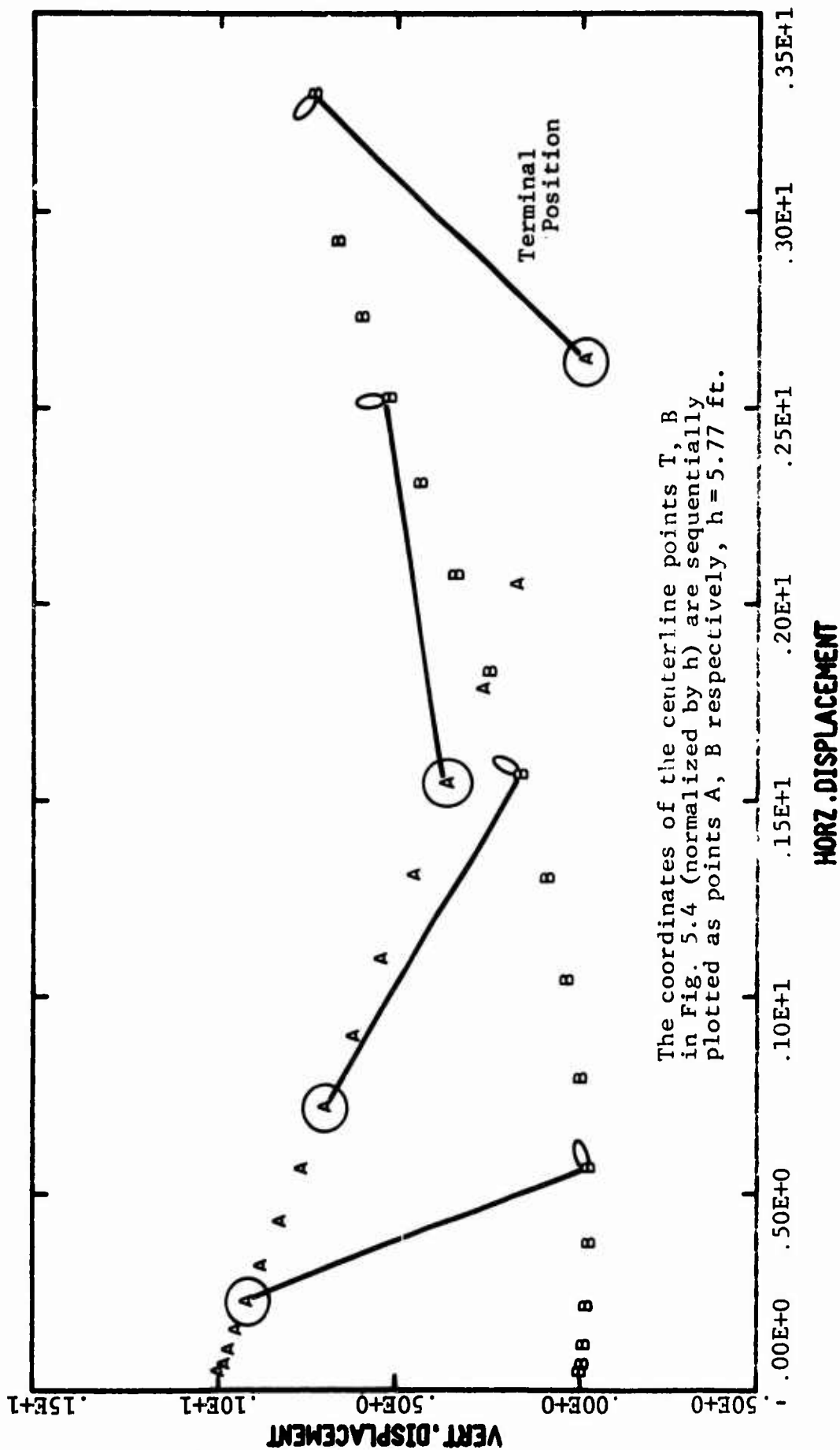


Fig. 5.13 TUMBLING MAN CENTERLINE (A-B) SPACIAL TRAJECTORY (Problem 10-U-M)

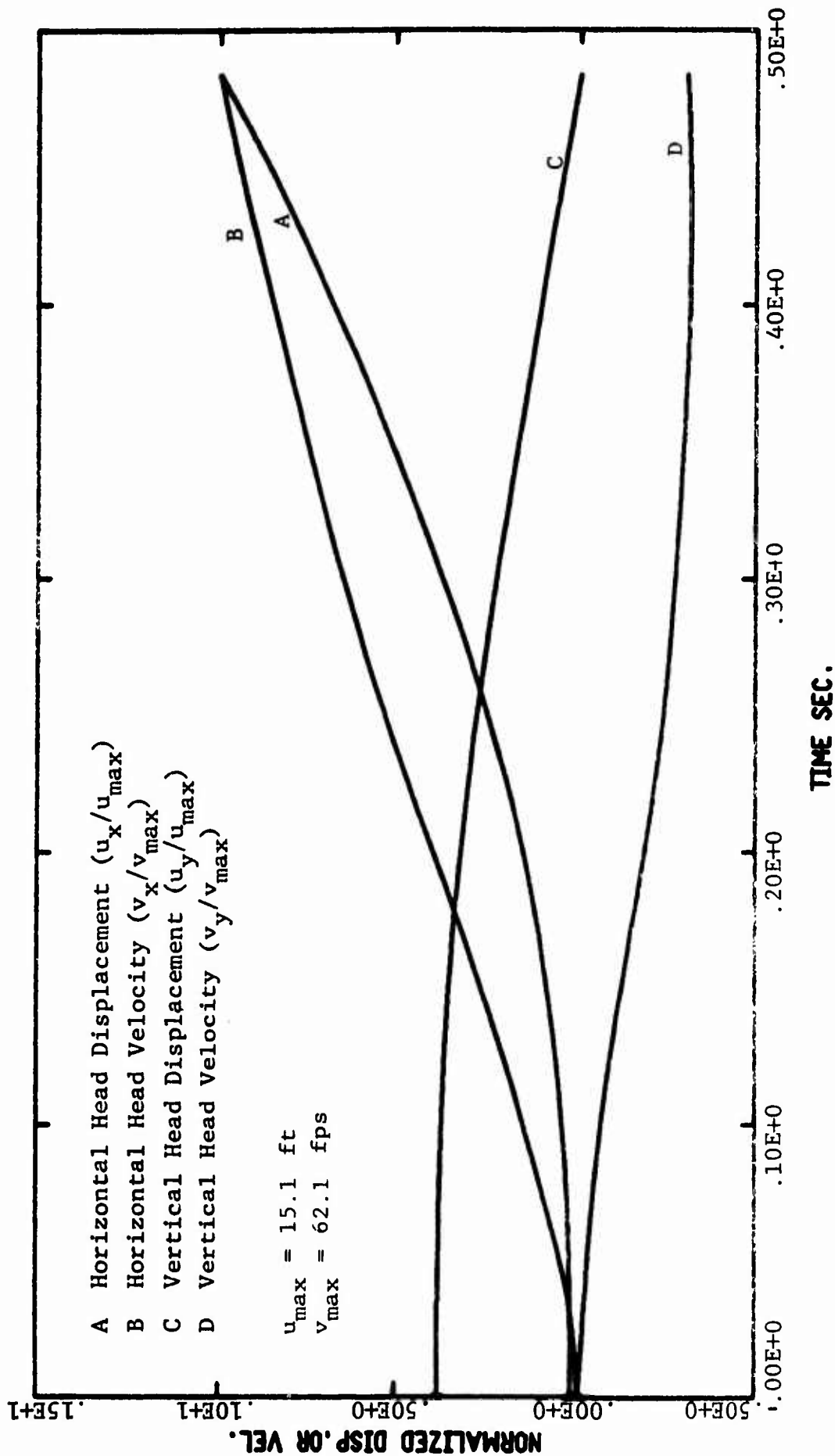


Fig. 5.14 TUMBLING MAN TIME TRAJECTORY
 (Problem 10-U-M)

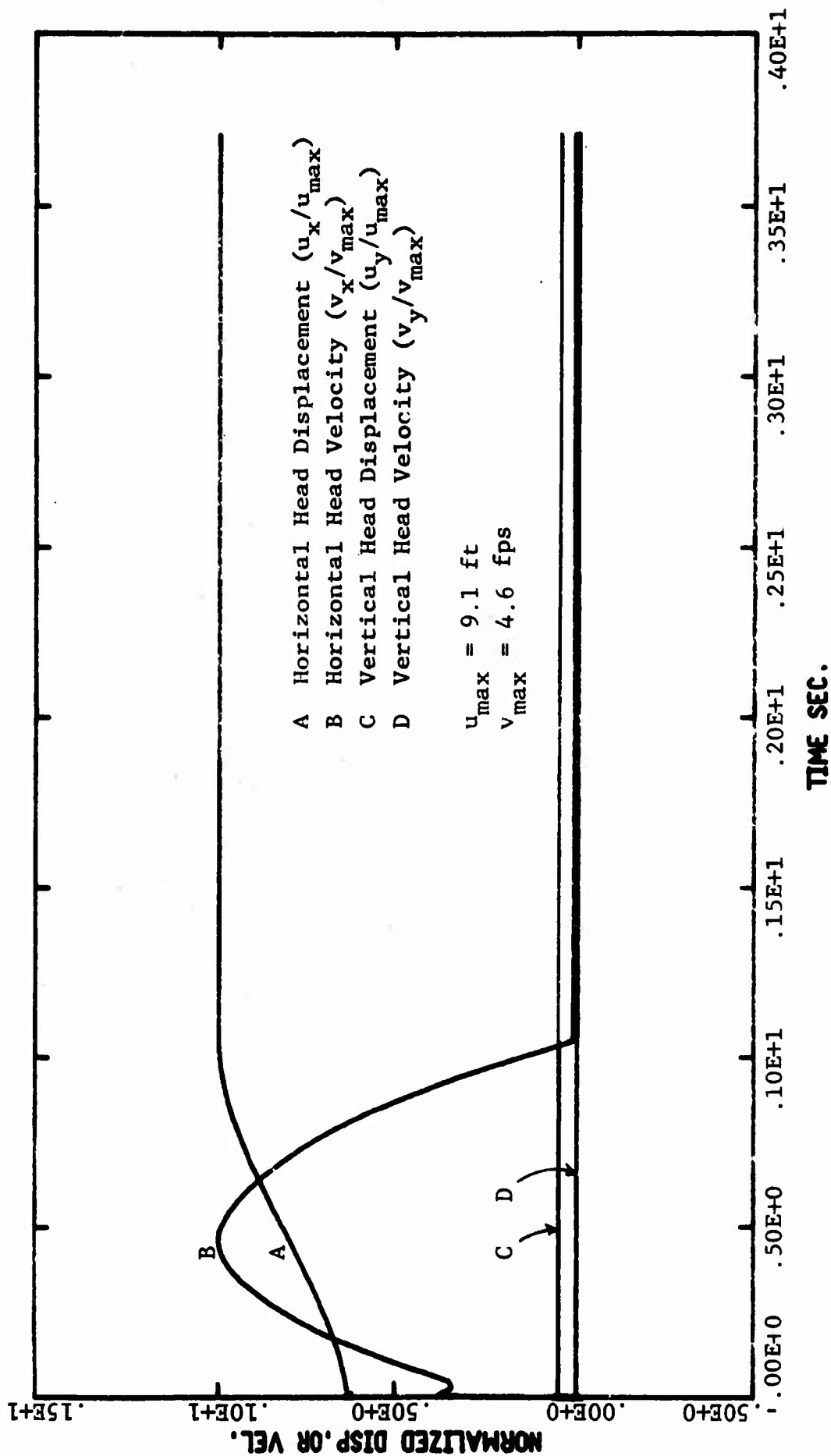


Fig. 5.15 TUMBLING MAN TIME TRAJECTORY
(Problem 10-P-M)

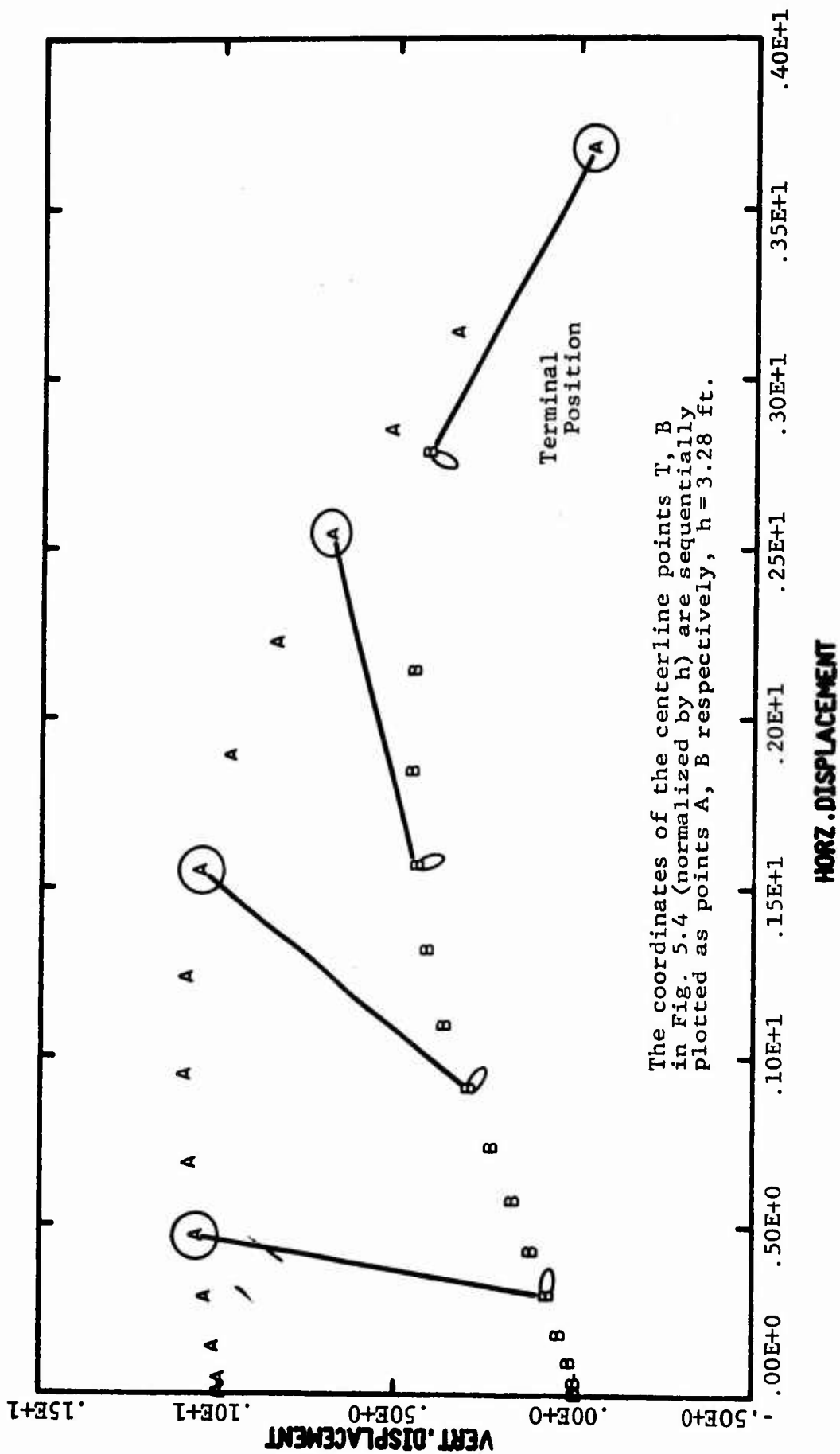


Fig. 5.1b TUMBLING MAN CENTERLINE (A-B) SPACIAL TRAJECTORY
(Problem 10-S-M)

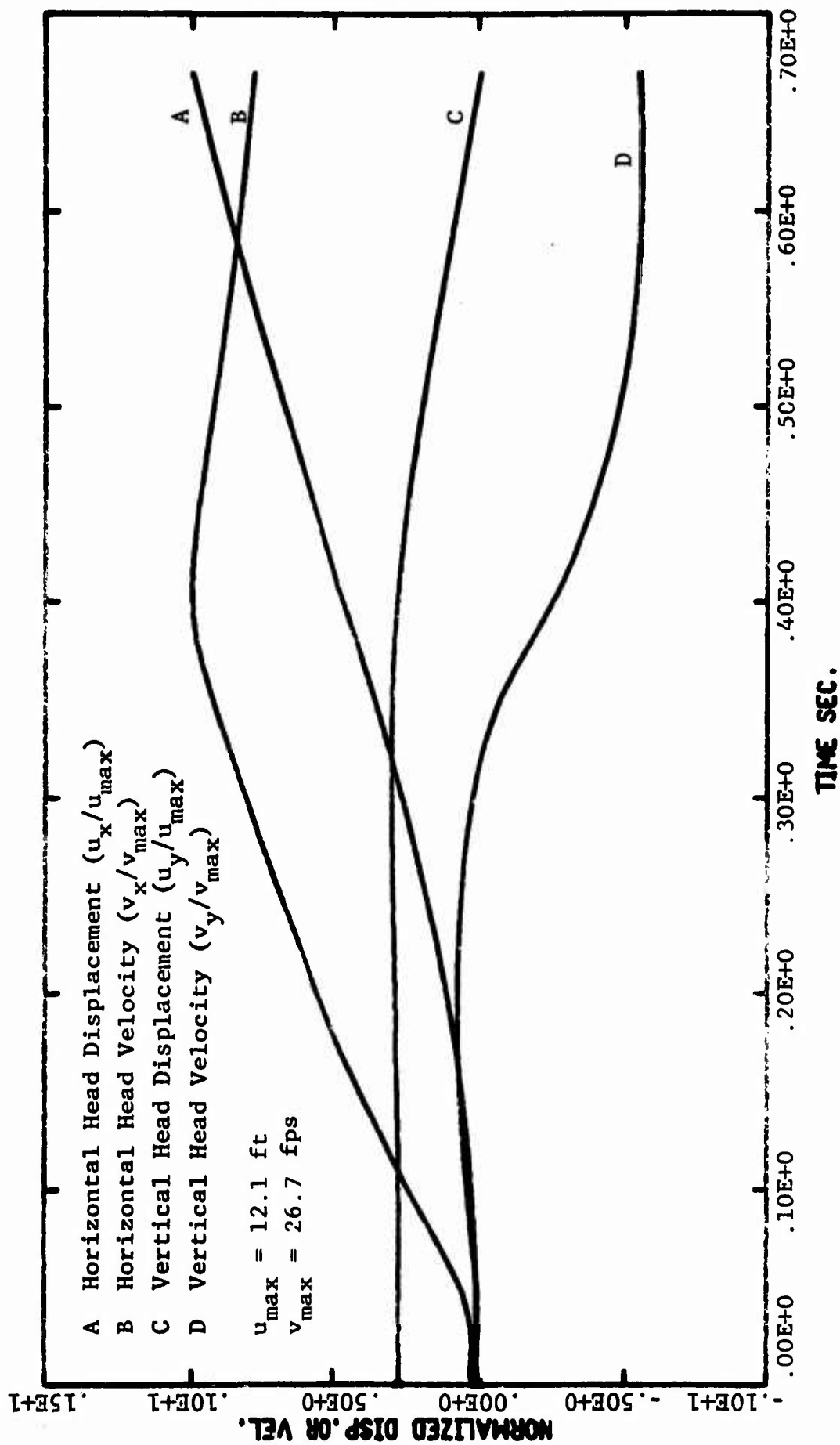


Fig. 5.17 TUMBLING MAN TIME TRAJECTORY
(Problem 10-S-M)

If a tangential component is present, we must have a means of incorporating V_x into the determination of survivability.

To illustrate the importance of the tangential effect, consider an impact situation where the vertical constraint force applied to the head just after contact is F_y . If the body has a sufficiently large tangential velocity (and hence a substantial horizontal momentum) the head will start to slide on the constraint at impact which will result in a horizontal force of $F_x = \mu F_y$ (where μ is the coefficient of friction). Consequently the net vectorial force, F_T , of the head is not just the normal force but rather a larger value of $F_T = (F_x^2 + F_y^2)^{1/2}$.

In order to properly account for the horizontal component in relation to fatality, we need more experimental information in the area of sliding impact effects on survivability. Since this information is unavailable at this time, we choose a simplified approach in which the vector magnitude of the head velocity at impact ($\sqrt{v_x^2 + v_y^2}$) is compared to the 27.9 fps critical velocity cited earlier.

5.4.2 Construction of Survivability Curves

Results given in Table 5.1 are used to construct survivability curves for shelterees located in that portion of the shelter which is directly affected by the jet. The floor area of the shelter studied that is directly affected by the jet is shown in Fig. 3.11. The resulting survivability curves are given in Fig. 5.18 and are constructed using the following approach.

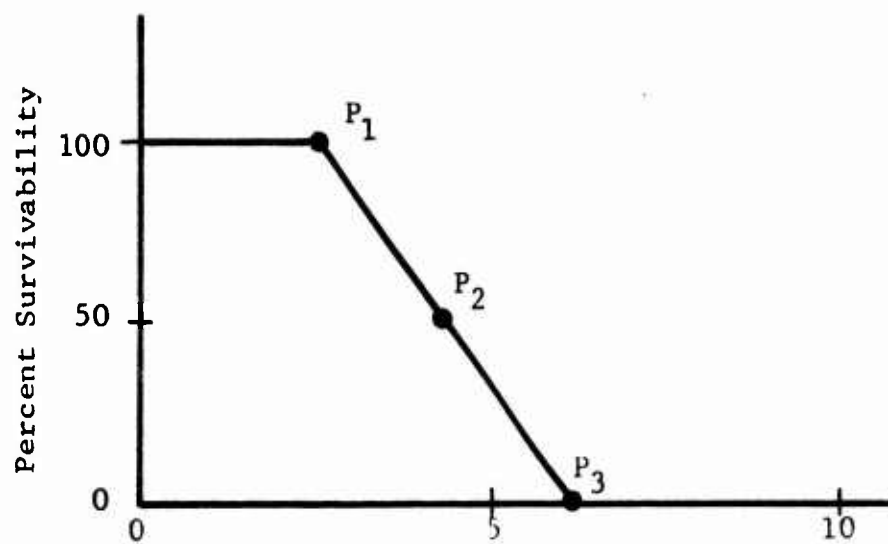
It will be observed from Table 5.1 that for any overpressure level and initial shelteree orientation, corresponding impact velocities decrease as we locate the shelteree further from the entrance. For example, at 10 psi a standing shelteree initially located near the entrance experiences a terminal velocity at 103.6 fps (see Table 5.1). The same shelteree located halfway between the entrance and the rear wall experiences a terminal velocity of 64.8 fps, while the one initially located

near the rear wall experiences 44.6 fps. This variation provides a basis for constructing an approximate survivability curve for the shelter population located in the affected area.

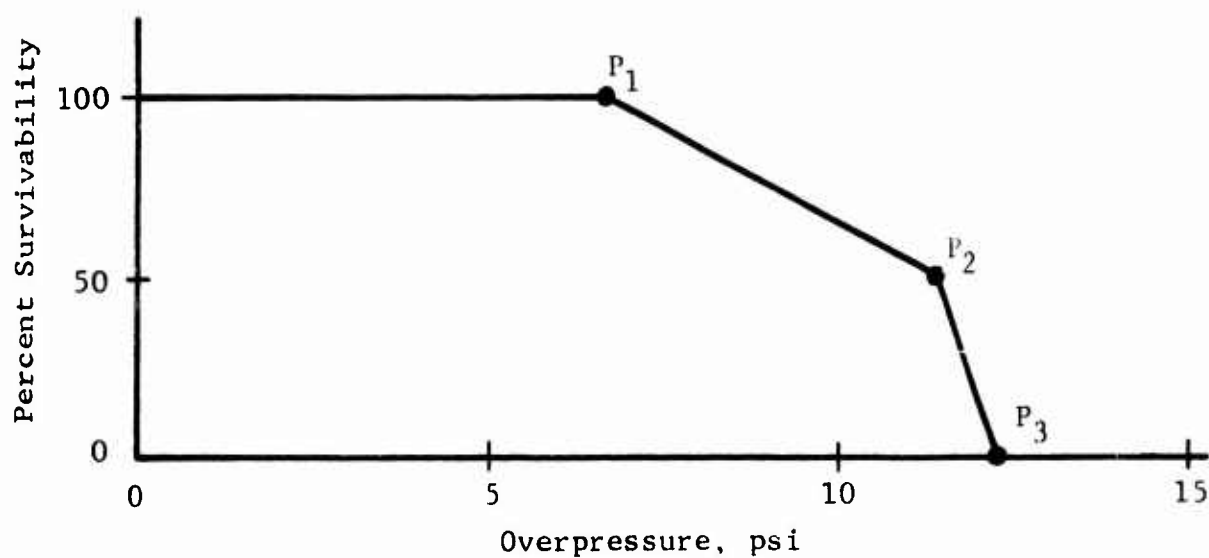
Assuming that shelterees are uniformly distributed, point P_1 (see Fig. 5.18) is established by seeking that overpressure level which will produce a 27.9 fps head impact velocity for a shelteree initially located near the entrance. Point P_2 is established by seeking that overpressure level which will produce a 27.9 fps head impact velocity for a shelteree located halfway between the entrance and the rear wall. Point P_3 is established by seeking that overpressure level which will produce a 27.9 fps head impact velocity for a shelteree located near the rear wall.

A curve for the prone man was not computed because the man does not impact a hard constraint (end wall) before coming to an at-rest position. There are exceptions where impact does occur, but the velocity level is insufficient to produce fatality. The fact that no fatal constraint impacts occur during the 10 to 50 psi range does not mean that there will be 100 percent survivors in an actual blast situation when all the shelterees are initially lying prone. A complicating factor which could alter the prone man velocity trajectory is the fact that the longitudinal sliding mode is not stable. Small eccentricities in the blast loading relative to the man's center of gravity could possibly rotationally slide the man at right angles to this initial head position. The man may then start rolling (similar to a log rolling action) instead of sliding, which of course could result in a completely different conclusion regarding his survivability.

Although we cannot give any reasonable quantitative results regarding survivability, what we can state qualitatively is that his survivability percentage in the initially prone position is substantially higher than either the standing or sitting positions. This conclusion is based on the prone man's velocity trajectory results which indicate that the peak velocity experienced by the man (and hence the impact force, should an object be encountered) is much lower than either of the other two orientations investigated.



(a) Man Initially Standing



(b) Man Initially Sitting

Fig. 5.18 SURVIVABILITY OF TUMBLING MAN AGAINST ENTRANCE JET VELOCITY

APPENDIX A

DESCRIPTION AND COST OF SHELTERS

Shelters considered in this study include two categories: single- and dual-purpose (Table A.1). Those considered herein are not existing structures but, rather, proposed feasible concepts, the physical characteristics of which are described.

A.1 SINGLE-PURPOSE SHELTERS

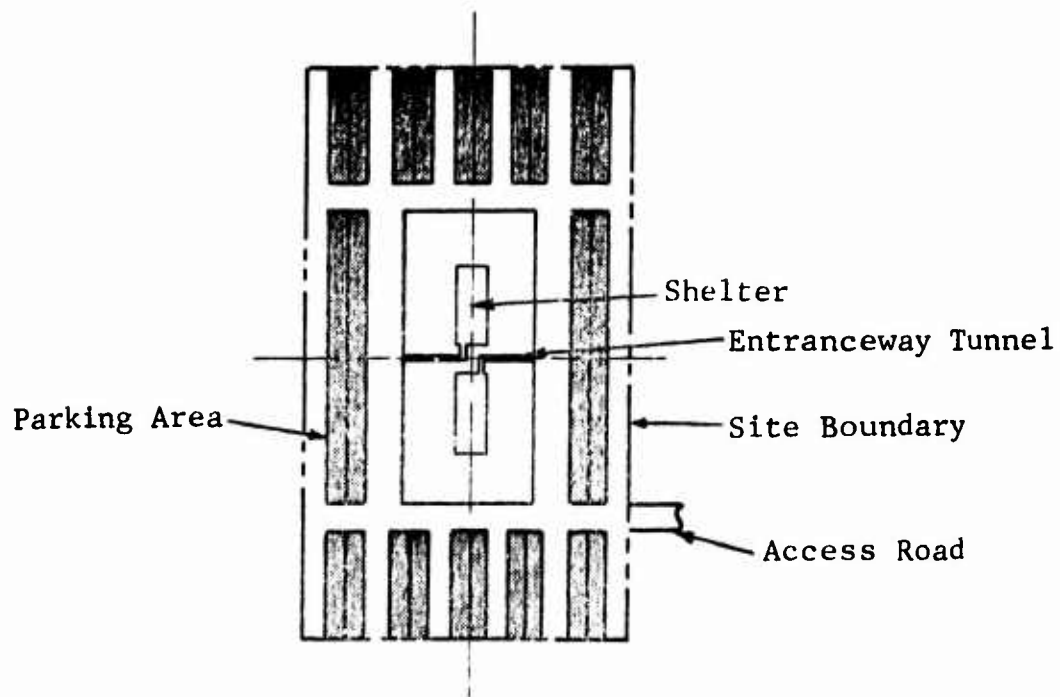
A.1.1 Arch Structures

Arch structures are subdivided with respect to materials of construction into two types: reinforced concrete, and corrugated and plate steel. With respect to "design weapon environment," these structures may be further divided into six categories to resist one of the following weapon environments:

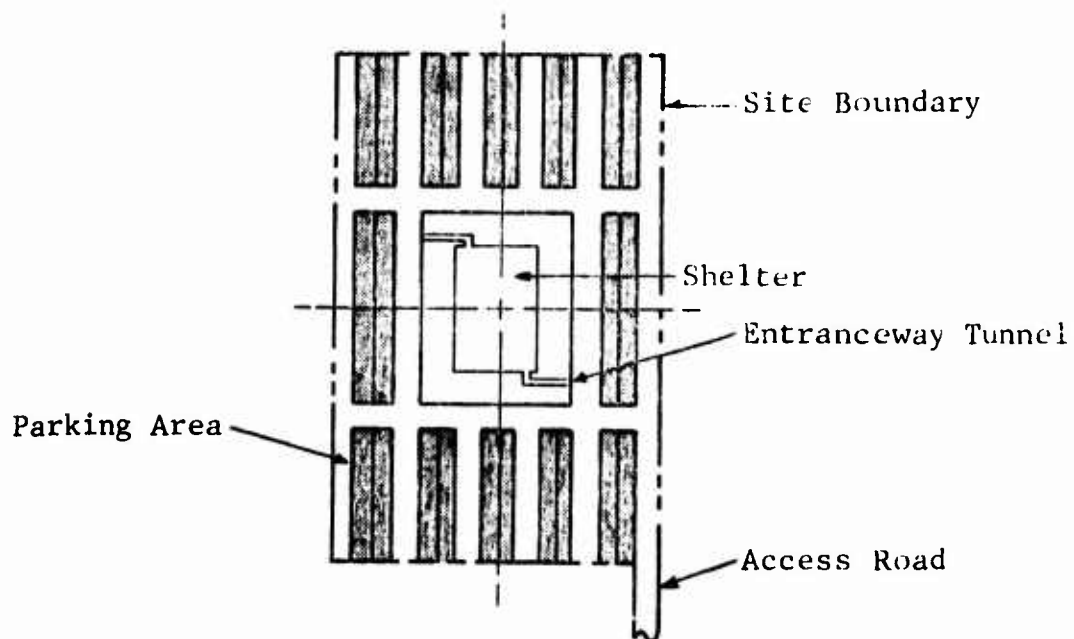
- | | |
|------------------------------|---|
| (a) fallout radiation alone, | |
| (b) 10 psi | } free-field overpressure and associated effects of prompt nuclear thermal and fallout radiation resulting from a single megaton weapon |
| (c) 20 psi | |
| (d) 30 psi | |
| (e) 100 psi | |
| (f) 150 psi | |

These shelters (10 in number) were designed to be located at specific sites (shelter complexes) on the peripheries of large population centers. The basic shelter, a single arch module, is capable of housing 500 persons at approximately 10 sq ft per person. Basic modules are combined to form larger complexes as the need dictates. A typical 1000-man peripheral shelter complex consisting of two basic shelters is shown in Fig. A.1a. Due to imposed siting conditions fires should not pose a serious hazard and for this reason were not specifically considered in their design. Consult Ref.14 for a more detailed description of peripheral shelter systems and their probable costs for midyear 1967.

Preceding page blank



(a) Arch Shelter Complex



(b) Rectangular Shelter Complex

Fig. A.1 SITE PLANS FOR 1000-MAN PERIPHERAL SHELTER COMPLEXES

Shelters (a) through (d) are referred to herein as "low level weapon effects designs." For purposes of comparison they were designed (Ref. 14) using reinforced concrete in one case and corrugated and plate steel in the other. They were also costed for 500- and 1000-man capacities.

Shelters (e) through (f) are referred to herein as "high level weapon effects designs". In general layout they are identical to the previous shelters except that these consist entirely of RC. Also, since single-purpose personnel shelters capable of resisting high overpressures are not of primary interest to Civil Defense, these were costed only for 500-man capacities.

The general configuration of an arch shelter (500-man) is shown in Fig. A.2. It has two levels with the second floor resting on two rows of reinforced concrete columns with footings separate from the rest of the structure. The second floor slab was designed to resist its own weight plus a live load of 150 psf. Location of this shelter relative to the ground surface (burial condition) is shown in Fig. A.3. Basic shelter dimensions and arch shell thicknesses of the structure are given in Fig. A.4 and Table A.2. Construction details are illustrated in Fig. A.5.

Reinforcement steel includes intermediate grade A15, A16, A408, with $f_y = 40,000$ psi for footings, foundation walls and floor slabs, and hard grade reinforcement A15, A16, A408 with $f_y = 50,000$ psi for arch shells and end walls. Welded wire fabric with a yield strength of 65,000 psi is used for slabs on ground. Percentages of main reinforcement are summarized in Table A.3.

Steel arch shelters (Table A.1) for fallout, 10 and 20 psi weapon environments were designed for the use of corrugated 12 gage steel plate with corrugations 2 in. deep and a pitch 6 in. wide. The shell of the 30 psi shelter was designed for the use of 0.5-in. flat plate formed into a circular arch and supported at intermediate positions by means of wide flange beam arch ribs. The basic dimensions of the steel arch shelter are the same as those of the reinforced concrete arch and are given in Figs. A.2 and A.4. Footing dimensions given in Table A.2 also apply to the steel arch.

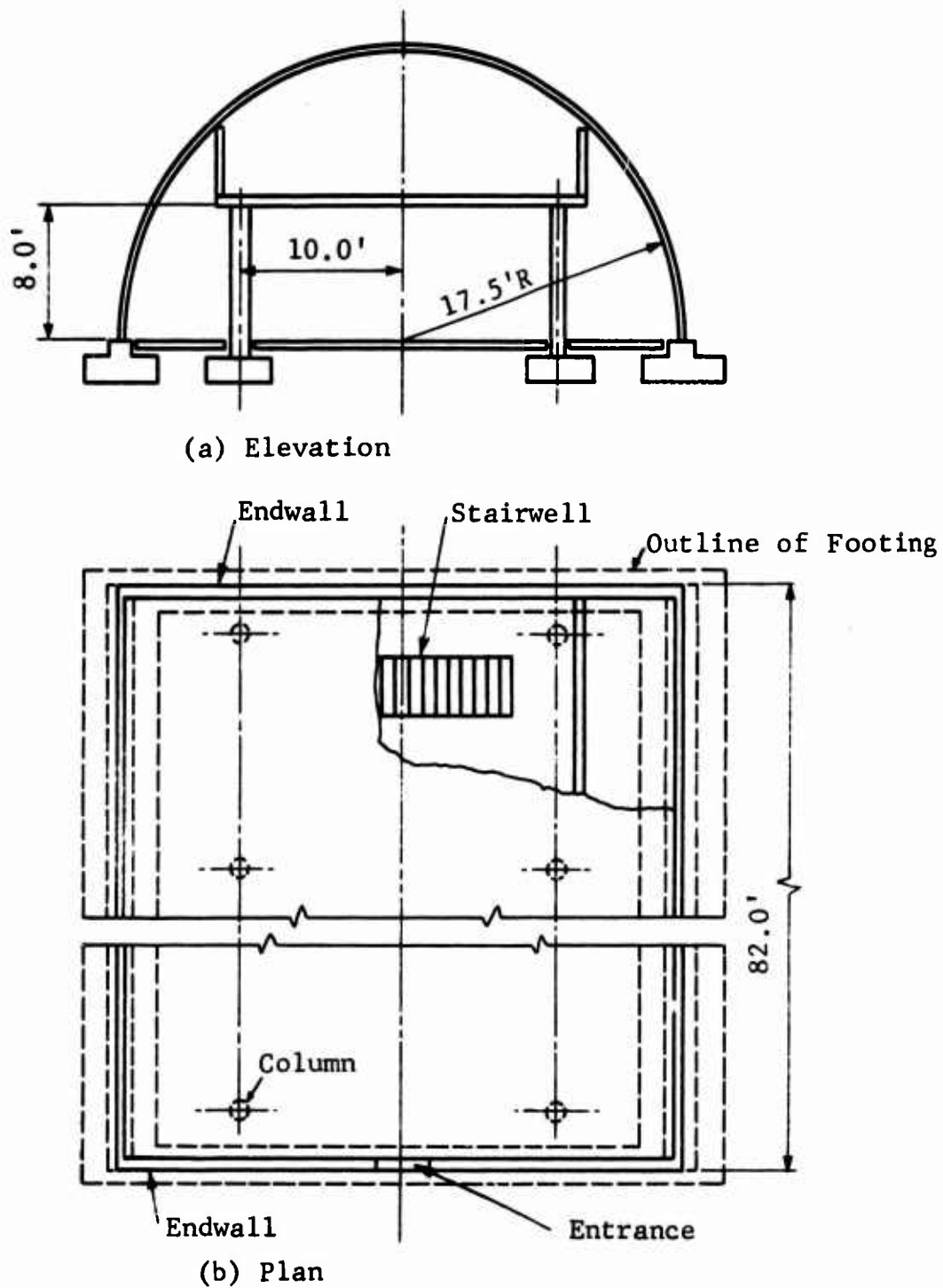


Fig. A.2 GENERAL CONFIGURATION OF BASIC 500-MAN ARCH SHELTER

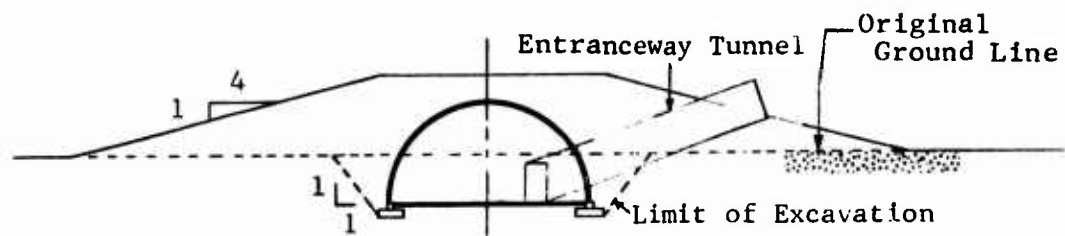
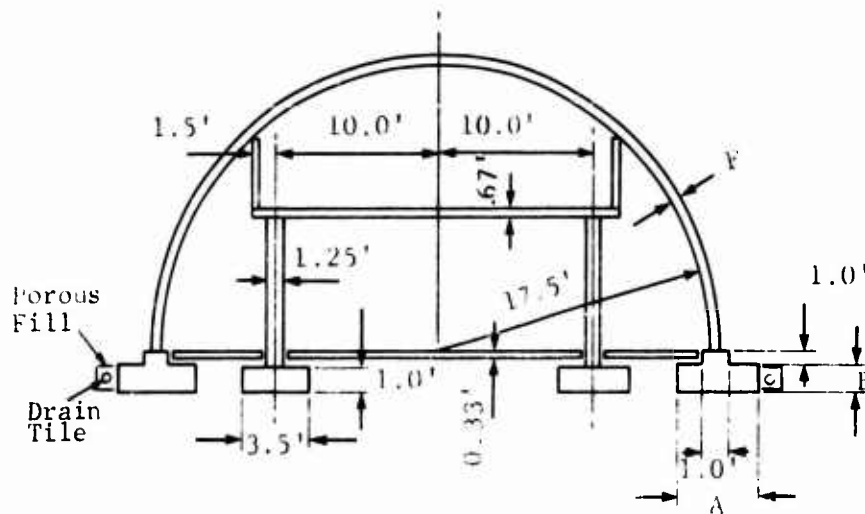
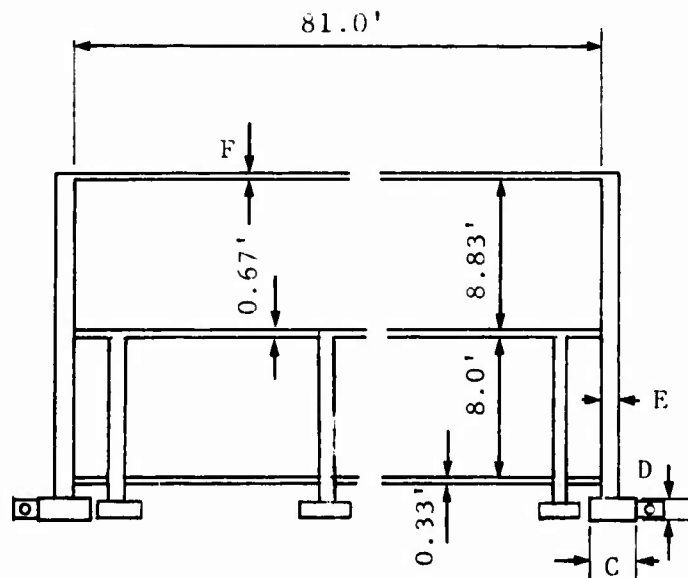


Fig. A.3 ARCH SHELTER LOCATION RELATIVE TO GROUND SURFACE



(a) Transverse Section
(For variable dimensions see Table A.2)



(b) Longitudinal Section

Fig. A.4 BASIC DIMENSIONS OF ARCH SHELTER

TABLE A.2
BASIC DIMENSIONS OF ARCH SHELTERS

Member	Dimensions for Indicated Design Weapon Environments, in.					
	FRE	10 psi	20 psi	30 psi	100 psi	150 psi
Arch Footing Width (A)	33	52	66	81	89	94
Arch Footing Depth (B)	8	10	14	17	22	30
End Wall Footing Width (C)	24	24	26	30	48	54
End Wall Footing Depth (D)	12	12	14	18	28	38
End Wall Thickness (E)	8	8	9	10	35	41
R/C Arch Shell Thickness (F)	4	4	4	4	8	13.5
Steel Arch Shelter Shell Thickness (gage)	12*	12*	12*	0.5**	--	--

FRE - fallout radiation environment (PF = 1000)

* corrugated steel plate } See text for description
** formed flat plate } of arch shells.

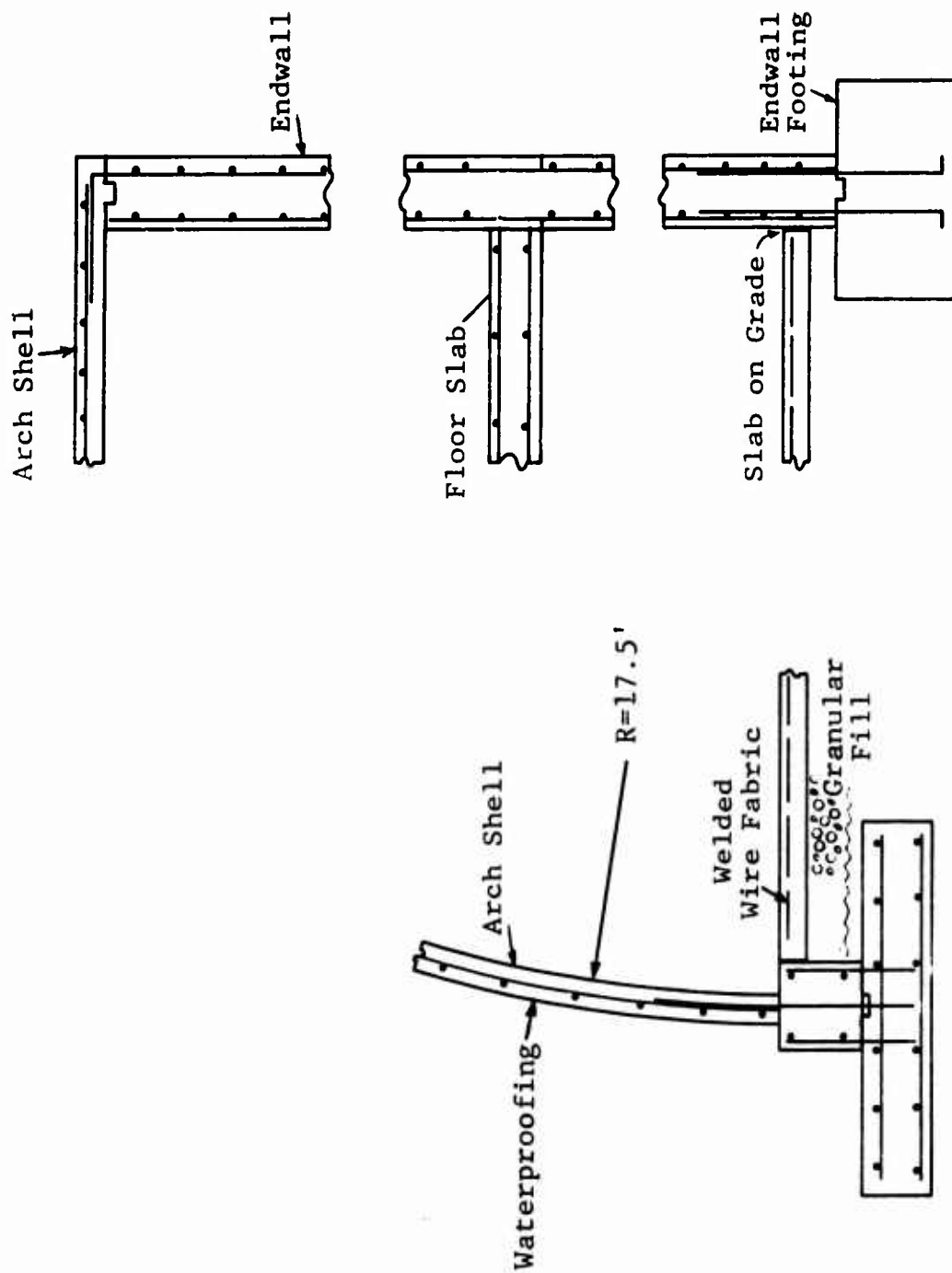


Fig. A.5 CONSTRUCTION DETAILS OF R/C ARCH

TABLE A.3
PERCENT REINFORCEMENT FOR INDICATED STRUCTURAL MEMBERS
(Arch Shelters, Single-Purpose)

Structural Member	Reinf.*	Design Weapon Environment					
		FRE	10 psi	20 psi	30 psi	100 psi	150 psi
Arch Shell	Φ'	1.0	1.0	1.0	1.0	1.0	2.0
Arch Footing	Φ'	0.13	0.13	0.13	0.13	0.25	0.25
	Φ	0.58	0.60	0.96	0.96	1.0	1.0
End Wall	Φ'	0.50	0.50	0.50	0.50	1.0	1.0
	Φ	1.0	1.0	1.0	1.0	1.0	1.0
End Wall Footing	Φ'	0.13	0.13	0.13	0.13	0.25	0.25
	Φ	1.75	1.75	1.75	1.75	1.75	1.75
Interior Floor Slab (second floor level)	Φ	1.5	1.5	1.5	1.5	1.5	1.5
	Φ'	1.5	1.5	1.5	1.5	1.5	1.5
Columns	Φ'	2.0	2.0	2.0	2.0	2.0	2.0
Column Footings	Φ	1.0	1.0	1.0	1.0	1.0	1.0
	Φ'	0.75	0.75	0.75	0.75	0.75	0.75
Lower Level Floor Slab	Φ	0.0025	0.0025	0.0025	0.0025	0.0025	0.0025

* Φ - tension reinforcement

Φ' - compression reinforcement

Note: This table contains percentages of main reinforcement only. Temperature reinforcement used corresponds to ACI Standard 318-63.

A.1.2 Rectangular Structures

As in the case of arch structures, reinforced concrete rectangular structures are subdivided into four design weapon environment categories in terms of ability to resist one of the following weapon environments:

- fallout radiation alone,
- 10 psi, free-field overpressure and associated effects of prompt nuclear, thermal and fallout radiation resulting from a single megaton weapon,
- 20 psi, as above, and
- 30 psi.

These are also "peripheral-type" shelters. They may be located within population centers, however, siting in such a case must correspond to peripheral shelter design criteria (Ref.14). A typical peripheral shelter complex (1000-man capacity) is shown in Fig. A.1b.

The general configuration of this shelter is shown in Fig. A.6. It is a basic 500-man module, exterior and interior walls forming a rectangular grid. Both exterior and interior walls are one-way slabs. The roof member is a two-way slab. Basic dimensions are given in Fig. A.7a and Table A.4. Percentages of reinforcement used in design are given in Table A.5. Reinforcement grades are the same as in the case of arch shelters: intermediate grade for footings and hard grade for walls and roof slabs. The depth of protective soil cover can be taken as 12 in. Figure A.7 also shows how two basic 500-man modules are combined to form a single 1000-man shelter. Construction details are found in Fig. A.8 and the location relative to the ground surface is shown in Fig. A.9.

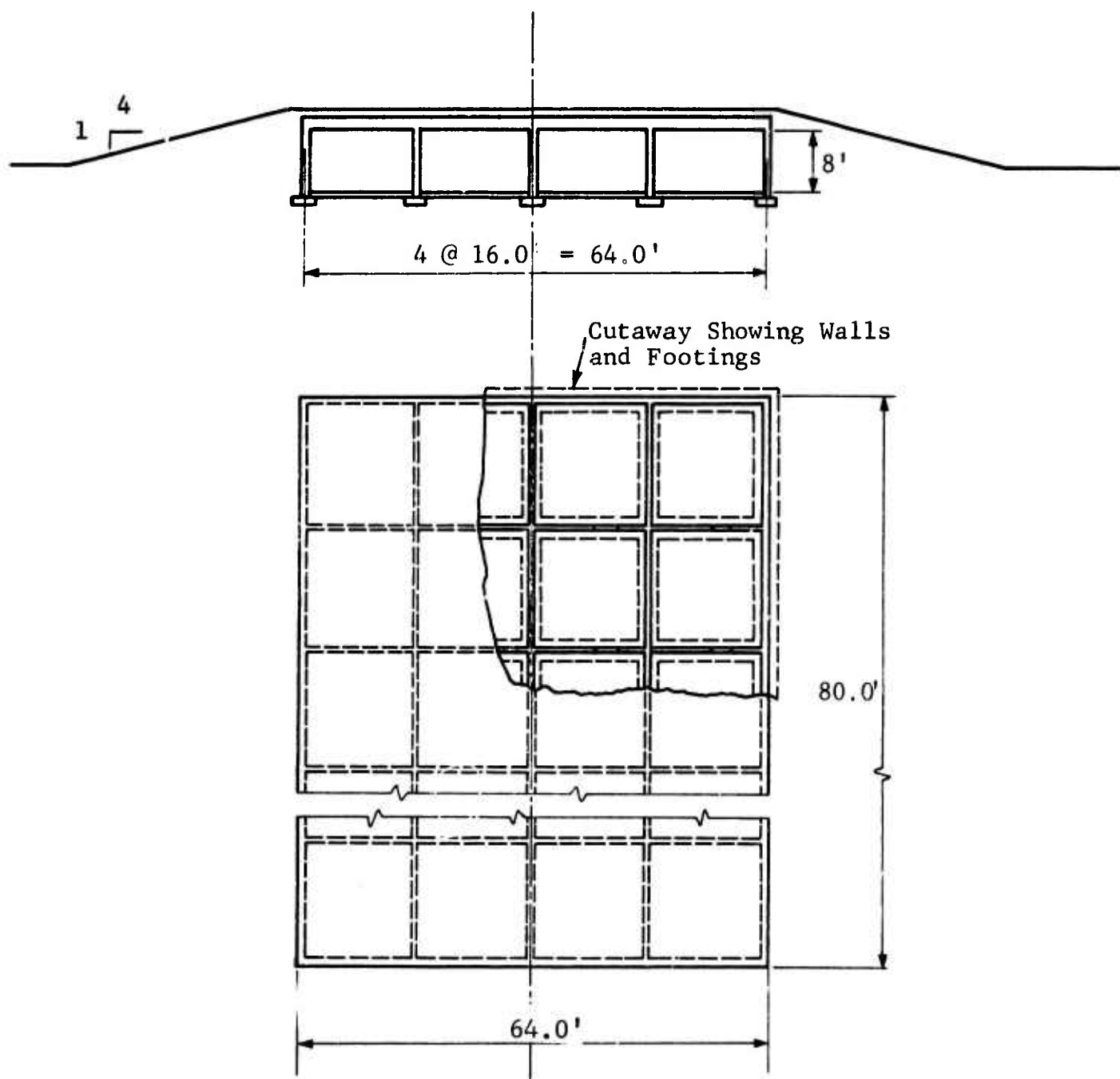
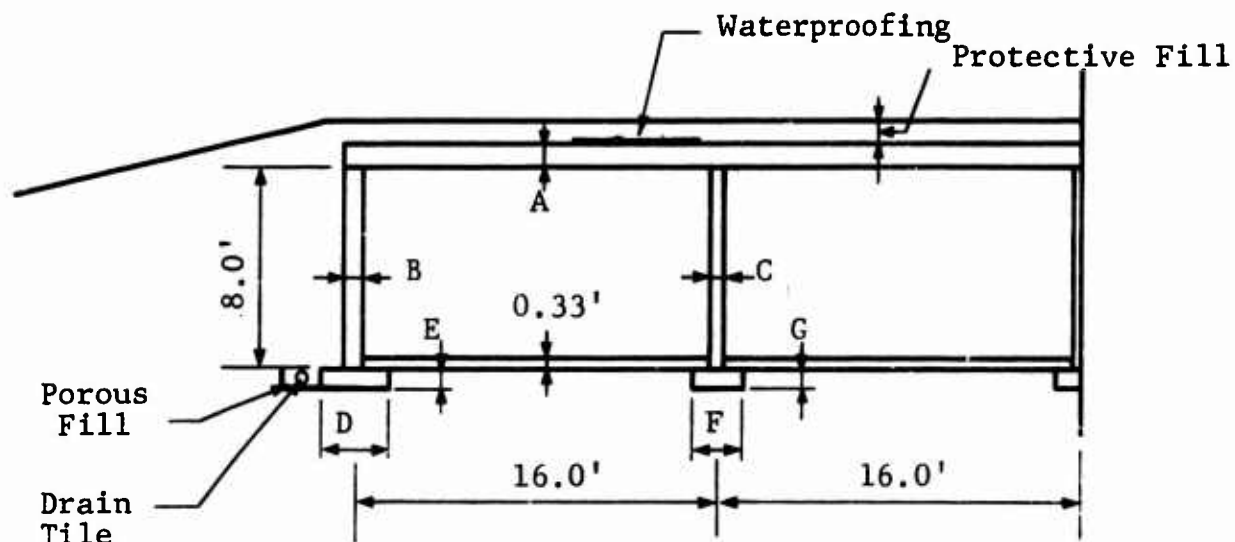


Fig. A.6 GENERAL CONFIGURATION OF BASIC 500-MAN
RECTANGULAR R/C SHELTER



(a) Half-Section Through Shelter
(For symbols see Table A.4)

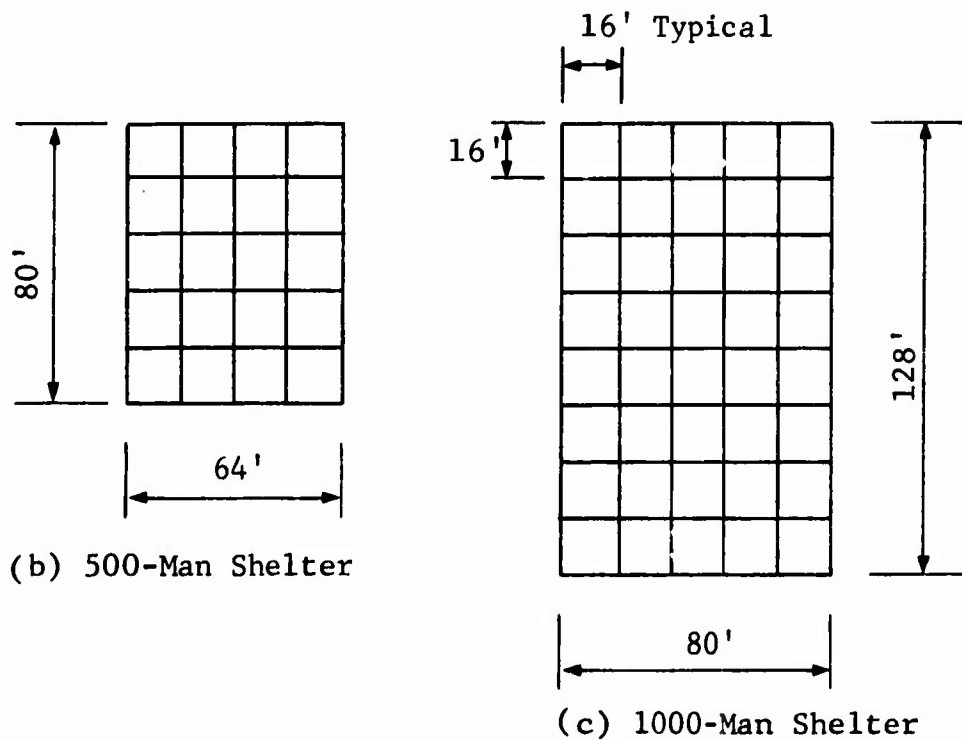


Fig. A.7 BASIC DIMENSIONS OF R/C RECTANGULAR SHELTER

TABLE A.4
BASIC DIMENSIONS OF R/C RECTANGULAR SHELTER

Member	Dimensions for Indicated Design Weapon Environment, in.			
	FRE	10 psi	20 psi	30 psi
Roof Thickness	6	9	12	18
Exterior Wall Thickness	8	8	9	10
Interior Wall Thickness	6	6	6	6
Exterior Footing Width	24	24	27	36
Exterior Footing Depth	8	8	8	8
Interior Footing Width	24	24	24	24
Interior Footing Depth	8	8	8	8

TABLE A.5
PERCENT REINFORCEMENT FOR INDICATED STRUCTURAL MEMBERS
(Rectangular R/C Shelters, Single-Purpose)

Structural Member	Percent Reinforcement*
Roof Slab	$\phi = \phi' = 1.0$ (both directions)
Exterior Wall	$\phi' = 0.5$ (outside reinforcement) $\phi = 1.0$ (inside reinforcement)
Exterior Wall Footing	$\phi_{top} = 0.13$ $\phi_{bottom} = 0.53$
Interior Wall	$\phi = \phi' = 0.75$
Interior Wall Footing	$\phi_{top} = 0.144$ $\phi_{bottom} = 0.576$
Floor Slab	$\phi = 0.0025$

* ϕ - tension reinforcement

ϕ' - compression reinforcement

Note: This table contains percentages of main reinforcement only.
Temperature reinforcement used corresponds to ACI Standard 318-63.

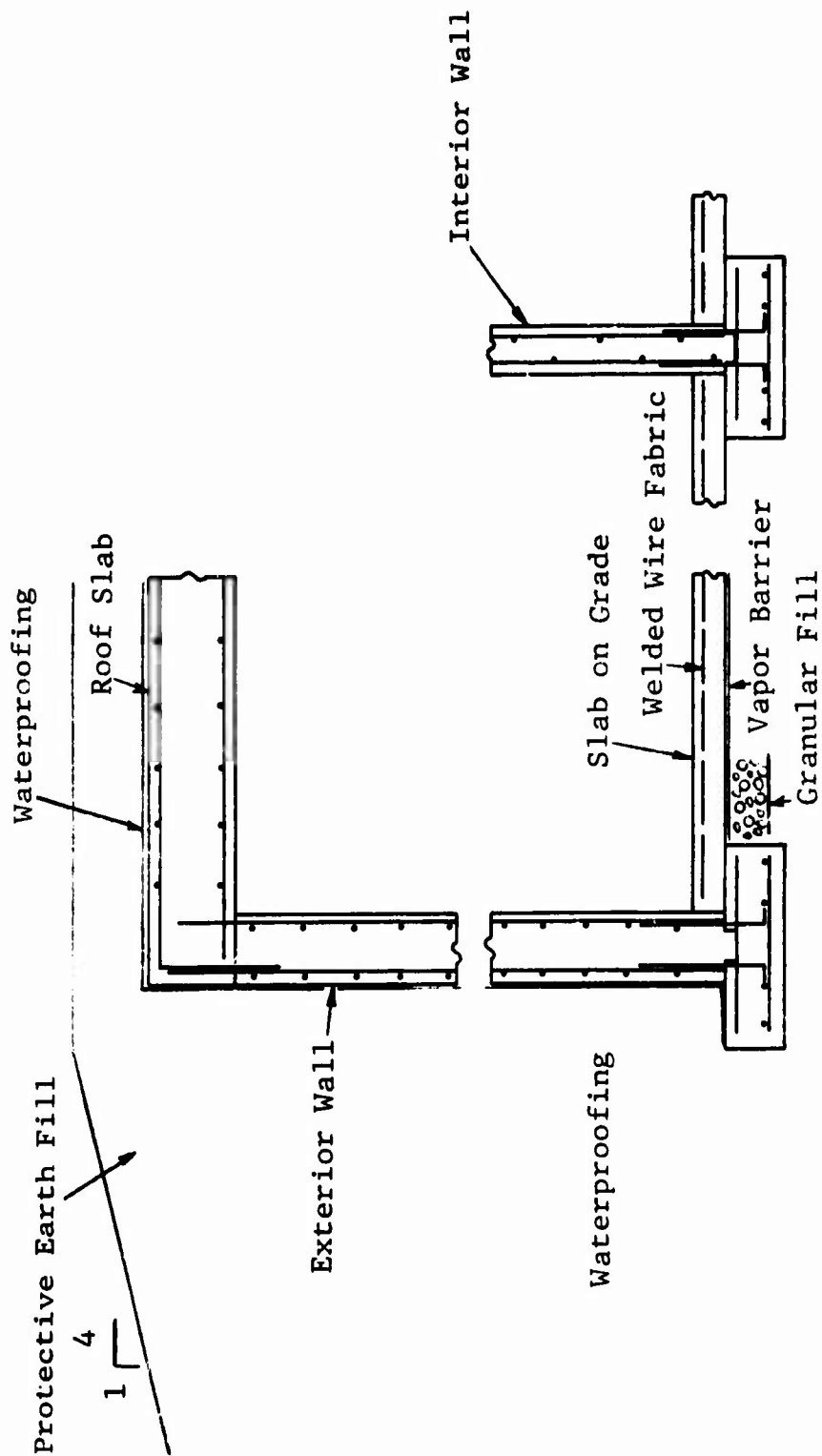


Fig. A.8 CONSTRUCTION DETAILS OF R/C RECTANGULAR SHELTER

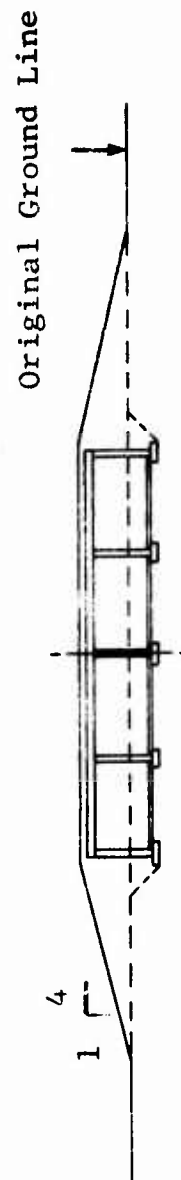


Fig. A.9 RECTANGULAR SHELTER LOCATION RELATIVE TO GROUND SURFACE

A.1.3 Entranceways for Arch and Rectangular Shelters

A.1.3.1 Low Level Weapon Effects Designs

A typical entranceway consists of:

- (1) an underpass type tunnel,
- (2) an internal shelter door,
- (3) an external shelter door (fallout radiation environment only),
- (4) a bulkhead, and
- (5) a blast door (no door is provided in the case of a fallout radiation environment).

Entranceway details are shown in Fig. A.10 and dimensions are given in Table A.6. The tunnel consists of corrugated steel plate section with corrugations 2-in. deep and a pitch of 6-in. The interior door is of standard commercial hollow metal construction, the external door is of stiffened steel plate. Entrance bulkheads are of structural steel plate formed with a 90-in. radius. The exterior blast door is made of two skins of galvanized metal and a core of aluminum honeycomb. The honeycomb is installed with its ribbon direction spanning the 24-in. door width. The design assumes one entranceway for each 500-man (arch or rectangular) shelter unit. The entranceway location relative to a shelter is illustrated in Figs. A.1 and A.3.

A.1.3.2 High Level Weapon Effects Designs

Entranceways for the 100 and 150 psi arch shelters are similar to those described earlier except that these consist of RC cast monolithically with the shelter. Due to high overpressures to be resisted the blast doors are also different. A typical entranceway is illustrated in Fig. A.11. The blast door consists of a structural steel grid filled with concrete. It rests on rails and is mechanically actuated. The blast door detail is shown in Fig. A.12 which also gives the overall dimensions of the entranceway. Dimensions of the entranceway cross section are given in Fig. A.13.

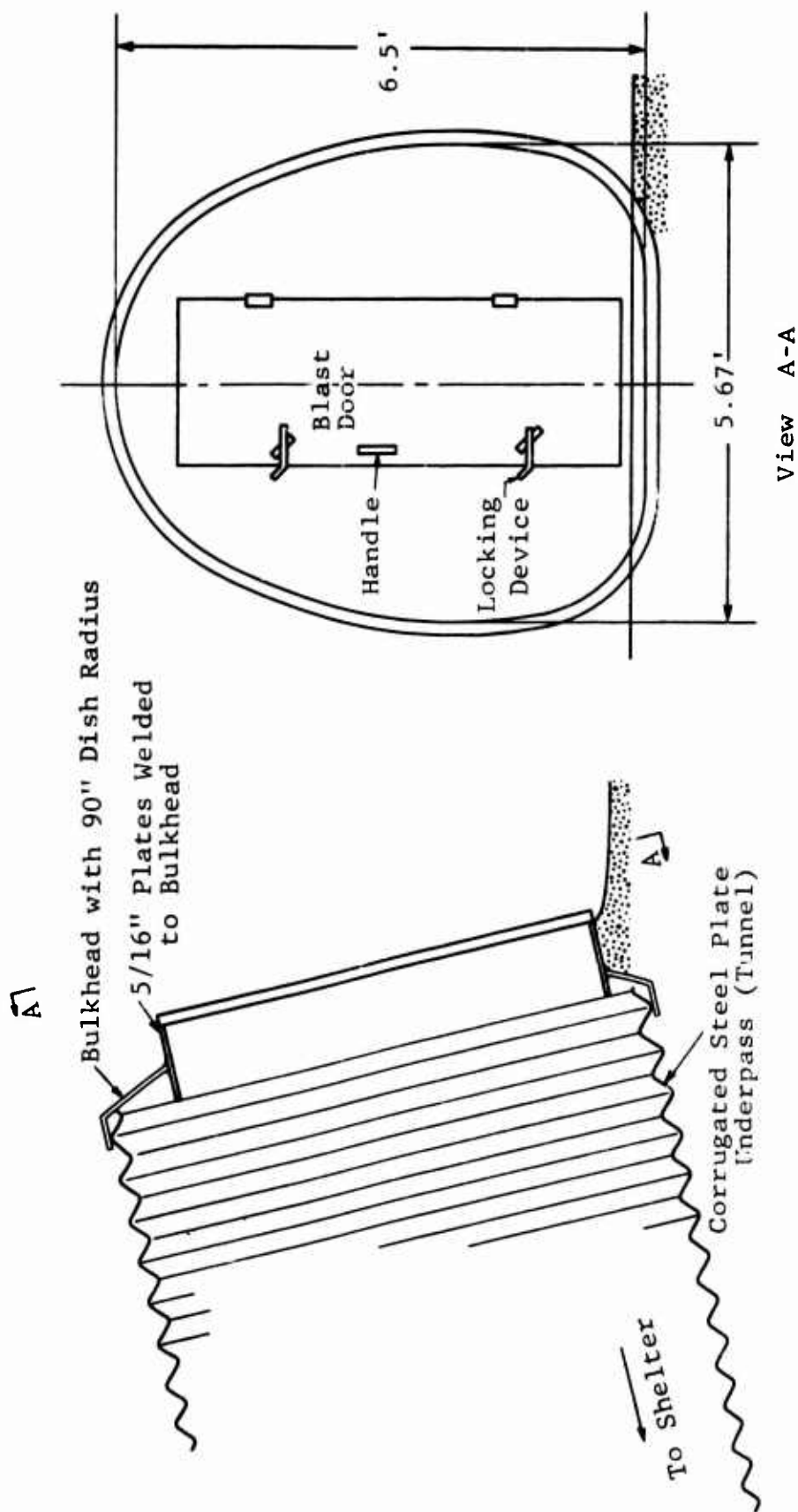


Fig. A.10 ENTRANCEWAY DETAILS FOR SINGLE-PURPOSE ARCH AND RECTANGULAR SHELTERS (SEE TABLE A.6)

TABLE A.6
ENTRANCEWAY DIMENSIONS (LOW LEVEL WEAPON EFFECTS DESIGNS)
(Single Basic Entrance)

Item	Dimensions for Indicated Design Weapon Environments			
	FRE	10 psi	20 psi	30 psi
Entranceway Tunnel, gage (corrugated steel plate sections with corrugations 2 in. deep and a pitch of 6 in.)	12	12	12	12
Entranceway Tunnel Length				
Arch Shelter	64.1'	64.1'	64.1'	64.1'
Rectangular Shelter	29.0'	29.0'	29.0'	29.0'
Internal Shelter Door (hollow, metal - commercial variety)	2'-10" x 6'-8", 1.75" thick	2'-10" x 6'-8", 1.75" thick	2'-10" x 6'-8", 1.75" thick	2'-10" x 6'-8", 1.75" thick
External Shelter Door (stiffened plate)	2'-10" x 6'-8"			
Bulkhead, plate thickness	0.25"	0.25"	0.25"	0.31"
Blast Door (galvanized metal with aluminum honeycomb core)	2' x 5'-6", 0.75" thick	2' x 5'-6", 0.75" thick	2' x 5'-6", 0.75" thick	2' x 5'-6", 0.75" thick

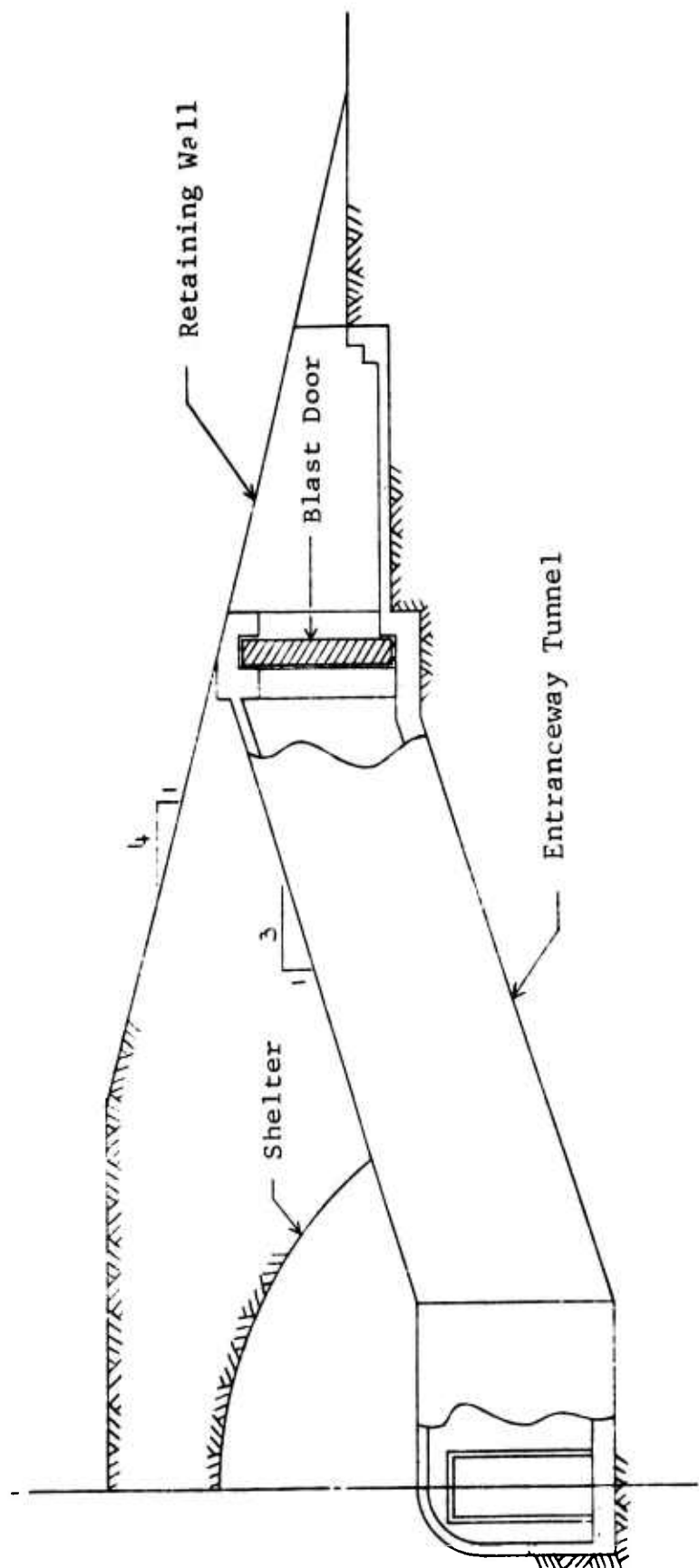


Fig. A.11 ENTRANCEWAY FOR 100 AND 150 psi DESIGN SHELTERS (ELEVATION)

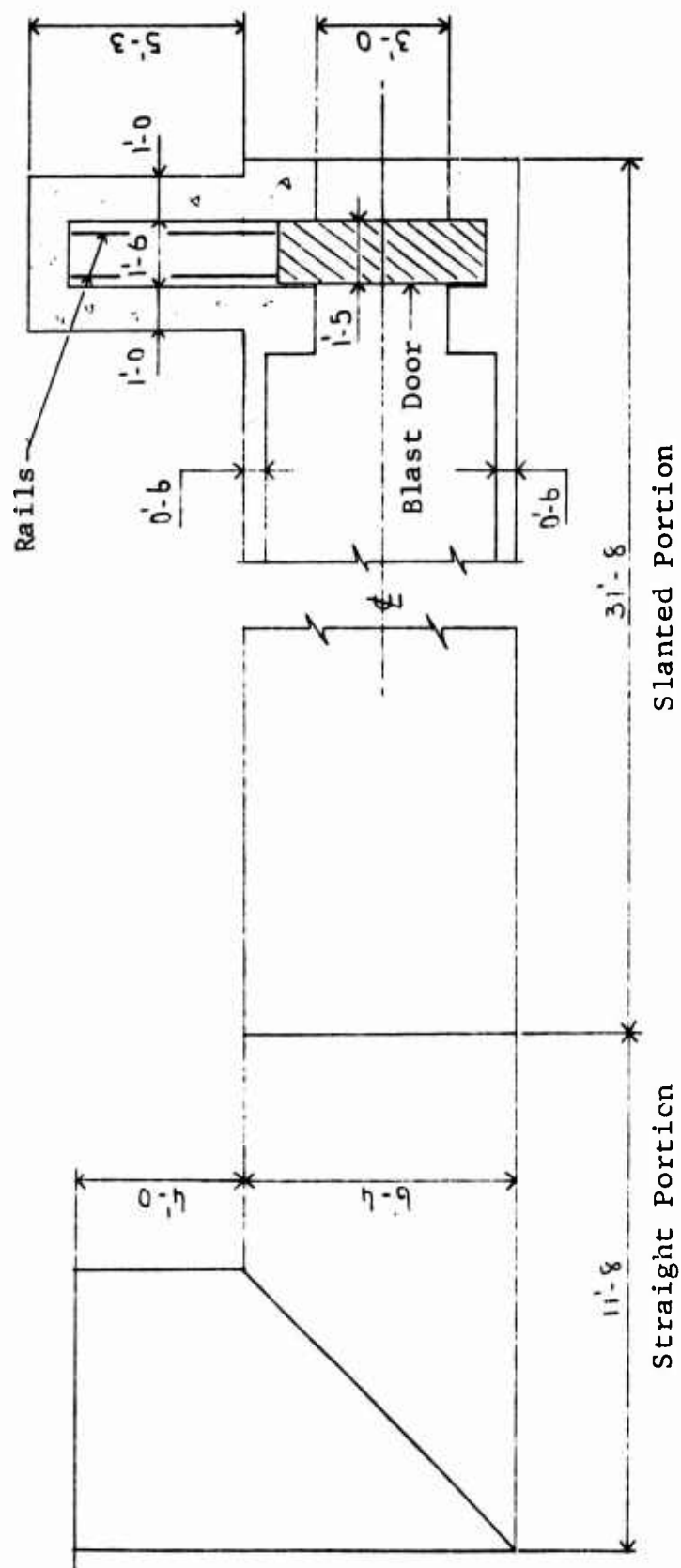
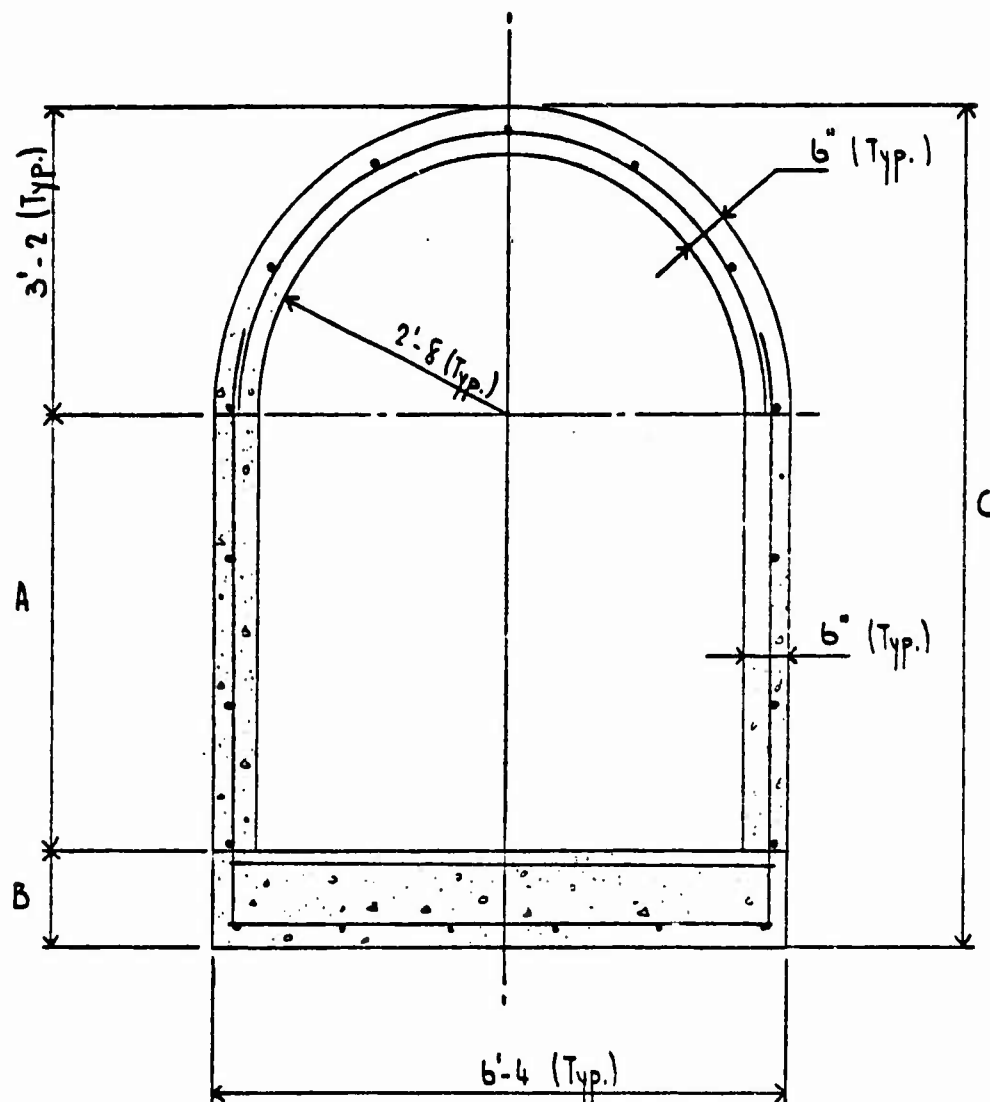


Fig. A.12 ENTRANCEWAY TUNNEL PLAN (100 AND 150 psi DESIGN SHELTERS)



	100 psi Design			150 psi Design		
	A	B	C	A	B	C
Horizontal Section	4'6"	0'11-1/4"	8'7-1/4"	4'6"	1'2"	8'10"
Slanted Section	4'11"	0'11-1/4"	9'0-1/4"	4'11"	1'2"	9'3"

Fig. A.13 ENTRANCEWAY CROSS SECTION (100 AND 150 psi DESIGNS)

A.2 COST OF SINGLE-PURPOSE SHELTERS

Total unit costs of the single-purpose (arch and rectangular) shelters described are given, the detailed costs of all items comprising these totals are presented in Appendix B. Although referred to as "shelter costs" they are in reality cost estimates, or probable costs. They are what an experienced contractor located in Chicago, Illinois would probably bid in the spring of 1969 in order to construct these structures in the same geographic area. Being defined in this manner, the given total costs are therefore subject to variations arising from contractor's profit and overhead contingencies (assuming that all materials and operations are explicitly specified).

Contractor's profit is simply the profit he expects to make on the job. This has a substantial variation depending on the particular situation. The contractor may want the job badly and accept a low profit, say less than 5 percent. In competitive bidding 10 percent is quite common. Overhead contingencies include such items as:

- field office and office expenses,
- construction equipment storage shack,
- construction equipment maintenance,
- job estimation, inspection and supervision,
- performance bond,
- unemployment taxes,
- social security,
- liability and risk insurance, etc.

For cost estimates given herein, the combined contractor's profit and overhead contingencies were taken at 20 percent of the total cost for labor and materials. This figure was recommended by the cost estimator* employed in the course of this study.

Cost estimates given relate to the immediate vicinity of Chicago, Illinois in the spring of 1969. For each shelter considered they include the following:

- site preparation (land clearance),
- shelter structure and habitability items (mechanical and electrical equipment),
- entranceway,
- service road and parking lot, and
- contractor's profit and overhead contingencies (20 percent).

They do not include:

- site costs such as land, surveys, soil borings, legal fees, real estate agent commissions, or title transfer costs.
- design costs such as architects and engineers fees, government supervision, administrative and inspective,
- financing costs,
- operating, remodeling and maintenance costs, and
- cost of food items and medical supplies.

Estimates given are for two shelter populations (500 and 1000 persons) and for each of the four design weapon environments described earlier.

Six cost options were considered with each shelter size and design weapon environment. These options are given in Table A.7 in the order of decreasing shelter austerity. Option 1 is the most austere and consists of a basic shelter structure with entranceways. No habitability items of any kind are provided.

*George A. Kennedy and Associates, Inc., Structural Engineers-Estimators, 75 E. Wacker Drive, Chicago, Illinois 60601

TABLE A.7
SHELTERING COST OPTIONS
(Cost Items Comprising Sheltering Options Considered)

Cost Option					
1	2	3	4	5	6
Site Clearance Access Road Shelter Structure Entranceway	Site Clearance Access Road Shelter Structure Entranceway	Site Clearance Access Road Shelter Structure Entranceway	↑	↑	↑
—	OCD Ventilation Package	Ventilation* System	Same as Option 1		
—	OCD Water Package	Water Supply* System Toilet System*	Same as Option 2		
—	OCD Electrical	Wiring, Fixtures and Outlets*	Same as Option 3		
—	—	Partitions	Parking Lot		
—	—	—	Parking Lot		

* commercial items

Note: A detailed breakdown of costs for these items is given in Appendix B.

In addition to structure and entranceways, costs include labor, materials and equipment necessary to clear the shelter site and build an access road. It will be remembered that shelters described are designed to be constructed close to highways or railways in uninhabited areas on the periphery of large population centers. In such areas access roads leading directly to the shelter site would not generally exist.

Cost option 2 is obtained from option 1 by adding OCD approved habitability items such as ventilation kits, water containers and basic electrical equipment. Cost option 3 is similarly obtained by adding habitability items of the commercial variety in accordance with requirements suggested in Refs. 15 and 16. This includes ventilation, plumbing and electrical systems and presupposes availability of normal power supply. Partitions included in this cost option separate the toilet from the living areas. Cost options 4, 5 and 6 are identical respectively to options 1, 2 and 3 with the exception that the shelter site is increased to provide parking. The size of a parking lot was planned on the basis of 0.4 cars per shelter occupant. Total unit costs are summarized in Tables A.8 and A.9 and the costs of individual items comprising the totals are given in Appendix B.

A.3 DUAL-PURPOSE SHELTERS

A.3.1 School Basements

Two school (Ref. 15) basements (ordinarily classrooms) were designed to act as shelters in the event of an emergency. Both schools are modern two-story structures consisting of a steel frame, filler walls and having large areas of window space. The first school accommodates a student body and staff of 500 persons, while the second accommodates 1100 persons. Basement shelter designs for 5, 25 and 50 psi overpressure levels and associated effects resulting from megaton range weapons are described.

The structures in question are illustrated in Figs. A.14 through A.17, and basic physical characteristics are described in Table A.10.

TABLE A.8
SUMMARY OF SINGLE-PURPOSE SHELTER COSTS PER SQUARE FOOT OF SHELTER AREA

Type of Structure	Capacity (No. of Persons)	Cost Option 1				Cost Option 2				Cost Option 3			
		Design Weapon Environment				Design Weapon Environment				Design Weapon Environment			
		FRE	10 psi	20 psi	30 psi	FRE	10 psi	20 psi	30 psi	FRE	10 psi	20 psi	30 psi
R/C Arch	500	10.85	11.08	11.88	12.20	11.15	11.38	12.18	12.51	15.60	15.83	16.63	16.95
	1000	10.30	10.56	11.07	11.65	10.61	10.86	11.38	11.95	15.05	15.31	15.83	16.40
Steel Arch	500	10.16	11.85	13.57	19.34	10.46	12.16	13.88	19.64	14.91	16.61	18.32	24.09
	1000	9.51	11.59	13.31	19.06	9.82	11.89	13.62	19.36	14.27	16.34	18.06	23.81
R/C Rectangular	500	10.93	12.94	15.12	19.14	11.20	12.11	15.40	19.41	15.21	17.22	19.41	23.42
	1000	9.76	11.74	13.77	17.40	10.03	12.01	14.05	17.68	14.04	16.02	18.06	21.69
		Cost Option 4				Cost Option 5				Cost Option 6			
		Design Weapon Environment				Design Weapon Environment				Design Weapon Environment			
		FRE	10 psi	20 psi	30 psi	FRE	10 psi	20 psi	30 psi	FRE	10 psi	20 psi	30 psi
R/C Arch	500	17.83	18.06	18.87	19.19	18.14	18.37	19.17	19.49	22.59	22.81	23.62	23.94
	1000	17.54	17.80	18.32	18.89	17.85	18.10	18.62	19.20	22.30	22.50	23.07	23.64
Steel Arch	500	17.17	18.84	20.56	26.33	17.45	19.14	20.86	26.63	21.90	23.59	25.31	31.08
	1000	16.76	18.83	20.55	26.30	17.06	19.13	20.86	26.60	21.51	23.58	25.31	31.05
R/C Rectangular	500	18.44	20.45	22.64	26.65	18.71	20.72	22.91	26.92	22.72	24.73	26.92	30.93
	1000	15.67	17.65	19.69	23.31	15.94	17.92	19.96	23.59	19.95	21.93	23.97	27.60

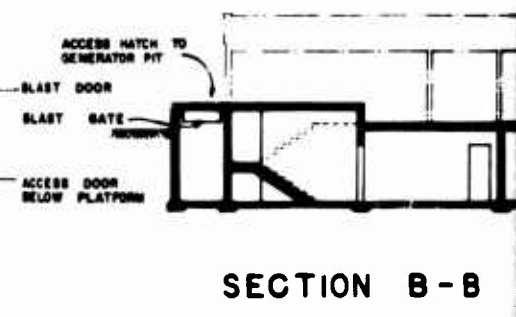
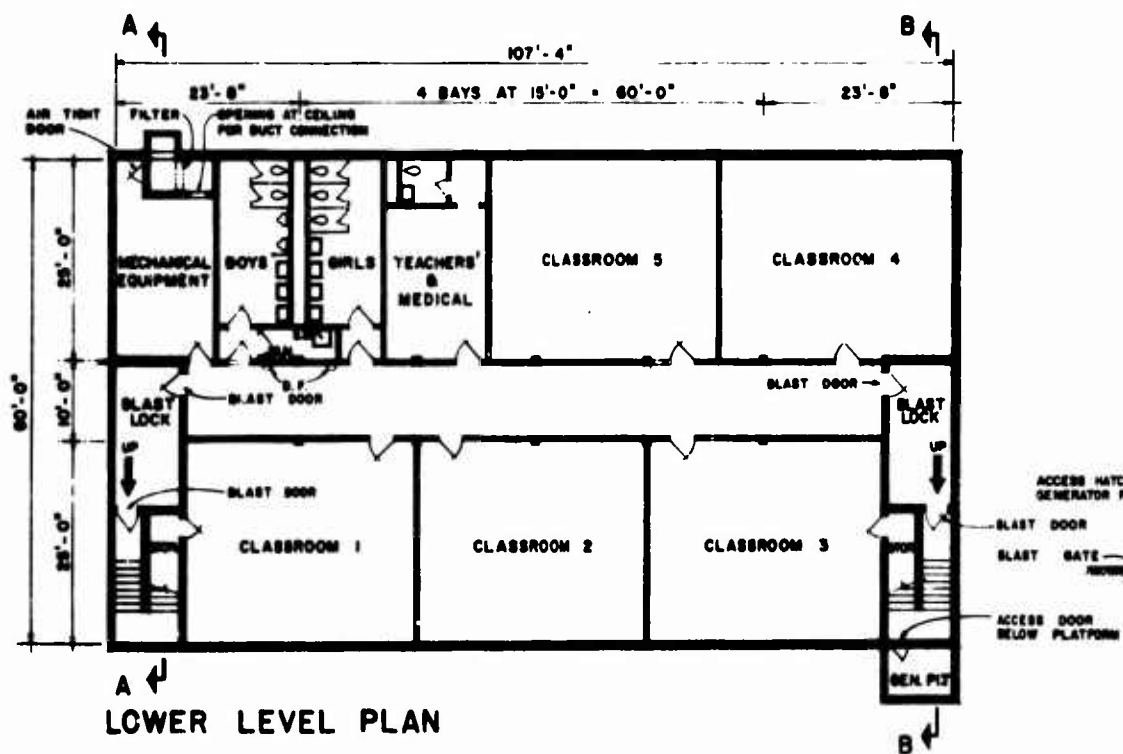
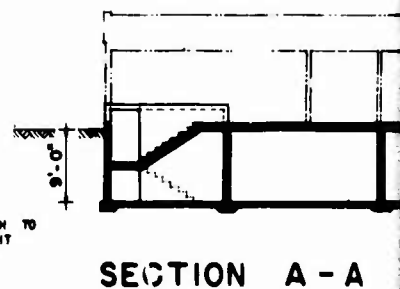
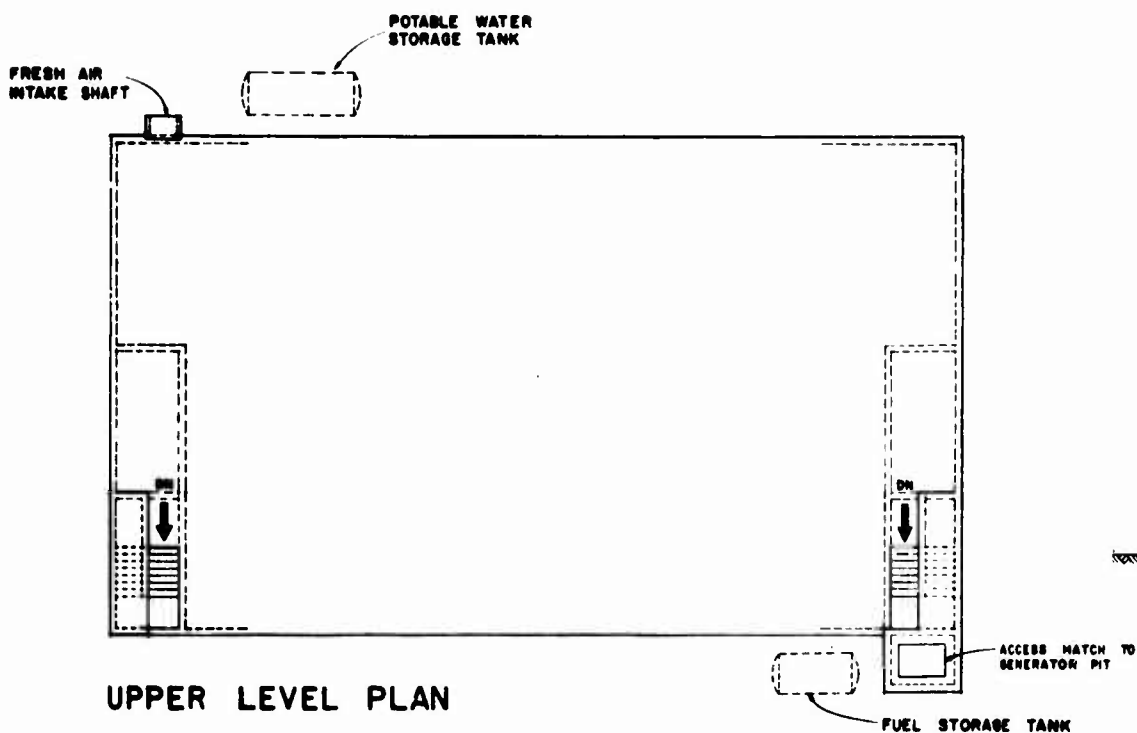
Costs given are valid for suburban areas of Chicago, Illinois for the spring of 1969.

TABLE A.9
SUMMARY OF SHELTER COSTS PER SQ FT OF SHELTER AREA
(RC Arch, 500-Man Capacity)

Design Weapon Environment	Cost Option					
	1	2	3	4	5	6
100 psi	17.06	17.33	22.78	25.45	25.71	31.15
150 psi	21.69	21.97	27.59	30.07	30.34	35.57

TABLE A.10
BASIC CHARACTERISTICS OF SCHOOL BASEMENT SHELTERS

Characteristic	Design Environments 5, 25 and 50 psi	
	Capacity, persons	
	550	1100
Gross Floor Area (sq ft)	6,440	12,260
Total Volume (cu ft)	57,960	110,340
Headroom (ft)	9	9
Shelter Area per Occupant (sq ft)	11.7	11.1
Shelter Volume per Occupant (cu ft)	105.3	99.9
Fallout Protection Factor	100	100
Maximum Inside Dose of Initial Radiation (rad)	20	20



B

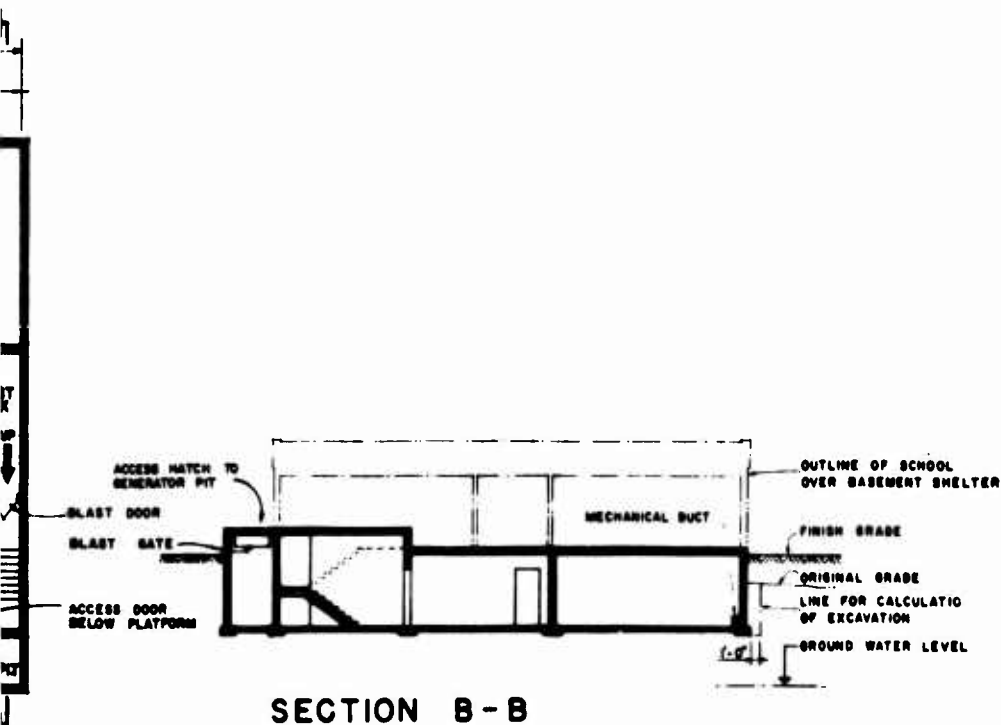
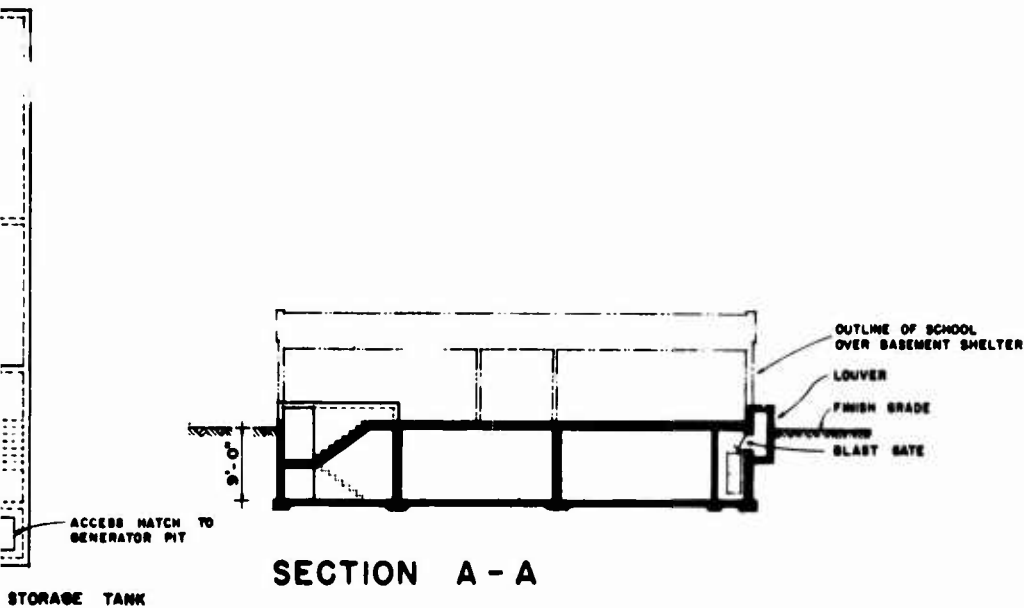


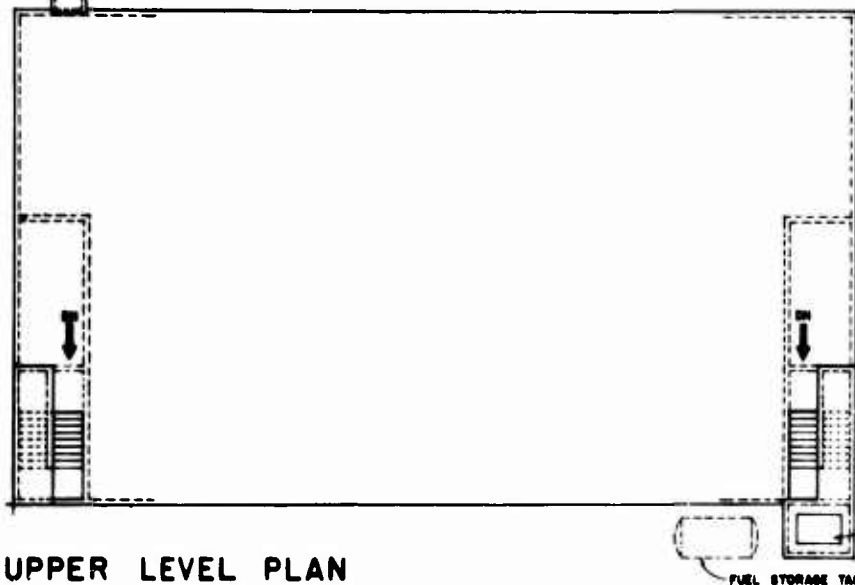
Fig. A.14

CLASSROOM SHELTER
FOR 550 PERSONS
5 PSI

SCALE 0' 0' 5' 10' 20'

FRESH AIR
INTAKE SHAFT

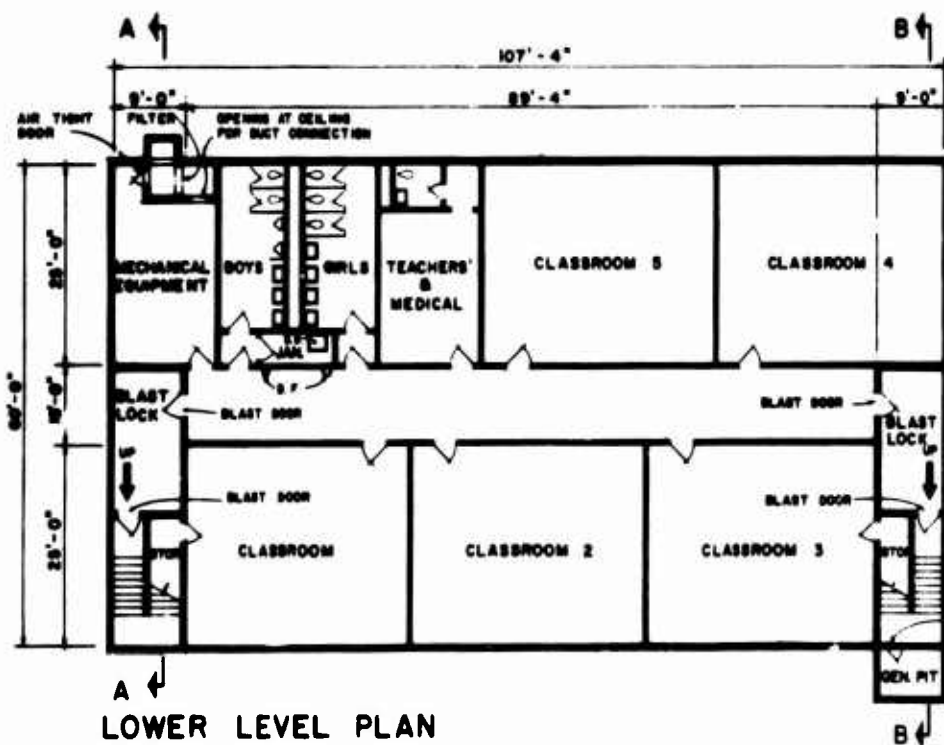
POTABLE WATER
STORAGE TANK



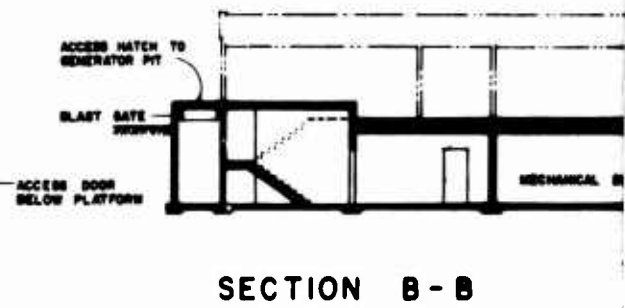
UPPER LEVEL PLAN



SECTION A - A



LOWER LEVEL PLAN



SECTION B - B

B

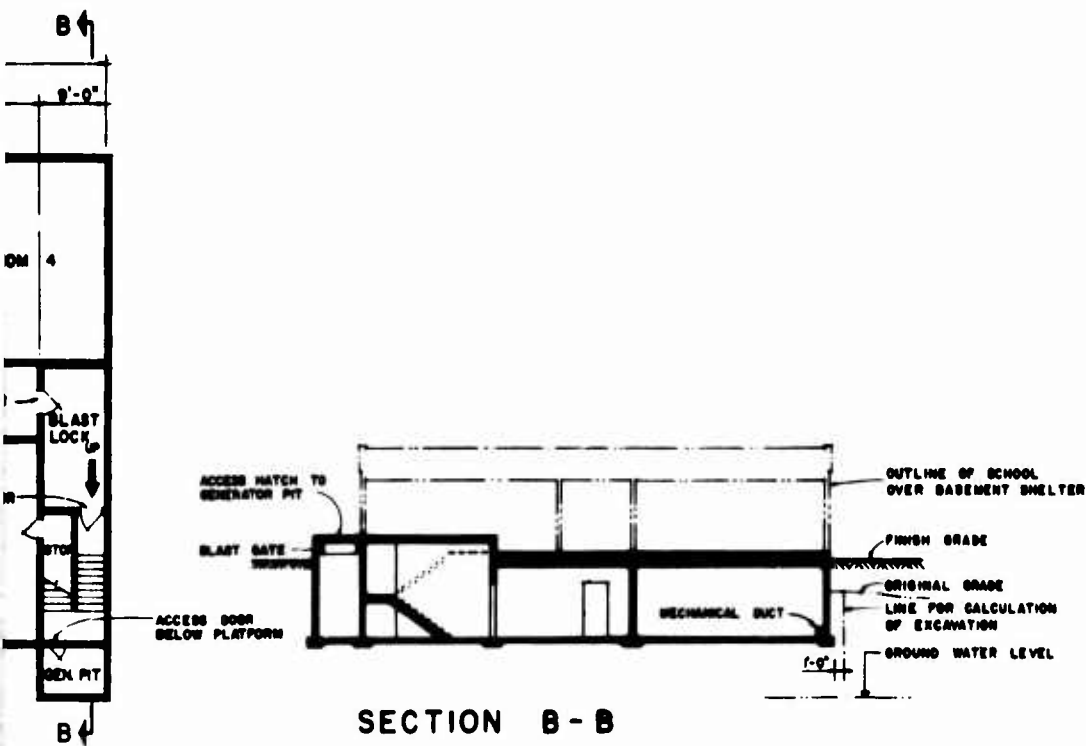
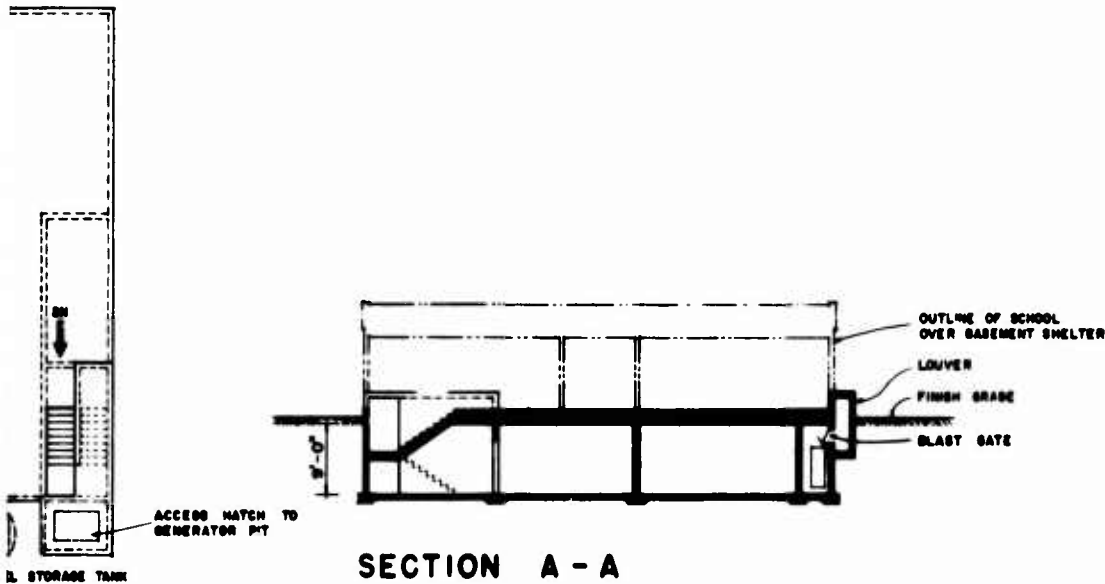


Fig. A.15

CLASSROOM SHELTER
FOR 550 PERSONS
25 AND 50 PSI

SCALE 0' 0' 5' 10' 20'

SECTION B - B

B

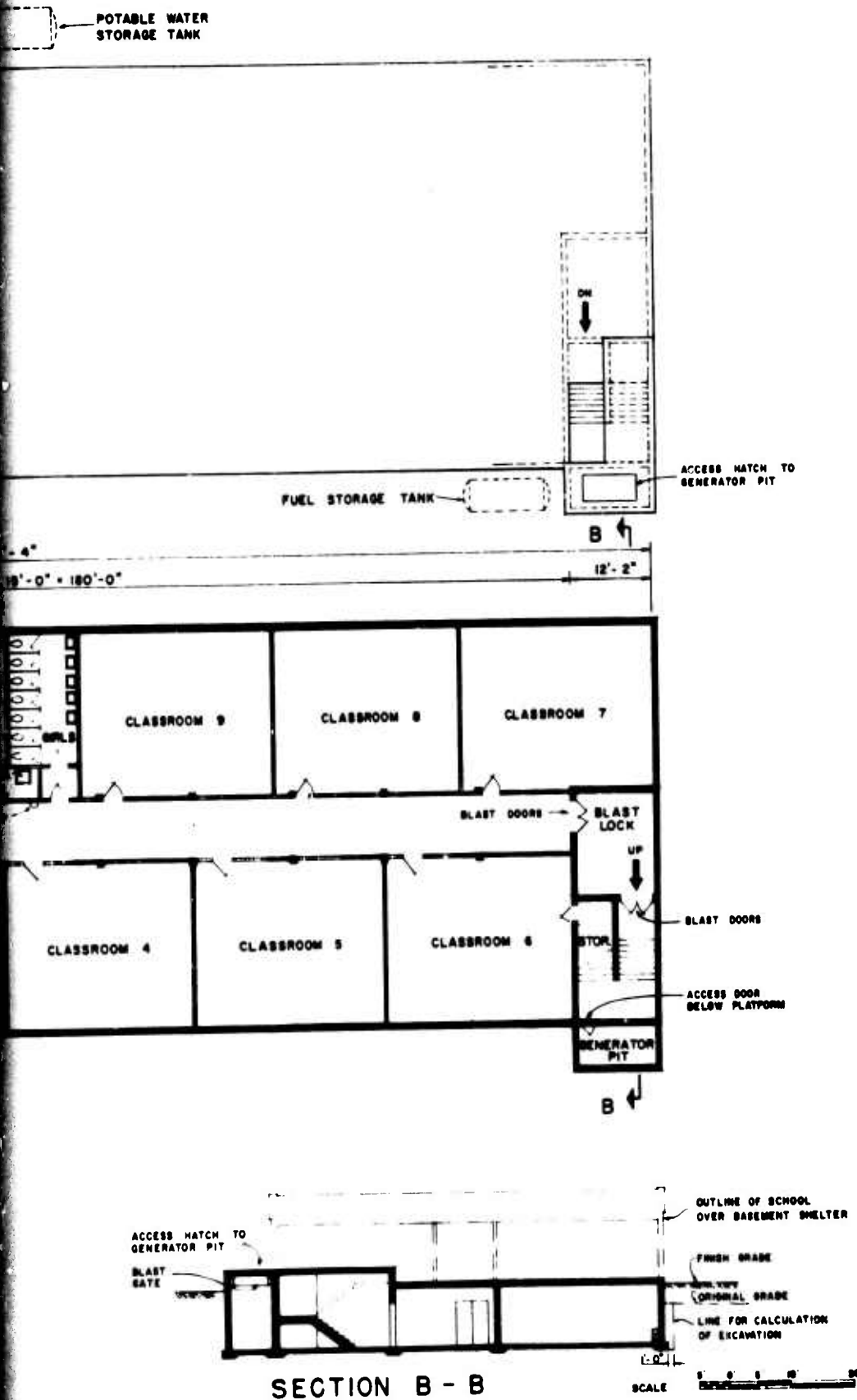
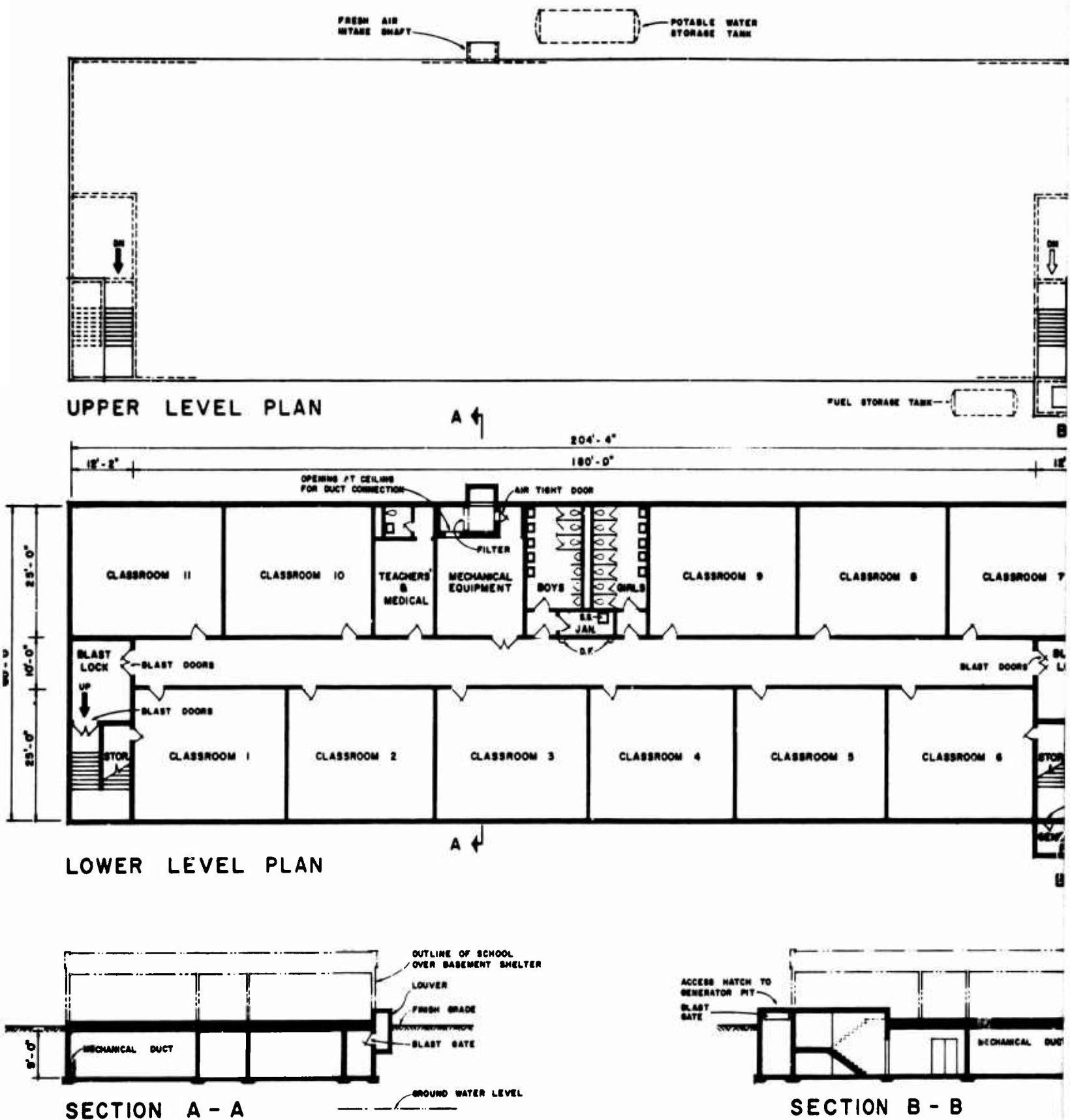


Fig. A.16
CLASSROOM SHELTER
FOR 1100 PERSONS
5 PSI

SECTION B - B



B

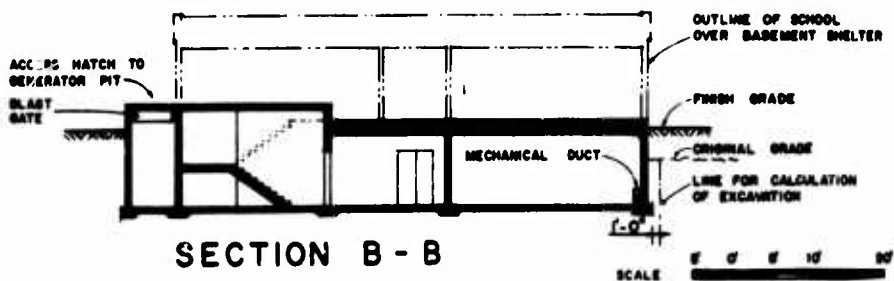
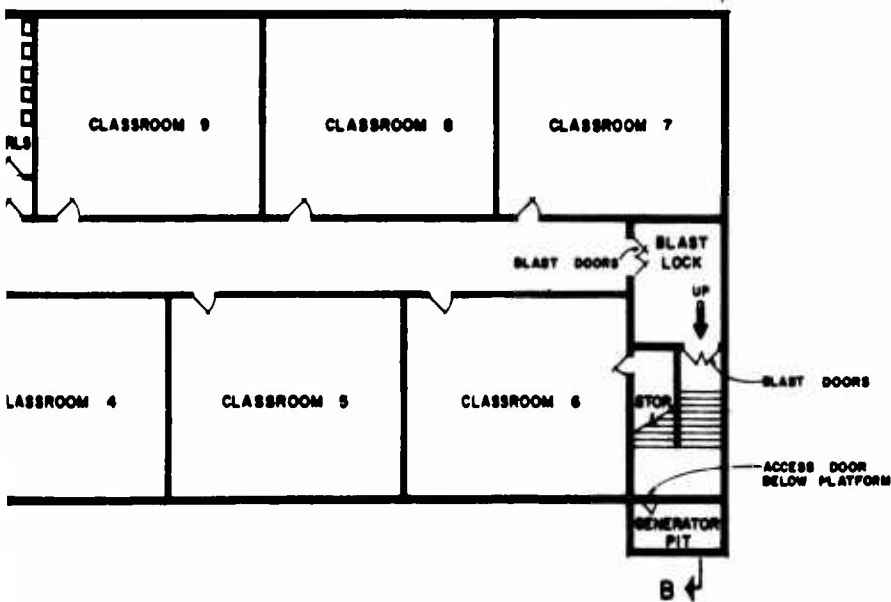
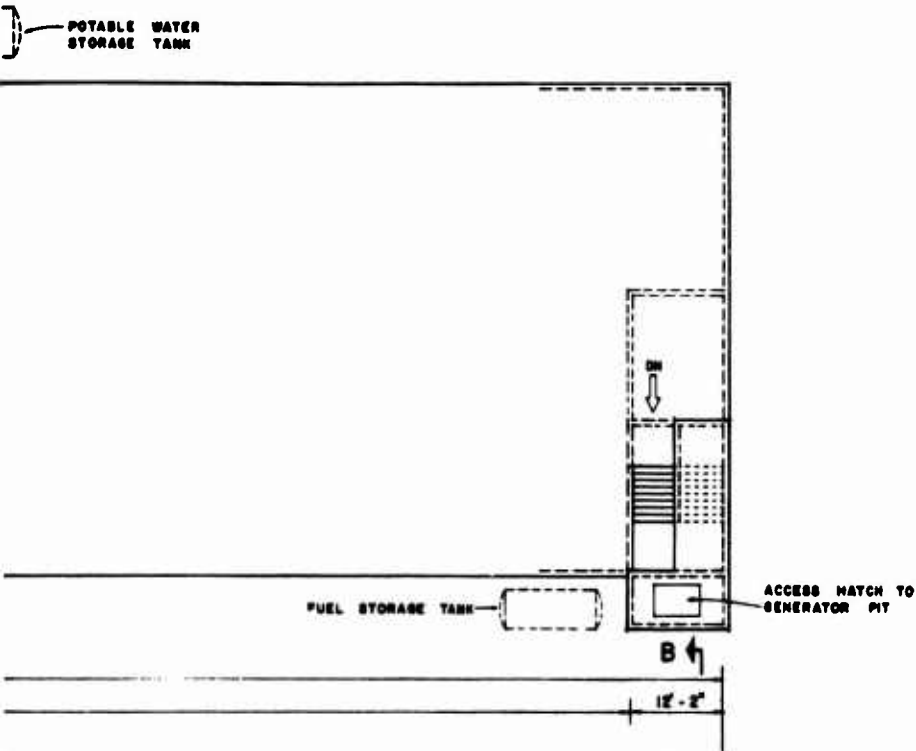


Fig. A.17
CLASSROOM SHELTER
FOR 1100 PERSONS
25 AND 50 PSI

Structural design is based on ultimate strength theory and, in most cases, is controlled by blast loading. The strength under normal conditions meets the requirements of the current ACI building code. Thicknesses of essential structural elements together with percent reinforcement are given in Table A.11.

The basement ceiling of the 5 psi structure has a one-way slab spanning between the exterior walls and longitudinal corridor beams. For the 25 and 50 psi designs, the ceiling spans two directions between transverse and longitudinal reinforced concrete tilt-up walls. The 10 in. slab thickness for the 5 psi structure is governed by fallout radiation requirements, and affords a minimum protection factor of 100.

The 21 and 30 in. roof slab thicknesses of the 25 and 50 psi basement schools satisfy structural requirements and afford the required radiation protection to reduce the initial radiation on the ground surface to a tolerable level of 20 rad or less within the shelter.

The 5 psi shelter has cinder block interior partitions; the 25 and 50 psi shelters have reinforced concrete tilt-up bearing walls. Reinforced concrete partitions were selected in the 25 and 50 psi schools for two reasons: to serve as bearing walls and to provide adequate lateral resistance.

The designs are based upon a minimum concrete strength of 3000 psi throughout for the 25 and 50 psi shelters and 3000 psi for the roof and columns, 2500 psi elsewhere, for the 5 psi shelter. The reinforcement conforms to ASTM A432 which has a minimum yield point of 60,000 psi. The live load on the basement roof is taken as 75 psf for the classrooms and 100 psf for the corridors. The dead load and live load from the upper level roof slab is assumed to be 10 and 40 psf, respectively. Debris loading is assumed to be negligible in combination with the blast load. The normal allowable soil bearing capacity is taken as 4 tons/sq ft.

TABLE A. 11
MEMBER SIZE AND PERCENT REINFORCEMENT (Ref. 15)

Structural Member	5 psi Design		25 psi Design		50 psi Design	
	Depth and/or Width in.	Percent Reinforcement *	Depth and/or Width in.	Percent Reinforcement *	Depth and/or Width in.	Percent Reinforcement *
Roof Slab	10	$\dot{t}_e = \dot{t}_c = 1.75, \dot{t}_v = 0.0$	21	$\dot{t}_{LC} = \dot{t}_{LE} = 1.0$ $\dot{t}_{SC} = \dot{t}_{SE} = 1.5, \dot{t}_v = 0.5$	30	$\dot{t}_{LC} = \dot{t}_{LE} = 1.0$ $\dot{t}_{SC} = \dot{t}_{SE} = 1.5, \dot{t}_v = 0.5$
Exterior Walls	10	$\dot{t}_e = \dot{t}_c = 0.25, \dot{t}_v = 0.0$	10	$\dot{t}_{LC} = \dot{t}_{LE} = 0.5$ $\dot{t}_{SC} = 1.5, \dot{t}_{SE} = 0.0, \dot{t}_v = 0.0$	10	$\dot{t}_{LC} = \dot{t}_{LE} = 0.5$ $\dot{t}_{SC} = 1.5, \dot{t}_{SE} = 0.0, \dot{t}_v = 0.0$
Corridor Beam Width Depth	12 36	$\dot{t}_e = \dot{t}_c = 0.65$	--	N/A	--	N/A
Partitions	6	--	6	$\dot{t} = \dot{t}' = 0.5$	6	$\dot{t} = \dot{t}' = 0.5$
Columns (square)	12 x 12	$\dot{t} = \dot{t}' = 0.5$	--	N/A	--	N/A
Column Footings Width Depth	48 x 48 20	$\dot{t}_e = 0.6, \dot{t}_v = 0.25$	--	N/A	--	N/A
Exterior Wall Footings Width Depth	22 8	$\dot{t}_e = 0.6$	24 10	$\dot{t}_e = 0.8$	48 12	$\dot{t}_e = 0.8$
Interior Wall Footings Width Depth	18 8	$\dot{t}_e = 0.6$	42 10	$\dot{t}_e = 0.8$	72 12	$\dot{t}_e = 0.8$

* Steel Reinforcement Symbols

- \dot{t}_e = percent steel at end, effective
- \dot{t}_c = percent steel at centerline
- \dot{t} = percent tension steel
- \dot{t}' = percent compression steel
- \dot{t}_v = percent web reinforcement
- \dot{t}_{LC} = percent steel in long direction at centerline of two-way slab
- \dot{t}_{LE} = percent steel in long direction at end of two-way lab, effective
- \dot{t}_{SC} = percent steel in short direction at centerline of two-way slab
- \dot{t}_{SE} = percent steel in short direction at end of two-way slab, effective

It should be noted that these basements, although designated as classrooms, can be easily and efficiently adapted to numerous conventional structures having different uses, i.e., office buildings, police stations, fire stations, hospitals, etc. Depending upon site conditions, such as type of foundation material, location of water table, etc., structures described may be completely or partially buried and may be located beneath or adjacent to the conventional above grade structure.

A.3.2 Parking Garages

Parking garage shelters (Ref.16) described are one-story below grade reinforced concrete structures proportioned so as to provide protection against the effects of megaton range nuclear weapons. They are designed to serve the obvious dual function of parking garage during normal operation and shelter during emergency for each of three design overpressure levels, 5, 25 and 50 psi. These shelters are illustrated in Figs. A.18 through A.20 and their basic physical characteristics are given in Tables A.12 and A.13. Layout is based on multiples of a 29 by 37 ft bay, proportioned to the dimensions of an average city block, with either parking facilities for 150 cars or shelter space for 5000 persons, as required. Typical locations for this type of shelter are (a) below a street-level parking area, or (b) below a city park site. The structure below the parking lot (Structure I) is designed with a roof slab which doubles as the deck of the parking lot. The structure below a city park site (Structure II) is modified to support 3 ft 6 in. of topsoil over the roof slab for landscaping. The structural design is based on ultimate strength theory and, in most cases, is controlled by the blast loading. The strength under normal loading meets the requirements of the current ACI building code.

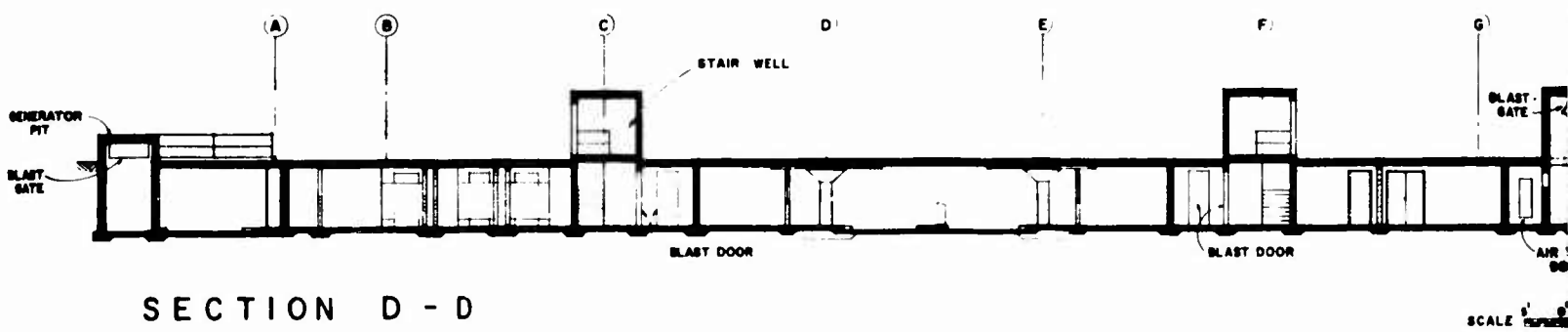
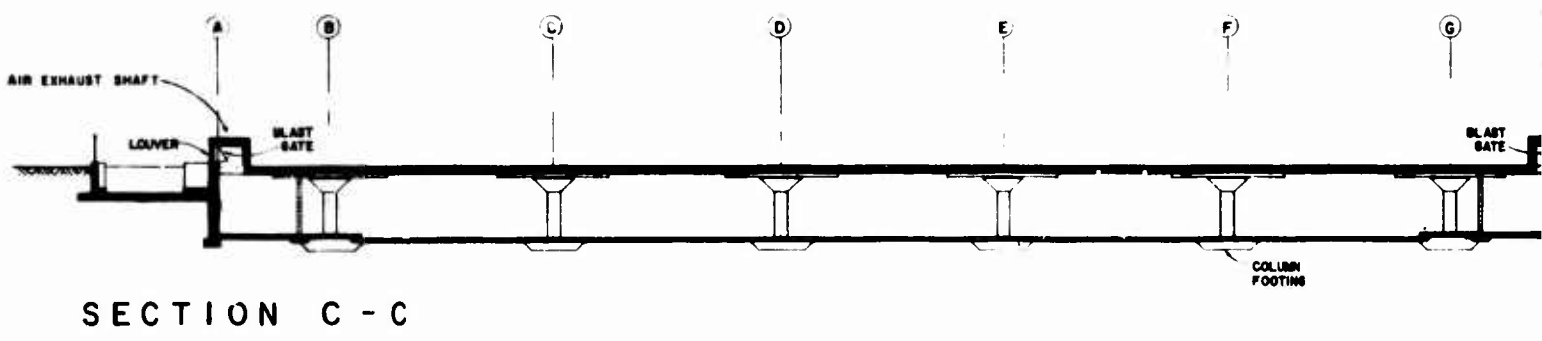
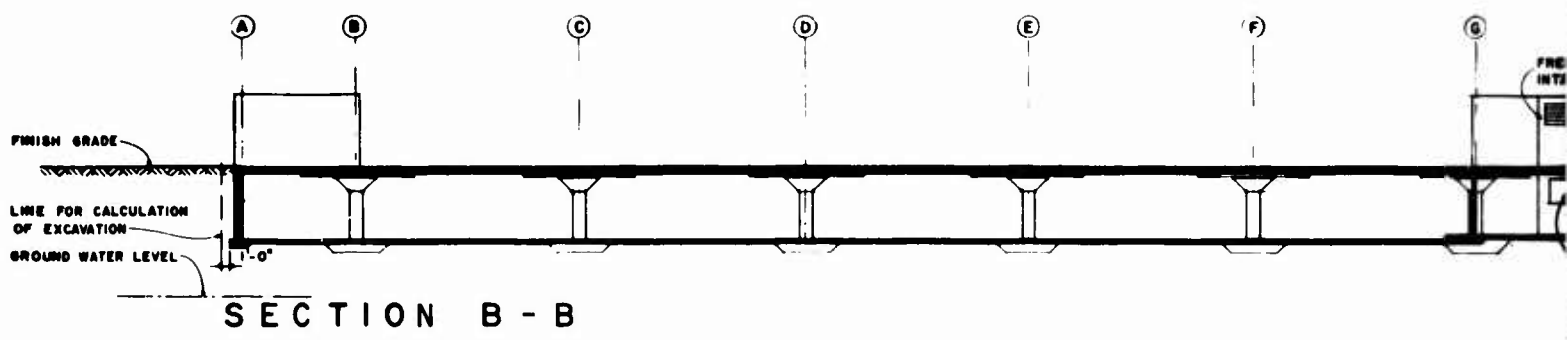
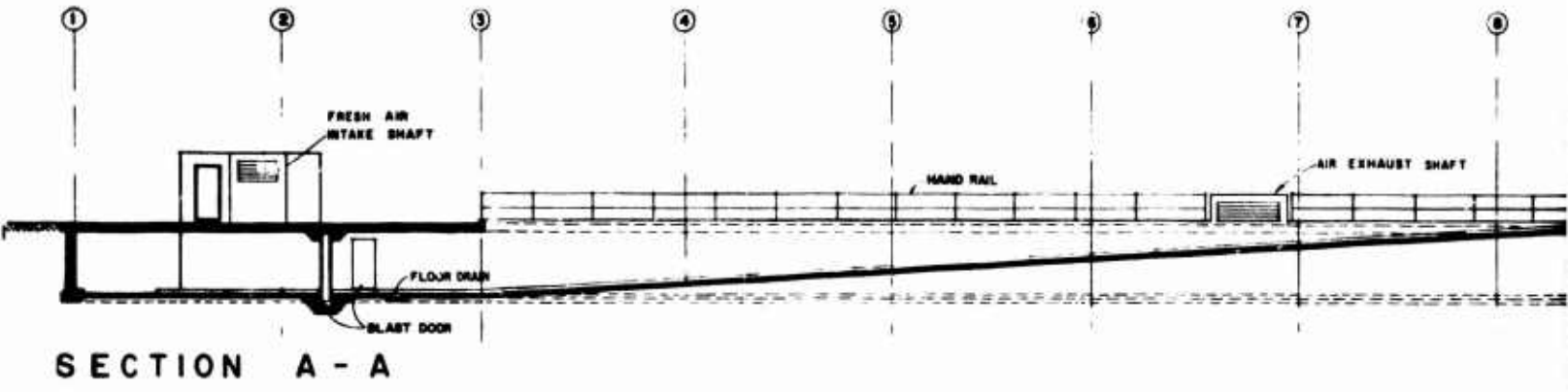
The garage ceiling for all three overpressure levels is a two-way flat slab which spans between the exterior walls and the interior columns.

TABLE A.12
BASIC CHARACTERISTICS OF PARKING GARAGE SHELTERS
(Capacity 5000 Persons)

Characteristic	Design Hardness Level		
	5 psi	25 psi	50 psi
Gross Floor Area (sq ft)	51,670	51,670	51,670
Total Volume (cu ft)	413,360	473,814	473,814
Headroom (ft)	8.00	9.17	9.17
Shelter Area per Occupant (sq ft)	10.33	10.33	10.33
Shelter Volume per Occupant (cu ft)	82.64	94.73	94.73
Fallout Protection Factor	100.00	100.00	100.00
Maximum Inside Dose of Initial Radiation (rad)	20.00	20.00	20.00

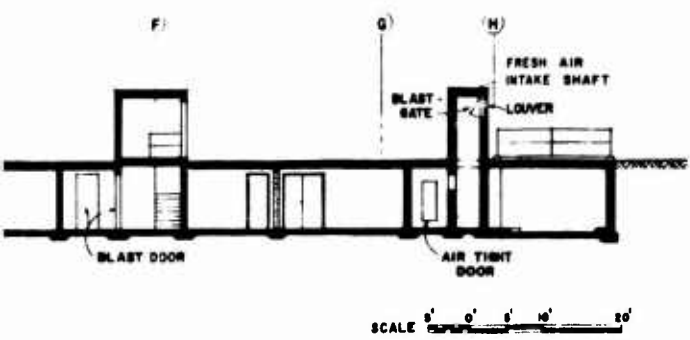
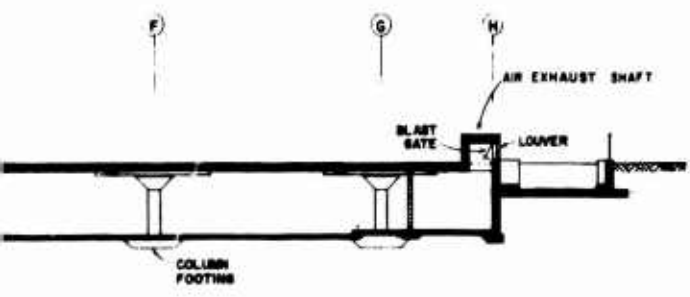
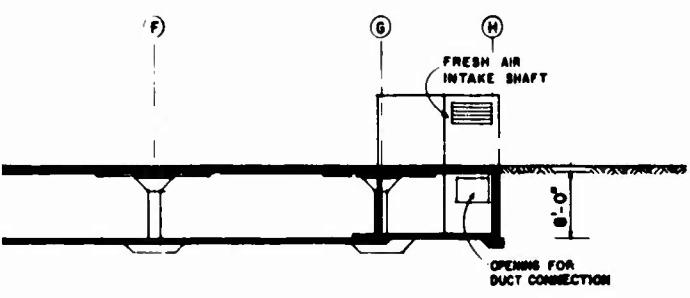
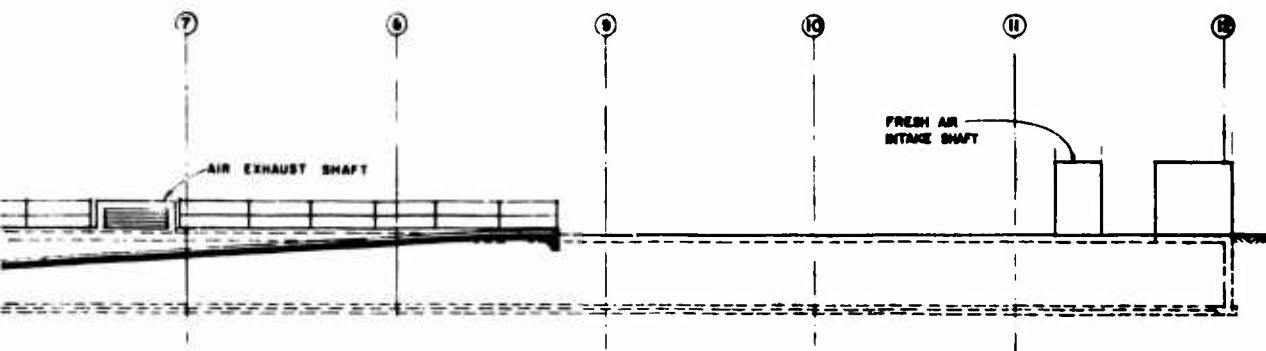
TABLE A.13
SIZES OF STRUCTURAL MEMBERS IN PARKING GARAGE SHELTERS

Structural Member	5 psi	25 psi	50 psi
Roof			
Slab Thickness	12"	21"	36"
Drop Panel Thickness	3"	3"	9"
Columns	12"	1'-6" x 3'-6"	1'-6" x 5'
Column Footings			
Width	6'-9" x 6'-9"	14' x 14'	20' x 20'
Depth	20"	30"	36"
Concrete Partitions			
Thickness	6"	6"	6"
Partition Footings			
Width	18"	18"	18"
Depth	8"	10"	12"
Exterior Walls			
Thickness	8"	8"	8"
Exterior Wall Footings			
Width	20"	22"	46"
Depth	12"	18"	30"



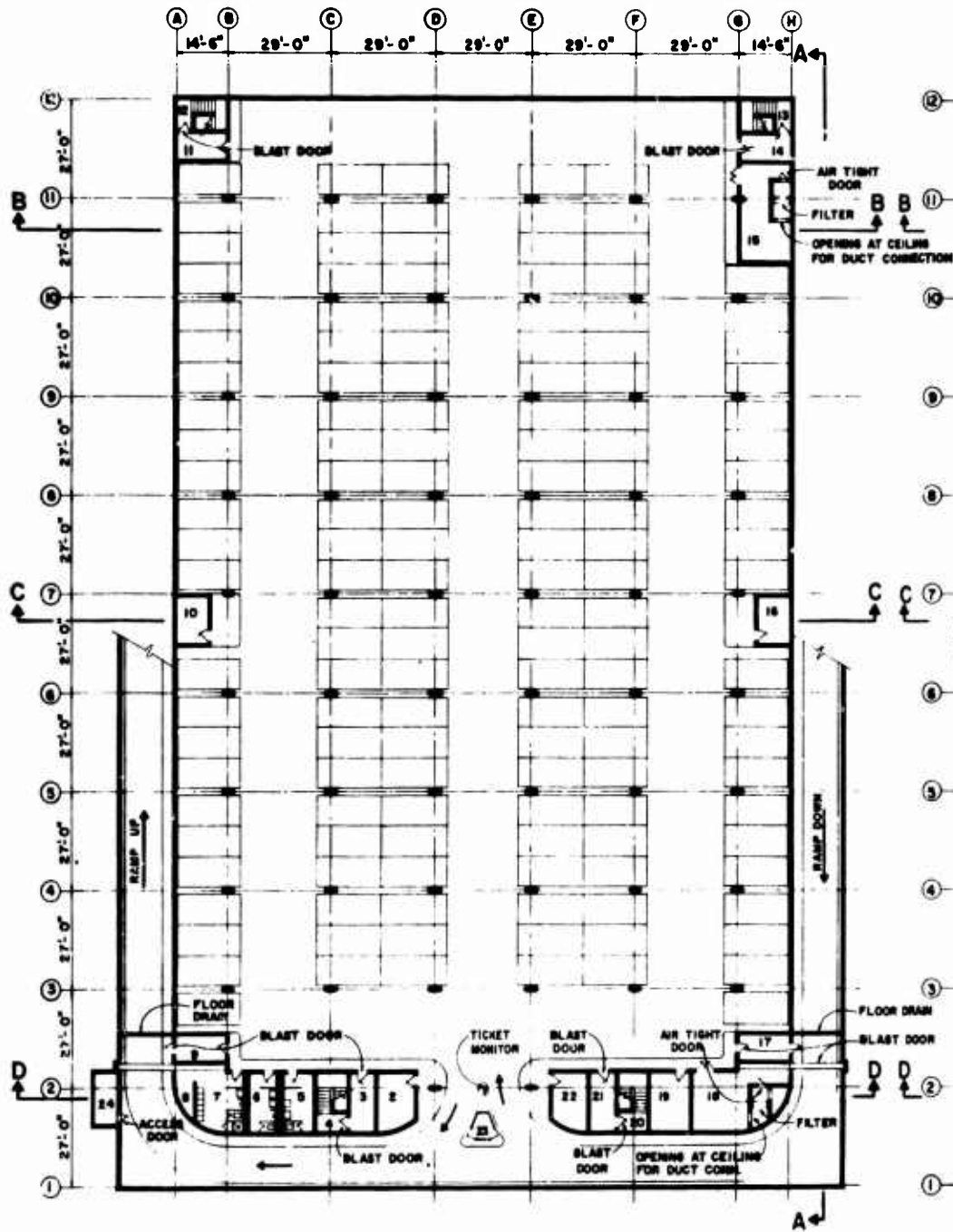
SCALE 1" = 10'

B

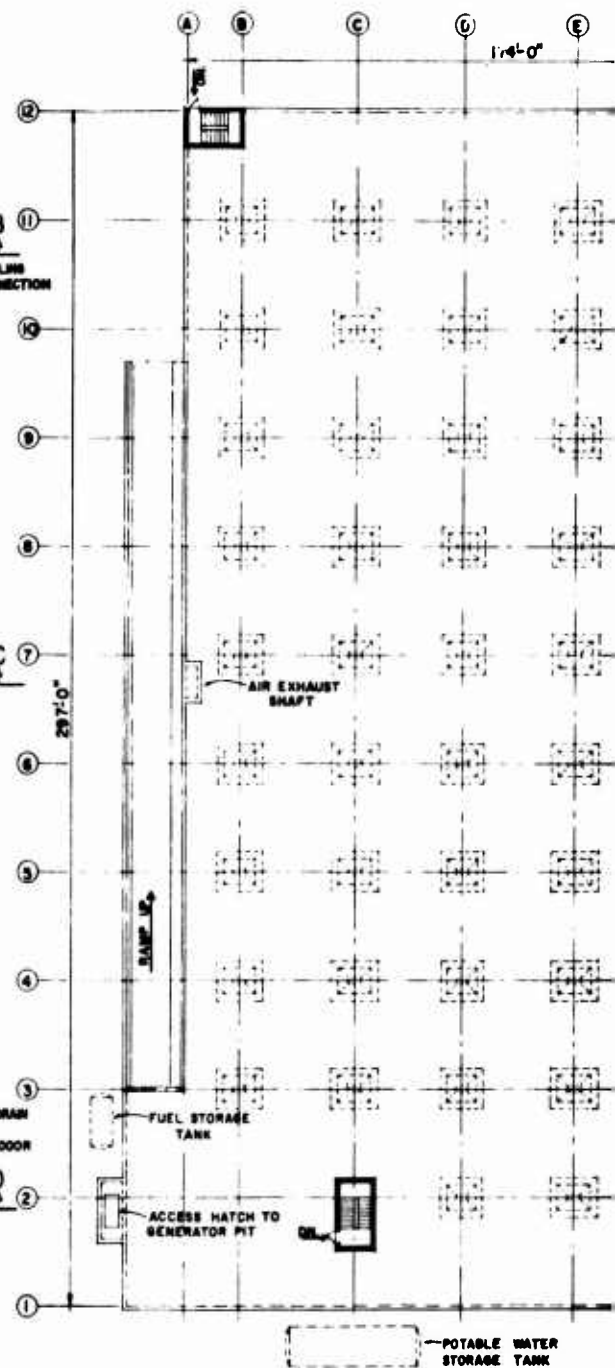


SCALE 0' 5' 10' 20'

Fig. A.18
PARKING GARAGE SHELTER
FOR 5,000 PERSONS
5 PSI

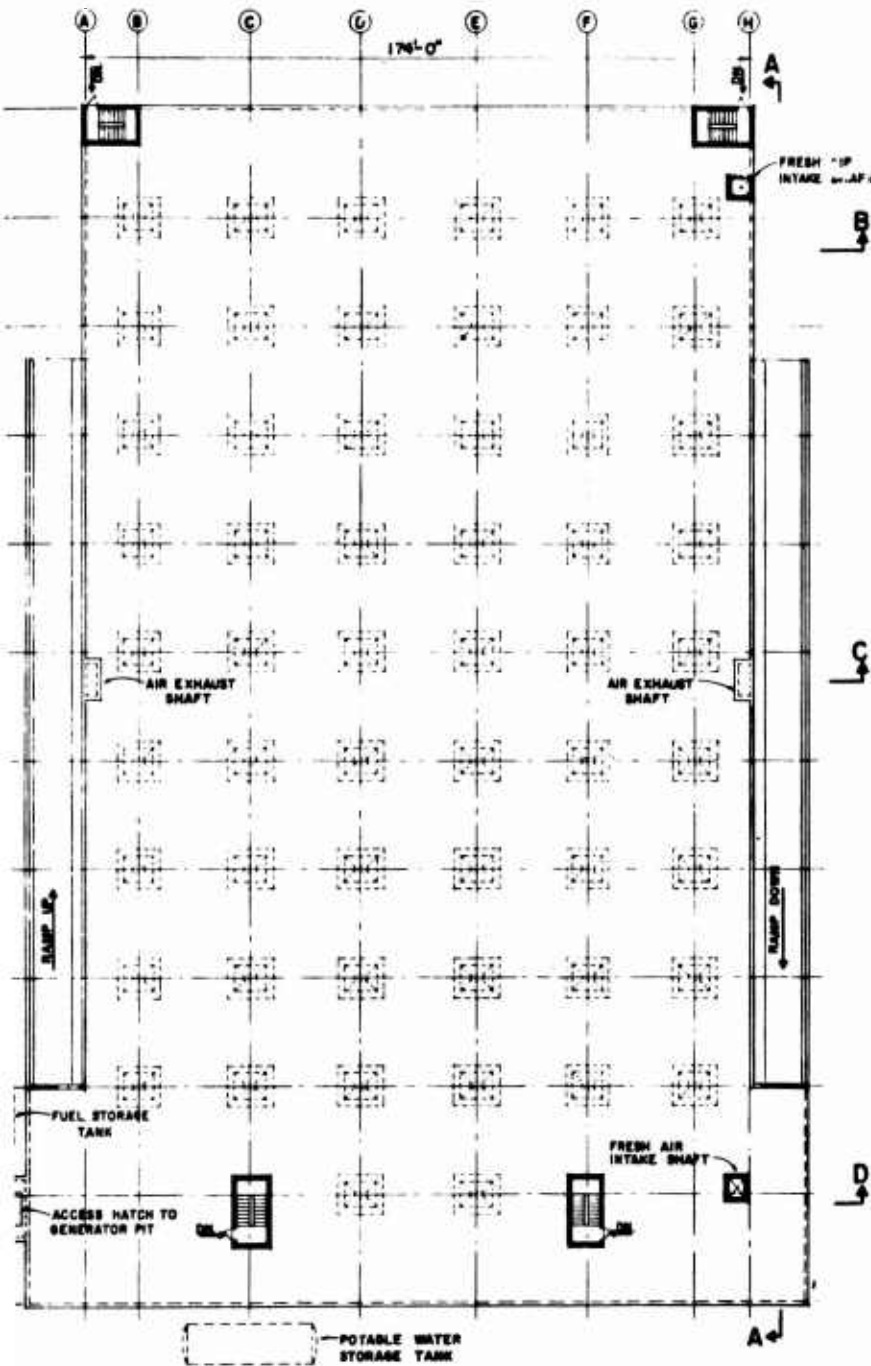


LOWER LEVEL PLAN



UPPER LEVEL PLAN

B



ROOM DESIGNATIONS

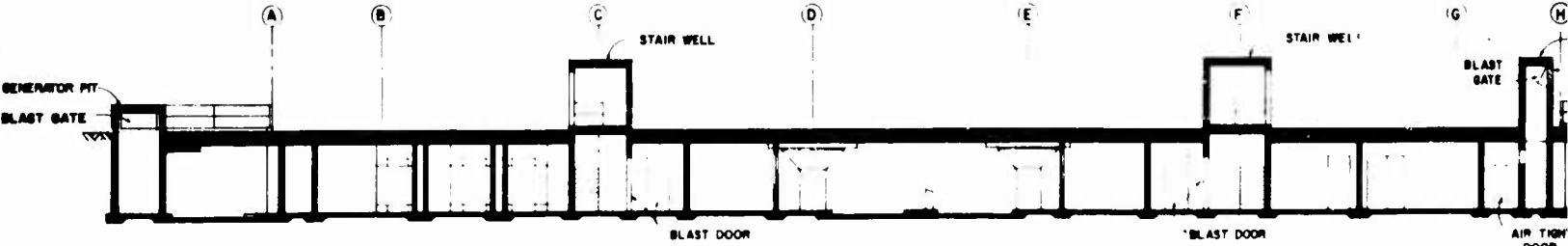
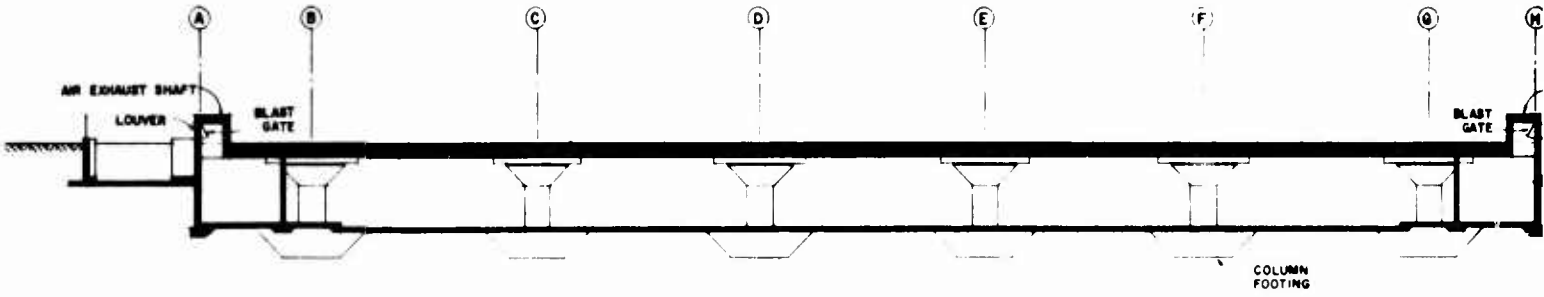
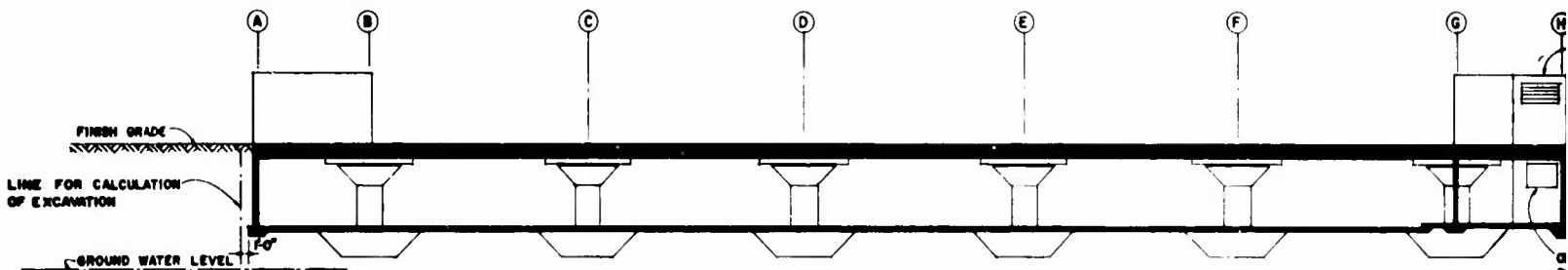
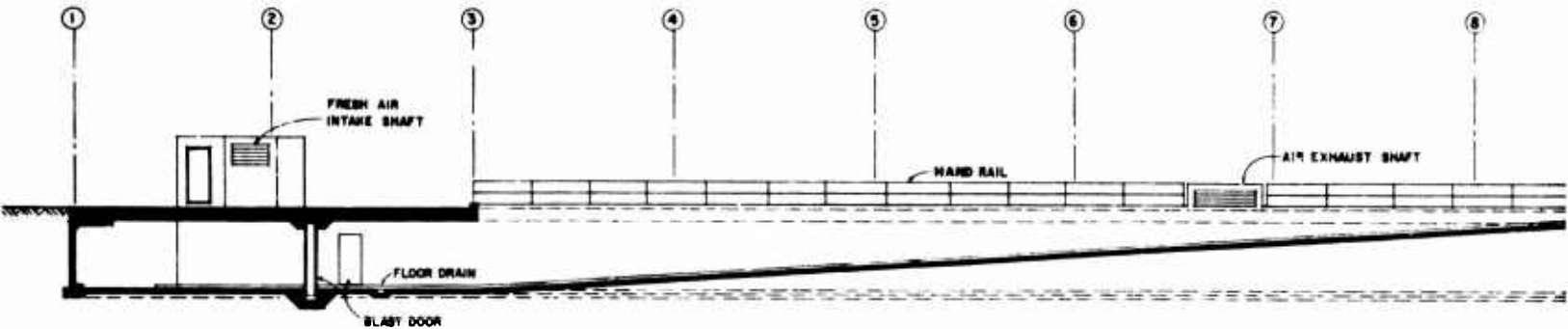
1. PARKING GARAGE
2. PUBLIC WAITING ROOM
3. BLAST LOCK
4. STAIR
5. WOMEN'S TOILET
6. MEN'S TOILET
7. EMPLOYEES TOILET & LOCKER ROOM
8. STORAGE
9. BLAST LOCK
10. MECHANICAL EQUIPMENT - AIR EXHAUST
11. BLAST LOCK
12. STAIR
13. STAIR
14. BLAST LOCK
15. MECHANICAL EQUIPMENT - AIR INTAKE
16. MECHANICAL EQUIPMENT - AIR EXHAUST
17. BLAST LOCK
18. MECHANICAL EQUIPMENT - AIR INTAKE
19. STORAGE
20. STAIR
21. BLAST LOCK
22. OFFICE
23. CHECK OUT BOOTH
24. GENERATOR PIT

UPPER LEVEL PLAN

Fig. A.19

PARKING GARAGE SHELTER FOR 5,000 PERSONS 25 AND 50 PSI

SCALE 10' 0 10' 20' 30'



SCALE 1" = 8'

B

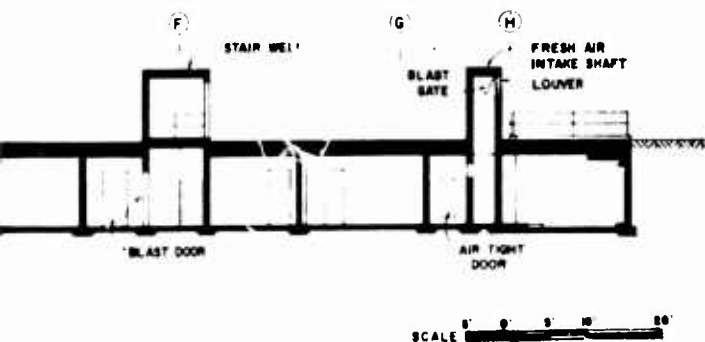
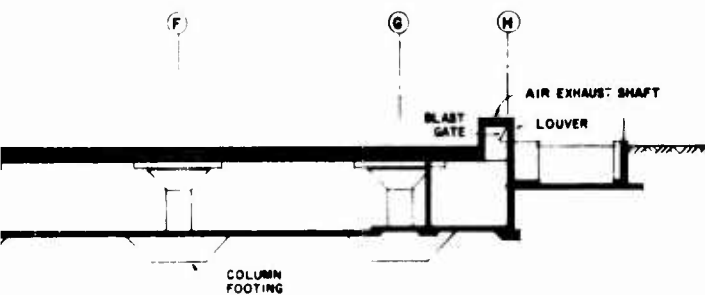
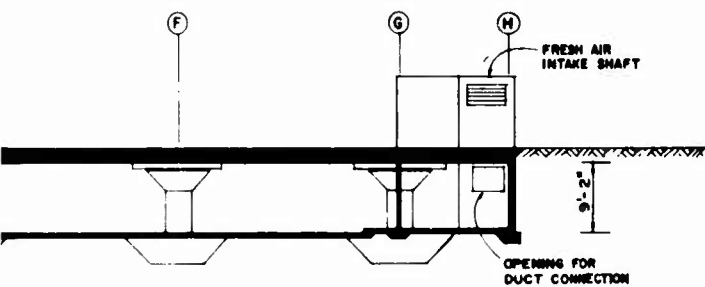
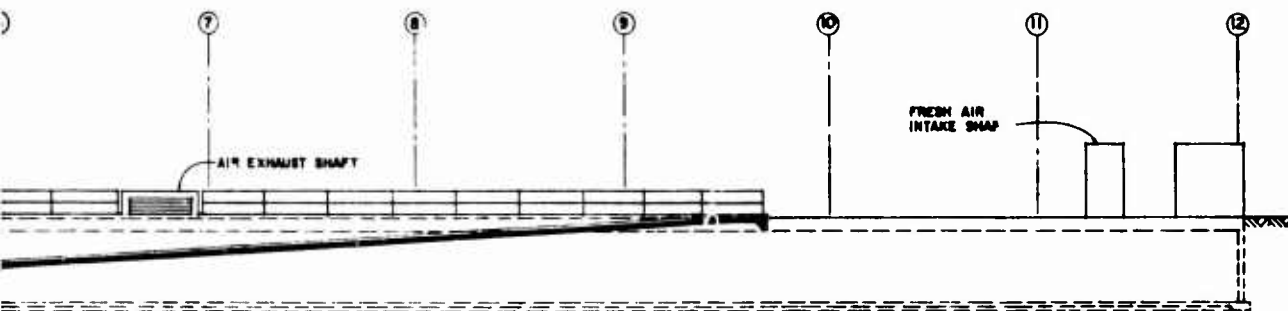


Fig. A.20
PARKING GARAGE SHELTER
FOR 5,000 PERSONS
25 AND 50 PSI

A 12-in. slab thickness is used for the 5 psi Structure I to fulfill structural requirements and afford a minimum protection factor of at least 100. This factor is somewhat greater for Structure II.

Roof slab thicknesses of 21 and 36 in. are used in the 25 and 50 psi garages which afford sufficient radiation protection to reduce initial radiation on the ground surface to a level of 20 rads or less within the shelter. The interior partitions are of cinder block construction in the 5 psi shelter and reinforced concrete tilt-up walls in the 25 and 50 psi shelters. The reinforced concrete partitions were selected to provide adequate lateral resistance against ground shock.

The designs are based upon a minimum concrete strength of 3000 psi throughout for the 25 and 50 psi shelters, and 3000 psi for the roof system and columns, 25 psi elsewhere for the 5 psi below ground garage. The reinforcement conforms to ASTM A432 which has a minimum yield point of 60,000 psi. Percent reinforcement is given in Table A.14. The combined live and dead loads on the garage roof of Structures I and II are taken as 100 and 450 psf, respectively, over the entire surface. Debris loading is assumed as negligible in combination with the blast load. The normal allowable soil bearing capacity is taken as 4 tons/sq ft. The equivalent static blast load on the garage roof is taken as equal to the peak incident overpressure at all three pressure levels based on allowable maximum deformations 1.3 times the peak elastic value.

The main blast doors at the ramp entrances of the 25 and 50 psi shelters consist of structural steel I-beams with steel cover plates. The hollow interior of the doors is filled with concrete to provide the required radiation protection within the tunnel portion of the ramps. The doors are mechanically (electrical power) rolled open and closed. Blast seals are provided around the door periphery to prevent pressure leakage within the structure. The ramp entrance doors of the 5 psi shelter consist of standard overhead rolling doors reinforced to resist the blast overpressure. These doors are operated manually.

TABLE A.14
PERCENT REINFORCEMENT FOR INDICATED STRUCTURAL MEMBERS
OF PARKING GARAGE SHELTERS

Structural Member	Design Weapon Environment		
	5 psi	25 psi	50 psi
Roof Slab	$\phi_e = \phi_c = 1.75$ $\phi_v = 0.0$	$\phi_e = \phi_c = 1.50$ $\phi_v = 0.5$	$\phi_e = \phi_c = 1.5$ $\phi_v = 0.5$
Columns	$\phi' = 2.0$	$\phi' = 2.0$	$\phi' = 2.0$
Column Footings	$\phi = 1.0$ $\phi' = 0.75$	$\phi = 1.0$ $\phi' = 0.75$	$\phi = 1.0$ $\phi' = 0.75$
Concrete Partitions	N/A	$\phi = \phi' = 0.75$	$\phi = \phi' = 0.75$
Partition Footings	$\phi = 0.576$ $\phi' = 0.144$	$\phi = 0.576$ $\phi' = 0.144$	$\phi = 0.576$ $\phi' = 0.144$
Exterior Walls	$\phi = 1.0$ $\phi' = 0.5$	$\phi = 1.0$ $\phi' = 0.5$	$\phi = 1.0$ $\phi' = 0.5$
Exterior Wall Footings	$\phi = 0.53$ $\phi' = 0.13$	$\phi = 0.53$ $\phi' = 0.13$	$\phi = 0.53$ $\phi' = 0.13$

ϕ_e = percent steel at end, effective

ϕ_c = percent steel at centerline

ϕ = percent tension steel

ϕ' = percent compression steel

ϕ_v = percent web reinforcement

A.3.3 Expressway Grade Separation Shelters

Expressway grade separation shelters were designed and costed in connection with the study described in Ref. 63. In the present study this group of shelter concepts were reexamined to determine their life-saving potential and to update their estimates of cost.

Shelters considered are illustrated in Fig. A.21, A.22 and A.23. These illustrations provide basic plans for the three shelters each designed to resist a different "design overpressure" level, i.e., 5, 25 and 50 psi. Figure A.21 shows a three-dimensional cut-away view of one side of the grade separation (bridge) modified to include a personnel shelter. The shelter has two levels. The upper level plan is given in Fig. A.22 and the lower in Fig. A.23. This is a RC shelter which makes use of the conventional structural portions of the bridge. Its interior and exterior walls carry vertical loads and are designed to act as shear walls and to resist flexure.

Structural design was carried out on the basis of ultimate strength with a ductility ratio of 1.3. In the case of 5 psi and 25 psi designs, the structure consists entirely of continuous one-way RC slabs; while in the case of the 50 psi design, additional supporting members such as beams and columns were found to be necessary. In addition to resisting flexure and axial load, the vertical members also act as shear walls. In all cases the roof slab, which carried vehicular and pedestrian traffic, satisfies the strength requirements of AASHTO 1953 specifications. Interior floor slabs (not subject to direct blast pressures) were designed for a uniformly distributed live load of 100 psf with load factors of 1.5 for dead load and 1.8 for live load. Properties of materials considered herein are summarized below.

- Compressive strength of concrete
(f'_c) = 4000 psi
- Dynamic compressive strength of concrete
($1.25 f'_c$) = 6000 psi
- Dynamic yield strength of reinforcing steel
(f_{yd}) = 52,000 psi

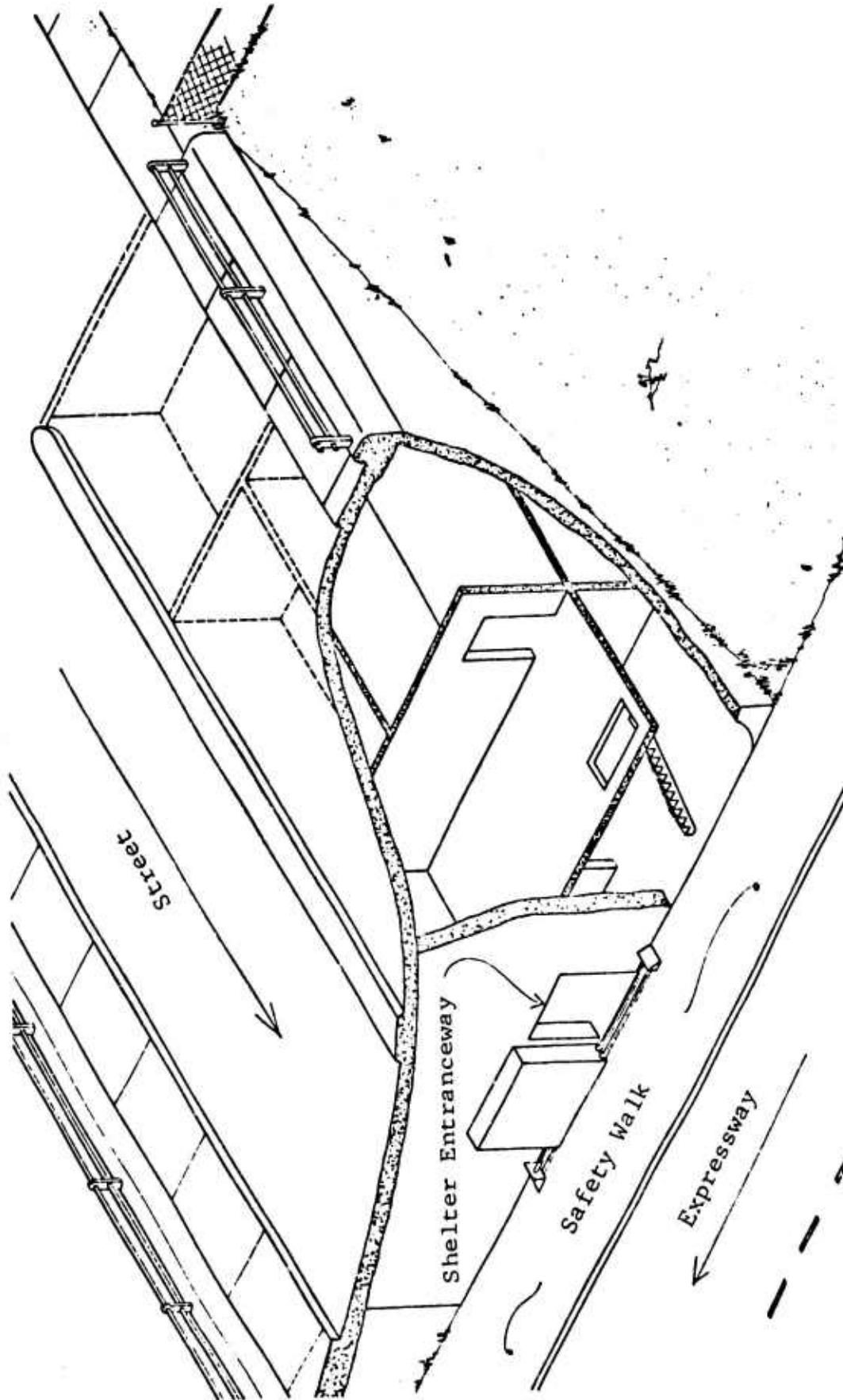


Fig. A.21 CUTAWAY VIEW OF AN EXPRESSWAY GRADE SEPARATION SHELTER

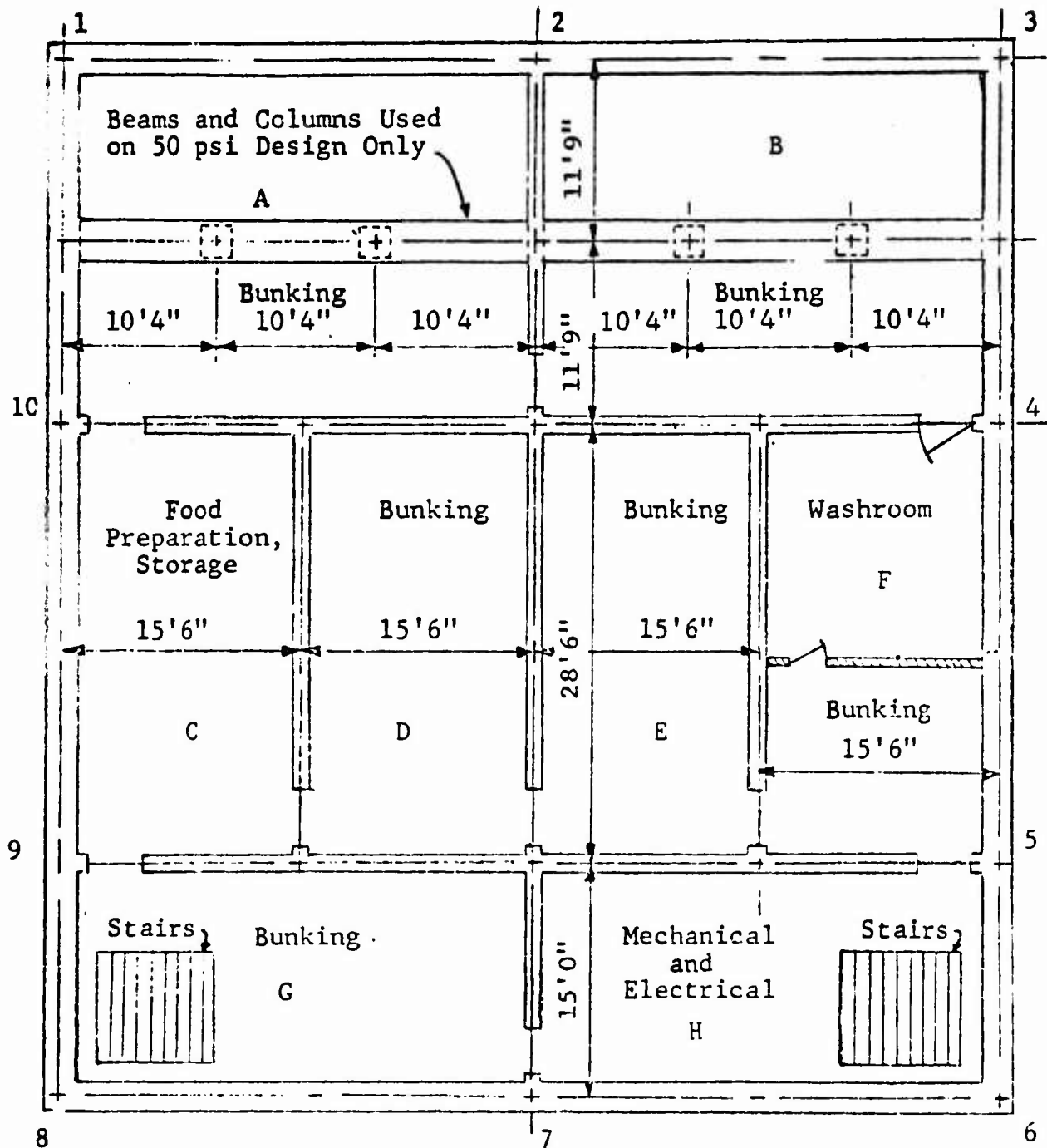


Fig. A.22 UPPER LEVEL FLOOR PLAN

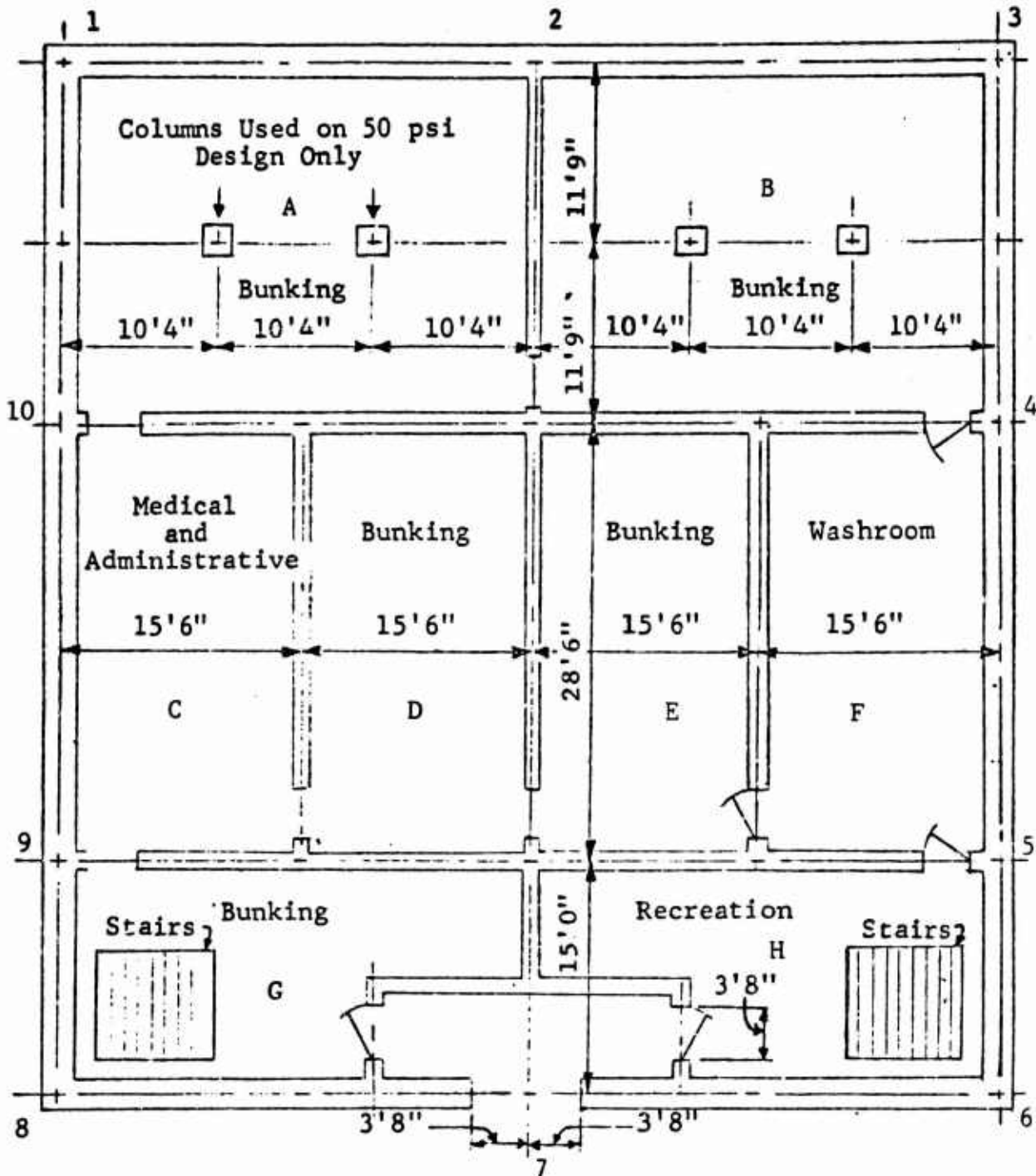


Fig. A.23 LOWER LEVEL FLOOR PLAN

- Allowable dynamic soil pressure $8^T/\text{sq ft}$
- Percent reinforcement $\phi = \phi' = 1.0$ percent*
- Depth of reinforcement 2 in. both sides

Structural component thicknesses for the three shelters are given in Table A.15.

TABLE A-15

STRUCTURAL COMPONENT THICKNESSES FOR THREE SHELTERS

Component	5 psi	25 psi	50 psi
Roof Slab			
Section A (Fig. B.8)	18"	22"	20"
Section B	18"	18"	22"
Section C	18"	18"	22"
External Walls			
Sections 1-2, 2-3	10"	12"	14"
All Others	18"	18"	22"
Partitions	6"	6"	6"
Floor Slabs	6"	6"	6"
Columns			15" x 15"
Beam			18.5" x 36"
Footings			
Wall	2'7" x 8"	4'3" x 10"	7'8" x 1'10"
Column			8'0" x 8'0"

* ϕ = percent tension steel

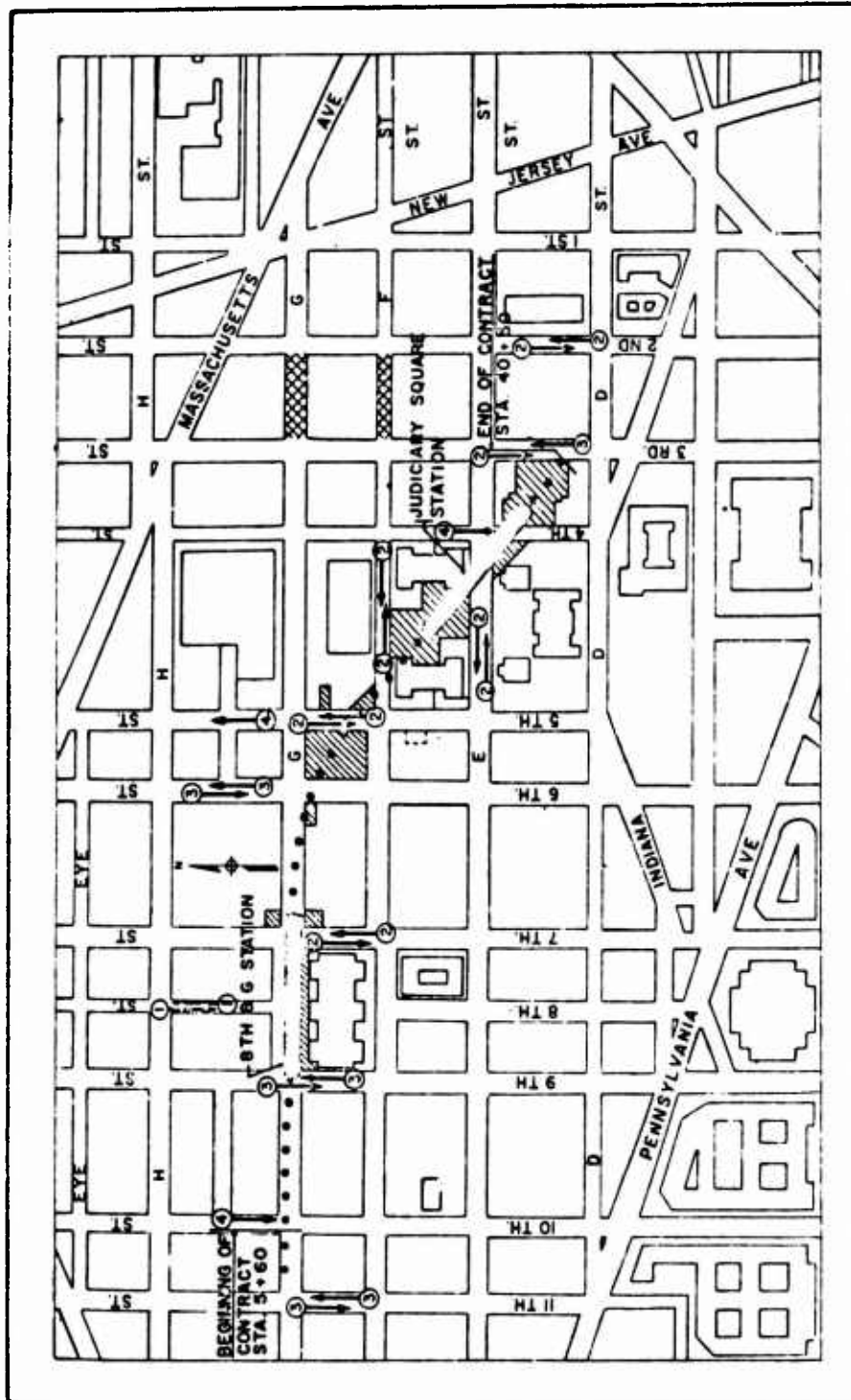
ϕ' = percent compression steel

A.3.4 Subway Passenger Station Shelter

The Judiciary Square passenger station is part of the proposed Washington Metropolitan Area Rapid Transit subway system. Its location within the proposed transportation network is shown in Fig. A.24. Its general plan and elevation are shown in Fig. A.25. This is a 600-ft long RC structure consisting of twelve 50-ft sections (units)(see Fig. A.26). Its cross section forms an elliptic arch with a flat base. A typical half-section through the arch is shown in Fig. A.27. The arch is of waffle-slab construction, variable thickness and is doubly-reinforced. It enclosed two mezzanines and two passenger stations (see Fig.A.25) and connects two entranceways. Transportation tunnels leading to and from the station are of rectangular cross section as is usual in cut and cover construction. Ventilation structures are located at both ends of the station (Fig. A.25) as are service rooms. Service rooms are located near the entrances at two levels, i.e., the mezzanine and the track level. Ventilation shafts are provided as shown in Fig. A.26. The spacing of ventilation shafts is approximately 75 ft except in the region occupied by the mezzanine. Concrete ducts with air supply registers are provided in the mezzanines (see Fig. A.27). These ducts emanate from the service areas. Total cross-sectional area of openings leading to the station is given in Table A.16.

The mezzanine is intermediate between the street level and the station platforms. It consists of two-way RC slabs supported on 24-in. diameter columns. The mezzanine is shown in Figs. A.25 and A.27. The net floor area of the two mezzanines is estimated at 7500 sq ft.

Passenger platforms are located within the station as shown in Fig. A.27. They consist of RC slabs and are located approximately 5-ft above the floor level. Space beneath the platforms is used for electric utilities and air supply. Passenger platforms are 600-ft long (each) and have a total width of 12 ft-1/2 in.



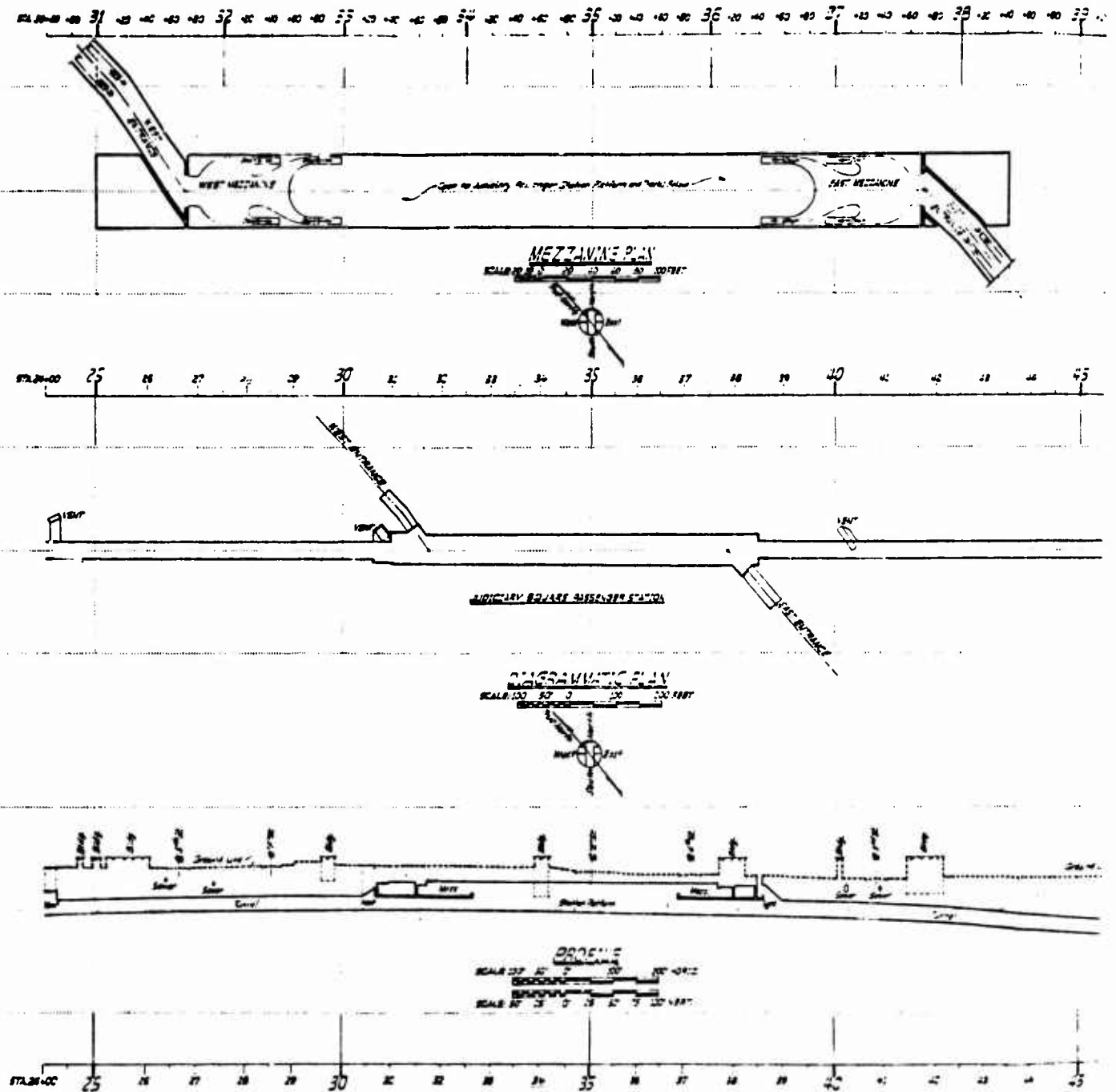


Fig. A.25 JUDICIARY SQUARE PASSENGER STATION, GENERAL PLAN AND ELEVATION

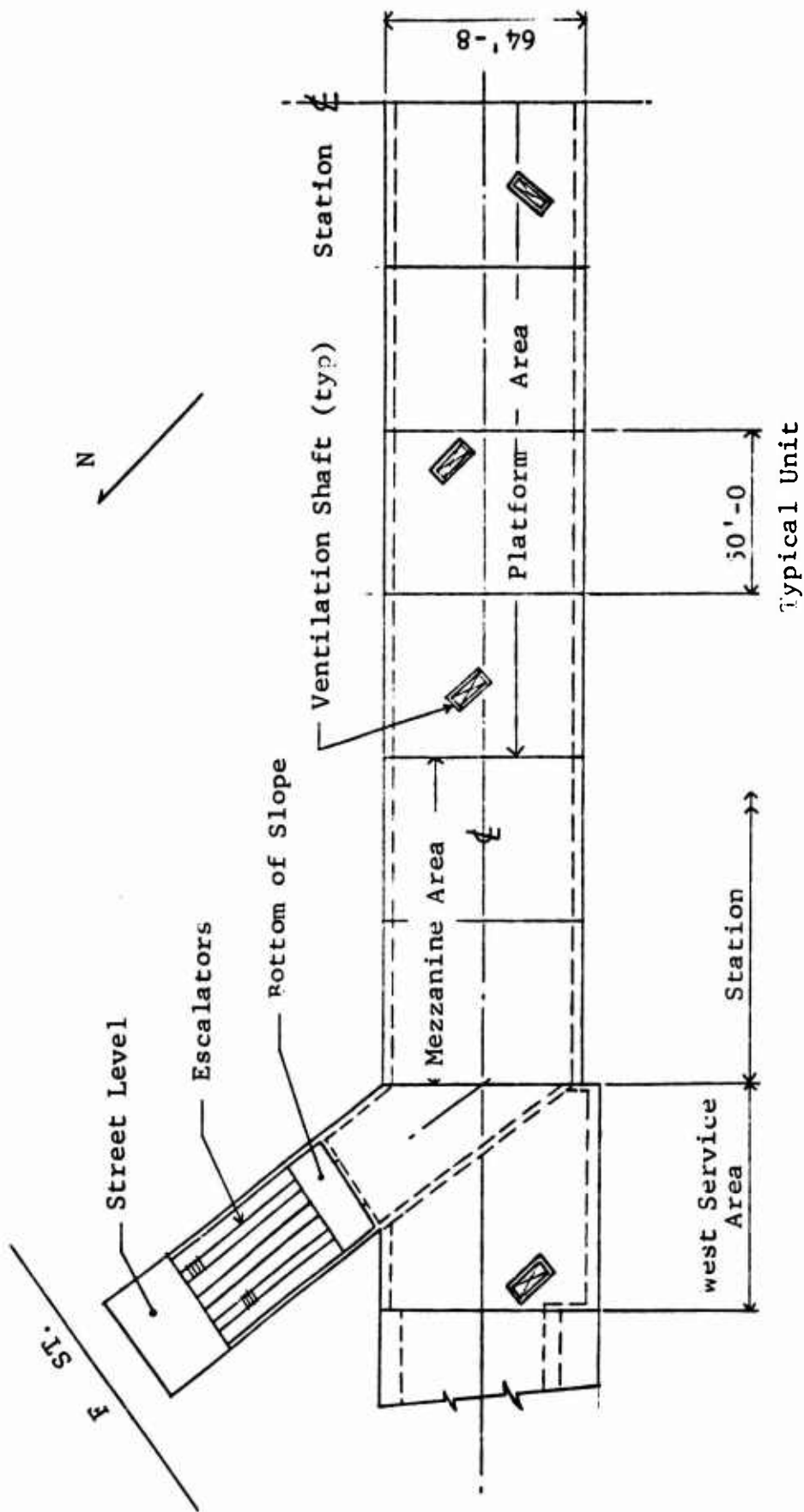


Fig. A.26 JUDICIARY SQUARE PASSENGER STATION, ROOF PLAN (HALF SECTION)

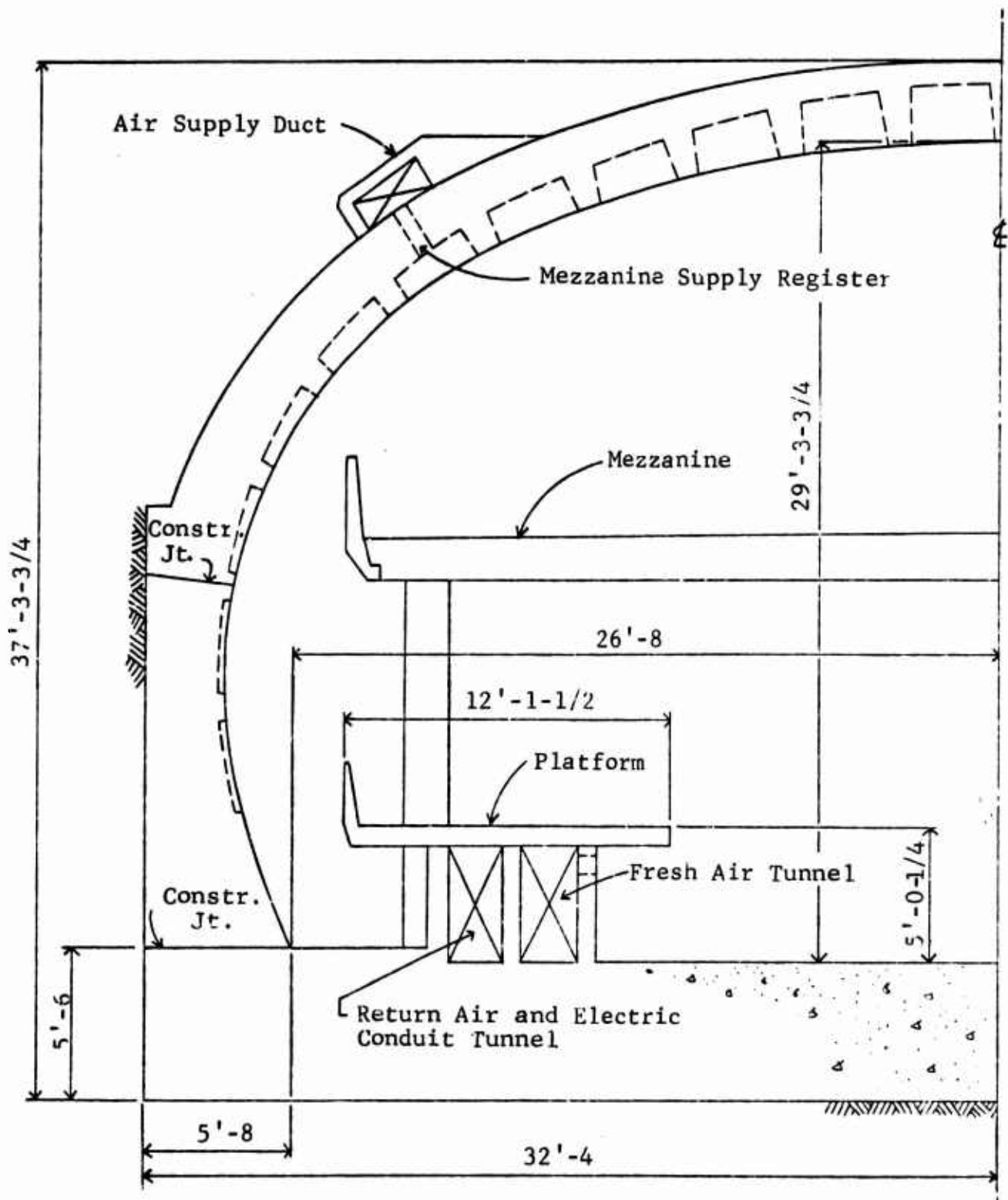


Fig. A.27 JUDICIARY SQUARE PASSENGER STATION ARCH
(SURVEY STATION 37 + 70)

TABLE A.16
OPENINGS LEADING INTO THE PASSENGER STATION

1. Ventilation shaft openings in the roof of the station and service areas; six openings with an average duct (cross-sectional) area of 23.1 sq ft each. One opening, 23.6 sq ft and one openings, 12.5 sq ft.
 2. Ventilation structure openings:
 West structure, 195 sq ft
 East structure, 228 sq ft
 3. Entranceways: 193 sq ft each
 4. Total duct area (excluding gratings and other obstructions)
 983.7 sq ft
-

The net usable area (sheltering purposes) of each platform (after deducting four escalator pits, six columns, parapet and a longitudinal edge distance of 1.5 ft) is 5622 sq ft or a total of 11,244 sq ft for this passenger station.

Assuming that only passenger platforms and mezzanines are used for sheltering purposes then the total usable floor area available is 18,744 sq ft. At 10 sq ft per person this is capable of accommodating 1874 shelterees. With the total (gross) station volume of 900,000 cu ft, the volume per occupant is 480 cu ft.

If the total floor area of the station (mezzanines, platforms, track area, etc.) is utilized, then the available floor area is 46,700 sq ft and is capable of accommodating 4670 shelterees. Shelter volume per occupant in this instance is 193 cu ft. The above calculations include only the station and not the service area (see Fig. A.26). Service areas would not be generally available for sheltering purposes.

Sheltering costs for this passenger station are given in Chapter One together with protective capabilities.

A.4 COSTS OF DUAL-PURPOSE

A.4.1 Schools and Parking Garages

The costs of dual-purpose shelters described are estimated. As previously clarified, these are in reality cost estimates based on what an experienced contractor located in Chicago, Illinois would most probably bid in the spring of 1969 in order to construct these structures in the same location. Being thus defined, the given costs are subject to variations, as is usually the case when bids are submitted for a given job. See Section A.2 for a brief discussion of such variations.

For each structure considered the costed items include:

shelter structure with entranceways,
habitability items, and
contractor's profit and overhead contingencies
(20 percent).

They do not include:

site costs such as land, land clearance, surveys,
soil borings, legal fees, real estate agent com-
missions or title costs,
design costs such as architect and engineer fees,
government supervision; administrative and inspective,
financing costs,
operating, remodeling and maintenance costs, and
cost of food items and medical supplies.

When considering dual-use shelters a clear understanding of "sheltering cost" is important. The sheltering cost is the cost incurred in providing the sheltering capability in a given structure. Depending on the weapon environment, this capability may be achieved through "slanting" or "hardening" a portion of such a building. The sheltering cost then is the difference between the cost of the building with shelter and without, and occurs due to additional labor, materials, equipment and supplies required in providing such a capability. Obviously, in order to determine sheltering costs in any one case we need two sets of

cost data: one for the building with shelter, and one without. For hardened structures discussed in this section, comparable conventional basements are not available. In order to determine sheltering costs, use is made of structures (school basements and parking garages) (Refs. 53 and 54) designed to resist conventional-use loads and fallout radiation. A review of their design, i.e., span lengths, member thicknesses, percent reinforcement, etc. indicates that for purposes of cost comparisons these structures may be considered as being of the conventional use type and are henceforth referred to as such. With the exception of member thicknesses, these conventional structures (school basements and parking garages) are in all other respects identical to the hardened structures discussed herein (see Figs. A.14 through A.17 for basement schools and Figs. A.18 through A.20 for parking garages) and are therefore not illustrated.

Three cost options are considered for both use classes. Cost option 1 consists of:

- (1) Shelter structure, conventional doors, blast doors, stairs and associated hardware.
- (2) Mechanical and electrical equipment of commercial variety commensurate with conventional as well as emergency use.

Cost option 2 consists of:

- (1) Shelter structure, conventional doors, blast doors, stairs and associated hardware.
- (2) Mechanical and electrical equipment of commercial variety commensurate with conventional use only. Special mechanical and electrical equipment capable of reliable functioning under emergency conditions is not provided.

Cost option 3 consists of:

- (1) Shelter structure, conventional doors, blast doors, stairs and associated hardware.
- (2) Mechanical and electrical equipment of commercial variety commensurate with conventional use only.

- (3) Recommended OCD items such as,
- ventilation kits
 - water containers convertible to chemical toilets
 - electrical package

Shelter costs for the three options discussed are summarized in Tables A.17 through A.19 for the basement shelters and Tables A.20 and A.21 for the parking garage shelters. Detailed costs of items comprising these options are given in Appendix B.

For accounting, scheduling as well as subcontract purposes, contract costs on a given project are generally subdivided into convenient categories which define distinct construction operations, labor skills, types of equipment and their usage, materials of construction, etc. Such categorization also provides a convenient means for determining the relative influence of various individual cost items on the total project costs. In the case of dual-use shelters discussed, the primary cost categories include:

- (1) Earthwork and Structural
- (2) Architectural
- (3) Mechanical
- (4) Electrical

The first category includes such cost items as excavation, back-fill, forming, framing, concrete, etc. The result is a complete structure without finishes or utilities. The second category includes finishes such as painting, floor tile as well as doors, partitions, etc. Category (3) includes all mechanical work and equipment such as plumbing, heating and ventilation. Installation of electrical equipment including wiring is contained in category (4).

The relative influence of these categories on the total cost is illustrated graphically for one cost option in Figs. A.28 and A.29. It will be noted that category (1) is the major contributor to the total shelter cost. This holds true for both single- and dual-purpose shelters.

TABLE A.17
SUMMARY OF TOTAL COSTS FOR SCHOOL BASEMENT SHELTERS, COST OPTION 1

Capacity	Description	Design Weapon Environment, psi					
		Conventional		5		25	
		Cost (\$)	Total Cost (%)	Cost (\$)	Total Cost (%)	Cost (\$)	Total Cost (%)
Population 550 Gross Floor Area 6440 sq ft	Earthwork and Structural	45,748	41.9	50,596	42.5	70,902	50.0
	Architectural	12,260	11.2	11,594	9.7	8,594	6.1
	Mechanical	21,027	19.2	21,330	17.9	22,187	15.6
	Electrical	11,948	11.0	15,755	13.2	16,538	11.6
	Total Direct Contract Cost	90,983	--	99,275	--	118,221	--
	Contractor's Profit and Overhead Contingencies (20%)	18,197	16.7	19,855	16.7	23,644	16.7
	Total Cost	109,180	100.0	119,130	100.0	141,865	100.0
	Cost Difference Over Conventional	--	--	9,950	--	32,685	--
	Unit Cost (total)	16.95	--	18.50	--	22.03	--
	Unit Cost Difference Over Conventional	--	--	1.55	--	5.08	--
Population 1100 Gross Floor Area 12,260 sq ft	Cost Increase Over Conventional (%)	--	--	9.1%	--	30.0%	--
	Earthwork and Structural	81,788	41.6	87,057	41.5	122,804	49.5
	Architectural	21,138	10.7	20,675	9.9	15,025	6.0
	Mechanical	38,313	19.5	38,678	18.4	39,799	16.0
	Electrical	22,680	11.5	28,350	13.5	29,430	11.8
	Total Direct Contract Cost	163,919	--	174,760	--	207,058	--
	Contractor's Profit and Overhead Contingencies (20%)	32,784	16.7	34,952	16.7	41,412	16.7
	Total Cost	196,703	100.0	209,712	100.0	248,470	100.0
	Cost Difference Over Conventional	--	--	13,009	--	41,767	--
	Unit Cost (total)	16.04	--	17.11	--	20.27	--
	Unit Cost Difference Over Conventional	--	--	1.07	--	4.23	--
	Cost Increase Over Conventional (%)	--	--	6.7%	--	26.4%	--

TABLE A.18
SUMMARY OF TOTAL COSTS FOR SCHOOL BASEMENT SHELTERS, COST OPTION 2

Capacity	Description	Design Weapon Environment, psi							
		Conventional		5		25		50	
		Cost (\$)	Total Cost (%)	Cost (\$)	Total Cost (%)	Cost (\$)	Total Cost (%)	Cost (\$)	Total Cost (%)
Population 550 Gross Floor Area 6440 sq ft	Earthwork and Structural	45,748	41.9	50,596	44.3	70,902	52.5	95,770	58.1
	Architectural	12,260	11.2	11,594	10.2	8,594	6.4	8,594	5.2
	Mechanical	21,027	19.2	21,027	18.3	21,027	15.5	21,027	12.7
	Electrical	11,948	11.0	11,948	10.5	11,948	8.9	11,948	7.3
	Total Direct Contract Cost	90,983	--	95,165	--	112,471	--	137,339	--
	Contractor's Profit and Overhead Contingencies (20%)	18,197	16.7	19,033	16.7	22,494	16.7	27,468	16.7
	Total Cost	109,180	100.0	114,198	100.0	134,965	100.0	164,807	100.0
	Cost Difference Over Conventional	--	--	--	--	--	--	--	--
	Unit Cost (total)	16.95	--	17.73	--	20.96	--	25.59	--
	Unit Cost Difference Over Conventional	--	--	0.78	--	4.01	--	8.64	--
	Cost Increase Over Conventional (%)	--	--	4.6%	--	23.6%	--	51.0%	--
Population 1100 Gross Floor Area 12,260 sq ft	Earthwork and Structural	81,788	41.6	87,057	43.0	122,804	51.5	166,604	57.2
	Architectural	21,138	10.7	20,675	10.2	15,025	6.3	15,025	5.2
	Mechanical	38,313	19.5	38,313	18.9	38,313	16.0	38,313	13.1
	Electrical	22,680	11.5	22,680	11.2	22,680	9.5	22,680	7.8
	Total Direct Contract Cost	163,919	--	168,725	--	198,822	--	242,622	--
	Contractor's Profit and Overhead Contingencies (20%)	32,784	16.7	33,745	16.7	39,764	16.7	48,524	16.7
	Total Cost	196,703	100.0	202,470	100.0	238,586	100.0	291,146	100.0
	Cost Difference Over Conventional	--	--	5,767	--	41,883	--	94,443	--
	Unit Cost (total)	16.04	--	16.51	--	19.46	--	23.75	--
	Unit Cost Difference Over Conventional	--	--	0.47	--	3.42	--	7.71	--
	Cost Increase Over Conventional (%)	--	--	2.9%	--	21.3%	--	48.0%	--

TABLE A.20

SUMMARY OF TOTAL COSTS FOR PARKING GARAGE SHELTERS, STRUCTURE I, FOR VARIOUS COST OPTIONS
(Capacity 5000 Persons, Gross Floor Area 51,670 sq ft)

Cost Option	Description	Conventional		Design Weapon Environments, psi					
				5		25		50	
		Cost (\$)	Total Cost (%)	Cost (\$)	Total Cost (%)	Cost (\$)	Total Cost (%)	Cost (\$)	Total Cost (%)
1	Earthwork and Structural	309,602	56.2	328,412	55.4	501,976	62.1	712,236	67.2
	Architectural	42,670	7.7	42,303	7.1	40,770	5.0	40,770	3.8
	Mechanical	83,511	15.2	88,480	14.9	93,940	11.6	93,940	8.9
	Electrical	23,126	4.2	34,706	5.9	36,918	4.6	36,918	3.4
	Total Direct Contract Cost	458,909	--	493,901	--	673,604	--	883,864	--
	Contractor's Profit and Overhead Contingencies (20%)	91,782	16.7	98,780	16.7	134,721	16.7	176,773	16.7
	Total Cost	550,691	100.0	592,681	100.0	808,325	100.0	1,060,637	100.0
	Cost Difference Over Conventional	--	--	41,990	--	257,634	--	509,946	--
	Unit Cost (total)	10.66	--	11.47	--	15.64	--	20.53	--
	Unit Cost Difference Over Conventional	--	--	0.81	--	4.98	--	9.87	--
	Cost Increase Over Conventional (%)	--	--	7.6%	--	46.7%	--	92.7%	--
2	Earthwork and Structural	309,602	56.2	328,412	57.3	501,976	64.4	712,236	69.0
	Architectural	42,670	7.7	42,303	7.4	40,770	5.2	40,770	4.0
	Mechanical	83,511	15.2	83,511	14.6	83,511	10.7	83,511	8.1
	Electrical	23,126	4.2	23,126	4.0	23,126	3.0	23,126	2.2
	Total Direct Contract Cost	458,909	--	477,352	--	649,333	--	859,643	--
	Contractor's Profit and Overhead Contingencies (20%)	91,782	16.7	95,470	16.7	129,877	16.7	171,929	16.7
	Total Cost	550,691	100.0	572,822	100.0	779,260	100.0	1,031,572	100.0
	Cost Difference Over Conventional	--	--	22,131	--	228,569	--	480,881	--
	Unit Cost (total)	10.66	--	11.09	--	15.08	--	19.96	--
	Unit Cost Difference Over Conventional	--	--	0.43	--	4.42	--	9.30	--
	Cost Difference Over Conventional (%)	--	--	4.0%	--	41.5%	--	87.2%	--
3	Earthwork and Structural	309,602	56.2	328,412	56.0	501,976	63.3	712,236	68.1
	Architectural	42,670	7.7	42,303	7.2	40,770	5.2	40,770	3.8
	Mechanical	83,511	15.2	92,711	15.8	92,711	11.7	92,711	8.9
	Electrical	23,126	4.2	25,626	4.3	25,626	3.1	25,626	2.5
	Total Direct Contract Cost	458,909	--	489,052	--	661,083	--	871,343	--
	Contractor's Profit and Overhead Contingencies (20%)	91,782	16.7	97,810	16.7	132,217	16.7	174,269	16.7
	Total Cost	550,691	100.0	586,862	100.0	793,300	100.0	1,045,612	100.0
	Cost Difference Over Conventional	--	--	36,171	--	242,609	--	494,921	--
	Unit Cost (total)	10.66	--	11.36	--	15.35	--	20.23	--
	Unit Cost Difference Over Conventional	--	--	0.70	--	4.69	--	9.57	--
	Cost Increase Over Conventional (%)	--	--	6.6%	--	44.0%	--	89.8%	--

TABLE A.21

SUMMARY OF TOTAL COSTS FOR PARKING GARAGE SHELTERS, STRUCTURE II, FOR VARIOUS COST OPTIONS
(Capacity 5000 Persons, Gross Floor Area 51,670 sq ft)

Cost Option	Description	Conventional		Design Weapon Environments, psi					
				5		25		50	
		Cost (\$)	Total Cost (%)	Cost (\$)	Total Cost (%)	Cost (\$)	Total Cost (%)	Cost (\$)	Total Cost (%)
1	Earthwork and Structural	395,101	61.7	408,288	60.9	545,476	64.5	752,392	68.8
	Architectural	31,480	4.9	27,648	4.1	28,290	3.3	28,290	2.6
	Mechanical	83,511	13.1	88,480	13.2	93,940	11.1	93,940	8.6
	Electrical	23,126	3.6	34,706	5.1	36,918	4.4	36,918	3.3
	Total Direct Contract Cost	533,218	--	559,122	--	704,624	--	911,540	--
	Contractor's Profit and Overhead Contingencies (20%)	106,644	16.7	111,824	16.7	140,925	16.7	182,308	16.7
	Total Cost	639,862	100.0	670,946	100.0	845,549	100.0	1,093,848	100.0
	Cost Difference Over Conventional	--	--	31,084	--	205,687	--	453,986	--
	Unit Cost (total)	12.38	--	12.99	--	16.36	--	21.17	--
	Unit Cost Difference Over Conventional	--	--	0.61	--	3.98	--	8.79	--
	Cost Increase Over Conventional (%)	--	--	4.9%	--	32.1%	--	71.0%	--
2	Earthwork and Structural	395,101	61.7	408,288	62.7	545,476	66.8	752,392	70.7
	Architectural	31,480	4.9	27,648	4.2	28,290	3.5	28,290	2.6
	Mechanical	83,511	13.1	83,511	12.8	83,511	10.2	83,511	7.8
	Electrical	23,126	3.6	23,126	3.6	23,126	2.8	23,126	2.2
	Total Direct Contract Cost	533,218	--	542,573	--	680,403	--	887,319	--
	Contractor's Profit and Overhead Contingencies (20%)	106,644	16.7	108,515	16.7	116,081	16.7	177,464	16.7
	Total Cost	639,862	100.0	651,088	100.0	816,484	100.0	1,064,783	100.0
	Cost Difference Over Conventional	--	--	11,226	--	176,622	--	424,921	--
	Unit Cost (total)	12.38	--	12.60	--	15.80	--	20.61	--
	Unit Cost Difference Over Conventional	--	--	0.22	--	3.42	--	8.23	--
	Cost Difference Over Conventional (%)	--	--	1.8%	--	27.6%	--	66.5%	--
3	Earthwork and Structural	395,101	61.7	408,288	61.4	545,476	65.7	752,392	69.7
	Architectural	31,480	4.9	27,648	4.2	28,290	3.3	28,290	2.6
	Mechanical	83,511	13.1	92,711	13.9	92,711	11.2	92,711	8.6
	Electrical	28,126	3.6	25,626	3.8	25,626	3.1	25,626	2.4
	Total Direct Contract Cost	533,218	--	554,273	--	692,103	--	899,019	--
	Contractor's Profit and Overhead Contingencies (20%)	106,644	16.7	110,855	16.7	138,421	16.7	179,804	16.7
	Total Cost	639,862	100.0	665,128	100.0	830,524	100.0	1,078,823	100.0
	Cost Difference Over Conventional	--	--	25,266	--	190,662	--	438,961	--
	Unit Cost (total)	12.38	--	12.87	--	16.07	--	20.88	--
	Unit Cost Difference Over Conventional	--	--	0.49	--	3.69	--	8.50	--
	Cost Difference Over Conventional (%)	--	--	4.0%	--	29.8%	--	68.7%	--

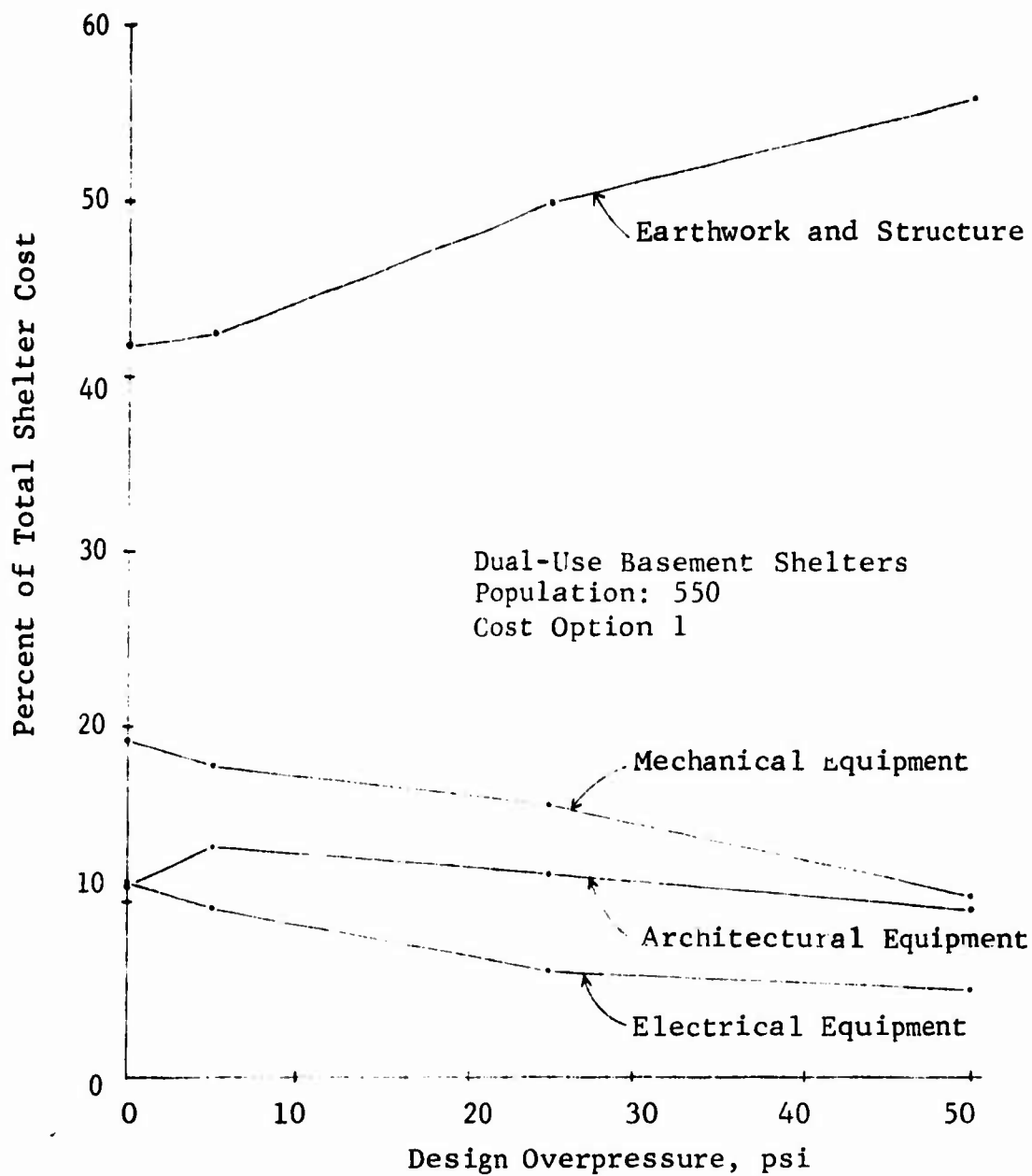


Fig. A.28 COST OF STRUCTURE AND EQUIPMENT SHELTER COMPONENTS AS PERCENT OF TOTAL SHELTER COST

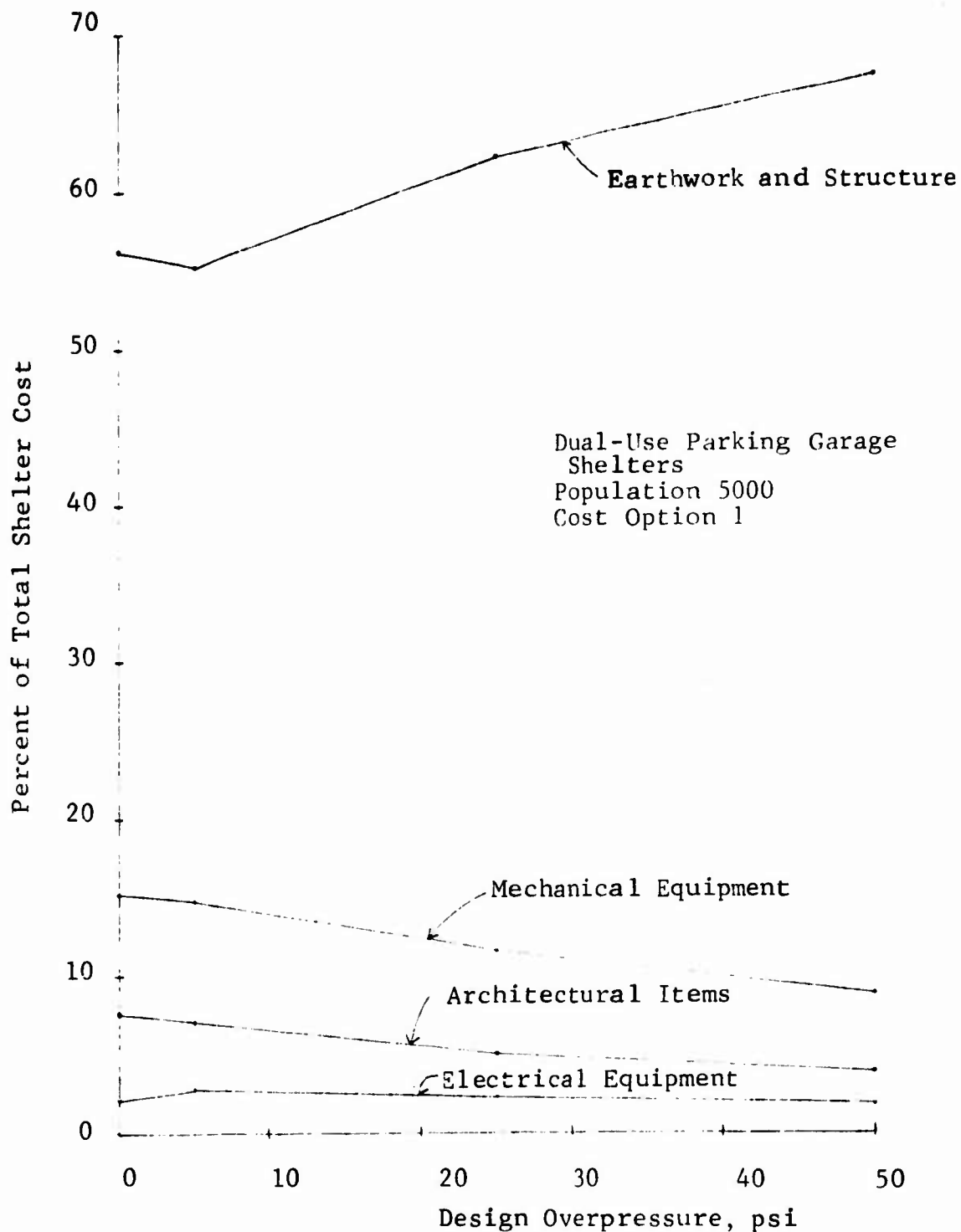


Fig. A.29 COST OF STRUCTURE AND EQUIPMENT SHELTER COMPONENTS AS PERCENT OF TOTAL SHELTER COST

In the example of dual-purpose basement structures, this category accounts for 41.6 percent (see Table A.17) of the cost for a conventional basement, and 55.3 percent of the cost for the same basement hardened to 50 psi. If we consider dual-use parking garages, category (1) accounts for 56.2 percent (see Table A.20) of the total cost in the case of a conventional garage, and 67.2 percent of the total cost for the same garage hardened to 50 psi. The remaining three cost categories (see Fig. A.28 and A.29) contribute significantly less. It is evident that in order to reduce sheltering costs, it is worthwhile to seek those structural configurations which are capable of reducing construction costs but not reducing survivability. In this respect, school basements considered herein are more efficient than parking garage shelters.

A.4.2 Grade Separation Shelters

Expressway grade separation shelters considered herein were designed and costed in connection with the study described in Ref. 63. The respective costs were for the Chicago, Ill. area in midyear 1964. This subsection contains costs for this group of shelters updated to midyear 1969.

Reference 63 considered one (habitability) cost option. This option was based on commercially available life-support equipment. In order to give the planner several choices, two cost options are considered in this study. Cost option 1 makes use of life-support equipment developed by OCD (see Table B.9). Cost option 2 makes use of commercially available habitability items together with package ventilation kits. It is based on the following assumptions.

1. Sanitary facilities are provided in accordance with Ref. 64 and are based on 800 occupants for a period of 14 days.

2. It is assumed that no outside utilities will be available in the event of an attack. Thus, storage tanks for potable water are provided. A motor generator set is provided to furnish a power source for electric lighting and other electric power requirements in accordance with Ref. 65. The generator is to be run by a diesel engine drawing fuel from an underground tank.
3. Ventilation is provided by shelter package ventilation kits with filters (Ref. 66). No period of complete closure to the outside is contemplated, thus no internal oxygen supply is considered.
4. Lighting is assumed to be provided by public service on AC current until the time of emergency, and thereafter by means of a DC generator within the shelter.
5. Medical supplies, food, sleeping accommodations, and communication equipment are not included in this cost option.

All emergency electrical power would be provided by means of a 20 kw generator powered by a 35 hp diesel engine (Ref. 64). The engine is provided with a 14-day fuel supply based on a continuous use. The 2000 gallons of fuel required is stored in an underground tank. Lighting provided is based on a 1-ft candle level in berthing and standing areas, 5-ft candles in exercise and toilet areas, and 15-ft candles in food preparation, reading and medical attention areas (Ref. 63). It is also assumed that lights will be wired to run on ordinary 115V 60-cycle AC power when it is available, and DC generator power when AC power is not available.

Sanitary facilities and water for shelter use are provided in accordance with Ref. 63 and are summarized below.

Item	Unit Quantity	Total Provided
Water	28 gal/person	22,400 gallons
Toilets	5/100 people	40
Urinals	1/100 people	8

Ventilation would be supplied by four shelter package ventilation kits (Ref. 66). Four of these units will supply a total of the minimum requirements set down (Ref. 63). The ventilation unit can ordinarily run off the generator, but in case there is a power failure, the generators are provided with bicycle drives.

Sheltering costs for the two cost options described are summarized in Tables A.22 and A.23. They represent average values in the Chicago Metropolitan area for midyear 1971. Items included in the mechanical, electrical and architectural portions are listed in Table A.24 for cost option 2. Mechanical and electrical items for cost option 1 are the same as for option 2. In Tables A.22 and A.23 the item labeled "Structural and Earthwork" includes labor and materials for excavation, backfill, grading, formwork, concrete, reinforcing steel, finishing, and blast doors which are of RC.

Costs given do not include price of land or architects and engineers fees.

TABLE A.22
SUMMARY OF COSTS, EXPRESSWAY GRADE SEPARATION SHELTERS
COST OPTION 1

Item	5 psi	25 psi	50 psi
Earthwork and Structural	\$90,700	\$96,000	\$117,000
Mechanical }	1,870	1,870	1,870
Electrical }			
Architectural	6,035	6,035	6,455
Credit for Portions of the Original Structure	-42,400	-42,400	-42,400
Net Contract Cost	56,205	61,505	82,925
Contractors Profit and Overhead Contingencies (20%)	11,200	12,300	16,600
Total Cost	67,405	73,805	99,525
Gross Floor Area, sq ft	7,725	7,725	7,725
Unit Cost	8.70	9.60	12.90

TABLE A.23
SUMMARY OF COSTS, EXPRESSWAY GRADE SEPARATION SHELTERS
COST OPTION 2

Item	5 psi	25 psi	50 psi
Earthwork and Structural	\$90,700	\$96,000	\$117,000
Mechanical	28,170	28,170	28,170
Electrical	12,060	12,060	12,060
Architectural	6,035	6,035	6,455
Credit for Portions of the Original Structure	-42,400	-42,400	-42,400
Net Contract Cost	94,565	100,265	121,285
Contractors Profit and Overhead Contingencies (20%)	18,900	20,000	24,300
Total Cost	113,465	120,265	145,585
Gross Floor Area, sq ft	7,725	7,725	7,635
Unit Cost	14.70	15.60	19.10

TABLE A.24
ARCHITECTURAL, ELECTRICAL AND MECHANICAL COSTS

Type	Description	Units	Cost dollars	Quantity	Total dollars
Mechanical	1. Toilet Units	each	300	40	12,000
	2. Urinal Trough	each	250	8	2,000
	3. Partitions	lot	500	1	500
	4. Preparation of Sanitary Pit	lot	2000	1	2,000
	5. Potable Water Tank	each	5500	1	5,500
	6. Piping	lot	1200	1	1,200
	7. Wash Fountains	each	375	10	3,750
	8. Ventilation Units	each	305	4	<u>1,220</u>
					28,170
Electrical	1. Public Hookup	lot	90	1	90
	2. Fuse and Switch Box	each	500	1	500
	3. Wiring	lot	1400	1	1,400
	4. Lighting Fixtures	lot	960	1	960
	5. Installation, items 2 to 4	lot	3800	1	3,800
	6. Engine Generator Set	each	4400	1	4,400
	7. Tank and Fuel for Item 6	lot	910	1	<u>910</u>
					12,060
Architectural	1. Stairs	each	670	2	1,340
	2. Roller Unit for Blast Door	each	3240*	1	3,240
	3. Blast Door Latch	each	615**	1	615
	4. Interior Doors	each	120	7	<u>840</u>
					6,035

* For 5 and 25 psi only, cost is \$3600 for 50 psi.

** For 5 and 25 psi only, cost is \$675 for 50 psi.

APPENDIX B

BREAKDOWN OF SHELTER COSTS

This appendix provides a detailed cost breakdown of shelter structure and habitability items which comprise the various options described in Appendix A. All costs given refer to suburban areas of Chicago, Illinois for the spring of 1969.

B.1 SINGLE-PURPOSE SHELTERS

Single-purpose shelters considered in this study include arch and rectangular structures designed for construction on sites located close to highways and/or railways in uninhabited areas on the periphery of large population centers. Such shelter sites may require access roads and parking areas.

Sheltering options considered are defined in Table B.1. Option 1 is the most austere and consists of a basic structure equipped with blast protected intake and exhaust ventilators and entranceways. No parking spaces or habitability items of any kind are provided. It is assumed that shelterees would be brought to the site using some mode of mass public transport. Shelter site data are given in Table B.2.

Cost option 2 is obtained from option 1 by adding certain OCD approved habitability items (Ref. 55) which include ventilation kits, water containers and basic electrical equipment. Costs of these items are given in Table B.3. Cost option 3 is obtained from option 1 by adding habitability items of commercial variety in accordance with requirements suggested in Ref. 15. This includes ventilation, plumbing and electrical systems and presupposes availability of normal power supply. Partitions in this option are for the purpose of separating the toilet from living areas. Items comprising this cost option are given in Tables B.4 through B.6. Table B.4 contains mechanical equipment which includes ventilation and plumbing items. Supplementary items such as a heater and a manual exhaust system are given.

TABLE B.1
SHELTERING COST OPTIONS

Cost Option					
1	2	3	4	5	6
Site Clearance Access Road Shelter Structure Entranceway	Site Clearance Access Road Shelter Structure Entranceway OCD Ventilation Package OCD Water Package OCD Electrical	Site Clearance Access Road Shelter Structure Entranceway Ventilation* System Water Supply* System Toilet System Wiring, Fixtures and Outlets* Partitions	↑ Same as Option 1 ↓ Parking Lot	↑ Same as Option 2 ↓ Parking Lot	↑ Same as Option 3 ↓ Parking Lot

TABLE B.2
SHELTER SITE DATA

Structure Type	Site Description*	Cost Option	Capacity, persons	
			500	1000
Arch	Dimensions for Minimum Site	1,2,3	140' x 199'	140' x 311'
	Acreage	-	0.64	1.0
	Dimensions for Site with Parking**	4,5,6	256' x 442'	344' x 613'
	Acreage	-	2.60	4.84
Rectangular	Dimensions for Minimum Site	1,2,3	140' x 224'	155' x 267'
	Acreage	-	0.72	0.95
	Dimensions for Site with Parking**	4,5,6	310' x 399'	344' x 552'
	Acreage	-	2.84	4.36

UNIT COSTS FOR SITE PREPARATION

Operation	Cost Option	Unit Cost \$/sq yd
Site Clearance***	1,2,3	
Preparation of Base and Rolling		0.30
6-in. Thick Crushed Stone Layer	4,5,6	2.00
Grading Dumped Material with Dozer		0.15
Final Grading by Machine Plus Roll and Finish		0.50

*Layout of typical shelter sites are illustrated in Fig. A.1.

**The size of parking lot is planned on the basis of 0.4 cars per shelter occupant.

***It is assumed herein that the shelter site is located on flat or slightly rolling terrain which is only slightly wooded. To clear and grub this kind of land would cost approximately \$275.00 per acre.

TABLE B.3
COST OF SPECIFIC OCD SHELTER HABITABILITY ITEMS
USING COST OPTIONS 2 AND 5 (Ref. 55)

Item Description	In-Place Cost \$/person
Package Ventilation Kit	1.14
Water Containers (convertible to chemical toilets)	0.70
Electrical Package	0.50

TABLE B.4
COST OF MECHANICAL EQUIPMENT FOR 500-MAN SHELTER USING COST OPTIONS 3 AND 6

Description	Unit	Unit Cost (\$)	Quantity	Total Cost (\$)
(1) Ventilation				
5 hp forced air supply van with filter section	each	1,650	1	1,650
Supply air duct work	lot	1,210	1	1,210
Diffusers and registers	lot	440	1	440
Air filters	lot	83	1	83
Fresh air intake with exhaust hatch	lot	2,200	1	2,200
5 hp forced exhaust fan	each	715	1	715
Forced exhaust fan duct work	each	550	1	550
Total (1)				6,848
(2) Blast Protection for One Intake and One Exhaust				704
(3) Plumbing				
Chemical toilets	each	176	10	1,760
Cast iron vent with 6 in. diam vent cap	each	660	1	660
Drain tile, 4 in. diam, 260 ft	lot	990	1	990
Water storage tank, 1750 gal., with 0.5 in. gate valve, and 50 ft of 0.5 in. pipe and fittings	lot	1,650	1	1,650
Double drain steel sink	each	330	1	330
Drinking fountain, wall hung cast iron, enameled	each	165	1	165
Septic tank, concrete	each	1,100	1	1,100
Total (3)				6,655
Total (1), (2) and (3)				14,207
Optional Mechanical Equipment Not Included in Shelter Cost Estimates				
(4) Supplementary Heater				
12 stage 130 kw electric duct heater	each	990	1	990
Thermostat, airflow switch and recycle control	each	495	1	495
Total (4)				1,485
(5) Manual Exhaust Fan				
Manual exhaust fan assembly	each	660	1	660
Exhaust fan ducts	lot	1,100	1	1,100
Total (5)				1,760

TABLE B.5
COST OF ELECTRICAL ITEMS FOR 500-MAN SHELTER USING COST OPTIONS 3 AND 6

Description	Unit	Unit Cost (\$)	Quantity	Total Cost (\$)
(1) Lighting				
Sleeping area, 6-100 w incandescent fixtures	each	22	6	132
Wiring, 200 ft, two No. 12 0.5 in. conduit and switches	lot	198	1	198
Administrative area, 2-40 w fluorescent fixtures	each	33	2	66
Wiring, 50 ft, two No. 12 0.5 in. conduit and switches	lot	72	1	72
Living area, 6-100 w incandescent fixtures	each	22	6	132
Wiring, 180 ft, two No. 12 0.5 in. conduit and switches	lot	143	1	143
Storage and toilet area 4-100 w incandescent fixtures	each	22	4	88
Wiring, 200 ft, two No. 12 0.5 in. conduit and switches	lot	198	1	198
Total (1)				1029
(2) Outlets				
Food warming outlets	each	11	3	33
Wiring, 300 ft, No. 12	lot	165	1	165
Conventional outlets and wiring	lot	176	1	176
Total (2)				374
(3) Wiring for Mechanical Equipment				
Power wiring for 2-5 hp motors, and disconnect switches	lot	440	1	440
Total (3)				440
(4) Service				
Wiring, 25 ft, two sets of 4-300 MCM in 2-3 in. conduit and service heads	lot	660	1	660
Power service switchboard	lot	1650	1	1650
Lighting panel, 18 circuit panel and feeder	lot	330	1	330
Total (4)				2640
Total (1),(2),(3) and (4)				4483
(5) Additional Wiring for Heater (not included in shelter cost)				
Power wiring for 130 kw duct heater, power panel (14-60 amp switches and 4-60 amp blanks in panel)	lot	880	1	880
14 disconnect switches	lot	660	1	660
Wiring from panel to heater, 40 ft	lot	825	1	825
Total (5)				2365

TABLE B.6
COST OF SPECIFIC ARCHITECTURAL ITEMS USING COST ITEMS 3 AND 6

Structure Type	Item Description	Unit	Unit Cost (\$)	Quantity	In-Place Cost (\$)
Arch	Partitions: 2 x 4 in. studs, 1/2 in. plasterboard, one side, no tape, no paint, 400 ft	lot	300	1	300
	Stairs: steel tread	each	1000	2	2000
Rectangular	Partitions: 2 x 4 in. studs, 1/2 in. plasterboard, one side, no tape, no paint, 400 ft	lot	300	1	300

However, these are optional and their costs are not included in the final estimates. Electrical items are given in Table B.5 and include wiring and associated hardware to be used in connection with the optional heater discussed. The two architectural items are given in Table B.6. Partitions, stairs and associated hardware are included.

Cost options 4, 5 and 6 are identical to options 1, 2 and 3 respectively, with the exception that in the former parking areas at the rate of 0.4 cars per shelter occupant are provided. Corresponding site data are given in Table B.2.

Entranceways are typical and common to all low level weapon effects designs. Entranceway costs for a single shelter (500 man capacity) are given in Table A.7. The manner in which these entranceways are used in connection with 1000 man shelters is illustrated in Fig. A.1. Entranceways for the 100 and 150 psi shelters are an integral part of the shelter structure and therefore do not constitute a separate cost option.

Total as well as individual costs comprising the six options described are given in Table B.8 for the low level weapon effects designs and in Table B.9 for the 100- and 150-psi designs.

B.2 DUAL-PURPOSE SHELTERS

Detailed cost breakdowns for school basement (Ref. 15) and parking garage (Ref. 16) shelters described in Appendix A are given. Sheltering (cost) options considered with this set of structures are defined in Table B.10. Option 3 is the least austere; in addition to a finished structure equipped with blast doors, it is fully equipped with mechanical and electrical systems commensurate with conventional as well as emergency use. Option 1 considers no additional equipment over that required by conventional use and is therefore the most austere of this set of options. Option 2 is identical to option 1 except that it includes emergency-use items recommended by OCD and identified in Table B.3. Contract cost categories considered include: Structural and Earthwork, Architectural, Mechanical and Electrical.

TABLE B.7
ENTRANCEWAY COSTS FOR 500-MAN CAPACITY ARCH AND RECTANGULAR SHELTERS

Structure Type	Description	Unit	Unit Cost (\$)	Quantity	In-Plane Cost for Indicated Design Hardness Levels (\$)			
					FRE	10 psi	20 psi	30 psi
Arch	Passageway (corrugated steel plate)	lin ft	46 52	64.1 64.1	3,393	3,393	3,393	3,830
	Interior Door (hollow, metal)	each	80	1	92	92	92	92
	Bulkhead	each	470	1	540	540	540	540
	Exterior Door (steel)	each	130	1	150	---	---	---
	Blast Door	each	210	1	---	242	242	242
	Total				4,175	4,267	4,267	4,704
Rectangular	Passageway (corrugated steel plate)	lin ft	53 60	29 29	1,537	1,537	1,537	1,740
	Interior Door (hollow, metal)	each	92	1	92	92	92	92
	Bulkhead	each	541	1	541	541	541	541
	Exterior Door (steel)	each	150	1	150	---	---	---
	Blast Door	each	242	1	---	242	242	242
	Total				2,320	2,412	2,412	2,615

Note: Location of an entranceway relative to a shelter is illustrated in Figs. A.1 and A.3.

Shelter Type (Capacity 500 Persons)	Description	Cost Option 1				Cost Option 2				Cost	
		FRE	10 psi	20 psi	30 psi	FRE	10 psi	20 psi	30 psi	FRE	10 psi
RC Arch	Site Preparation	176	176	176	176	176	176	176	176	176	176
	Shelter:										
	Earthwork and Structural	34,346	35,130	38,225	39,027	34,346	35,130	38,225	39,027	34,346	35,130
	Mechanical	704	704	704	704	1,624	1,624	1,624	1,624	14,207	14,207
	Electrical					250	250	250	250	4,483	4,483
	Architectural	2,000	2,000	2,000	2,000	2,000	2,000	2,000	2,000	2,300	2,300
	Entranceway	4,175	4,267	4,267	4,704	4,175	4,267	4,267	4,704	4,175	4,267
	Service Road	335	335	335	335	335	335	335	335	335	335
	Cost Sum	41,736	42,612	45,707	46,946	42,906	43,782	46,877	48,116	60,022	60,898
	Contractor's Profit and Overhead Contingencies (20%)	8,347	8,522	9,141	9,389	8,581	8,756	9,375	9,623	12,004	12,180
	Total Cost	50,083	51,134	54,848	56,335	51,487	52,538	56,252	57,739	72,026	73,078
	Total Cost per sq ft	10.85	11.08	11.88	12.20	11.15	11.38	12.18	12.51	15.60	15.83
Steel Arch	Site Preparation	176	176	176	176	176	176	176	176	176	176
	Shelter:										
	Earthwork and Structural	31,699	38,121	44,732	66,490	31,699	38,121	44,732	66,490	31,699	38,121
	Mechanical	704	704	704	704	1,624	1,624	1,624	1,624	14,207	14,207
	Electrical					250	250	250	250	4,483	4,483
	Architectural	2,000	2,000	2,000	2,000	2,000	2,000	2,000	2,000	2,000	2,000
	Entranceway	4,175	4,267	4,267	4,704	4,175	4,267	4,267	4,704	4,175	4,267
	Service Road	335	335	335	335	335	335	335	335	335	335
	Cost Sum	39,089	45,603	52,214	74,409	40,259	46,773	53,384	75,579	57,375	63,889
	Contractor's Profit and Overhead Contingencies (20%)	7,818	9,121	10,443	14,882	8,052	9,355	10,677	15,116	11,475	12,778
	Total Cost	46,907	54,724	62,657	89,291	48,311	56,128	64,061	90,695	68,850	76,667
	Total Cost per sq ft	10.16	11.85	13.57	19.34	10.46	12.16	13.88	19.64	14.91	16.61
RC Rectangular	Site Preparation	198	198	198	198	198	198	198	198	198	198
	Shelter:										
	Earthwork and Structural	43,609	51,557	60,890	77,806	43,069	51,557	60,890	77,806	43,069	51,557
	Mechanical	704	704	704	704	1,624	1,624	1,624	1,624	14,207	14,207
	Electrical					250	250	250	250	4,483	4,483
	Architectural									300	300
	Entranceway	2,312	2,404	2,404	2,611	2,312	2,404	2,404	2,611	2,312	2,404
	Service Road	335	335	335	335	335	335	335	335	335	335
	Cost Sum	46,618	55,198	64,531	81,654	47,788	56,368	65,701	82,824	64,904	73,484
	Contractor's Profit and Overhead Contingencies (20%)	9,324	11,040	12,906	16,331	9,558	11,274	13,140	16,565	12,981	14,697
	Total Cost	55,942	66,238	77,437	97,985	57,346	67,642	78,841	99,389	77,885	88,181
	Total Cost per sq ft	10.93	12.94	15.12	19.14	11.20	13.21	15.40	19.41	15.21	17.22

B

TABLE B.8
TOTAL COSTS FOR SINGLE-PURPOSE SHELTERS

Design Weapon Environment															
Cost Option 3				Cost Option 4				Cost Option 5				Cost Option 6			
FRE	10 psi	20 psi	30 psi	FRE	10 psi	20 psi	30 psi	FRE	10 psi	20 psi	30 psi	FRE	10 psi	20 psi	30 psi
176	176	176	176	715	715	715	715	715	715	715	715	715	715	715	715
34,346	35,130	38,225	39,027	34,346	35,130	38,335	39,027	34,346	35,130	38,225	29,027	34,346	25,130	38,225	39,027
14,207	14,207	14,207	14,207	704	704	704	704	1,624	1,624	1,624	1,624	14,207	14,207	14,207	14,207
4,483	4,483	4,483	4,483					250	250	250	250	4,483	4,483	4,483	4,483
2,300	2,300	2,300	2,300	2,000	2,000	2,000	2,000	2,000	2,000	2,000	2,000	2,300	2,300	2,300	2,300
4,175	4,267	4,267	4,704	4,175	4,267	4,267	4,704	4,175	4,267	4,267	4,704	4,175	4,267	4,267	4,704
335	335	335	335	26,672	26,672	26,672	26,672	26,672	26,672	26,672	26,672	26,672	26,672	26,672	26,672
60,022	60,898	63,993	65,232	68,612	69,488	72,583	73,822	69,782	70,658	73,753	74,992	86,898	87,774	90,869	92,108
12,004	12,180	12,799	13,046	13,722	13,898	14,517	14,764	13,956	14,132	14,751	14,998	17,380	17,555	18,174	18,422
72,026	73,078	76,792	78,278	82,334	83,386	87,100	88,586	83,738	84,790	88,504	89,990	104,278	105,329	109,043	110,530
15.60	15.83	16.63	16.96	17.83	18.06	18.87	19.19	18.14	18.37	19.17	19.49	22.59	22.81	23.62	23.94
176	176	176	176	715	715	715	715	715	715	715	715	715	715	715	715
31,699	38,121	44,732	66,490	31,699	38,121	44,732	66,490	31,699	38,121	44,732	66,490	31,699	38,121	44,732	66,490
14,207	14,207	14,207	14,207	704	704	704	704	1,624	1,624	1,624	1,624	14,207	14,207	14,207	14,207
4,483	4,483	4,483	4,483					250	250	250	250	4,483	4,483	4,483	4,483
2,000	2,000	2,300	2,300	2,000	2,000	2,000	2,000	2,000	2,000	2,000	2,000	2,300	2,300	2,300	2,300
4,175	4,267	4,267	4,704	4,175	4,267	4,267	4,704	4,175	4,267	4,267	4,704	4,175	4,267	4,267	4,704
335	335	335	335	26,672	26,672	26,672	26,672	26,672	26,672	26,672	26,672	26,672	26,672	26,672	26,672
59,275	63,889	70,500	92,695	65,965	72,479	79,090	101,285	67,135	73,649	80,260	102,455	84,251	90,765	97,376	119,571
11,475	11,778	14,100	18,539	13,193	14,496	15,818	20,257	13,427	14,730	16,052	20,491	16,850	18,153	19,475	23,914
68,850	76,665	84,600	111,234	79,158	86,975	94,908	121,542	80,562	88,379	96,312	122,946	101,101	108,918	116,851	143,485
14.91	16.61	18.32	24.09	17.15	18.84	20.56	26.33	17.45	19.14	20.86	26.63	21.90	23.59	25.31	31.08
198	198	198	198	781	781	781	781	781	781	781	781	781	781	781	781
43,069	51,557	60,890	77,806	43,069	51,557	69,890	77,806	43,069	51,557	60,890	77,806	43,069	51,557	60,890	77,806
14,207	14,207	14,207	14,207	704	704	704	704	1,624	1,624	1,624	1,624	14,207	14,207	14,207	14,207
4,483	4,483	4,483	4,483					250	250	250	250	4,483	4,483	4,483	4,483
300	300	300	300									300	300	300	300
2,312	2,404	2,404	2,611	2,312	2,404	2,404	2,611	2,312	2,404	2,404	2,611	2,312	2,404	2,404	2,611
335	335	335	335	31,806	31,806	31,806	31,806	31,806	31,806	31,806	31,806	31,806	31,806	31,806	31,806
64,904	73,484	82,817	99,940	78,672	87,252	96,585	113,708	79,842	88,422	97,755	114,878	96,958	105,538	114,871	131,994
12,981	14,697	16,653	19,988	15,734	17,450	19,317	22,742	15,968	17,684	19,551	22,976	19,392	21,108	22,974	26,399
77,885	88,181	99,380	119,928	94,406	104,702	115,902	136,450	95,810	106,106	117,306	137,854	116,350	126,646	137,845	158,393
15.21	17.22	19.41	23.42	18.44	20.45	22.64	26.65	18.71	20.72	22.91	26.92	22.72	24.73	26.92	30.93

A

Shelter Type (Capacity 1000 Persons)	Description	Cost Option 1				Cost Option 2				FRE
		FRE	10 psi	20 psi	30 psi	FRE	10 psi	20 psi	30 psi	
RC Arch	Site Preparation	275	275	275	275	275	275	275	275	275
	Shelter:									
	Earthwork and Structural	64,903	66,671	70,659	74,215	64,903	66,671	70,659	74,215	64,903
	Mechanical	1,408	1,408	1,408	1,408	3,248	3,248	3,248	3,248	28,411
	Electrical					500	500	500	500	8,961
	Architectural	4,000	4,000	4,000	4,000	4,000	4,000	4,000	4,000	4,601
	Entranceway	8,349	8,533	8,533	9,407	8,349	8,533	8,533	9,407	8,349
	Service Road	335	335	335	335	335	335	335	335	335
	Cost Sum	79,270	81,222	85,210	89,640	81,610	83,562	87,550	91,980	115,840
	Contractor's Profit and Overhead Contingencies (20%)	15,854	16,244	17,042	17,928	16,322	16,712	17,510	18,396	23,166
	Total Cost	95,124	97,466	102,252	107,568	97,932	100,274	105,060	110,376	139,006
	Total Cost per sq ft	10.30	10.56	11.07	11.65	10.61	10.86	11.38	11.95	15.05
Steel Arch	Site Preparation	275	275	275	275	275	275	275	275	275
	Shelter:									
	Earthwork and Structural	58,842	74,608	87,881	131,226	58,842	74,608	87,881	131,226	58,842
	Mechanical	1,408	1,408	1,408	1,408	3,248	3,248	3,248	3,248	28,411
	Electrical					500	500	500	500	8,961
	Architectural	4,000	4,000	4,000	4,000	4,000	4,000	4,000	4,000	4,601
	Entranceway	8,349	8,533	8,533	9,407	8,349	8,533	8,533	9,407	8,349
	Service Road	335	335	335	335	335	335	335	335	335
	Cost Sum	73,209	89,159	102,432	146,651	75,549	91,499	104,772	148,991	109,775
	Contractor's Profit and Overhead Contingencies (20%)	14,642	17,832	20,486	29,330	15,110	18,299	20,954	29,798	21,956
	Total Cost	87,851	106,991	122,918	175,981	90,659	109,798	125,726	178,789	131,731
	Total Cost per sq ft	9.51	11.59	13.31	19.06	9.82	11.89	13.62	19.36	14.27
RC Rectangular	Site Preparation	262	262	262	262	262	262	262	262	262
	Shelter:									
	Earthwork and Structural	76,624	93,337	110,736	141,273	76,624	93,337	110,736	141,273	76,624
	Mechanical	1,408	1,408	1,408	1,408	3,248	3,248	3,248	3,248	28,411
	Electrical					500	500	500	500	8,961
	Architectural									601
	Entranceway	4,635	4,819	4,819	5,221	4,635	4,819	4,819	5,221	4,635
	Service Road	335	335	335	335	335	335	335	335	335
	Cost Sum	83,264	100,161	117,560	148,499	85,604	102,501	119,900	150,839	119,834
	Contractor's Profit and Overhead Contingencies (20%)	16,653	20,032	23,512	29,700	17,121	20,500	23,980	30,168	23,961
	Total Cost	99,917	120,193	141,072	178,199	102,725	123,001	143,880	181,007	143,801
	Total Cost per sq ft	9.76	11.74	13.77	17.40	10.03	12.01	14.05	17.68	14.04

TABLE B.8 (Contd)

Design Weapon Environment															
Cost Option 3			Cost Option 4				Cost Option 5				Cost Option 6				
10 psi	20 psi	30 psi	FRE	10 psi	20 psi	30 psi	FRE	10 psi	20 psi	30 psi	FRE	10 psi	20 psi	30 psi	
275	275	275	1,331	1,331	1,331	1,331	1,331	1,331	1,331	1,331	1,331	1,331	1,331	1,331	
66,671	70,659	74,215	64,903	66,671	70,659	74,215	64,903	66,671	70,659	74,215	64,903	66,671	70,659	74,215	
28,413	28,413	28,413	1,408	1,408	1,408	1,408	3,248	3,248	3,248	3,248	28,413	28,413	28,413	28,413	
8,965	8,965	8,965					500	500	500	500	8,965	8,965	8,965	8,965	
4,600	4,600	4,600	4,000	4,000	4,000	4,000	4,000	4,000	4,000	4,000	4,600	4,600	4,600	4,600	
8,533	8,533	9,407	8,349	8,533	8,533	9,407	8,349	8,533	8,533	9,407	8,349	8,533	8,533	9,407	
335	335	335	55,000	55,000	55,000	55,000	55,000	55,000	55,000	55,000	55,000	55,000	55,000	55,000	
117,792	121,780	126,210	134,991	136,943	140,931	145,361	137,331	139,283	143,271	147,701	171,561	173,513	177,501	181,931	
23,558	24,356	25,242	26,998	27,389	28,186	29,072	27,466	27,857	28,654	29,540	34,312	34,703	35,500	36,386	
141,350	146,136	151,452	161,989	164,332	169,117	174,433	164,797	167,140	171,925	177,241	205,873	208,216	213,001	218,317	
15.31	15.83	16.40	17.57	17.80	18.32	18.89	17.85	18.10	18.62	19.20	22.30	22.55	23.07	23.64	
275	275	275	1,331	1,331	1,331	1,331	1,331	1,331	1,331	1,331	1,331	1,331	1,331	1,331	
74,608	87,881	131,226	58,842	74,608	87,881	131,226	58,842	74,608	87,881	131,226	58,842	74,608	87,881	131,226	
28,413	28,413	28,413	1,408	1,408	1,408	1,408	3,248	3,248	3,248	3,248	28,413	28,413	28,413	28,413	
8,965	8,965	8,965					500	500	500	500	8,965	8,965	8,965	8,965	
4,600	4,600	4,600	4,000	4,000	4,000	4,000	4,000	4,000	4,000	4,000	4,600	4,600	4,600	4,600	
8,533	8,533	9,407	8,349	8,533	8,533	9,407	8,349	8,533	8,533	9,407	8,349	8,533	8,533	9,407	
335	335	335	55,000	55,000	55,000	55,000	55,000	55,000	55,000	55,000	55,000	55,000	55,000	55,000	
125,729	139,002	183,221	128,930	144,880	158,153	202,372	131,270	147,220	160,493	204,712	165,500	181,450	194,723	238,942	
25,146	27,800	36,644	25,786	28,976	31,631	40,474	26,254	29,444	32,099	40,942	33,100	36,290	38,945	47,788	
150,875	166,802	219,865	154,716	173,856	189,784	242,846	157,524	176,664	192,592	245,654	198,600	217,740	233,668	286,730	
16.34	18.06	23.81	16.76	18.83	20.55	26.30	17.06	19.13	20.86	26.60	21.51	23.58	25.31	31.05	
262	262	262	1,199	1,199	1,199	1,199	1,199	1,199	1,199	1,199	1,199	1,199	1,199	1,199	
93,337	110,736	141,273	76,624	93,337	110,736	141,273	76,624	93,337	110,736	141,273	76,624	93,337	110,736	141,273	
28,413	28,413	28,413	1,408	1,408	1,408	1,408	3,248	3,248	3,248	3,248	28,413	28,413	28,413	28,413	
8,965	8,965	8,965					500	500	500	500	8,965	8,965	8,965	8,965	
600	600	600									600	600	600	600	
4,819	4,819	5,221	4,635	4,819	4,819	5,221	4,635	4,819	4,819	5,221	4,635	4,819	4,819	5,221	
335	335	335	49,848	49,848	49,848	49,848	49,848	49,848	49,848	49,848	49,848	49,848	49,848	49,848	
136,731	154,130	185,069	133,714	150,611	168,010	198,949	136,054	152,951	170,350	201,289	170,284	187,181	204,580	235,519	
27,346	30,286	37,014	26,743	30,122	33,602	39,790	27,211	30,590	34,070	40,258	34,057	37,436	40,916	47,104	
164,077	184,956	222,083	160,457	180,733	201,612	238,739	163,265	183,541	204,420	241,547	204,341	224,617	245,496	282,623	
16.02	18.06	21.69	15.67	17.65	19.69	23.31	15.94	17.92	19.96	23.59	19.95	21.93	23.97	27.60	

TABLE B.9
TOTAL COSTS FOR SINGLE PURPOSE SHELTERS
SHELTER TYPE: RC ARCH CAPACITY: 500 PERSONS

Description	Option 1		Option 2		Option 3	
	100 psi	150 psi	100 psi	150 psi	100 psi	150 psi
Site Preparation	211	211	211	211	211	211
Shelter:						
(a) Earth & Struc.	61796	79577	61796	79577	61796	79577
(b) Mech	845	845	1624	1624	17048	17048
(c) Elec	-	-	250	250	5380	5380
(d) Arch	2400	2400	2400	2400	2760	2760
Service Road	402	402	402	402	402	402
Cost Sum	65654	83435	66683	84464	87597	105378
20% Contractor's	13131	16687	13337	16893	17519	21076
Total Cost	78785	100122	80020	101357	105116	126454
Total Cost/ft ²	17.06	21.69	17.33	21.95	22.78	27.39

Description	Option 4		Option 5		Option 6	
	100 psi	150 psi	100 psi	150 psi	100 psi	150 psi
Site Preparation	858	858	858	858	858	858
Shelter:						
(a) Earth & Struc.	61796	79577	61796	79577	61796	79577
(b) Mech	845	845	1624	1624	17048	17048
(c) Elec	-	-	250	250	5380	5380
(d) Arch	2400	2400	2400	2400	2760	2760
Service Road	32006	32006	32006	32006	32006	32006
Cost Sum	97905	115686	98934	116715	119348	137629
20% Contractor's	19581	23137	19787	23343	23970	27526
Total Cost	117486	138823	118721	140058	143818	165155
Total Cost/ft ²	25.45	30.07	25.71	30.34	31.15	35.77

TABLE B.10
DEFINITION OF SHELTERING COST OPTIONS
FOR DUAL-PURPOSE SHELTERS

Cost Item	Cost Option
(1) Shelter structure, blast doors, stairs and associated hardware	1,2,3
(2) Mechanical and electrical equipment of commercial variety commensurate with conventional use only	1,2,3
(3) Special mechanical and electrical equipment of commercial variety commensurate with emergency use	3
(4) Civil Defense equipment: package ventilation kits, water containers, electrical equipment	2

Labor, materials and equipment costs are given in Tables B.11 through B.13 for school basement shelters and in Tables B.14 through B.16 for parking garage shelters. Total costs for each of the three options are summarized in Tables A.14 through A.18.

Detailed costs of conventional school basements (Ref. 53) are given in Tables B.17 and B.18 and for conventional parking garages (Ref. 54) are given in Tables B.19 and B.20. Cost of these conventional structures were used for determining incremental sheltering costs which are also included in Tables A.17 and A.18.

TABLE B.11
STRUCTURAL CONSTRUCTION COST AND QUANTITY BREAKDOWN FOR SCHOOL SHELTERS

Design Overpressure psi	Description	Units	Price (\$)	1100 Population		550 Population	
				Quantity	Cost (\$)	Quantity	Cost (\$)
5	Excavation, Backfill and Grading	cu yd	1.50	4,750	7,125	2,550	3,825
	Concrete, Not Including Forms or Reinforcing	cu yd	30.00	935	28,050	546	16,380
	Reinforcement	tons	320.00	44.8	14,336	25.3	8,096
	Wire Mesh	sq	11.00	130	1,430	69	759
	Forms						
	Roof Slab, Beams and Columns	sq ft	1.50	14,740	22,110	7,750	11,625
	Walls and Footings	sq ft	0.85	13,480	11,458	9,550	8,118
	Damp Proofing (polyethylene)	sq ft	0.05	18,750	937.5	10,550	527.5
	Blast Doors						
	3' x 6'-8"	each	172.50	--	--	4	690
	5' x 6'-8"	each	230.00	4	920	--	--
	Blast Gates	each	115.00	6	690	5	575
	Total Cost				87,057		50,596
25	Excavation, Backfill and Grading	cu yd	1.50	4,750	7,125	2,550	3,825
	Concrete	cu yd	30.00	1,338	40,140	752	22,560
	Tilt-Up Concrete Partitions	sq ft	2.00	6,400	12,800	3,680	7,360
	Reinforcement	tons	320.00	48.8	15,616	27.4	8,768
	Wire Mesh	sq	11.00	130	1,430	69	759
	Forms						
	Roof Slab and Columns	sq ft	1.50	12,080	18,120	6,330	9,495
	Walls and Footings	sq ft	0.85	14,020	11,917	9,990	8,492
	Damp Proofing (polyethylene)	sq ft	0.05	18,750	938	10,550	528
	Blast Doors						
	3' x 6'-8"	each	2025.00	--	--	4	8,100
	5' x 6'-8"	each	3375.00	4	13,500	--	--
	Blast Gates	each	203.00	6	1,218	5	1,015
	Total Cost				122,804		70,902
50	Excavation, Backfill and Grading	cu yd	1.50	4,980	7,470	2,690	4,035
	Concrete	cu yd	30.00	2,135	64,050	1,204	36,120
	Tilt-Up Concrete Partitions	sq ft	2.00	6,400	12,800	3,680	7,360
	Reinforcement	tons	320.00	90.1	28,832	51.8	16,576
	Wire Mesh	sq	11.00	130	1,430	69	759
	Forms						
	Roof Slab and Columns	sq ft	1.50	12,080	18,120	6,330	9,495
	Walls and Footings	sq ft	0.85	14,640	12,444	10,290	8,747
	Damp Proofing (polyethylene)	sq ft	0.05	19,850	938	10,550	528
	Blast Doors						
	3' x 6'-8"	each	2700.00	--	--	4	10,800
	5' x 6'-8"	each	4725.00	4	18,900	--	--
	Blast Gates	each	270.00	6	1,620	5	1,350
	Total Cost				166,604		95,770

TABLE B.12
ESTIMATED ARCHITECTURAL CONSTRUCTION COST AND QUANTITY BREAKDOWN

Incident Design Overpressure psi	Description	Units	Price (\$)	1100 Population		550 Population	
				Quantity	Cost (\$)	Quantity	Cost (\$)
5	Cinder Block, 8 in.	sq ft	1.00	5,650	5,650	3,000	3,000
	Toilet Partitions	lin ft	10.00	80	800	45	450
	Resilient Tile, Asphalt	sq ft	0.28	9,900	2,772	4,600	1,288
	Concrete Hardener/Sealer Liquid	sq ft	0.08	3,100	248	1,220	98
	Insulation Board 1/2 in. Thick (ceiling)	sq ft	0.40	11,840	4,736	5,500	2,200
	Painting (interior)	sq ft	0.16	15,800	2,528	10,450	1,672
	Cement Enamel Finish	sq ft	0.42	1,600	672	1,420	596
	Doors						
	2'-6" x 6'-8"	each	85.00	2	170	2	170
	3'-0" x 6'-8"	each	95.00	16	1,520	12	1,140
	5'-0" x 6'-8"	each	130.00	1	130	-	-
	Air Tight Metal Doors 2' x 5'	each	100.00	1	100	1	100
	Metal Access Hatch 2' x 3'	each	40.00	1	40	1	40
	Aluminum Louver	sq ft	5.00	34	170	26	130
	Stair Nosing	lin ft	3.00	225	675	130	390
	Handrail	lin ft	4.00	116	464	80	320
	Total Cost				20,675		11,594
25 & 50	Toilet Partitions	lin ft	10.00	80	800	45	450
	Resilient Tile, Asphalt	sq ft	0.28	9,900	2,772	4,600	1,288
	Concrete Hardener/Sealer Liquid	sq ft	0.08	3,100	248	1,220	98
	Insulation Board 1/2 in. Thick (ceiling)	sq ft	0.40	11,840	4,736	5,500	2,200
	Painting (interior)	sq ft	0.16	15,800	2,528	10,450	1,672
	Cement Enamel Finish	sq ft	0.42	1,600	672	1,420	596
	Doors						
	2'-6" x 6'-8"	each	85.00	2	170	2	170
	3'-0" x 6'-8"	each	95.00	16	1,520	12	1,140
	5'-0" x 6'-8"	each	130.00	1	130	-	-
	Air Tight Metal Doors 2' x 5'	each	100.00	1	100	1	100
	Metal Access Hatch 2' x 3'	each	40.00	1	40	1	40
	Aluminum Louver	sq ft	5.00	34	170	26	130
	Stair Nosing	lin ft	3.00	225	675	130	390
	Handrail	lin ft	4.00	116	464	80	320
	Total Cost				15,025		8,594

TABLE B.13
ESTIMATED MECHANICAL AND ELECTRICAL CONSTRUCTION COST
AND QUANTITY BREAKDOWN FOR COST OPTION 1

Design Overpressure Level psi	Item	1100 Population (\$)	550 Population (\$)
5	Mechanical		
	Heating, ventilation and fuel storage Plumbing system	23,085 15,593	11,880 9,450
	Total Cost	<u>38,678</u>	<u>21,330</u>
25 & 50	Heating, ventilation and fuel storage Plumbing system	24,071 15,728	12,602 9,585
	Total cost	<u>39,799</u>	<u>22,187</u>
5	Electrical		
	Total cost including lighting, wire, switches and outlets	28,350	15,755
	Total cost including lighting, wire, switches and outlets	29,430	16,538

TABLE B.14

ESTIMATED STRUCTURAL CONSTRUCTION COST AND QUANTITY BREAKDOWN FOR PARKING GARAGE SHELTERS

Design Overpressure Level psi	Description	Units	Price (\$)	Structure I		Structure II	
				Quantity	Cost (\$)	Quantity	Cost (\$)
5	Excavation and Hauling	cu yd	1.50	21,400	32,100	28,800	43,200
	Backfill	cu yd	0.75	530	398	7,700	5,775
	Concrete	cu yd	30.00	4,052	121,560	4,444	133,320
	Reinforcement	tons	320.00	154.8	49,536	288.5	92,256
	Wire Mesh	sq	11.00	556	6,116	556	6,116
	Forms						
	Roof Slab and Columns	sq ft	1.50	55,500	83,250	56,020	84,030
	Walls and Footings	sq ft	0.85	28,720	24,412	34,930	29,691
	Damp Proofing (Polyethylene)	sq ft	0.05	68,700	3,435	125,900	6,295
	Personnel Blast Doors 3' x 6'-8"	each	172.50	12	2,070	12	2,070
	Main Entrance Blast Doors	each	2430.00	2	4,860	2	4,860
	Blast Gates	each	135.00	5	675	5	675
	Total Cost				328,412		408,288
25	Excavation and Hauling	cu yd	1.50	25,600	38,400	32,360	48,540
	Backfill	cu yd	0.75	760	570	8,200	6,150
	Concrete	cu yd	30.00	6,585	197,550	6,961	208,830
	Tilt-Up Concrete Partitions	sq ft	2.00	2,500	5,000	2,500	5,000
	Reinforcement	tons	320.00	310.4	99,328	332.6	106,432
	Wire Mesh	sq	11.00	556	6,116	556	6,116
	Forms						
	Roof Slab and Columns	sq ft	1.50	59,360	89,040	59,460	89,190
	Walls and Footings	sq ft	0.85	30,920	26,282	38,480	32,708
	Damp Proofing (Polyethylene)	sq ft	0.05	71,500	3,575	127,900	6,395
	Personnel Blast Doors 3' x 6'-8"	each	2025.00	12	24,300	12	24,300
	Main Entrance Blast Doors	each	5400.00	2	10,800	2	10,800
	Blast Gates	each	203.00	5	1,015	5	1,015
	Total Cost				501,976		545,476
50	Excavation and Hauling	cu yd	1.50	30,420	45,630	37,670	56,505
	Backfill	cu yd	0.75	920	690	8,325	6,244
	Concrete	cu yd	30.00	11,287	338,610	11,506	345,180
	Tilt-Up Concrete Partitions	sq ft	2.00	2,500	5,000	2,500	5,000
	Reinforcement	tons	320.00	453.5	145,120	478.7	153,184
	Wire Mesh	sq	11.00	556	6,116	556	6,116
	Forms						
	Roof Slab and Columns	sq ft	1.50	60,520	90,780	60,520	90,780
	Walls and Footings	sq ft	0.85	33,000	28,050	40,380	34,323
	Damp Proofing (Polyethylene)	sq ft	0.05	72,800	3,640	129,200	6,460
	Personnel Blast Doors 3' x 6'-8"	each	2700.00	12	32,400	12	32,400
	Main Entrance Blast Doors	each	7425.00	2	14,850	2	14,850
	Blast Gates	each	270.00	5	1,350	5	1,350
	Total Cost				712,236		752,392

TABLE B.15

ESTIMATED ARCHITECTURAL CONSTRUCTION COST AND QUANTITY BREAKDOWN FOR PARKING GARAGE SHELTERS

Design Overpressure Level psi	Description	Units	Price (\$)	Structure I		Structure II	
				Quantity	Cost (\$)	Quantity	Cost (\$)
5	Cinder Block, 6 in.	sq ft	1.00	2,175	2,175	--	--
	Toilet Partitions	lin ft	10.00	50	500	50	500
	Resilient Tile, Asphalt	sq ft	0.28	300	84	300	84
	Concrete Hardener/Sealer Liquid	sq ft	0.08	52,500	4,200	52,500	4,200
	Insulation Board 1/2 in. Thick (ceiling)	sq ft	0.40	52,000	20,800	--	--
	Painting	sq ft	0.16	32,550	5,208	84,550	13,528
	Cement Enamel Finish	sq ft	0.42	725	305	725	305
	Doors						
	3' x 6'-8"	each	95.00	7	665	7	665
	5' x 6'-8"	each	130.00	2	260	2	260
	Air Tight Metal Doors 2' x 5'	each	115.00	2	230	2	230
	Metal Access Hatch 2' x 3'	each	40.00	1	40	1	40
	Aluminum Louver	sq ft	5.00	100	500	100	500
	Stair Nosing	lin ft	3.00	512	1,536	512	1,536
	Handrail	lin ft	4.00	1,150	4,600	1,150	4,600
	Metal Partition (includes glazing)	lin ft	35.00	30	1,050	30	1,050
	Metal Grating	sq ft	5.00	30	150	30	150
	Total Cost				42,303		27,648
25 & 50	Toilet Partitions	lin ft	10.00	50	500	50	500
	Resilient Tile, Asphalt	sq ft	0.28	300	84	300	84
	Concrete Hardener/Sealer Liquid	sq ft	0.08	52,500	4,200	52,500	4,200
	Insulation Board 1/2 in. Thick (ceiling)	sq ft	0.40	52,000	20,800	--	--
	Painting	sq ft	0.16	34,600	5,536	86,600	13,856
	Cement Enamel Finish	sq ft	0.42	725	305	725	305
	Doors						
	3' x 6'-8"	each	95.00	7	665	7	665
	5' x 6'-8"	each	130.00	2	260	2	260
	Air Tight Metal Doors 2' x 5'	each	115.00	1	230	2	230
	Metal Access Hatch 2' x 3'	each	40.00	1	40	1	40
	Aluminum Louver	sq ft	5.00	100	500	100	500
	Stair Nosing	lin ft	3.00	550	1,650	550	1,650
	Handrail	lin ft	4.00	1,200	4,800	1,200	4,800
	Metal Partition (includes glazing)	lin ft	35.00	30	1,050	30	1,050
	Metal Grating	sq ft	5.00	30	150	30	150
	Total Cost				40,770		28,290

TABLE B.16
ESTIMATED MECHANICAL AND ELECTRICAL CONSTRUCTION COST
AND QUANTITY BREAKDOWN FOR PARKING GARAGE SHELTERS, COST OPTION 1

Design Overpressure Level	Item	Structure I	Structure II
		Cost (\$)	Cost (\$)
5 psi	Mechanical		
	Heating, ventilation and fuel storage	31,500	31,500
	Plumbing system	25,480	25,480
	Sprinkler system	31,500	31,500
	Total Cost	88,480	88,480
25 & 50 psi	Heating, ventilation and fuel storage	35,560	35,560
	Plumbing system	26,880	26,880
	Sprinkler system	31,500	31,500
	Total Cost	93,940	93,040
5 psi	Electrical		
	Total cost including emergency generator, lighting, wire, switches and outlets	34,706	34,706
	Total cost including emergency generator, lighting, wire, switches and outlets	36,918	36,918
25 & 50 psi			

TABLE B.17
ESTIMATED CONSTRUCTION COST AND QUANTITY BREAKDOWN
FOR CONVENTIONAL SCHOOL BASEMENT SHELTERS

Description	Units	Price (\$)	1100 Population		550 Population	
			Quantity	Cost (\$)	Quantity	Cost (\$)
Structural and Earthwork						
Excavation, Backfill and Grading	cu yd	1.50	4,750	7,125	2,550	3,825
Concrete	cu yd	30.00	928	27,840	519	15,570
Reinforcement	tons	320.00	39.1	12,512	21.2	6,784
Wire Mesh	sq	11.00	130	1,430	69	759
Forms						
Roof Slab, Beams and Columns	sq ft	1.50	14,410	21,615	7,530	11,295
Walls	sq ft	0.85	12,150	10,328	8,220	6,987
Damp Proofing (polyethylene)	sq ft	0.05	18,750	938	10,550	528
Total Cost				81,788	45,748	
Architectural						
Cinder Block, 6 in.	sq ft	1.00	6,050	6,050	3,400	3,400
Toilet Partitions	lin ft	10.00	80	810	45	450
Resilient Tile, Asphalt	sq ft	0.28	10,310	2,887	4,900	1,372
Concrete Hardener/Sealer Liquid	sq ft	0.08	2,700	216	920	74
Insulation Board 1/2 in. Thick (ceiling)	sq ft	0.40	12,240	4,896	5,800	2,320
Painting (interior walls)	sq ft	0.16	15,300	2,448	10,050	1,608
Cement Enamel Finish	sq ft	0.42	1,600	672	1,420	596
Doors						
2'-6" x 6'-8"	each	85.00	1	85	2	170
3'-0" x 6'-8"	each	95.00	17	1,615	15	1,425
5'-0" x 6'-8"	each	130.00	3	390	-	-
Aluminum Louver	sq ft	5.00	14	70	7	35
Air Tight Metal Door 2' x 5'	each	100.00	1	100	1	100
Stair Nosing	lin ft	3.00	225	675	130	390
Handrail	lin ft	4.00	56	225	80	320
Total Cost				24,138		12,260

TABLE B.18
MECHANICAL AND ELECTRICAL ITEMS
FOR CONVENTIONAL BASEMENT SHELTERS

Item	1100 Population Cost(\$)	550 Population Cost(\$)
(1) Heating Ventilating, and Fuel Storage	338	162
Filters	338	162
Heating Coil	432	304
Supply air blower, etc.	1,822	1,080
Sheet metal ductwork	8,900	4,563
Registers and grilles	891	405
Insulation	2,700	1,350
Automatic temperature control	5,940	2,700
Total (1)	21,033	10,564
(2) Plumbing System		
Pumps and motors	540	405
Piping	1,215	675
Fixtures	12,150	6,885
Emergency storage	2,700	2,025
Insulation	675	473
Total (2)	17,280	10,463
Total (1) and (2)	38,313	21,027
(3) Electrical Items		
Total cost including lighting, wiring, out- lets, etc.	22,680	11,948

TABLE B.19
ESTIMATED CONSTRUCTION COST AND QUANTITY BREAKDOWN FOR CONVENTIONAL PARKING GARAGE SHELTER

Description	Units	Price (\$)	Structure I		Structure II	
			Quantity	Cost (\$)	Quantity	Cost (\$)
Structural and Earthwork						
Excavation and Hauling	cu yd	1.50	21,400	32,100	28,800	43,200
Backfill	cu yd	0.75	530	398	7,700	5,775
Concrete	cu yd	30.00	3,376	101,280	4,311	129,330
Reinforcement	tons	320.00	189.8	60,736	285	91,200
Wire Mesh	sq	11.00	556	6,116	556	6,116
Forms						
Roof Slab and Columns	sq ft	1.50	54,440	81,660	56,020	84,030
Walls and Footings	sq ft	0.85	28,090	23,877	34,300	29,155
Damp Proofing (polyethylene)	sq ft	0.05	63,700	3,435	125,900	6,295
Total Cost				309,602		395,101
Architectural						
Under Block, 6 in.	sq ft	1.00	2,650	2,650	2,650	2,650
Toilet Partitions	lin ft	10.00	50	500	50	500
Resilient Tile, Asphalt	sq ft	0.28	360	101	360	101
Concrete Hardener/Sealer Liquid	sq ft	0.08	42,560	4,205	52,560	4,205
Insulation Board, 1 in. Thick (ceiling)	sq ft	0.40	51,560	20,624	1,450	580
Painting (interior)	sq ft	0.16	22,750	3,640	73,000	11,680
Painting (exterior)	sq ft	0.16	8,850	1,416	10,190	1,630
Cement Enamel Finish	sq ft	0.42	725	305	725	305
Doors						
2'-6" x 6'-8"	each	85.00	10	850	10	850
3'-0" x 6'-8"	each	95.00	5	475	5	475
5'-0" x 6'-8"	each	130.00	2	260	2	260
Aluminum Louver	sq ft	5.00	100	500	100	500
Air Tight Metal Doors 2' x 5'	each	100.00	2	200	2	200
Stair Nosing	lin ft	3.00	128	384	128	384
Hand Rail	lin ft	4.00	600	3,200	950	3,800
Metal Partition (includes glazing)	lin ft	35.00	30	1,050	30	1,050
Metal Grating	sq ft	5.00	30	150	30	150
Steel Roll-Up Door 15' x 8'	each	1080.00	2	2,160	2	2,160
Total Cost				42,670		31,480

TABLE B.20
MECHANICAL AND ELECTRICAL ITEMS
FOR CONVENTIONAL PARKING GARAGE SHELTERS

	Structure I and II Cost (\$)
(1) Mechanical	
Heating, Ventilating and Fuel Storage	
Filters	891
Supply air blowers, etc.	4,320
Exhaust air blowers, etc.	4,590
Sheet metal ductwork	15,930
Registers	1,620
Electrical duct heaters	608
Automatic temperature control	473
Total (1)	28,432
(2) Plumbing	
Pump and motor	338
Domestic HW storage tank	203
Plumbing fixtures	12,150
Emergency storage water tank	10,125
Oil intercaptor	1,890
Sprinkler system	30,375
Total (2)	55,081
Total (1) and (2)	83,513
(3) Electrical System	23,126

APPENDIX C

DESCRIPTION AND DOCUMENTATION OF COMPUTER PROGRAMS

Descriptions of computer programs used for calculating incipient failure loads for various components of rectangular and arch shelters considered in this study are presented.

C.1 RECTANGULAR REINFORCED CONCRETE SLAB ANALYSIS PROGRAM

This computer program is capable of determining the incipient failure load for one- and two-way RC slabs, flat plates and flat slabs when subjected to free-field blast overpressures produced by nuclear weapons. It is capable of treating one- and two-way slabs as roof elements or as wall elements of basement-like rectangular structures. Slab end conditions may be simple supports, fixed supports or mixed, i.e., a given slab may be fixed along one edge and simply supported along the other three. The theory behind this computer program is discussed in Chapter Two.

This computer program is specifically geared for slabs where the quantities of tension and compression reinforcement along any one of the two span directions is the same. However the total reinforcement in span one may be different from that of span two. Slabs falling in this category may be analyzed automatically. Slabs which do not satisfy this condition may still be analyzed using this computer program, however the resistance function needs first to be determined and input as part of input data. This would require minor modification in the "main" program. The modification would be to bypass statements which are used to compute resistance functions for slabs with uniform reinforcement.

The most expedient way to construct a resistance function is by the use of an elasto-plastic finite element computer program which is capable of treating reinforced concrete. Such computer programs exist (Ref. 72). The major difficulty is that the use of such codes is time-consuming if a large number of complex slab systems are analyzed. An easier approach, though less accurate, is to use the approach outlined in Ref. 4 and Ref. 13.

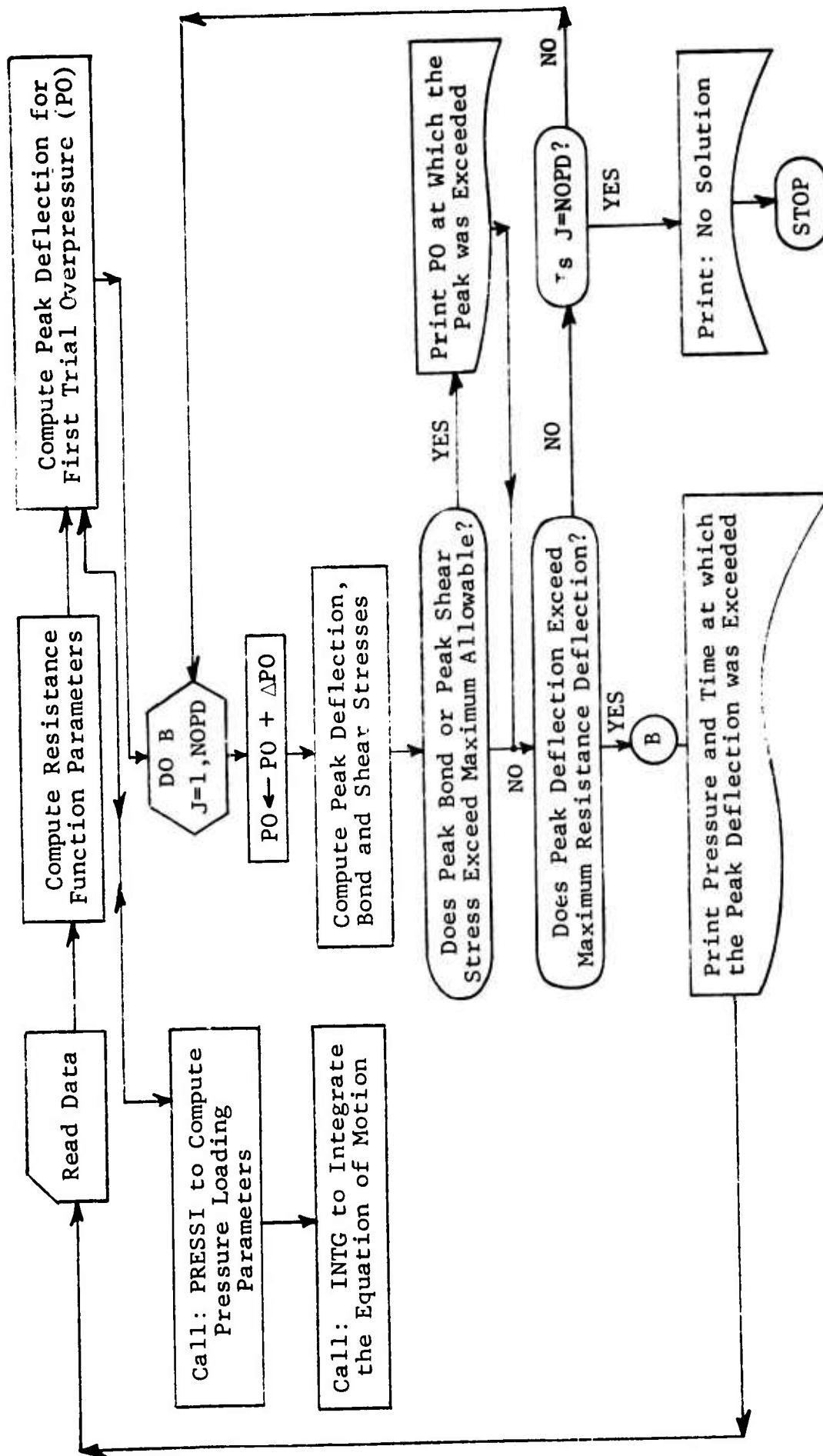


Fig. C.1 GENERAL FLOW CHART FOR SLAB ANALYSIS COMPUTER PROGRAM

The overall computational process is illustrated in Fig. C.1. The computer program consists of a MAIN program and six subroutines. The subroutines are PRESSI, INTG, CRIT, FUN, FINT and STEPIT. The MAIN program reads data, coordinates the computational process among these subroutines and prints the results. Instructions for using this computer program are given in Subsection C.1.2.

C.1.1 MAIN Program

As mentioned, the function of the MAIN program is to read input data, coordinate the auxiliary subroutines required for the computation of the incipient failure overpressure, and print results. Its general computational process is as shown in Fig. C.1.

Given a weapon yield, initial overpressure and a set of specific slab data consisting of geometry, section and strength properties, end conditions, etc., the program proceeds to construct the corresponding resistance function as a first step. Based on initial peak overpressure, the corresponding peak deflection is calculated next. This is an initializing step. In the process the program communicates with subroutine PRESSI which provides the pressure time history and subroutine INTG which integrates the equation of motion. The peak overpressure is then incremented within a loop with peak deflections, and bond and shear stresses are calculated and compared with corresponding terminal values at each increment. In this manner the incipient failure overpressure based on one of the three failure mechanisms (flexure, bond or shear) is determined.

A list of input data parameters and their corresponding text notation is given. They are presented in the same order as that of input data statements in the MAIN program.

<u>Computer Variable</u>	<u>Definition</u>
NW	Number of data points (not including origin) needed to describe the resistance function (e.g., NW=3 for trilinear slab resistance function illustrated in Chapter Two)

FNPD	Controls maximum time range of integration, FNPD is the number of natural periods of the single degree-of-freedom model (i.e., $T_{MAX} = FNPD$ natural period of vibration), FNPD=2 is a conservative value to use
TOO	Initial integration time is given in seconds (usually 0.0 sec)
NDE	Number of first order differential equations needed to describe equations of motion (e.g., NDE=2 if the one degree-of-freedom model is used)
NTI	Number of time intervals used in integration scheme (e.g., NTI=50 is usually sufficient)
TMASS	Total mass (m_t) of equivalent single degree-of-freedom system (lb-sec ² /in.)
PO	Initial peak overpressure value used in the search for the incipient failure overpressure (psi)
YIELD	Weapon yield (MT)
FKMASS(J),KLOAD(J); J=1,...,NW	Mass and load factors, K_m , K_L for the resistance function (e.g., can be obtained from Tables D.1 through D.5, Appendix D)
TH1S(J),TH2S(J), TH1L(J),TH2L(J); J=1,...,NW	Shear coefficients θ_{1s} , θ_{2s} , θ_{1l} , θ_{2l} (e.g., can be obtained from Tables D.1 through D.5)
XOO(K), K=1,...,NDE	Initial conditions for equations of motion (usually zero)
NOPD	Number of overpressure iterations used in the search for the incipient failure overpressure
POEND	Final overpressure value (psi) used in the search for the incipient failure overpressure (psi)
IWRT	Intermediate printout switch governing printout of complete time history for each trial overpressure value; =0 switch off; =1 switch on (usually set =0)
FKS,FKL	Cracked section factor for the short and long side respectively (k_s , k_l) (see Chapter Two for definition)

DS,DL	Short and long side depths respectively, measured from the compression face of the beam (slab) to the centroid of the longitudinal tensile reinforcement (in.)(d_s , d_ℓ)
PS	Percent steel in rods perpendicular to short side (p_s)
PL	Percent steel in rods perpendicular to long side (p_ℓ)
FNS,FNL	Ratio of steel modulus, E_s , to concrete modulus, E_c , for short and long side respectively (n_s , n_ℓ)
DPS,DPL	Distance between centroids of compression and tensile steel in doubly reinforced member for short and long side respectively (d'_s , d'_ℓ) (in.)
FA,FB	Short and long side of slab respectively (a , b)(in.)
QDL	Total dead weight acting normal to slab surface ($Q_{d\ell}$) (lb/in ²)
FDY	Dynamic yield strength of steel (f_{dy})(psi)
ALF	Coefficient used in bending resistance formula (α) (see Tables D.1 through D.5)
BET	Coefficient used in bending resistance formula (β) (see Tables D.1 through D.5)
GAM	Coefficient used in bending resistance formula (γ) (see Tables D.1 through D.5)
RHO	Coefficient used in bending resistance formula (ρ) (see Tables D.1 through D.5)
EC	Modulus of elasticity for concrete (E_c)(psi)
DTOT	Total depth of slab (D)(in.)
FMU	Coefficient used in bending resistance formula (μ)(see Tables D.1 through D.5)
PHI	Coefficient used in bending resistance formula (ϕ) (see Tables D.1 through D.5)
PMULT	Lateral pressure multiplier (M_ℓ), the amount by which overpressure is reduced in magnitude (usually set equal to +1 for roof slabs, 0.5 for buried external walls)

DCAP	Width of capitol (d_c)(in.), when this variable is not left blank in the program input, the computer is instructed to solve a flat plate problem (with reference to Table D.4), if the variable is left blank the computer assumes it is solving a slab supported along the entire periphery (e.g., Tables D.1 through D.3, or D.5)
SPS,SPL	Reinforcement rod shear perimeter per unit slab length for the short and long side respectively (in./in.)
FMAXBS,FMAXBL	Maximum allowable bond stress for the short and long side respectively (psi)
FMAXSS,FMAXSL	Maximum allowable shear stress for the short and long side respectively (psi)
VBAC	Leave blank

C.1.2 Slab Analysis Program User Instructions

A description of the input data and its format is given in Table C.1. The description is for a typical, single problem run. In the event that more than one problem is to be solved, the data may be stacked back-to-back and executed during a single run.

Before proceeding, the user should be familiar with the basic theory and assumptions concerning the analysis of rectangular RC slabs presented in Chapter Two. It should be noted that this program calculates the incipient overpressure only. Catastrophic failure overpressure is a separate calculation involving the procedure outlined in Chapter Two.

TABLE C.1
INPUT DATA FORMAT

1 Card (1I5, 2E10.5, 2I5)		
Col. 1-5	NW	Resistance function data points (excluding origin)
6-15	FNPD	Integration time range multiplier
16-25	TOO	Initial integration time (sec)
26-30	NDE	Number of first order differential equations (2)
31-35	NTI	Number of integration time intervals
1 Card (3E10.5)		
Col. 1-10	TMASS	Total mass of equivalent single degree-of-freedom system (lb-sec ² /in.)
11-20	PO	Initial overpressure search value (psi)
21-30	YIELD	Weapon yield (MT)
NW Cards (6E10.5)		
Typical Card	Col. 1-10	FKMASS() Mass factor, K_m
	11-20	KLOAD() Load factor, K_L
	21-30	TH1S() Shear coefficient, Q_{1s}
	31-40	TH2S() Shear coefficient, Q_{2s}
	41-50	TH1L() Shear coefficient, Q_{1L}
	51-60	TH2L() Shear coefficient, Q_{2L}
1 Card (8E10.5)		
Col. 1-10	X00(1)	Initial velocity, ips
11-20	X00(2)	Initial displacement, (in.)
		} Initial conditions for integration
1 Card (1I5, 1E10.5, 1I5)		
Col. 1-5	NOPD	Number of failure overpressure iterations
6-15	POEND	Upper bound on overpressure search (psi)
16-20	IWRT	Detail printout switch, 0 off; 1 on
1 Card (8E10.5)		
Col. 1-10	FKS	Cracked section factors (short and long side)
11-20	FKL	
21-30	DS	Compression face to steel centroid depths (short and long side)(in.)
31-40	DL	
41-50	PS	Ratio of steel in the short and long directions respectively
51-60	PL	
61-70	FNS	Ratio of steel to concrete modulus
71-80	FNL	
1 Card (8E10.5)		
Col. 1-10	DPS	Distance between tension and compression rods (in.)
11-20	DPL	
21-30	FA	Short and long side of slab respectively (in.)
31-40	FB	
41-50	QDL	Total dead weight normal to slab surface (lb/in. ²)
51-60	FDY	Dynamic yield strength of reinforcing steel (F_{dy})(psi)
61-70	ALF	} Coefficients in bending resistance formula (see Appendix D)
71-80	BET	
1 Card (8E10.5)		
Col. 1-10	GAM	} Coefficients in bending resistance formula (see Appendix D)
11-20	RHO	
21-30	EC	Concrete modulus of elasticity (psi)
31-40	DTOT	Total depth of slab (in.)
41-50	FMU	} Coefficients in bending resistance formula (see Appendix D)
51-60	PHI	
61-70	PMULT	Lateral pressure multiplier
71-80	DCAP	Capital width (leave blank if not applicable)(in.)
1 Card (7E10.5)		
Col. 1-10	SPS	Reinforcement shear perimeter per unit length, short and long side (in /in.)
11-20	SPL	
21-30	FMAXBS	Maximum allowable bond stress for short and long side (psi)
31-40	FMAXBL	
41-50	FMAXSS	Maximum allowable shear stress for short and long side (psi)
51-60	FMAXSL	
61-70	VBAC	Leave blank

MAIN PROGRAM LISTING

Reproduced from
best available copy.

```
COMMON/RWT/RW,P,TH1S,TH2S,TH1L,TH2L
COMMON/RIT/IWRT
COMMON/74/XSTAT,PMULT,VBAC
COMMON/AY/ TO,A,AA,B,BB,C,CC,PO,YIELD
DIMENSION W(50),R(50),FKMASS(50),FKLOAD(50)
COMMON/AX/W,R,FKMASS,FKLOAD,NW,TMASS,TPGL
DIMENSION TH1S(50),TH2S(50),TH1L(50),TH2L(50)
DIMENSION X00(50),CV(20)
```

```
COMPUTE DYNAMIC RESPONSE
THE DIFFERENTIAL EQUATION IS OF THE FORM.
```

```

      D2W=(KL/KM)*(P(T)-R(W))/MT
50 READ(5,10)NW,FNPD,TOO,NDE,NTI,TMASS, PO,YIELD
10 FORMAT(11F10.5,2I5/3F10.5)
      READ(5,12)((FKMASS(J),FKLOAD(J),TH1S(J),TH2S(J),TH1L(J),
11TH2L(J)),J=1,NW)
12 FORMAT(6E10.5)
      READ(5,15)(X00(J),J=1,NDE)
15 FORMAT(8E10.5)
      READ(5,101)NORD, POEND,IWRT
101 FORMAT(15,1E10.5,15)
      READ(5,350)FKS,FKL,DS,DL,PS,PL,FNS,FNL,DPS,DPL,FA,FB,GDL,FDY,
11ALE,BFT,GAM,RHO,EC,DTOT,FMU,PHI,PMULT,DCAP
350 FORMAT(8E10.5/8F10.5/8F10.5)
      READ(5,450)SPS,SPC,FMAXRS,FMAXRL,FMAXSS,FMAXSL,VBAC
450 FORMAT(7E10.5)
```

```
IF(PMULT.EQ.0.0)MULT=1.0
```

```
COMPUTE CRACKED SECTION FACTORS FKS FKL
COVER IS .1*DTOT
```

```

FMMS=PS*(3.*FNS-1.)
FMML=PL*(3.*FNL-1.)
QS=PS*(FNS+(2.*FNS-1.)*.1*DTOT/DS)
QL=PL*(FNL+(2.*FNL-1.)*.1*DTOT/DL)
FKS=SQRT(FMMS**2+2.*QS)-FMMS
FKL=SQRT(FMML**2+2.*QL)-FMML
```

```
TPGL IS THE SLAB AREA SUBJECTED TO PRESSURE WHICH WILL
CAUSE BENDING
```

```
TPGL=FA*FB -DCAP**2
COMPUTE RESISTANCE AND K FACTORS
```

```

IRESET=0
BS=1.0
BL=1.0
```

COMPUTE AVG. I

```

FITS=BS*(FKS*DS)**3/3.+FNS*PS*((1.-FKS)*DS)**2+
1(FNS-1.)*PS*BS*DS*(FKS*DS-3.))**2
FIGS=BS*DTOT**3/12.
FIS=(FITS+FIGS)/2.
FITL=BL*(FKL*DL)**3/3.+FNL*PL*((1.-FKL)*DL)**2+
1(FNL-1.)*PL*BL*DL*(FKL*DL-3.))**2
FIGL=BL*DTOT**3/12.
FIL=(FITL+FIGL)/2.
FIAVG=(FIS+FIL)/2.
R1A=PL*DL*DPL*FDY*FMU-FA*FB*QDL +PS*DS*DPS*FDY*PHI
R2A=FDY*(2.*ALF*PL*DL*DPL*FB/FA+2.*BET*PS*DS*DPS)-FA*FB*QDL
FK1=GAM*EC*FIAVG/(FA*FA)
FK2=RHO*EC*FIAVG/(FA*FA)
DEL1A=R1A/FK1
DEL2A=DEL1A+(R2A-R1A)/FK2

```

COMPUTE R AND W TABLE

```

W(1)=0.0
R(1)=0.0
W(2)=DEL1A
R(2)=R1A
W(3)=DEL2A
R(3)=R2A
W(4)=DEL2A*10.
R(4)=R2A
FKLOAD=DEL2A
WEL=DEL1A

```

COMPUTE NATURAL FREQ.

```

OMGSQ=R(2)*FKLOAD/(W(2)*FKMASS(2)*TMASS)
INATE=6.283/SQRT(OMGSQ)
INPD=2.0
*****WRITE INPUT*****
WRITE(6,11)NW,INPD,TOO,NDE,NTI,TMASS,WEL,PO,YIELD
11 FORMAT(1H1/15X,33HNUMBER OF DEFLECTION DATA POINTS=,I3/
1      15X,47HNUMBER OF INATE DURATIONS FOR TIME INTEGRATION=,F
2      10.5/15X,29HINITIAL TIME FOR INTEGRATION=,E16.8/
3      15X,45HNUMBER OF FIRST ORDER DIFFERENTIAL EQUATIONS=,I3/
4      15X,37HNUMBER OF INTEGRATION TIME INTERVALS=,I5/
5      15X,25HTOTAL MASS OF THE SYSTEM=,E16.8/
6      15X,19HELASTIC DEFLECTION=,E16.8/
7      15X,27HSTART SEARCH OVER PRESSURE=,F16.8/
8      15X,10HYIELD(MT)=,E16.8////)
WRITE(6,13)
13 FORMAT(9X,1HW,16X,1HR,16X,6HFKMASS,16X,6HFKLOAD)
WRITE(6,14)(W(K),R(K),FKMASS(K),FKLOAD(K),K=1,NW)
14 FORMAT(1X,4(E16.8,2X))
WRITE(6,19)
19 FORMAT(9X,1HW,13X,4HTH1S,13X,4HTH2S,13X,4HTH1L,13X,4HTH2L)
WRITE(6,29)(W(J),TH1S(J),TH2S(J),TH1L(J),TH2L(J),J=1,NW)
29 FORMAT(1X,5(E16.8,2X))
WRITE(6,16)
16 FORMAT(20X,38H***DIFFERENTIAL EQ. INITIAL CONDITIONS)
WRITE(6,17)(J,XOO(J),J=1,NDE)

```

```

17 FORMAT(1X/5X,4HX00(,12,2H)=,E16.8)
WRITE(6,102)NOPD,FAILDF,POEND,IWRT
102 FORMAT(1X//1X,25HMAX NUMBER OF ITERATIONS=,I3 //
1      1X,19HFAILURE DEFLECTION=,E16.8//
2      1X,20HMAX SEARCH PRESSURE=,E16.8//
3      1X,35HDETAIL PRINTOUT SWITCH,ZERO IS OFF=,I2////)
WRITE(6,351)FKS,FKL,DS,DL,PS,PL,FNS,FNL,DPS,DPL,FA,FB,QDL,FDY,
1ALF,BET,GAM
351 FORMAT(1X//1X,35HCRACKED SECTION FACTOR(SHORT SIDE)=,E16.8//
1      1X,34HCRACKED SECTION FACTOR(LONG SIDE)=,E16.8//
2      1X,32HEQUIVALENT DEPTH D (SHORT SIDE)=,E16.8//
3      1X,31HEQUIVALENT DEPTH D (LONG SIDE)=,E16.8//
4      1X,27HPERCENT STEEL (SHORT SIDE)=,E16.8//
5      1X,26HPERCENT STEEL (LONG SIDE)=,E16.8//
6      1X,27HMODULUS RATIO (SHORT SIDE)=,E16.8//
7      1X,26HMODULUS RATIO (LONG SIDE)=,E16.8//
8      1X,52HDEPTH BETWEEN POS.AND NEG.STEEL,DPRIME,(SHORT SID
9E)=,E16.8//
A      1X,51HDEPTH BETWEEN POS.AND NEG.STEEL,DPRIME,(LONG SIDE
R)=,E16.8//
C      1X,18HSHORT SIDE LENGTH=,E16.8//
D      1X,17HLONG SIDE LENGTH=,E16.8//
E      1X,31HSTATIC DEAD LOAD PRESSURE(PSI)=,E16.8//
F      1X,32HDYNAMIC YIELD STRENGTH OF STEEL=,E16.8//
G      1X,28HRESISTANCE CURVE COEFF. ALF=,E16.8//
H      1X,28HRESISTANCE CURVE COEFF. BET=,E16.8//
I      1X,28HRESISTANCE CURVE COEFF. GAM=,E16.8)
WRITE(6,355)RHO,EC,DTOT,FMU,PHI,PMULT,DCAP
355 FORMAT(1X,28HRESISTANCE CURVE COEFF. RHO=,E16.8//
1      1X,20HMODULUS OF CONCRETE=,E16.8//
2      1X,17HTOTAL SLAB DEPTH=,E16.8//
3      1X,31HRESISTANCE CURVE COEFF. (FMU) =,E16.8//
4      1X,31HRESISTANCE CURVE COEFF. (PHI) =,E16.8//
5      1X,24HVERPRESSURE MULTIPLIER=,E16.8//
6      1X,15HCAPITOL WIDTH=,E16.8//)
WRITE(6,451)SPS,SPL,FMAXBS,FMAXBL,FMAXSS,FMAXSL,VRAC
451 FORMAT(1X//1X,42HSTEEL SHEAR PERIMETER PER IN.(SHORT SIDE)=,E16.8/
1      1X,41HSTEEL SHEAR PERIMETER PER IN.(LONG SIDE)=,E16.8//
2      1X,33HMAX ALL. BOND STRESS(SHORT SIDE)=,E16.8//
3      1X,33HMAX ALL. BOND STRESS(LONG SIDE)=,E16.8//
4      1X,34HMAX ALL. SHEAR STRESS(SHORT SIDE)=,E16.8//
5      1X,33HMAX ALL. SHEAR STRESS(LONG SIDE)=,E16.8//
6      1X,25HVOLUME/AREA*CO      RATIO=,E16.8//)
WRITE(6,731)TNAT
731 FORMAT(1X///1X,25HPERIOD OF FREE VIBRATION=,E16.8///)
C*****
CALL PRESS1
TMAX=TNAT*FNPD
IF(TO.GT.,.99E+30)TMAX=FNPD

C
C      TMAX=FNPD OPTION ONLY USED WHEN SOLVING THE STEP SOLUTION I. E. TO VERY
C      LARGE
C
C      INITIALIZE
C
C      CV(20)=0.0
C      CV(19)=0.0
C      CV(18)=0.0
C      CV(17)=0.0

```



```

CV(16)=0.0
CV(15)=0.0
CV(1)=WEL
CALL INTG(TMAX,T00,X00,NDE,NTI,CV)

```

```

CV(20) IS THE PEAK DEFLECTION

```

```

CV(19) IS THE TIME AT WHICH THE PEAK OCCURED

```

```

XPAST=CV(20)
DELP=(POEND-PO)/FLOAT(NOPD)
DO 103 J=1,NOPD
PO=PO+DELP
CALL PRESSI
TMAX=TNAIF*FNPD
IF(T0.GT..99E+30)TMAX=FNPD

```

```

TMAX=FNPD OPTION ONLY USED WHEN SOLVING THE STEP SOLUTION I, E. TO VERY
LARGE

```

```

CV(20)=0.0
CV(19)=0.0
CV(18)=0.0
CV(17)=0.0
CV(16)=0.0
CV(15)=0.0
CALL INTG(TMAX,T00,X00,NDE,NTI,CV)

```

```

IF DCAP IS NOT ZERO,THIS IMPLYS SLAB IS SUPPORTED BY CAPITOLS,
OTHERWISE IT IS AN EDGE SUPPORT

```

```

IF(DCAP.GT.0.0)GO TO 7000

```

```

COMPUTE TOTAL SHEAR PER INCH OF SIDE (DYNAMIC SHEAR + DEAD WT.SHEAR)

```

```

RHO+PHI+BET=0 OPTION IS EMPLOYED ONLY FOR ONE WAY SLABS,WHERE SHEAR IS
IS ACTING ONLY ON SIDE FB

```

```

IF(RHO+PHI+BET.EQ.0.0) GO TO 7100
VTOTS=(CV(18)+FA*FB*QDL/(2.*(1.+FB/FA)))/FA
VTOTL=(CV(16)+FA*FB*QDL/(2.*(1.+FA/FB)))/FB
GO TO 7001

```

```

7100 VTOTS=0.0
VTOTL=(CV(16)+FA*FB*QDL/2.)/FB
GO TO 7001

```

```

7000 VTOTS=(CV(18)+FA*FB*QDL)/(4.*(DCAP+DTOT))
VTOTL=VTOTS
GO TO 7001

```

```

COMPUTE BOND AND SHEAR STRESSES ON SHORT AND LONG SIDES

```

```

7001 BSS=VTOTS/(SPS*.875*DS)
BSL=VTOTL/(SPL*.875*DL)
SSS=VTOTS/(DS*.875)
SSL=VTOTL/(DL*.875)
IF(FMAXBS.LT.BSS) GO TO 70
IF(FMAXBL.LT.BSL) GO TO 70
IF(FMAXSS.LT.SSS) GO TO 70

```

```

      IF(FMAXSL.LT.SSL) GO TO 70
      GO TO 71
70 IF(IRESET.EQ.1) GO TO 71
      WRITE(6,72)PO,BSS,FMAXBS,BSL,FMAXBL,SSS,FMAXSS,SSL,FMAXSL
      1,CV(18),CV(17),CV(16),CV(15)
72 FORMAT(1X///1X,51HSHEAR AND/OR BOND STRESS VIOLATED AT OVER PRESSU
      1RE=,E16.8,2X,3HPS1.1X//
      21X,24HBOND STRESS(SHORT SIDE)=,E16.8,2X,14HMAX ALLOWABLE=,E16.8//
      31X,24HBOND STRESS(LONG SIDE)=,E16.8,2X,14HMAX ALLOWABLE=,E16.8//
      41X,25HSHEAR STRESS(SHORT SIDE)=,E16.8,2X,14HMAX ALLOWABLE=,E16.8//
      51X,25HSHEAR STRESS(LONG SIDE)=,E16.8,2X,14HMAX ALLOWABLE=,E16.8//
      61X,34HPEAK DYNAMIC SHEAR PER SHORT SIDE=,E16.8//
      71X,29HPEAK SHEAR TIME (SHORT SIDE)=,E16.8//
      81X,33HPEAK DYNAMIC SHEAR PER LONG SIDE=,E16.8//
      91X,28HPEAK SHEAR TIME (LONG SIDE)=,E16.8//
      IRESET=1
71 CONTINUE

```

DEFINE PRESENT DEFLECTION

```

      XPRES=CV(20)
      IF(XPRES-FAILDF.GT.0.) GO TO 111
      XPAST=XPRES
103 CONTINUE
      WRITE(6,105)
105 FORMAT(1X,11HNO SOLUTION)
      GO TO 50
111 DELTXV=XPRES-XPAST
      DF=DELP/DELT XV
      F=DF*(FAILDF-XPAST)+PO-DELP
      PO=F
      CALL PRESS1
      TMAX=TNAIF*FNPD
      IF(TO.GT..99E+30)TMAX=FNPD

```

TMAX=FNPD OPTION ONLY USED WHEN SOLVING THE STEP SOLUTION I. E. TO VERY LARGE

```

      CV(20)=0.0
      CV(19)=0.0
      CV(18)=0.0
      CV(17)=0.0
      CV(16)=0.0
      CV(15)=0.0
      CALL INTG(TMAX,TOO,XOO,NDE,NT1,CV)
      XND=CV(20)/WEL
      TND=CV(19)/TO
      WRITE(6,20)XND,TND,CV(20),CV(19),PO,YIELD
      1,CV(18),CV(17),CV(16),CV(15)
20 FORMAT(1X,08HSOLUTION//1X,24HNUMBER OF YIELD DEFLECTIONS=,E16.8//
      11X,31HNON DIM PEAK TIME (W.R.T. TO) =,E16.8//
      21X,25HACTUAL PEAK DISPLACEMENT=,E16.8//
      31X,17HACTUAL PEAK TIME=,E16.8//
      41X,20HOVER PRESSURE (PSI)=,E16.8//
      51X,11HYIELD (MT)=,E16.8//
      61X,34HPEAK DYNAMIC SHEAR PER SHORT SIDE=,E16.8//
      71X,29HPEAK SHEAR TIME (SHORT SIDE)=,E16.8//
      81X,33HPEAK DYNAMIC SHEAR PER LONG SIDE=,E16.8//
      91X,28HPEAK SHEAR TIME (LONG SIDE)=,E16.8//
      IF(IRESET-1)672,671,671

```

```

671 WRITE(6,673) '
673 FORMAT(1X69HSHEAR AND/OR BOND STRESS FAILURE OCCURED, SEE PRINTOUT
1ABOVE ***** ///)
GO TO 672

C
C COMPUTE TOTAL SHEAR PER INCH OF SIDE(DYNAMIC SHEAR + DEAD WT, SHEAR)
C
672 IF(DCAP.GT.0.0)GO TO 7003
C
C RHO+PHI+DET=0 OPTION IS EMPLOYED ONLY FOR ONE WAY SLABS,WHERE SHEAR IS
C IS ACTING ONLY ON SIDE FB
C

IF(RHO+PHI+DET.EQ.0.0) GO TO 7101
VTOTS=(CV(18)+FA*FB*QDL/(2.*(1.+FB/FA)))/FA
VTOTL=(CV(16)+FA*FB*QDL/(2.*(1.+FA/FB)))/FB
GO TO 7004
7101 VTOTS=0.0
VTOTL=(CV(16)+FA*FB*QDL/2.)/FB
GO TO 7004
7003 VTOTS=(CV(18)+QDL*FA*FB)/(4.*(DCAP+DTOT))
VTOTL=VTOTS
GO TO 7004
7004 BSS=VTOTS/(SPS*.875*DS)
BSL=VTOTL/(SPL*.875*DL)
SSS=VTOTS/(DS*.875)
SSL=VTOTL/(DL*.875)
WRITE(6,677)BSS,FMAXBS,BSL,FMAXBL,SSS,FMAXSS,SSL,FMAXSL
677 FORMAT(1X///1X,43HSHEAR AND BOND STRESSES AT FLEXURE FAILURE ///
11X,24HBOND STRESS(SHORT SIDE)=,E16.8,2X,14HMAX ALLOWABLE=,E16.8//
21X,24HBOND STRESS(LONG SIDE)=,E16.8,2X,14HMAX ALLOWABLE=,E16.8//
31X,25HSHEAR STRESS(SHORT SIDE)=,E16.8,2X,14HMAX ALLOWABLE=,E16.8//
41X,25HSHEAR STRESS(LONG SIDE)=,E16.8,2X,14HMAX ALLOWABLE=,E16.8
5////)
TRATIO=TU/TNATF
WRITE(6,732)TRATIO
732 FORMAT(1X//1X,34IMPULSE DURATION/NATURAL FREQ.RATIO=,E16.8//)
674 CONTINUE
IF(TMAX-CV(19)*1.05)2000,2000,50
2000 WRITE(6,2001)
2001 FORMAT(1X,55H*****CAUTION,SOLUTION HAS NOT PEAKED OUT,EXTEND FNP
1PD )
GO TO 50
END

```

C.1.3 Subroutines INTG and FUN

Integration of the differential equation of motion described earlier (Chapter Two) was performed by means of the Runge-Kutta (Ref. 56) fourth order process which was programmed and is represented by subroutines INTG and FUN. Actual integration is performed within the body of subroutine INTG which initiates the process. The function of subroutine FUN is to express the given differential equation first order form:

$$\dot{x}_1 = \left(- \frac{R(x_2)}{m_t} + \frac{p(t)}{m_t} \right) K_m / K_L$$

$$\dot{x}_2 = x_1$$

In these equations R represents the resistance function, p the loading function and m_t the mass of the system

<u>Computer Variable</u>	<u>Definition</u>
TMAX	Time range (sec) over which the integration is to be performed
TO	Initial time (sec)
NDE	Number of first order differential equations
NTI	Number of time increments (Δt)
TMASS	Total mass (m_t) of equivalent single degree-of-freedom model
X00	Vector of initial conditions
CV	Vector which transmits information from subroutine INTG to MAIN
X0	Solution at the start of a typical time step
XN	Solution at the end of a typical time step
FK1,FK2,FK3,FK4	Value of \dot{x}_1 or \dot{x}_2 evaluated at the corresponding x_1, x_2 (i.e., at X01ST, X02ST,X03ST,X04ST)
T	Time
F()	Value of \dot{x}_1 and \dot{x}_2 evaluated at a given x_1 or x_2

X()	Dummy variable for x_1 and x_2
G()	Dummy variable for CV
RW	Represents R, the resistance function
PT	Overpressure ($P(t)$)
P	Applied force to one degree-of-freedom model ($p(t)$)
PMULT	Multiplier used to proportion of the amount of surface force applied to the slab
W()	Values of abscissa which define the junction points of the piecewise linear resistance function
R()	Values of the ordinate which define the junction points of the piecewise linear resistance function
FKMASS	Mass factor (K_m)
FKLOAD	Load factor (K_L)
TPGL	Projected area of slab (or arch) being analyzed, thus $P=PT*PMULT*TPGL$
A,AA,B,BB,C,CC	Shock parameters $a,\alpha,b,\beta,c,\gamma$ (see subroutine PRESSI discussion)
PO	Peak overpressure (psi)
YIELD	Weapon size (MT)

SUBROUTINE INTG LISTING

```

SUBROUTINE INTG(TMAX,IO,X00,NDE,NTI,CV)
C
C RUNGE-KUTTA 4TH ORDER INTEGRATION PROCESS
C
  DIMENSION X0(50),XN(50),X00(50),CV(20),FK1(50),FK2(50),FK3(50),
1FK4(50),X01ST(50),X02ST(50),X03ST(50)
C
C SET INITIAL VALUES FOR T, XN, AND FK1
C
  H=(TMAX-IO)/FLOAT(NTI)
  DO 2 K=1,NDE
2  XN(K)=X00(K)
  T=IO
  CALL FUN(T,X00,FK1,CV)
C
C END INITIALIZATION
C
  DO 1 J=1,NTI
  DO 3 L=1,NDE
  X0(L)=XN(L)
3  X01ST(L)=FK1(L)*H*.5 + X0(L)
  T1ST=T+H*.5
  CALL FUN(T1ST,X01ST,FK2,CV)
  DO 4 M=1,NDE
4  X02ST(M)=FK2(M)*H*.5 + X0(M)
  T2ST= T1ST
  CALL FUN(T2ST,X02ST,FK3,CV)
  DO 5 N=1,NDE
5  X03ST(N)=FK3(N)*H + X0(N)
  T3ST= T + H
  CALL FUN(T3ST,X03ST,FK4,CV)
  DO 6 JJ=1,NDE
6  XN(JJ)= X0(JJ)+ H*(FK1(JJ)+2.*FK2(JJ) + 2.*FK3(JJ)+FK4(JJ))/6.
C SET NEW TIME INCREMENT FOR NEXT STEP IN SOLUTION
  T=T3ST
C SET NEW VALUE FOR FK1 FOR NEXT STEP IN SOLUTION
  CALL FUN(T,XN,FK1,CV)
C FK1 IS NOW XNDOT
  CALL CRIT(XN,X0,FK1,CV,T)
C GO ON TO CALCULATE NEXT TIME STEP IN SOLUTION
1 CONTINUE
  RETURN
  END

```

SUBROUTINE FUN LISTING

```

SUBROUTINE FUN(T,X,F,G)
COMMON/RWT/RW,P,TH1S,TH2S,TH1L,TH2L
COMMON/ZZ/XSTAT,PMULT,VRAC
DIMENSION F(50),X(50),G(20)
COMMON/AX/W,R,EKMASS,EKLOAD,NW,TMASS,TPGL
COMMON/AY/ TO,A,AA,B,BB,C,CC,PO,YIELD
DIMENSION W(50),R(50),EKMASS(50),EKLOAD(50)
DIMENSION TH1S(50),TH2S(50),TH1L(50),TH2L(50)

```

DESCRIPTION OF FIRST ORDER DIFFERENTIAL EQUATIONS

X(1)=.....VELOCITY

X(2)=.....DISPLACEMENT

PT= SURFACE PRESSURE

PMULT IS AN OVERPRESSURE MULTIPLIER (USUALLY 1. OR LESS.) E.G. FOR USE C
UNDER GROUND WALL PROBLEMS

P=PT*TPGL IS THE SURFACE FORCE

Z=1.0

TAU=T/TO

IF(TAU.GT.1.) Z=0.0

PT=PO*(A*EXP(-AA*TAU) + B*EXP(-BB*TAU)+ C*EXP(-CC*TAU))*(1.-TAU)*Z

P=PT*TPGL*PMULT

G(1) =GV(1)=WEL (ELASTIC DEFLECTION

RW ,EKM , EKL ARE THE INTERPOLATED VALUES

11 CALL FINT(R,W,NW,RW,X(2))

CALL STEPIT(EKMASS,W,NW,EKM,X(2))

CALL STEPIT(EKLOAD,W,NW,EKL,X(2))

2 F(1)=(EKL/EKM)*(P-RW)/TMASS

F(2)=X(1)

RETURN

END

C.1.4 Subroutines FINT and STEPIT

The function of these two subroutines is to perform interpolation. Subroutine FINT is used for interpolating functions with linear variations, as in the case of resistance functions for structural members discussed earlier. Subroutine STEPIT is used for those functions which vary in a step fashion. Program variables are described below.

<u>Computer Variables</u>	<u>Definition</u>
FV	Stored function value (dependent variable)
XV	Corresponding stored independent variable
NX	Number of dependent and independent values stored
F	Interpolated function value corresponding to X
X	Independent variable value corresponding to F
XREM	Variable records original sign of X before taking absolute value of X
JSAVE	Location of nearest stored function value
DELTXV	Distance between two nearest stored values

SUBROUTINE FINT LISTING

```

SUBROUTINE FINT(FV,XV,NX,F,X)
DIMENSION FV(50),XV(50)
C INTERPOLATION ROUTINE
XREM=X
X=ABS(X)
FMUL=1.0
C FV ARE FUNCTION VALUES (NX OF THEM)
C XV ARE IND. VAR. (NX OF THEM)
C F,X ARE THE FUNCTION AND IND. VAR FOR SOME INTERMEDIATE POINT
C (IF F IS THE INTERPOLATED VALUE)
C FIRST BRACKET X TO NEAREST GIVEN PT.
C
DO 10 J=2,NX
  USAVE=J
  IF (XV(J)-X.GT.0.) GO TO 11
10 CONTINUE
  IF (XREM.LT.0.0) FMUL=-1.0
  F=FV(NX)*FMUL
  X=XREM
  RETURN
11 DELTXV=XV(USAVE)-XV(USAVE-1)
  DF=(FV(USAVE)-FV(USAVE-1))/DELT XV
  IF (XREM.LT.0.0) FMUL=-1.0
  F=(DF*(X-XV(USAVE-1))+FV(USAVE-1))*FMUL
  X=XREM
  RETURN
END

```

SUBROUTINE STEPIT LISTING

```

SUBROUTINE STEPIT(FV,XV,NX,F,X)
DIMENSION FV(50),XV(50)
STEP INTERPOLATION ROUTINE

FV ARE FUNCTION VALUES (NX OF THEM)
XV ARE INDEP. VAR (NX OF THEM)

FIRST BRACKET X AND TAKE FUNCTION VALUE TO THE RIGHT
      1
      1 .....*FV(4)
      1 .....*FV(3)
      1 . 1
      1 . 1 E.G.
      1...*FV(2) 1 AT X , F=FV(4)
      1 1
      1FV(1) 1
      *-----
      X(1) X X(4)

XREM=X
X=ABS(X)
FMUL=1.0
DO 10 J=2,NX
USAVE=J
IF(XV(J)-X,GT.0.) GO TO 11
10 CONTINUE
IF(XREM.LT.0.0)FMUL=-1.
F=FV(NX)*FMUL
X=XREM
RETURN
11 IF(XREM.LT.0.0)FMUL=-1.0
F=FV(USAVE)*FMUL
X=XREM
RETURN
END

```

C.1.5 Subroutine CRIT

The purpose of the subroutine CRIT is to keep track of the maximum value (in time) of selected critical time varying parameters and the corresponding time at which the peaks occur. The critical values of interest are updated after each step in the integration process.

<u>Computer Variable</u>	<u>Definition</u>
CV(18)	Current maximum value of the total shear force acting on the slab short side (lb)
CV(17)	Time value corresponding to CV(18)(sec)
CV(16)	Current maximum value of total shear force acting on the slab long side (lb)
CV(15)	Time value corresponding to CV(16)(sec)
CV(20)	Current maximum value of the displacement of the slab centermost point (in.)
CV(19)	Time value corresponding to CV(20)(sec)

SUBROUTINE CRIT LISTING

```

SUBROUTINE CRIT(XN,X0,XNDOT,CV,T)
COMMON/AX/W,R,FKMASS,FKLOAD,NW,TMASS,TPGL
DIMENSION W(50),R(50),FKMASS(50),FKLOAD(50)
COMMON/RWT/RW,P,TH1S,TH2S,TH1L,TH2L
DIMENSION TH1S(50),TH2S(50),TH1L(50),TH2L(50)
DIMENSION XN(50),X0(50),XNDOT(50),CV(20)
COMMON/RIT/IWRT
DISP=XN(2)
DISPP=ABS(DISP)
IF(CV(20)-DISPP)1,1,2
1 CV(19)=T
  CV(20)=DISPP
2 CONTINUE
C COMPUTE MAX VS AND MAX VL
  DO 10 J=2,NW
    JSAVE=J
    IF(W(J)-DISPP.GT.0.) GO TO 11
10 CONTINUE
11 TH1SX=TH1S(JSAVE)
    TH2SX=TH2S(JSAVE)
    TH1LX=TH1L(JSAVE)
    TH2LX=TH2L(JSAVE)
    VS=TH1SX*P+TH2SX*RW
    VL=TH1LX*P+TH2LX*RW
    IF(CV(18)-VS)4,4,5
4 CV(17)=T
  CV(18)=VS
5 CONTINUE
  IF(CV(16)-VL)6,6,7
6 CV(15)=T
  CV(16)=VL
7 CONTINUE
  IF(IWRT.EQ.0)GO TO 50
  WRITE(6,30)XN(2),XN(1),T
30 FORMAT(1X/1X,19HCROWN DISPLACEMENT=,E16.8,3X,9HVELOCITY=,E16.8,3X,
15HTIME=,E16.8)
50 CONTINUE
  RETURN
  END

```

C.1.6 Subroutine PRESSI

The function of subroutine PRESSI is to calculate magnitudes of free-field overpressure generated by KT and MT size nuclear weapons. For a given peak overpressure, weapon size and time after the arrival of the blast wave, the corresponding overpressure level is calculated using the following equation (Ref. 57):

$$\Delta P = \Delta P_s (ae^{-\alpha\tau} + be^{-\beta\tau} + ce^{-\gamma\tau})(1 - \tau), \text{ psi} \quad (\text{C.1})$$

where

ΔP is the overpressure, psi

ΔP_s is the peak overpressure, psi

t is the time after shock arrival measured in units of positive phase duration, i.e.,

$$\tau = \frac{t - t_s}{D_p^+}$$

and

t_s is the shock arrival time, sec

D_p^+ is the duration of the positive phase, sec.

Coefficients a , b and c and α , β , γ are shock parameters which are given in Ref. 57 in graphical form (see Fig. C.2) as functions of ΔP_s . Graphical forms of shock parameters are not simple functions (curves); and before Eq.(C.1) could be programmed for electronic computation, it was necessary to develop approximate equations for curves a , b , c , α , β , γ and D_p^+ .

Curves representing the variation of the given shock parameters (Fig. C.2) were divided into a number of regions (peak overpressure ranges) characterized by the type of variation, i.e., linear or nonlinear. Nonlinear portions were approximated by means of parabolas. A typical idealization performed is shown in Fig. C.3 and represents the variation of shock parameter b . This curve was divided into five regions with respect to peak overpressure. The variations in these regions are given

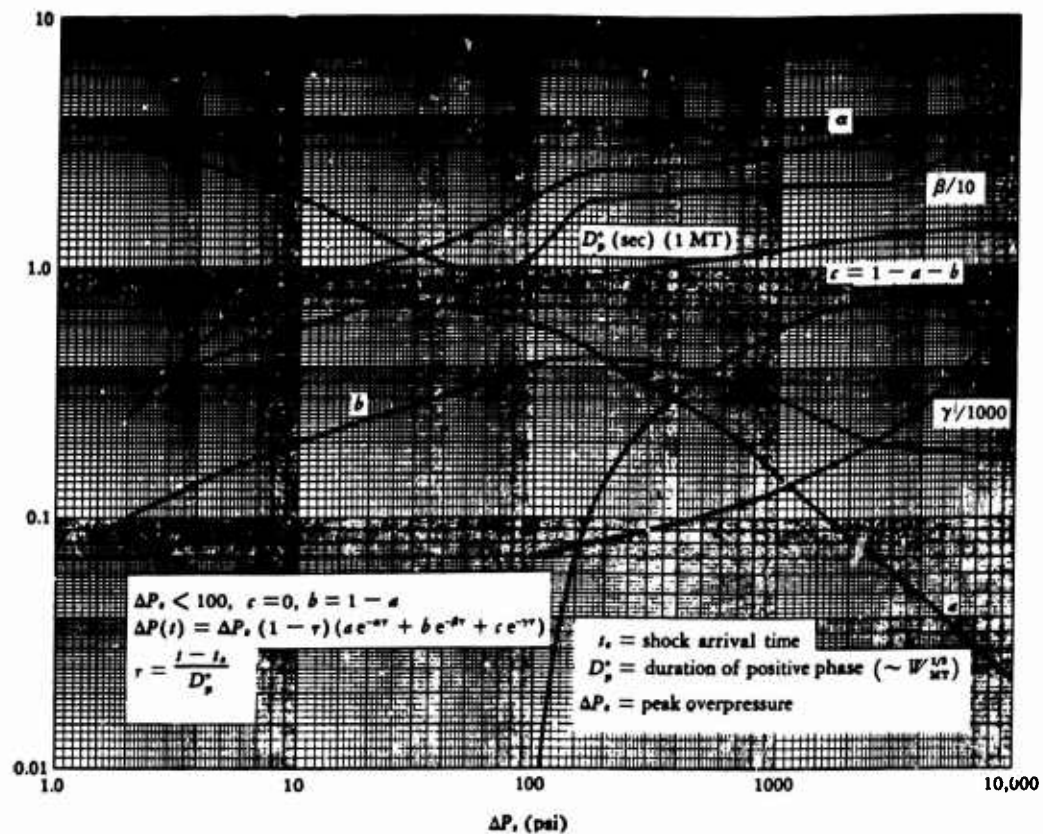


Fig. C.2 APPROXIMATE ANALYTIC FORM FOR OVERPRESSURE VS TIME FOR NUCLEAR BLAST WAVE IN TERMS OF PEAK OVERPRESSURE

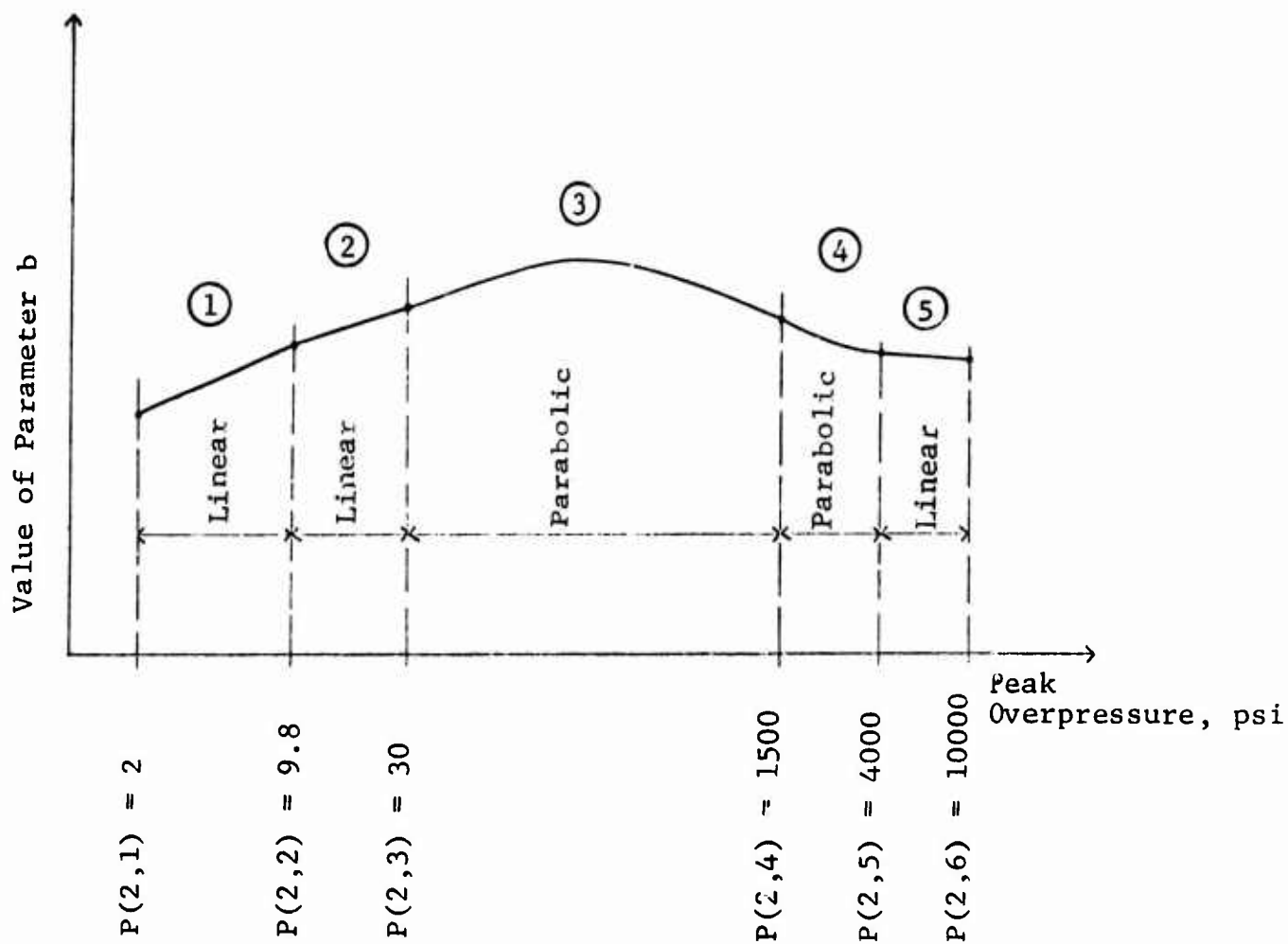


Fig. C.3 IDEALIZATION OF SHOCK PARAMETER b CURVE

by the following equations:

Linear Variation

$$V(k) = C_1(k,i) P_o^{C_2(k,i)} \quad (C.2)$$

Nonlinear Variation

$$V(k) = C_1(k,i) + C_2(k,i) \ln P_o + C_3(k,i) [\ln P_o]^2 \quad (C.3)$$

In Eqs. (C.2) and (C.3) the index k designates the shock parameter curve being considered. These designations are shown below.

Shock Parameter	Program Designation (k)
a	1
b	2
α	3
β	4
γ	5

Index i designates the overpressure range being considered. The type of variation being considered in any one case is designated by KIND(k,i) = 1 or 2, where 1 refers to a linear variation and 2 to a nonlinear variation. The number of overpressure ranges NRANGE(k) in any one case varies with the type of variation. Overpressure ranges and Eqs. (C.2) and (C.3) corresponding to each overpressure range for the five shock parameters listed are given in Table C.2. The shock parameter c is not included since it is obtained from $c = 1 - a - b$. Numerical values of curve equation parameters are set in data statements in the program (see program listing).

Subroutine PRESS may be used where the value of the peak overpressure is within the range $2 \leq \Delta P_s \leq 10,000$ psi. Figure C.4 presents PRESS in flowchart form. As input the subroutine requires: peak overpressure (psi); weapon size (MT); and the time after the arrival of the shock front (sec).

TABLE C.2
SHOCK PARAMETER IDEALIZATION

Shock Parameter	Overpressure Range	Type of Curve	Equation
a	2-15	Straight Line	$a = 0.94127992 P_0^{-0.06469880}$
	15-35	Straight Line	$a = 1.16282745 P_0^{-0.14275098}$
	35-75	Straight Line	$a = 1.06328338 P_0^{-0.11757965}$
	75-220	Parabola	$\ln a = -2.1696237 + 1.0499078 \ln P_0 - 0.15072543 (\ln P_0)^2$
	220-300	Straight Line	$a = 10.63372195 P_0^{-0.60360648}$
	300-900	Parabola	$\ln a = -3.5915442 + 1.3617450 \ln P_0 - 0.16150803 (\ln P_0)^2$
	900-2000	Straight Line	$a = 38.49753141 P_0^{-0.80154185}$
	2000-10000	Straight Line	$a = 57.46864462 P_0^{-0.85425206}$
b	2-9.8	Straight Line	$b = 0.07391036 P_0^{0.43615142}$
	9.8-30	Straight Line	$b = 0.10067667 P_0^{0.30073985}$
	30-1500	Parabola	$\ln b = -4.4409313 + 1.3757287 \ln P_0 - 0.13063109 (\ln P_0)^2$
	1500-4000	Parabola	$\ln b = 23.490011 - 6.1312383 \ln P_0 + 0.37362382 (\ln P_0)^2$
	4000-10000	Straight Line	$b = 0.51999155 P_0^{-0.12138683}$
α	2-3	Straight Line	$\alpha = 0.125 P_0^{1.0}$
	3-20	Parabola	$\ln \alpha = -2.3415881 + 1.5032479 \ln P_0 - 0.24087817 (\ln P_0)^2$
	20-30	Straight Line	$\alpha = 0.35607458 P_0^{0.34469537}$
	30-100	Parabola	$\ln \alpha = 0.34285702 - 0.42775009 \ln P_0 + 0.10820815 (\ln P_0)^2$
	100-300	Parabola	$\ln \alpha = -9.2697949 + 3.7176161 \ln P_0 - 0.33868201 (\ln P_0)^2$
	300-500	Straight Line	$\alpha = 2.00406623 P_0^{0.03876594}$
	500-6000	Straight Line	$\alpha = 0.75434693 P_0^{0.19598924}$
	6000-10000	Parabola	$\ln \alpha = 68.131084 - 15.363012 \ln P_0 + 0.88453218 (\ln P_0)^2$
β	2-22	Straight Line	$\beta = 0.25521219 P_0^{0.34874251}$
	22-40	Straight Line	$\beta = 0.44409685 P_0^{0.16953199}$
	40-110	Parabola	$\ln \beta = 6.8634444 - 3.7469502 \ln P_0 + 0.49767470 (\ln P_0)^2$
	110-280	Parabola	$\ln \beta = -24.211087 + 9.1911457 \ln P_0 - 0.84839391 (\ln P_0)^2$
	280-1700	Straight Line	$\beta = 1.38981839 P_0^{0.05549113}$
	1700-5000	Parabola	$\ln \beta = 19.986486 - 5.0649923 \ln P_0 + 0.33310964 (\ln P_0)^2$
	5000-10000	Straight Line	$\beta = 0.00853424 P_0^{0.67807190}$
γ	2-200	Straight Line	$\gamma = 0.02446584 P_0^{0.22826899}$
	200-10000	Parabola	$\ln \gamma = 0.14168432 - 1.0923874 \ln P_0 + 0.11203606 (\ln P_0)^2$
D_p^+	2-10	Straight Line	$D_p^+ = 4.02376729 P_0^{-0.33047502}$
	10-30	Straight Line	$D_p^+ = 5.26683086 P_0^{-0.44739151}$
	30-200	Parabola	$\ln D_p^+ = 3.4743932 - 1.5451558 \ln P_0 + 0.16603774 (\ln P_0)^2$
	200-500	Straight Line	$D_p^+ = 0.42904253 P_0^{0.15002989}$
	500-4000	Straight Line	$D_p^+ = 0.52706705 P_0^{0.11691892}$
	4000-10000	Straight Line	$D_p^+ = 0.89097957 P_0^{0.05362128}$

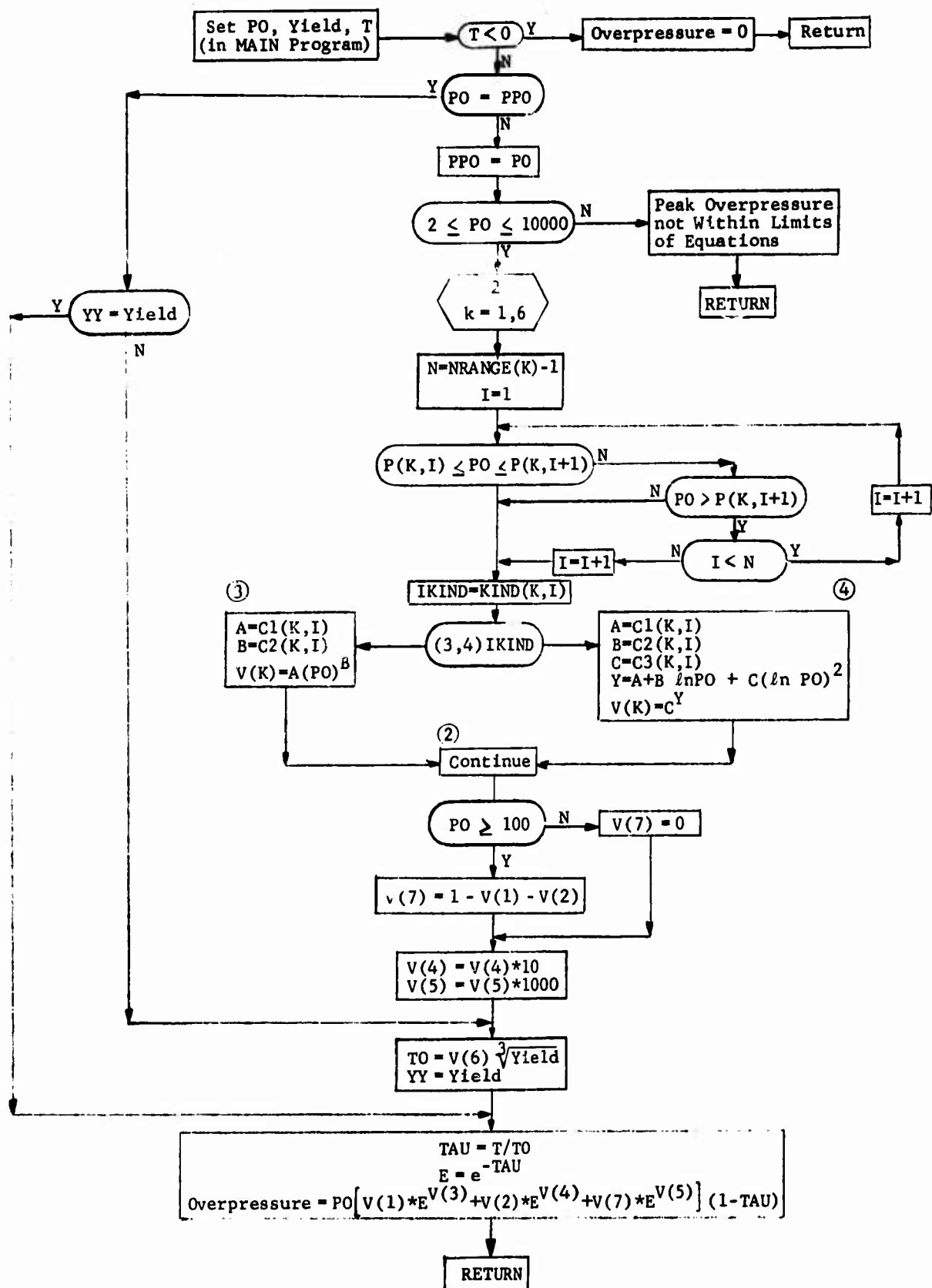


Fig. C.4 SUBROUTINE PRESS FLOWCHART

SUBROUTINE PRESSI LISTING

```

SUBROUTINE PRESSI
COMMON/RT/IRI
COMMON/AY/ IO, A, AA, B, BB, C, CC, PO, YIELD
DIMENSION KIND(6,10), NRANGE(10), P(6,10), C2(6,10), C3(6,10), V(10), C1
1(6,10)
DATA(KIND(1,J),J=1,8)/1,1,1,2,1,2,1,1/
DATA(KIND(2,J),J=1,5)/1,1,2,2,1/
DATA(KIND(3,J),J=1,8)/1,2,1,2,2,1,1,2/
DATA(KIND(4,J),J=1,7)/1,1,2,2,1,2,1/
DATA(KIND(5,J),J=1,2)/1,2/
DATA(KIND(6,J),J=1,6)/1,1,2,1,1,1/
DATA(NRANGE(1),J=1,6)/8,5,8,7,2,6/
DATA(P(1,J),J=1,8)/2.,15.,35.,75.,220.,300.,900.,2000./
DATA(P(2,J),J=1,5)/2.,9.8,30.,1500.,4000./
DATA(P(3,J),J=1,8)/2.,3.,20.,30.,100.,300.,500.,6000./
DATA(P(4,J),J=1,7)/2.,22.,40.,110.,280.,1700.,5000./
DATA(P(5,J),J=1,2)/2.,200./
DATA(P(6,J),J=1,6)/2.,10.,30.,200.,500.,4000./
DATA(C1(1,J),J=1,8)/.94127992,1.1628274,1.0432833,-2.1696237,10.63
15722,-3.5915442,38.497531,57.468645/
DATA(C1(2,J),J=1,5)/.07391036,.10067667,-4.4409313,23.490011,.5199
19155/
DATA(C1(3,J),J=1,8)/.125,-2.3415881,.35607458,.34285702,-9.2697949
1,2.0040662,.75434693,68.131084/
DATA(C1(4,J),J=1,7)/.25521219,.44409685,6.8634444,-24.211087,1.389
1818,19.986486,.00853424/
DATA(C1(5,J),J=1,2)/.02446584,.14168432/
DATA(C1(6,J),J=1,6)/4.0237673,5.2668309,3.4743932,.42904353,.52706
1705,.89097957/
DATA(C2(1,J),J=1,8)/-.06469880,-.14275098,-.11757965,1.0499078,-.6
10360648,1.3617450,-.80154185,-.85425206/
DATA(C2(2,J),J=1,5)/.43615142,.30073985,1.3757287,-6.1312383,-.121
178683/
DATA(C2(3,J),J=1,8)/1.,1.5032479,.34469537,-.42775009,3.7176161,.0
13876594,.19598924,-15.363012/
DATA(C2(4,J),J=1,7)/.34874251,.1693199,-3.7469502,9.1911457,.05549
1113,-5.0649923,.6780719/
DATA(C2(5,J),J=1,2)/.22826899,-1.0923074/
DATA(C2(6,J),J=1,6)/-.33047502,-.44739151,-1.5451558,.15002989,.11
1691892,.05362128/
DATA(C3(1,J),J=1,8)/0.,0.,0.,-.15072543,0.,-.16150803,0.,0./
DATA(C3(2,J),J=1,5)/0.,0.,-.13063109,.37362382,0./
DATA(C3(3,J),J=1,8)/0.,-.24087817,0.,.10820815,-.33968201,0.,0.,.8
18453218/
DATA(C3(4,J),J=1,7)/0.,0.,.49767470,-.84839391,0.,.33310964,0./
DATA(C3(5,J),J=1,2)/0.,.11203606/
DATA(C3(6,J),J=1,6)/0.,0.,.1660374,0.,0.,0./

```



SUBROUTINE PRESSI LISTING

```

SUBROUTINE PRESSI
COMMON/RT/IRI
COMMON/AY/ IO, A, AA, B, BB, C, CC, PO, YIELD
DIMENSION KIND(6,10), NRANGE(10), P(6,10), C2(6,10), C3(6,10), V(10), C1
1(6,10)
DATA(KIND(1,J),J=1,8)/1,1,1,2,1,2,1,1/
DATA(KIND(2,J),J=1,5)/1,1,2,2,1/
DATA(KIND(3,J),J=1,8)/1,2,1,2,2,1,1,2/
DATA(KIND(4,J),J=1,7)/1,1,2,2,1,2,1/
DATA(KIND(5,J),J=1,2)/1,2/
DATA(KIND(6,J),J=1,6)/1,1,2,1,1,1/
DATA(NRANGE(1),J=1,6)/8,5,8,7,2,6/
DATA(P(1,J),J=1,8)/2.,15.,35.,75.,220.,330.,900.,2300./
DATA(P(2,J),J=1,5)/2.,9.8,30.,1500.,4000./
DATA(P(3,J),J=1,8)/2.,3.,20.,30.,100.,300.,500.,6000./
DATA(P(4,J),J=1,7)/2.,22.,40.,110.,280.,1700.,5000./
DATA(P(5,J),J=1,2)/2.,200./
DATA(P(6,J),J=1,6)/2.,10.,30.,200.,500.,4000./
DATA(C1(1,J),J=1,8)/.94127992,1.1628274,1.2632833,-2.1696237,10.63
15722,-1.5915442,38.497531,57.468645/
DATA(C1(2,J),J=1,5)/.07391036,1.1006766,-4.4409313,23.490011,.5199
19155/
DATA(C1(3,J),J=1,8)/.125,-2.3415881,.35607458,.34285702,-9.2697949
1.2,0.040662,.75434693,68.131084/
DATA(C1(4,J),J=1,7)/.25521219,.44409685,6.8634444,-24.211087,1.389
1818,19.986486,.00853424/
DATA(C1(5,J),J=1,2)/.02446584,.14168432/
DATA(C1(6,J),J=1,6)/4.0237673,5.2668309,3.4743932,.42904353,.52706
1705,.89097957/
DATA(C2(1,J),J=1,8)/-.06469880,-.14275098,-.11757965,1.3499078,-.6
10360648,1.3617450,-.80154185,-.85425206/
DATA(C2(2,J),J=1,5)/.43615142,.30073985,1.3757287,-6.1312383,-.121
138683/
DATA(C2(3,J),J=1,8)/1.,1.5032479,.34469537,-.42775009,3.7176161,.0
13876594,.19598924,-15.363012/
DATA(C2(4,J),J=1,7)/.34874251,.1693199,-3.7469502,9.1911457,.05549
1113,-5.0649923,.67807190/
DATA(C2(5,J),J=1,2)/.22826899,-1.0923874/
DATA(C2(6,J),J=1,6)/-.33047502,-.44739151,-1.5451558,.15002989,.11
1691892,.05362128/
DATA(C3(1,J),J=1,8)/0.,0.,0.,-.15072543,0.,-.16150803,0.,0./
DATA(C3(2,J),J=1,5)/0.,0.,-.13063109,.37362382,0./
DATA(C3(3,J),J=1,8)/0.,-.24087817,0.,.10820815,-.33968201,0.,0.,.8
18453218/
DATA(C3(4,J),J=1,7)/0.,0.,.49767470,-.84839391,0.,.33310964,0./
DATA(C3(5,J),J=1,2)/0.,.11203606/
DATA(C3(6,J),J=1,6)/0.,0.,.16603774,0.,0.,0./

```



```

      IF(P0.EQ.PP0) GO TO 13
      PP0=PP0
      IF(P0.GE.2..AND.P0.LE.10000.) GO TO 11
      GO TO 16
11 DO 2 K=1,6
      N=NRANGE(K)-1
      I=1
      IF(P0.GE.P(K,I).AND.P0.LE.P(K,I+1)) GO TO 5
      IF(P0.GT.P(K,I+1)) GO TO 6
      GO TO 5
      6 IF(I.LT.N) GO TO 7
      I=I+1
      GO TO 5
      7 I=I+1
      GO TO 8
      5 IKIND=KIND(K,I)
      GO TO(3,4),IKIND
      3 A=C1(K,I)
      B=C2(K,I)
      V(K)=A*P0**B
      GO TO 2
      4 A=C1(K,I)
      B=C2(K,I)
      C=C3(K,I)
      Y=A+B*ALOG(P0)+C*ALOG(P0)*ALOG(P0)
      V(K)=EXP(Y)
      2 CONTINUE
      IF(P0.GE.100.) GO TO 14
      V(7)=0.
      V(5)=0.0
      V(1)=1.0-V(2)
      GO TO 15
14 V(7)=1.-V(1)-V(2)
15 V(4)=V(4)*10.
      V(5)=V(5)*1000.
      GO TO 17

13 IF(YY.EQ.YIELD) GO TO 9
17 TO=V(6)*YIELD**(1./3.)
      YY=YIELD
      IF(IWRT.EQ.0)GO TO 50
      WRITE(6,18)YIELD,P0,TO,V(1),V(3),V(2),V(4),V(7),V(5)
18 FORMAT(7H0YIELD=,E15.8,3H MT/22H PEAK OVERPRESSURE,P0=E15.8,4H PSI
1/23H POS.PHASE DURATION,TO=,E15.8,5H SEC./22H0OVERPRESSURE,P(T)=P0
2* 55H(A*EXP(-AA*TAU)+B*EXP(-BB*TAU)+C*EXP(-CC*TAU))*(
31.-TAU)/9H0WHERE A=,E15.8,4X,4H AA=,E15.8/6X,3H B=E15.8,4X,4H BB=,
4E15.8/6X,3H C=,E15.8,4X,4H CC=,E15.8/6X,9H TAU=T/TO)
50 CONTINUE
      A=V(1)
      AA=V(3)
      B=V(2)
      BB=V(4)
      C=V(7)
      CC=V(5)

```

```

      RETURN
      ENTRY PRESS(OVERP,T)
      IF(T,LT,U.) GO TO 10
9     TAU=T/T0
      E=EXP(-TAU)
      OVERP=PO*(V(1)*(L**V(3))+V(2)*(F**V(4))+V(7)*(E**V(5)))*(1.0-TAU)
      RETURN
10    OVERP=0.0
      RETURN
16    WRITE(6,12)
12    FORMAT(49HOPEAK OVERPRESSURE NOT WITHIN LIMITS OF EQUATIONS)
      RETURN
      END

```

C.2 BURIED ARCH SHELTER ANALYSIS PROGRAM

Since we are dealing with a single degree-of-freedom idealization of structures, the major difference between the methods of analysis for an arch and a rectangular plate is in the means for generating resistance functions. In the case of RC beams and slabs having various edge conditions, resistance functions are generally known and well-documented. For these types of structures a complete, all-inclusive computational procedure is thus capable of being easily programmed as described in the previous section.

In the case of buried arches the situation is somewhat different. Readily usable equations describing resistance functions for buried arches under various soil conditions do not exist as such. The problem of the behavior of various soils in the vicinity of a buried arch is not well understood. It is therefore considerably more difficult than the one dealing with the behavior of RC slabs at grade. However, a fairly good approximation to the arch resistance function can be made by the use of a nonlinear finite element approach. This involves modeling the arch as well as a portion of the soil media surrounding the arch as described in Chapter Two and illustrated in Fig. 2.17. The computer program (Ref. 24) used in generating resistance functions for buried arch shelters is an existing program developed at IITRI and is generally available, therefore, its documentation is not included in this report. Instead we describe how the program was used in calculating incipient failure pressures for buried arch shelters.

The computer program mentioned is a finite element program and was developed for the purpose of analyzing plane structures in the elastic-plastic range. It can handle bar and triangular plate elements so that it is applicable to trusses and to the analysis of in-plane stresses in reinforced plates, arches, etc. The material behavior is assumed to be isotropic. The user has a choice of 3 stress-strain laws and 10 different materials.

The stress-strain laws are: Ramberg-Osgood, Goldberg-Richard, and Bilinear.

A numerical step-by-step procedure for obtaining solutions which satisfy the requirements of the incremental theory of plasticity for materials which obey the Mises yield condition and the associated flow rule is used in the program. At each step in the solution an iterative procedure is used to find the correct values of the strain increments. Changes in plastic strain are accounted for by the addition of fictitious plastic forces to the actual loading on the structure in such a way that the deflections of the structure under the modified loading with elastic behavior assumed are equal to the actual ones. A modified form of the computer program given in Ref. 58 is used to obtain elastic solutions.

Once the resistance function is obtained using the computer program described, the procedure for obtaining the incipient failure overpressure for the arch shell is essentially the same as that used in connection with rectangular structures described in Subsection C.1 and involves using the same subroutines. The computational procedure is as described in Fig. C.1 except that failure criteria are as established in Chapter Two. The arch shell analysis program used is not included in this report because it would be necessary to include the computer program of Ref. 24, which is lengthy, and as mentioned earlier, is generally available. The reader may readily assemble the package from the information provided herein should this be desirable.

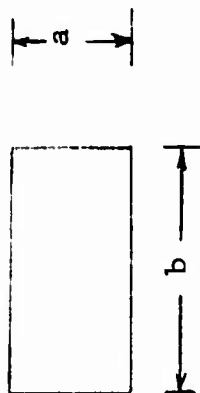
APPENDIX D

SLAB COEFFICIENTS

Tables which list coefficients required in the analysis of RC slabs when using the slab analysis computer program described and documented in Appendix C are presented. These tables are a modified version of those given in Ref. 13. The manner in which these coefficients are used in solving a given problem is described in Chapter Two, input format is provided in Appendix C.

TABLE D.1

COEFFICIENTS FOR TWO-WAY SLAB FIXED ON FOUR SIDES, WITH UNIFORM LOAD

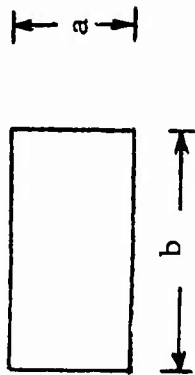


Strain Range	a/b	K_L	K_m	ϕ	μ	β	α	γ	ρ	θ_{1s}	θ_{2s}	$\theta_{1\ell}$	$\theta_{2\ell}$
Elastic	1.0	0.33	0.21	0.0	30.2			870		0.10	0.15	0.10	0.15
	0.9	0.34	0.23	0.0	27.8			798		0.09	0.14	0.10	0.17
	0.8	0.36	0.25	0.0	26.0			757		0.08	0.12	0.11	0.19
	0.7	0.38	0.27	0.0	26.0			744		0.07	0.11	0.11	0.21
	0.6	0.41	0.29	0.0	26.4			778		0.06	0.09	0.12	0.23
	0.5	0.43	0.31	0.0	25.0			866		0.05	0.08	0.12	0.25
Elasto- Plastic	1.0	0.46	0.31			12.0	12.0		271	0.07	0.18	0.07	0.18
	0.9	0.47	0.33			12.0	11.0		248	0.06	0.16	0.08	0.20
	0.8	0.49	0.35			12.0	10.3		228	0.06	0.14	0.08	0.22
	0.7	0.51	0.37			12.0	9.8		216	0.05	0.13	0.08	0.24
	0.6	0.53	0.39			12.0	9.3		212	0.04	0.11	0.09	0.26
	0.5	0.55	0.41			12.0	9.0		216	0.04	0.09	0.09	0.28
Fully- Plastic	1.0	0.33	0.17			12.0	12.0			0.09	0.16	0.09	0.16
	0.9	0.35	0.18			12.0	11.0			0.08	0.15	0.09	0.18
	0.8	0.37	0.20			12.0	10.3			0.07	0.13	0.10	0.20
	0.7	0.38	0.22			12.0	9.8			0.06	0.12	0.10	0.22
	0.6	0.40	0.23			12.0	9.3			0.05	0.10	0.10	0.25
	0.5	0.42	0.25			12.0	9.0			0.04	0.08	0.11	0.27

Note: Blank spaces indicate nonapplicability.

TABLE D.2

COEFFICIENTS FOR TWO-WAY SLAB WITH SIMPLE SUPPORTS ON TWO LONG SIDES,
FIXED SUPPORTS ON TWO SHORT SIDES AND UNIFORM LOAD

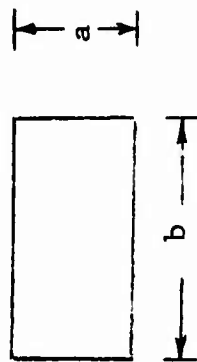


Strain Range	a/b	K_L	K_m	ϕ	$\mu \cdot \frac{a}{b}$	β	$2 \cdot \alpha$	γ	ρ	θ_{1s}	θ_{2s}	θ_{1l}	θ_{2l}
Elastic	1.0	0.39	0.26	20.4	0.0			575		0.09	0.10	0.07	0.18
	0.9	0.41	0.28	10.2	11.0			476		0.08	0.14	0.08	0.20
	0.8	0.44	0.30	10.2	10.3			396		0.68	0.12	0.08	0.22
	0.7	0.46	0.33	9.3	9.7			328		0.07	0.11	0.08	0.24
	0.6	0.48	0.35	8.5	9.3			283		0.06	0.09	0.09	0.26
Elasto- Plastic	0.5	0.51	0.37	7.4	9.0			243		0.05	0.08	0.09	0.28
	1.0	0.46	0.31			12.0	12.0		271	0.07	0.18	0.07	0.18
	0.9	0.47	0.33			12.0	11.0		248	0.06	0.16	0.08	0.20
	0.8	0.49	0.35			12.0	10.3		228	0.06	0.14	0.08	0.22
	0.7	0.51	0.37			12.0	9.7		216	0.05	0.13	0.08	0.24
Fully- Plastic	0.6	0.53	0.37			12.0	9.3		212	0.04	0.11	0.09	0.26
	0.5	0.55	0.41			12.0	9.0		216	0.04	0.09	0.09	0.28
	1.0	0.33	0.17			12.0	12.0			0.09	0.16	0.09	0.16
	0.9	0.35	0.18			12.0	11.0			0.08	0.15	0.09	0.18
	0.8	0.37	0.20			12.0	10.3			0.07	0.13	0.10	0.20
	0.7	0.38	0.22			12.0	9.7			0.06	0.12	0.10	0.22
	0.6	0.40	0.23			12.0	9.3			0.05	0.10	0.10	0.25
	0.5	0.42	0.25			12.0	9.0			0.04	0.08	0.11	0.27

Note: Blank spaces indicate nonapplicability.

TABLE D.3

COEFFICIENTS FOR TWO-WAY SLAB WITH SIMPLE SUPPORTS ON FOUR SIDES AND UNIFORM LOAD



Strain Range	a/b	K_L	K_m	ϕ	$\mu \cdot \frac{a}{b}$	$2 \cdot \beta$	$2 \cdot \alpha$	γ	ρ	θ_{1s}	θ_{2s}	$\theta_{1\ell}$	$\theta_{2\ell}$
Elastic	1.0	0.45	0.31	12.0	12.0			271		0.07	0.18	0.07	0.18
	0.9	0.47	0.33	12.0	11.0			248		0.06	0.16	0.08	0.20
	0.8	0.49	0.35	12.0	10.3			228		0.06	0.14	0.08	0.22
	0.7	0.51	0.37	12.0	9.8			216		0.05	0.13	0.08	0.24
	0.6	0.53	0.39	12.0	9.3			212		0.04	0.11	0.09	0.26
Elasto-Plastic	0.5	0.55	0.41	12.0	9.0			216		0.04	0.09	0.09	0.28
	1.0	0.33	0.17			12.0	12.0		0.0	0.09	0.16	0.09	0.16
	0.9	0.35	0.18			12.0	11.0		0.0	0.08	0.15	0.09	0.18
	0.8	0.37	0.20			12.0	10.3		0.0	0.07	0.13	0.10	0.20
	0.7	0.38	0.22			12.0	9.8		0.0	0.06	0.12	0.10	0.22
Fully-Plastic	0.6	0.40	0.23			12.0	9.3		0.0	0.05	0.10	0.10	0.25
	0.5	0.42	0.25			12.0	9.0		0.0	0.04	0.08	0.11	0.27
	1.0	0.33				12.0	12.0			0.09	0.16	0.09	0.16
	0.9	0.35				12.0	11.0			0.08	0.15	0.09	0.18
	0.8	0.37				12.0	10.3			0.07	0.13	0.10	0.20
	0.7	0.38				12.0	9.8			0.06	0.12	0.10	0.22
	0.6	0.40				12.0	9.3			0.05	0.10	0.10	0.25
	0.5	0.42				12.0	9.0			0.04	0.08	0.11	0.27

Note: Blank spaces indicate nonapplicability.

TABLE D.4

COLUMN SUPPORTED SLAB WITH SQUARE INTERIOR UNIFORM LOAD



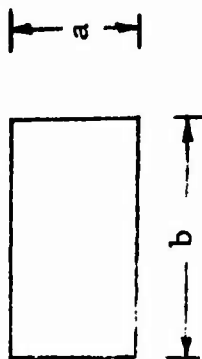
Typical Quadrant

Strain Range	d_c/a	K_L	K_m	$\phi/4$	μ	$\beta/2$	α	144γ	ρ	θ_{1s}	θ_{2s}	$\theta_{1\ell}$	$\theta_{2\ell}$
Elastic	0.05	0.53	0.34	4.2	0.0			1.45		0.16	0.84	0.16	0.84
	0.10	0.53	0.34	4.4	0.0			1.60		0.16	0.84	0.16	0.84
	0.15	0.53	0.34	4.6	0.0			1.75		0.16	0.89	0.16	0.84
	0.20	0.53	0.34	4.8	0.0			1.92		0.16	0.84	0.16	0.84
	0.25	0.53	0.34	5.0	0.0			2.10		0.16	0.84	0.16	0.84
Elastic	0.05	0.50	0.29			4.2	0.0		0.0	0.14	0.86	0.14	0.86
	0.10	0.50	0.29			4.4	0.0		0.0	0.14	0.86	0.14	0.86
	0.15	0.50	0.29			4.6	0.0		0.0	0.14	0.86	0.14	0.86
	0.20	0.50	0.29			4.8	0.0		0.0	0.14	0.86	0.14	0.86
	0.25	0.50	0.29			5.0	0.0		0.0	0.14	0.86	0.14	0.86
Plastic	0.05	0.50	0.29			4.2	0.0			0.14	0.86	0.14	0.86
	0.10	0.50	0.29			4.4	0.0			0.14	0.86	0.14	0.86
	0.15	0.50	0.29			4.6	0.0			0.14	0.86	0.14	0.86
	0.20	0.50	0.29			4.8	0.0			0.14	0.86	0.14	0.86
	0.25	0.50	0.29			5.0	0.0			0.14	0.86	0.14	0.86

Note: Blank spaces indicate nonapplicability.

TABLE D.5

TWO-WAY SLAB WITH SIMPLE SUPPORTS ON TWO SHORT SIDES,
FIXED SUPPORTS ON TWO LONG SIDES AND UNIFORM LOAD



Strain Range	a/b	K_L	K_m	ϕ	μ	2β	α	γ	ρ	θ_{1s}	θ_{2s}	θ_{1l}	θ_{2l}
Elastic	1.0	0.39	0.26	0.0	20.4			575		0.07	0.18	0.09	0.16
	0.9	0.40	0.28	0.0	19.5			600		0.06	0.16	0.10	0.18
	0.8	0.42	0.29	0.0	19.5			610		0.06	0.14	0.11	0.19
	0.7	0.43	0.31	0.0	20.2			662		0.05	0.13	0.11	0.21
	0.6	0.45	0.33	0.0	21.2			731		0.04	0.11	0.12	0.23
Elasto- Plastic	0.5	0.47	0.34	0.0	22.2			850		0.04	0.09	0.12	0.25
	1.0	0.46	0.31			12.0	12.0		271	0.07	0.18	0.07	0.18
	0.9	0.47	0.33			12.0	11.0		248	0.06	0.16	0.08	0.20
	0.8	0.49	0.35			12.0	10.3		228	0.06	0.14	0.08	0.22
	0.7	0.51	0.37			12.0	9.8		2.6	0.05	0.13	0.08	0.24
Fully Plastic	0.6	0.53	0.39			12.0	9.3		212	0.04	0.11	0.09	0.26
	0.5	0.55	0.41			12.0	9.0		216	0.04	0.09	0.09	0.28
	1.0	0.46	0.31			12.0	12.0			0.07	0.18	0.07	0.18
	0.9	0.47	0.33			12.0	11.0			0.06	0.16	0.08	0.20
	0.8	0.49	0.35			12.0	10.3			0.06	0.14	0.08	0.22
	0.7	0.51	0.37			12.0	9.8			0.05	0.13	0.08	0.24
	0.6	0.53	0.39			12.0	9.3			0.04	0.11	0.09	0.26
	0.5	0.55	0.41			12.0	9.0			0.04	0.09	0.09	0.28

Note: Blank spaces indicate nonapplicability.

APPENDIX E

DESCRIPTION OF TUMBLING MAN COMPUTER PROGRAM

The tumbling man computer program computes the trajectory of a rigid body shelteree model (Figs. 5.1 through 5.3) located inside a shelter (with the blast doors open) and establishes the velocity experienced by the model upon impact with any prescribed obstacle (floor, end wall, ceiling). The loadings for the tumbling mass model are characterized by the lift, drag and point of application distances (L, D, δ, Δ) and are, in general, functions of time and the position of the mass center of gravity (x, y, θ). The program subroutines (FORCE and INPUT) define the loading related quantities for one particular shelter and one particular weapon size. These subroutines of course apply to any assumptions used in developing the loading (e.g., the one-dimensionality of the flow assumption). The program has been written with enough generality so that it may be used to solve other problems with different force loadings. For example, should a more refined two-dimensional flow field be developed, one would only have to replace the FORCE and INPUT subroutines; the remainder of the program would essentially be untouched.

E.1 COMPUTER PROGRAM DESCRIPTION

The overall computer program is composed of 16 program routines which may be grouped into the following 5 categories:

<u>Routine(s)</u>	<u>Function</u>	<u>Program Name</u>
1.	Overall coordinating of major program steps	MAIN
2.	Definition of tumbling man loading	FORCE INPUT
3.	Integration of governing equations of motion	FUN, FUN1, FUN2, FUN3, FUN4, FUN5, FUN6, FUN7, INTGVI, CRIT
4.	Program output control	PLOTS
5.	Auxiliary operations	MAXVEC, SGN

A flowchart (Fig. E.1) gives an overall view of the computational process. A listing of the subroutine, a description of the key program variable involved, and a description of the basic program input format are provided. The input required by the force calculations (called by subroutine INPUT) is not general and is to be regarded as special input needed by the FORCE subroutine only. Input descriptions for this latter data will therefore not be provided.

E.2 MAIN PROGRAM INPUT

The input cards and corresponding format required for the main program are given herein. All input cards relating to the particular FORCE and INPUT subroutine are normally placed directly behind the three cards specified below.

Card	Columns	Computer Variable	Text Variable	Description
1	1-10	H	h (ft)	Appropriate model height corresponding to Figs. 5.1, 5.2, 5.3
	11-20	D1	d_1 (ft)	Distance to center of gravity (see Fig. 5.4)
	21-30	FM	m (lb-sec ² /ft)	Man mass
	31-40	FI	\bar{I} (lb-sec ² -ft)	Man mass moment of inertia about center of gravity
	41-45	NTP		Number of integration time intervals if no constraints are hit (must be less than 200)
	46-55	FMULT		Multiplier on force duration (where the force time duration is supplied though the call argument of user supplied subroutine INPUT(TFINE;DUR). In other words this variable controls the time range of integration (TMAX) where $TMAX=FMULT*DUR$

*Note: TFINE is the value of time up to which a fine time integration is used. This value is to be supplied by the INPUT subroutine call argument.

2	1-10	S1	S_1 (ft)	Distance to center of gravity (see appropriate Fig. 5.1, 5.2, 5.3)
	11-20	S2	S_2 (ft)	Distance to center of gravity (see appropriate Fig. 5.1, 5.2, 5.3)
	21-30	TB (sec)		First time value used in argument of applied forces for the determination of loads which cause incipient motion (usually taken as zero)
	31-45	NTEE		Number of iterations used to determine force to cause incipient motion. (NZMAX-1 additional times to further refine the incipient starting time. NZMAX is a variable preset to 5.
	46-55	FMU		Coefficient of sliding friction for the man's contact points with the floor
	56-60	IPIV		Switch relating to the initial position configuration. For the initial position of standing and sitting, set IPIV=3; for the prone position set IPIV=2.
3	1-10	XHMAX	x_{\max} (ft)	Distance to hard constraint from initial position of man (e.g., see appropriate Fig. 5.1, 5.2, 5.3)
	11-20	XHMIN	x_{\min} (ft)	Same description as x_{\max}
	21-30	YHMAX	y_{\max} (ft)	Same description as x_{\max}
	31-40	YHMIN	y_{\min} (ft)	Same description as x_{\max}

All Cards Called
by Subroutine INPJT
are Stacked After Card 3

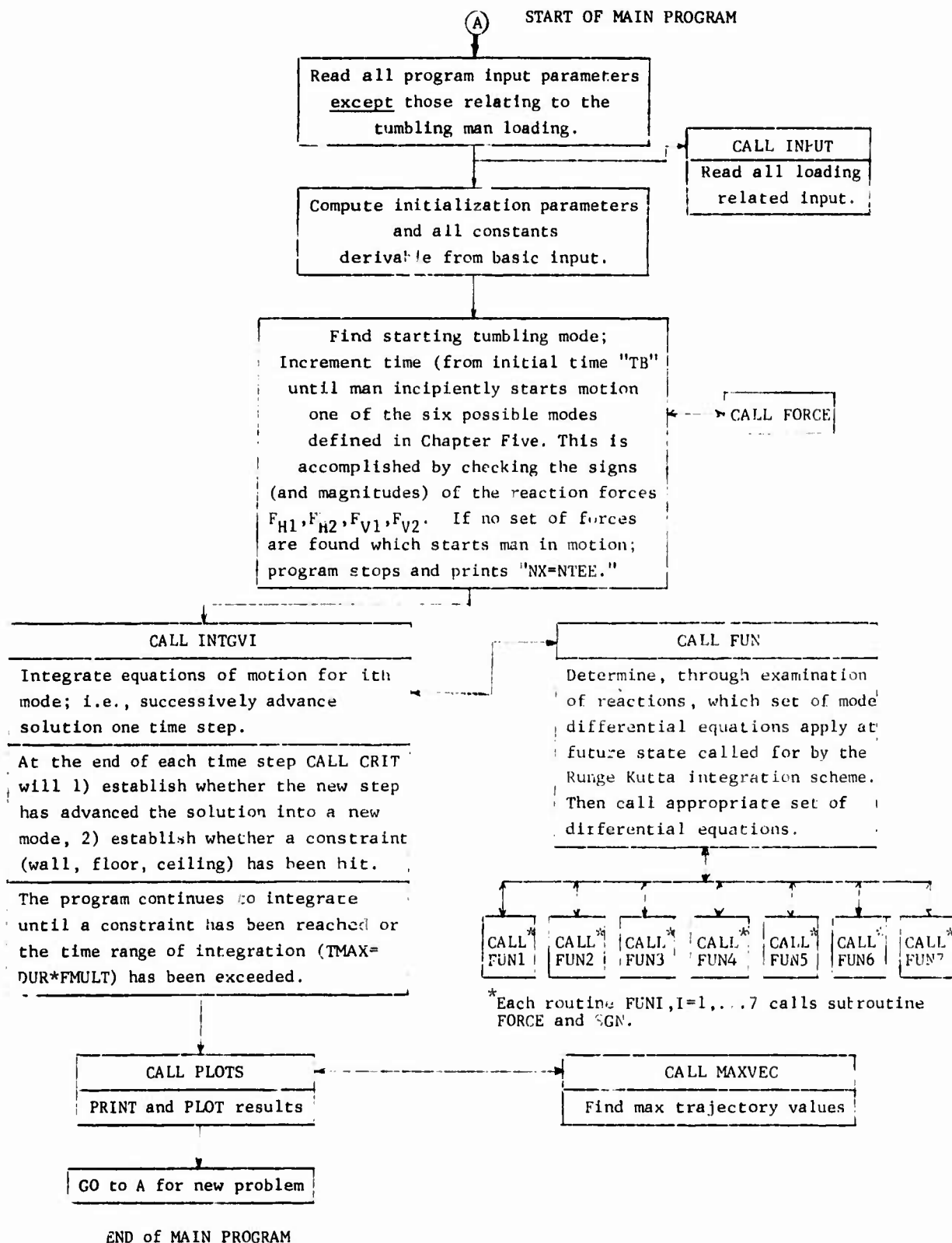


Fig. E.1 TUMBLING MAN COMPUTER PROGRAM FLOW CHART

E.3 PROGRAM OUTPUT

The first portion of the problem output is an echo printout of the input variables. In addition to these, the following variables are printed out:

TMAX = maximum time in seconds of the range of integration.

TFINE = the time value in seconds up to which a fine time integration interval is used. For example, large forces change rapidly during the shock diffraction phase, thus TFINE is taken as t_d in Fig. 5.7. The value is fed to the main program through the calling argument of INPUT.

TE = denoted as "time range for start cycle" on printout sheet. This value is the upper time value to which the search for the start of incipient motion is made. Currently this value is set equal to TFINE automatically in the program.

PH1D, PH2D = these angles refer to the test variables ϕ_1 and ϕ_2 of Fig. 5.4 and are measured in degrees.

Next a printout of the starting mode number and incipient forces FV1, FV2, FH1 (lbs) are printed in the respective order listed (the two numbers printed below these four numbers may be disregarded).

If a boundary constraint is reached, for example, if x_{\max} is exceeded, a notation reading "XHMAX EXCEEDED" is printed out. Similar printouts appear for the three other possible constraints. Following this heading the corresponding time of head impact (sec) and coordinates of the head at time of impact (ft) are printed. If this information is not printed, it means that the head did not hit any constraints over the time range specified by TMAX.

Next, "NONDIMENSIONAL VEL. AND DISP. FACTORS FOR CASE NPAGE" is printed out where NPAGE is the problem case number. Following this is a list of the factors used to nondimensionalize the velocity and displacement plots which come later. The horizontal head velocity trajectory is divided by VXTMAX; the vertical

head velocity is divided by VYTMAX, the horizontal head displacement is divided by UXTMAX, and the vertical head displacement is divided by UYTMAX.

Finally a listing of important trajectory information is given headed by the printout:

T UXF UYF UXT UYT VXT VYT VYF VFT VHZ MD

where:

T = time (sec). Note that the first time value is the time at which incipient motion starts.

UXF,UYF = Horizontal and vertical coordinates (in ft of the point B in Figs. 5.1 and 5.3 (when IPIV=3) or the coordinates point B1 in Fig. 5.2 (when IPIV=2).

UXT,UYT = Horizontal and vertical coordinates (in ft) of the point T in Figs. 5.1, 5.2 and 5.3.

VXT,VYT = Horizontal and vertical velocity (in fps) of the point T in Figs. 5.1, 5.2 and 5.3.

VYF = Vertical velocity (in fps) of variable UYF.

VFT,VHZ = Vertical and horizontal force (in lbs) of the applied lift and drag forces.

MD = integer number indicating mode of motion (Nos. 1 through 7). Mode numbers 1 through 6 are defined in Fig. 5.5 and Mode 7 indicates that the body has come to rest from a sliding position.

Finally plots of the type shown in Figs. 5.17 and 5.18 are produced which show the trajectories of the tumbling man. This plotting routine is a special program (subroutine ONEPLOT) and is obtainable from the Westinghouse Corporation. The plots are not essential to the operation of the program or the interpretation of results; thus, the call for these routines may be physically removed from the deck should the program be run on some other computer facility that does not possess the ONEPLOT option.

E.4 PROGRAM LISTINGS AND DESCRIPTIONS

The listings of the 16 subroutines which comprise the tumbling man program are presented. Brief descriptions of the operation of each subprogram and the key variables involved are given.

E.5 MAIN PROGRAM LISTING

The purpose of the main program is to control the overall logic flow for the problem solution. This routine reads and writes the problem input, computes the starting mode and calls the integration and plotting routines. The key variables for this routine are the input variables which have already been described in detail in the problem input discussion given earlier in this appendix.

```
C
C   MAIN PROGRAM
C
COMMON/FSBT/IFSET
COMMON/GR1E/IZIONCL
COMMON/INTOW/ISW
COMMON/PAGE/ZPAGE
COMMON/IRISS/ITRIS
COMMON/BOUND/XMAX,XMIN,YMAX,YMIN
COMMON/EDRSW/IEDRSW
COMMON/ZBL AT/100,1,PRSD,LD,TC
COMMON/ALDOM/IRISE
COMMON/ADJUV/100F(200)
COMMON/XPAST/XP(15)
DIMENSION XOU(15),CV(20)
COMMON/MODE/MOD,NL,10
COMMON/DATT/FINP,H,D1,D2,F4,FI,NTP,IMULT,DELO,S1,S2,TR,NTEF,UT1,IN
XAX,TE,P1,PH2,R1,R2,D3,GRV,F4U,IPIV
NPAGE=0
ITRIS=0
2 READ(5,25)      H,D1,FM,FI,NTP,IMULT,      S1,S2,TR,NTEF,      FMU
X,IPIV
IDRNT=IPIV
25 FORMAT(4E10,5,15,E10,5/3E10,5,115,E10,5,15)
READ(5,740)XMAX,XMIN,YMAX,YMIN
740 FORMAT(4E10,5)
C
C   CALL INPUT FOR BLAST ROUTINE
C   CALL INPUT(TFINF,DUP)
C
```

Reproduced from
best available copy.

```

C      INITLIZE
C
      IFORSW=0
      ISA=0
      IFSET=1
      NDE=6
      NTP=NTIP
      PH1=ATAN(S1/D1)
      PH1D=PH1*180./3.14159
      PH2=ATAN(S2/D1)
      PH2D=PH2*180./3.14159
      R1=S1/SIN(PH1)
      NL=1
      R2=S2/SIN(PH2)
      GRV=32.2
      D2=D1
      D3=H-D1
      XP(1)=0.0
      DURRX=DUR/10.
      CALL FORCE(DURRX,S1,D1,0.0,4,D1,S1,S2,FTDUR,HTDUR,DELX,DELHY)
      FIMP=.5*DUR*FTDUR
      IMAX=DUR*FMULT
      TE=TFINE
      WRITE(6,26)      H,D1,      FM,F1,NTIP,FMULT,      S1,S2,TR,NTEE,NTI
26  FORMAT(140,      //
X      1X,'MAN HEIGHT='E16.8//
X      1X,'DISTANCE TO C.G. (D1)='E16.8//
X      1X,'MAN MASS='E16.8//
X      1X,'MAN MASS MOMENT OF INERTIA='E16.8//
X      1X,'NO. PLOT POINTS='E15.8//
X      1X,'TIME RANGE MULTIPLY FACTORS='E16.8//
Y      1X,'S1='E16.8//
X      1X,'S2='E16.8//
X      1X,'START TIME FOR START CYCLE='E16.8//
X      1X,'NO.OF START CYCLE POINTS='E13.8//
X      1X,'NO. OF TOTAL INTEGRATION TIME STEPS='E15.8// )
      WRITE(6,27)
      XIMAX,TE,PH1D,PH2D,FMD,TFINE,DUR,IPIV
27  FORMAT(1X/
X      1X,'TIME RANGE OF INTEGRATION='E16.8//
X      1X,'TIME RANGE FOR START CYCLE='E16.8//
X      1X,'PH1D='E16.8//
Y      1X,'PH2D='E16.8//
X      1X,'COEF.OF FRICTION='E16.8//
X      1X,'TFINE='E16.8//
X      1X,'INPUT FORCE DURATION='E16.8//
X      1X,'IPIV IS AN INITIAL ORIENTATION CODE='E15.8//)
      WRITE(6,741)XHMAX,XHMIN,YHMAX,YHMIN
741  FORMAT(1X,' HORIZONTAL DISPLACEMENT MAX BOUND='E16.8//
1      1X,' HORIZONTAL DISPLACEMENT MIN BOUND='E16.8//
1      1X,' VERTICAL DISPLACEMENT MAX BOUND='E16.8//
1      1X,' VERTICAL DISPLACEMENT MIN BOUND ='E16.8////////)
C
C      FIND STARTING MODE, AND STARTING TIME TC , **PASS HERE ONCE

```



```

NZMAX=5
DO 200 NZ=1,NZMAX
DLL=(TE-TB)/FLOAT(NTEE)
T=TB-DLL
DO 20 NX=1,NTEE
T=T+DLL
CALL FORCE(T,S1,D1,0.0,H,D1,S1,S2,FT,HT,DEL,DELH)
FV1=(FM*GRV*S2-(DEL+D1)*FT)/(S1+S2)-HT*(S2+DELH)/(S1+S2)
FV2=FM*GRV-FV1-HT
FH1=-FT*.5
DL1=FMU*FV1-ABS(FH1)
DL2=FMU*FV2-ABS(FH1)
CHECK LIFT (MOD=1)

C
C
IF(FV1.LT.0.0.AND.FV2.LT.0.0) GO TO 11
C
SLIDE OR LOCK
IF(FV1.GE.0.0.AND.FV2.GE.0.0)GO TO 12
C
C
NEXT , EITHER FV1 OR FV2 IS NEG. ROT OR SLIDE + ROT CASES
C
IF(FV1.LT.0.0) GO TO 15
C
C
THUS FV2 IS NEG. WILL PIVOT ON END B1, DL1 PLUS IMPLYS LOCK
C
SLIDE OF B1
C
IF(DL1.GE.0.0) GO TO 17
MOD=6
TO=T
GO TO 10
C
C
AT , WE HAVE LIFT
C
11 MOD=1
TO=T
GO TO 10
C
C
CHECK SLIDE OR LOCK DL1 OR DL2 PLUS IMPLYS LOCK OF THAT POINT
C
12 IF(DL1.GE.0.0.OR.DL2.GE.0.0) GO TO 13
C
PASSED TEST 12, THEREFORE DL1 AND DL2 BOTH NEG.,THEREFORE SLIDES
MOD=2
TO=T
GO TO 10
C
LOCKED,THEREFORE MOD=7, CYCLE TO NEXT TIME
13 MOD=7
GO TO 20
C
PIVOT ON END B2 , DL2 PLUS IMPLYS LOCK SLIDE OF B2
15 IF(DL2.GE.0.0) GO TO 16
MOD=5
TO=T
GO TO 10
16 MOD= 3
TO=T
GO TO 10

```



C AT 17, WILL ROT. ONLY

```
17 MOD =4
   TO=T
   GO TO 10
20 CONTINUE
   IF(NX.EQ.NTEE) GO TO 21
10 CONTINUE
   GO TO 32
21 WRITE(6,30)
30 FORMAT(1X,'***** NX=NTEE',///)
   STOP
32 CONTINUE
   IE=TO+DLL
   IF(TO-DLL.GT,0.0)GO TO 700
   TB=0.0
   GO TO 701
700 TB=TO-DLL
701 CONTINUE
200 CONTINUE
   IF(TO.LT,1.0001+DLL)TO=1.0
```

C
C NOW WE HAVE MOD AND TO
X00(1)=0.0
X00(2)=0.0
X00(3)=81
X00(4)=0.0
X00(5)=01
X00(6)=0.0

C
C INITIALIZE A PAST VECTOR
C

```
DO 420 JL=1,NDE
420 XP(JL)=X00(JL)
   XP(7)=FV1
   XP(8)=FH1
   XP(9)=FV2
   XP(10)=FH1
   XP(11)=0.0
   XP(12)=0.0
   WRITE(6,100)MOD,FV1,FV2,FH1,DL1,DL2
100 FORMAT(1X,///1X,'MOD,FV1,FV2,FH1,DL1,DL2 =',15,2X,3(E16.8,2X)///1X,2
X(15,8,2X)///)
   MODE(1)=MOD
   NTIF=N+1/10 +1
```

C
CALL INTGV1(TMAX,TO,X00,NDE,NT1,OV,TFINE,NTIFIN)
CALL PLOTS
GO TO 2
END



E.5.1 Subroutines FORCE and INPUT Listings

The blast loading experienced by a shelteree is estimated by means of the two subroutines discussed herein. The first of these, INPUT, reads the airblast parameters and geometric variables of the problem. These include such items as blast wave pressure, shock pressure in the shelter, maximum drag and lift area, initial position and area of the shelteree, etc. Also read are complete tables of the average and maximum jet velocities at seven shelter locations (distances from the entrance, at specific times during the filling process). The subroutine computes all required shock parameters and initial jet values such as velocities and dynamic pressures.

The second subroutine, FORCE, performs the actual load calculations. No inputs are read in this subroutine and it communicates with the subroutine INPUT via block common. The computations performed by subroutine FORCE are those outlined in Chapter Five and include estimates of the shock diffraction and drag phase loads. The latter are obtained by interpolation in the velocity and cavity density tables for the appropriate time and position. The key variables appearing in the calling arguments of FORCE and INPUT are listed as follows:

<u>Computer Variable</u>		<u>Text Variable</u>	<u>Description</u>
FORCE Call Arguments	T	t	Integration time
	XCG	x(t)	Horizontal distance to man center of gravity (see Fig. 5.4)
	YCG	y(t)	Vertical distance to man center of gravity (see Fig. 5.4)
	TCG	$\theta(t)$	Angular rotation of man mass (see Fig. 5.4)
	H,D1,S1,S2	h,d_1,s_1,s_2	Dimensions of man model (see Fig. 5.4)
	FT,HT	D,L	Drag and lift respectively
	DEL,DELH	Δ,δ	Points of application of drag and lift (see Fig. 5.4)

INPUT Call
Arguments

TFINE

Time range over which fine time interval intergration applies. TFINE was taken as t_d in Fig. 5.7 in this particular subroutine.

DUR

Time duration over which forces act

The input variables read by the subroutine INPUT are given by:

Computer Variable

Description

LVEL

T - Load based on maximum velocity
F - Load based on average velocity

NTIME

Number of time data points for load determination

DPB

Blast wave overpressure, psi

DPS

Shock overpressure in shelter

UEO

Entrance velocity at $t = 0$

DIA

Diameter of shelteree

APR

Projected area in initial position

ALMAX

Maximum lift area

ADMAX

Maximum drag area

ADMIN

Minimum drag area

BE

Half-width of entrance

XXCO

Initial position of center of gravity to entrance

XP(I)

Shelter position for load determination

TT(I)

Time data points for load determination

DC(I)

Chamber densities at times TT(I)

UU(I,J)

Average jet velocities at position X(I) and time TT(J)

UUM(I,J)

Maximum jet velocities at position X(I) and time TT(J)

```

SUBROUTINE FORCE(T,XCG,YCG,TCG,H,D1,S1,S2,FT,HT,DEL,DELH)
COMMON /AIRRL/ XP(7),TI(21),DC(21),V(7,21),NTIME,UPM,APR,BE,
1 ALMAX,ADMAX,ADMIN,XX0,TJET,TRISE,TDFR,QJET,QDFR
COMMON/FORSW/IFORSW
COMMON /ORIENT/ IORNT
THETA=TCG
SIGMA=TCG
IF(IORNT.EQ,2) SIGMA=SIGMA+1.57079
XX=XX0+XCG/BE
IF(T.LT.TDFR) GO TO 470
IF(T.LT.TJET) GO TO 425
IF(T.GT.T(NTIME)) GO TO 499
DO 405 I2=2,7
IF(XX.GT.XP(I2)) GO TO 405
I1=I2-1
GO TO 410
405 CONTINUE
IF(XX.GT.XP(7)) GO TO 499

410 DO 420 K2=2,NTIME
IF(T.GT.TI(K2)) GO TO 420
K1=K2-1
DXX=(XX-XP(I1))/(XP(I2)-XP(I1))
V1=V(I1,K1)+DXX*(V(I2,K1)-V(I1,K1))
V2=V(I1,K2)+DXX*(V(I2,K2)-V(I1,K2))
DTI=(T-TI(K1))/(TI(K2)-TI(K1))
VV=V1+DTI*(V2-V1)
DD=DC(K1)+DTI*(DC(K2)-DC(K1))
Q=0.5*DD*VV*VV
GO TO 430
420 CONTINUE
425 Q=QDFR+(T-TDFR)*(QJET-QDFR)/(TJET-TDFR)
430 AD=ADMIN+(ADMAX-ADMIN)* SIN(SIGMA-1.57079) **2
AL=ALMAX*SIN(2.*SIGMA-3.14159)
FT=G*AL
HT=Q*AL
GO TO 490
470 HT=0.
IF(T.LT.TRISE) GO TO 472
QDRG=QDFR*ADMAX/APR
Q=UPM+(T-TRISE)*(QDRG-UPM)/(TDFR-TRISE)
GO TO 472
472 Q=1*QDFR/TRISE
475 FT=G*APR
490 DEL=(H/2.-D1)*COS(THETA)+(S1-S2)*SIN(THETA)/2.
DELH=0.
IF(IFORSW.NE,0) GO TO 2121
FPAST=FT
HPAST=HT
2121 CONTINUE
RETURN
495 FT=FPAST
HT=HPAST
IFORSW=1
GO TO 490
499 FT=0.0
HT=0.0
GO TO 490
END

```



```

SUBROUTINE INPUT(TFINE,DUR)
COMMON /TRIGSW/ITRIG
COMMON /AIRRL/ XP(7),TT(21),DC(21),V(7,21),NTIME,DPM,APR,RE,
1      ALMAX,ADMAX,ADMIN,XX0,TJET,TRISE,TDFR,QUET,QDFR
COMMON /ORIENT/ IORNT
DIMENSION UU(7,21),UUJ(7,21)
LOGICAL LEVEL
PB=14.7
DB=0.0025264
CB=1120
GAN=1.4
FMU=6.
READ(5,501) LEVEL,VTIME,DPA,DPS,QED
501 FORMAT (L5,I5,3F10.4)
READ(5,505) DIA,APR,ALMAX,ADMAX,ADMIN,RE,XXCGO
505 FORMAT (7L10.4)
PR=DPS/PB+1.
DS=DB*(1.+6.*PR)/(6.+PR)
US=5.*(PR-1.)/SQRT(7.*(1.+6.*PR))*CB
VS=CB*SQRT((1.+6.*PR)/7.)
IF(IORNT.LE.2) GO TO 5
DP=144.*(1.7+).023*DPS)*DPS
TRISE=DIA/VS/2.
TDFR=5.*DIA/VS
GO TO 8
3 DP=144.*(DP+DPS)*(4.*PR-1.)/(6.+PR)
TRISE=0.000001
TDFR=6./VS
8 CONTINUE
IF(ITRIG.EQ.1) GO TO 825
READ(5,505) (XP(I),I=1,7)
READ(5,505) (TT(I),I=1,NTIME)
READ(5,505) (DC(I),I=1,NTIME)
READ(5,505) ((UU(I,J),I=1,7),J=1,NTIME)
READ(5,505) ((UUJ(I,J),I=1,7),J=1,NTIME)
825 ITRIG=1
XX0=XXCGO/AF
IG=10 I=2.7
L=1-1
IF(XX0.GT.XP(1)) GO TO 10
QUJ=QU(I,1)+(XX0-XP(L))*(QU(I,1)-QU(L,1))/(XP(1)-XP(L))
QU=QUJ
IF(LEVEL) GO TO 20
QUJ=QU(I,1)+(XX0-XP(L))*(QU(I,1)-QU(L,1))/(XP(1)-XP(L))
GO TO 20
10 CONTINUE
20 TJET=XX0/(4.-0.5*(QU+QUJ))
VJET=0.5*3600*IS
TJET=0.5*3600*QUJ*QUJ
DO 30 I=1,7
DO 30 J=1,NTIME
V(2,J)=QU(I,J)
IF(LEVEL) V(1,J)=QUJ(I,J)
30 CONTINUE
TFINE=TJET
DUR=TT(TFINE)
RETURN
END

```



E.5.2 Subroutine INTGVI Listing

The purpose of the subroutine INTGVI is to integrate the governing equations of motion by means of a fourth order Runge-Kutta integration algorithm. The routine is capable of handling two integration regions. In the first (from $t = T_0$ to $t = T_{\text{FINE}}$) a fine integration interval is used where NT_{IFINE} time steps are employed. In the second region (from $t = T_{\text{FINE}}$ to $t = T_{\text{MAX}}$) a courser interval is used where $NTI - NT_{\text{IFINE}}$ time steps are employed. The variable NTI refers to the total number of prescribed time steps in the overall integration process.

The call arguments for INTGVI are:

<u>Computer Variable</u>	<u>Description</u>
TMAX	Maximum time range of integration
T0	Starting time for integration
X00(I), I=1,...6	Vector of initial conditions for integration variables
NDE	Number of first order differential equations (six in our type of problem)
NTI	Total number of integration time steps
CV()	Storage vector (not used here)
TFINE, NTIFINE	(See written description of INTGVI above)

The key variable in the routine is the solution at each time step and is denoted by $XN(JJ)$ $JJ=1,...,6$ where the following correspondence can be made between the text notation of Chapter Five and the $XN(JJ)$ variables:

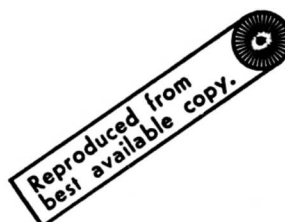
$$\begin{aligned} XN(1) &\equiv x_1 \\ XN(2) &\equiv x_2 \\ XN(3) &\equiv x_3 \\ XN(4) &\equiv x_4 \\ XN(5) &\equiv x_5 \\ XN(6) &\equiv x_6 \end{aligned}$$

The two important subroutines that communicate with INTGVI are FUN and CRIT which are described in the next set of listings.

```

SUBROUTINE INTGVI(TMAX,TO,X00,NDE,NTI,CV,TFINE,NTIFIN)
C
C RUNGE-KUTTA 4TH ORDER INTEGRATION PROCESS
C
COMMON/INTSW/ISW
DIMENSION X0(15),XN(15),X00(15),CV(20),FK1(15),FK2(15),FK3(15),
XFK4(15),X01ST(15),X02ST(15),X03ST(15)
C
C SET INITIAL VALUES FOR T, XN, AND FK1
C
IF(NTIFIN.EQ.0) GO TO 10
H=(TFINE-TO)/FLOAT(NTIFIN)
GO TO 11
10 H=(TMAX-TO)/FLOAT(NTI)
11 DO 2 K=1,NDE
2 XN(K)=X00(K)
T=TO
CALL FUN(TO,X00,FK1,CV)
C
C END INITIALIZATION
C
DO 1 JJ=1,NTI
DO 3 L=1,NDE
X0(L)=XN(L)
3 X01ST(L)=FK1(L)*H*.5 + X0(L)
T1ST=T+H*.5
CALL FUN(T1ST,X01ST,FK2,CV)
DO 4 M=1,NDE
4 X02ST(M)=FK2(M)*H*.5 + X0(M)
T2ST=T1ST+H*.5
CALL FUN(T2ST,X02ST,FK3,CV)
DO 5 N=1,NDE
5 X03ST(N)=FK3(N)*H + X0(N)
T3ST=T + H
CALL FUN(T3ST,X03ST,FK4,CV)
DO 6 JJ=1,NDE
6 XN(JJ)= X0(JJ)+ H*(FK1(JJ)+2.*FK2(JJ) + 2.*FK3(JJ)+FK4(JJ))/6.
C SET NEW TIME INCREMENT FOR NEXT STEP IN SOLUTION
IF(NTIFIN.EQ.0) GO TO 12
IF(JJ.GE.NTIFIN) H=(TMAX-TFINE)/FLOAT(NTI-NTIFIN)
12 T=T3ST
C SET NEW VALUE FOR FK1 FOR NEXT STEP IN SOLUTION
CALL FUN(T,XN,FK1,CV)
C FK1 IS NOW XNDOT
CALL CRIT(XN,X0,FK1,CV,T)
IF(ISW.EQ.1) GO TO 14
C GO ON TO CALCULATE NEXT TIME STEP IN SOLUTION
1 CONTINUE
14 RETURN
END

```



E.5.3 Subroutine FUN Listing

The purpose of the FUN subroutine (in conjunction with subroutines FUN1, FUN2, FUN3, FUN4, FUN5, FUN6, and FUN7) is to decide which of the six sets of equations (given in Chapter Five) is applicable, and then to compute the right-hand side of the appropriate set (for prescribed values of x_1 , x_2 , x_3 , x_4 , x_5 and x_6). The right-hand side of the set (actually the first derivatives of x_1 , x_2 , x_3 , x_4 , x_5 , x_6) are used in various places in the tumbling man program, in particular in INTGVI and CRIT.

A test is made at the beginning of the program to see what the previous mode of motion was in the last time step. Based on this fact, certain invalid modes are ruled out for the next step. For example, we can pass from mode 3 to mode 1 but not from mode 1 to mode 3. The latter combination would involve impacting a constraint. The program cannot proceed beyond the first contact with a surface and would automatically stop integrating upon reaching the constraint. The FUN calling arguments are:

<u>Computer Variable</u>	<u>Description</u>
T	Dummy integration time
X(J), J=1,...6	Correspond to text variables $x_1(t)$, $x_2(t)$, $x_3(t)$, $x_4(t)$, $x_5(t)$, $x_6(t)$ evaluated at $t=T$
FON(J), J=1,...6	Corresponds to right-hand side of the appropriate set of mode equations of Chapter Five, Eqs. (5.3) through (5.8)
FON(J), J=7,...12	The locations of FON from 7 to 12 are stored as a storage vector for transferring the following values: FON(7) = F_{V1} , FON(8) = F_{H1} FON(9) = F_{V2} , FON(10) = F_{H2} FON(11) = \dot{x}_{B2} , FON(12) = \dot{x}_{B1}
G(K), K=1,20	Storage vector (not used)

```

SUBROUTINE FUN(T,X,FON,G)
COMMON/XPAST/XP(15)
DIMENSION X(15),FON(15),G(20)
COMMON /MODE/MOD,NL,TO
COMMON/DATT/FIMP,H,D1,D2,FM,FI,NTP,IMULT,DELO,S1,S2,TR,NTEE,NT1,FM
XAX,TE,PH1,PH2,RL,P2,D3,GRV,F10,IPIV

```

```

C
C   SET PROPER BRANCH *****
C

```

```

CALL FORCE(T,X(3),X(5),X(1),4,D1,S1,S2,FT,HT,DEL,DELH)
GO TO (1,2,3,4,5,6,7),MOD

```

```

C   LOGIC FROM STATE MOD=1 *****

```

```

1 CALL FUN1(FON,X,T)

```

```

C   END MOD=1 LOGIC *****

```

```

RETURN

```

```

C   LOGIC FROM STATE MOD=2 *****

```

```

2 CALL FUN2(FON,X,T)

```

```

UXCDDT=FON(3)

```

```

SG=SGN(UXCDDT)

```

```

FV1=FON(7)

```

```

FV2=FON(9)

```

```

IF(FV1.GT.0.0.AND.FV2.GT.0.0)GO TO 40

```

```

IF(FV1.LE.0.0.AND.FV2.LE.0.0)GO TO 81

```

```

IF(FV1.LE.0.0)GO TO 82

```

```

IF(UXCDDT*(P(4).GT.0.0)GO TO 84

```

```

IF(SG*FV0*FV1.LT.FT)GO TO 84

```

```

CALL FUN4(FON,X,T)

```

```

RETURN

```

```

80 IF(UXCDDT*XP(4).GT.0.0)RETURN

```

```

IF(SG*FV0*(FV1+FV2).LT.FT)RETURN

```

```

CALL FUN7(FON,X,T)

```

```

RETURN

```

```

C   FUN2 IMPLIED WITH RETURN 80

```

```

81 CALL FUN1(FON,X,T)

```

```

RETURN

```

```

82 IF(UXCDDT*XP(4).GT.0.0)GO TO 85

```

```

IF(SG*FV0*FV2.LT.FT)GO TO 85

```

```

CALL FUN3(FON,X,T)

```

```

RETURN

```

```

85 CALL FUN5(FON,X,T)

```

```

RETURN

```

```

84 CALL FUN6(FON,X,T)

```

```

RETURN

```

```

C   END LOGIC FROM MOD=2 *****

```

```

C   LOGIC FROM STATE MOD=3 ***

```

```

3 CALL FUN3(FON,X,T)

```

```

FV2=FON(9)

```

```

FV2=FON(10)

```

```

IF(FV2.GT.0.0)GO TO 90

```




```

      CALL FUN1(FON,X,T)
      RETURN
90 IF(FH2.GT.-FV2*FV2.AND.FH2.LT.FV2*FV2)
  XRETURN
C
C   RETURN AT 90 IMPLYS FUN=FUN3
C
      CALL FUN3(FON,X,T)
      RETURN
C
C   END LOGIC FROM MOD=3 ****
C
C   LOGIC FROM STATE MOD=4 ****
C
4  CALL FUN4(FON,X,T)
  FV1=FON(7)
  FH1=FON(8)
  IF(FV1.GT.0.0)GO TO 92
  CALL FUN1(FON,X,T)
  RETURN
92 IF(-FMJ*FV1.LT.FH1.AND.FH1.LT.FM1*FV1)
  XRETURN
C   RETURN AT 92 IMPLYS FUN=FUN4
      CALL FUN6(FON,X,T)
      RETURN
C
C   END LOGIC FROM MOD=4 ****
C
C   LOGIC FROM MOD=5 ****
C
5  CALL FUN5(FON,X,T)
  FV2=FON(9)
  FH2=FON(10)
  UXB2DT=FON(11)
  SG=SGN(UXB2DT)
  IF(FV2.GT.0.0)GO TO 95
  CALL FUN1(FON,X,T)
  RETURN
95 IF(XP(11)*UXB2DT.GT.0.0)RETURN
  IF(SG*FV2*FV2.LT.FT)RETURN
C
C   RETURN AT 95 IMPLYS FUN=FUN5
C
      CALL FUN3(FON,X,T)
      RETURN
C
C   END LOGIC FROM MOD=5 ****
C
C   LOGIC FROM MOD=6 ****
C
6  CALL FUN6(FON,X,T)

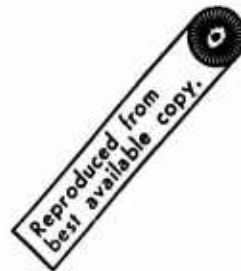
```



```

FV1=FON(7)
FV2=FON(8)
UB1XDT=FON(12)
SG=SGN(UB1XDT)
IF(FV1.GT.0.0)GO TO 96
CALL FUN1(FON,X,T)
RETURN
96 IF(XP(12)*UB1XDT.GT.0.0)RETURN
IF(SG*FV2*FV1.LT.FT )RETURN
C
C RETURN 96 IMPLYS FON=FON6
C
C CALL FUN4(FON,X,T)
C RETURN
C
C END LOGIC FROM MOD=6 ****
C
C LOGIC FROM MOD=7
C
C 7 CALL FUN7(FON,X,T)
C RETURN
C
C END LOGIC FROM MOD=7
C
C END

```



E.5.4 Subroutines FUN1 through FUN7 Listings

This group of seven subroutines computes the right-hand side of Eqs. (5.3) through (5.8) (i.e., $FON(J), J=1,12$) given the values $X(K), K=1,6$ at time T . The calling arguments of a typical subroutine in this group are:

<u>Computer Variable</u>	<u>Description</u>
T	Dummy variable for time
X(K), K=1,6	Corresponds to text variables $x_1(t), x_2(t), x_3(t), x_4(t), x_5(t), x_6(t)$ evaluated at $t = T$
FON(J), J=1,12	(See description for FUN subroutine)
G(I), I=1,20	Storage vector (not used)

Subroutine FUN1 corresponds to the right side of Eq. (5.3); FUN2 to Eq. (5.4); FUN3 to Eq. (5.5); FUN4 to Eq. (5.6); FUN5 to Eq. (5.7); FUN6 to Eq. (5.8); and FUN7 is a routine which is employed if the man comes to rest (it has no text equation correspondence) which simply states that all future velocities are zero.

```

SUBROUTINE FUN1(F,X,T)
COMMON/DATT/FIMP,H,D1,D2,F,FI,TP,IMULT,DELO,S1,S2,TB,NTEE,NT1,TH
XAX,TE,PH1,PH2,R1,R2,D3,GRV,FMU,IPIV
DIMENSION F(15),X(15)
CALL FORCE(T,X(3),X(5),X(1),H,D1,S1,S2,FT,HT,DEL,DELM)
F(1)=X(2)
F(2)=(DEL*FI+HT*DELM)/FI
F(3)=X(4)
F(4)=FT/PM
F(5)=X(6)
F(6)=-GRV+HT/PM
RETURN
END

```



```

SUBROUTINE FUN2(F,X,T)
COMMON/DATT/FIMP,H,D1,D2,FM,FI,TP,IMULT,DELO,S1,S2,TB,NTEE,NT1,TH
XAX,TE,PH1,PH2,R1,R2,D3,GRV,FMU,IPIV
DIMENSION F(15),X(15)
CALL FORCE(T,X(3),X(5),X(1),H,D1,S1,S2,FT,HT,DEL,DELM)
HD=HT*DELM
F(1)=0.0
F(2)=0.0
F(3)=X(4)

```

```

FV1=((FM*GRV-HT)*(S2-FMU*D1*SGN(X(4)))-(FT*DEL+HD))/(S1+S2)
FV2=FM*GRV-FV1-HT
F(4)=(FT-FMU*FV1*SGN(X(4))-FMU*FV2*SGN(X(4)))/FM
F(5)=0.0
F(6)=0.0
F(7)=FV1
F(8)=FV2
RETURN
END

```

Reproduced from
best available copy.

```

SUBROUTINE FUN3(F,X,I)
COMMON/DA17/FIMP,H,D1,D2,F1,F2,TP,INULT,DEL0,S1,S2,TR,NTER,NTI,IN
XAX,TE,PH1,PH2,R1,R2,D3,GRV,FMU,IPIV
DIMENSION F(15),X(15)
CALL FORCE(T,X(3),X(5),X(1),H,D1,S1,S2,F1,HT,DEL,DELH)
HD=HT*DELH
P=PH2-X(1)
SP=SIN(P)
CP=COS(P)
F(1)=X(2)
F(2)=(FT*(DEL+S2*CP)+HI-(FM*GRV-HT)*H2*SP)/(F1+FM*R2*H2)
F(3)=X(4)
F(4)=R2*CP+F(2)+H2*X(2)*X(2)*SP
F(5)=X(6)
F(6)=R2*F(2)*SP-R2*X(2)*X(2)*CP
F(7)=FV2 AND F(8)=FH2
F(9)=F1+(R2*F(2)*SP-H2*F(1)*F(1)*CP)+FM*GRV-HT
F(10)=F2+(R2*F(2)*CP+H2*F(1)*F(1)*SP)-FT
RETURN
END

```

```

SUBROUTINE FUN4(F,X,I)
COMMON/DA17/FIMP,H,D1,D2,F1,F2,TP,INULT,DEL0,S1,S2,TR,NTER,NTI,IN
XAX,TE,PH1,PH2,R1,R2,D3,GRV,FMU,IPIV
DIMENSION F(15),X(15)
PT=PH1+X(1)
CALL FORCE(T,X(3),X(5),X(1),H,D1,S1,S2,F1,HT,DEL,DELH)
HD=HT*DELH
CPT=COS(PT)
SPT=SIN(PT)
F(1)=X(2)
F(2)=(FT*(DEL+R1*CPT)+HD+(FM*GRV-H1)*R1*SPT)/(F1+FM*R1*R1)
F(3)=X(4)
F(4)=F(2)*R1*CPT-R1*X(2)*X(2)*SPT
F(5)=X(6)
F(6)=-F(2)*R1*SPT-R1*X(2)*X(2)*CPT
F(7)=FV1 AND F(8)=FH1
F(9)=F1+(-F(2)*R1*SPT-R1*F(1)*F(1)*CPT)+FM*GRV-HT
F(10)=FM*(F(2)*R1*CPT-R1*F(1)*F(1)*SPT)-FT
RETURN
END

```

```

SUBROUTINE FUN5(F,X,T)
COMMON/DAT1/FIMP,H,D1,D2,F1,F1,NTP,IMULT,DELO,S1,S2,TB,NTEE,NT1,T
XAX,TE,PH1,PH2,R1,R2,D3,GRV,FMU,IPIV
DIMENSION F(15),X(15)
CALL FORCE(T,X(3),X(5),X(1),H,D1,S1,S2,FT,HT,DEL,DELH)
HD=HT*DELH
HBH=HT/FM
P = PH2-X(1)
SP=SIN(P)
CP=COS(P)
UDXB2= X(4)-R2*X(2)*CP
F(1)=X(2)
F(2)=(FT *DEL +HD + FM*(-R2*X(2)*X(2)*CP+GRV-HB* )*(R2
X*CP*SGN(UDXB2)*FMU -R2*SP))/(F1-FM*R2*R2*SP*(CP*SGN(UDXB2)*FMU-SP)
X)
F(5)=X(6)
F(6)=-R2*X(2)*X(2)*CP +R2*SP*F(2)
F(3)=X(4)
F(4)=(FT -SGN(UDXB2)*FMU*(FM*F(6)+GRV*FM -HT))/FM
F(9)=FM*(F(6)+GRV) -HT
F(10)=-SGN(UDXB2)*FMU*(F(6)+FM*GRV-HT)
F(11)=UDXB2
RETURN
END

```

```

SUBROUTINE FUN6(F,X,T)
COMMON/DAT1/FIMP,H,D1,D2,F1,F1,NTP,IMULT,DELO,S1,S2,TB,NTEE,NT1,T
XAX,TE,PH1,PH2,R1,R2,D3,GRV,FMU,IPIV
DIMENSION F(15),X(15)
CALL FORCE(T,X(3),X(5),X(1),H,D1,S1,S2,FT,HT,DEL,DELH)
HD=HT*DELH
HBH=HT/FM
PT=PH1+ X(1)
SPT=SIN(PT)
CPT=COS(PT)
SG =SGN( X(4)-X(2)*R1*CPT)
F(1)=X(2)
F(2)=(FT *DEL+HD+FM*(-X(2)**2 *R1*CPT+GRV-HB* )*(R1*CPT+R1*SPT+SG*
X*FMU)+.0 )/(F1+ FM*R1*R1*SPT*(CPT+SPT*SG*FMU))
F(5)=X(6)
F(6)=-X(2)*X(2)*R1*CPT -F(2)*R1*SPT
F(3)=X(4)
F(4)=(FT -SG*FMU*(FM*F(6)+FM*GRV-HT) )/FM
C
C
C
F(7)= FM1 AND F(8)= FM1 AND F(9)= UR1*DT
F(7)=FM*(F(6)+GRV) -HT
F(8)=-SG*FMU*(FM*F(6)+FM*GRV-HT )
F(12)= X(4)-X(2)*R1*SPT
RETURN
END

```



```

SUBROUTINE FUN7(F,X,T)
DIMENSION F(15),X(15)
F(1)=0.0
F(2)=0.0
F(3)=0.0
F(4)=0.0
F(5)=0.0
F(6)=0.0
RETURN
END

```

E.5.5 Subroutine CRIT Listing

The subroutine CRIT is called at the end of each time step in the integration process. The routine checks the reactions (using the past mode equations) to determine if a transition from one mode to another has taken place. Also the trajectory coordinates of the center of gravity are converted into head trajectory coordinates to determine whether a constraint (floor, ceiling, wall) has been exceeded. If a constraint is reached, the problem stops integrating and returns to the main program for the execution of the print and plotting routines.

The calling arguments of CRIT are

<u>Computer Variable</u>	<u>Description</u>
XN(K),K=1,...6	Advanced time step solution for the unknowns $x_1(t+\Delta t)$, where $x_1 \dots x_6$ are the differential equations unknown
XO(K),K=1,6	Vector of initial conditions corresponding to $x_1 \dots x_6$
XNDOT(K),K=1,6	Advanced time step solution for velocities $\frac{dx_1(t+\Delta t)}{dt} \quad \dots \quad \frac{dx_6(t+\Delta t)}{dt}$
CV(J),J=1,20	Storage vector (not used)
T	Integration time at $t+\Delta t$

```

SUBROUTINE CRIT(XN,X0,XNDOT,CV,T)
COMMON/MDMV/MODE(200)
COMMON/XPAST/XP(15)
DIMENSION XN(15),X0(15),XNDOT(15),
XCV(20),FUNK(15)
COMMON/INTSL/ISV
COMMON/ROUNDS/XHMAX,XHMIN,YHMAX,YHMIN
COMMON /MODE/MOD,NL,TO
COMMON /PREL/UXB(200),UYB(200),EXT(200),UYT(200),VXT(200),VYT(200)
XTH(200),UXBL(200),UYBL(200),FORC(200)
X,UYF(200),UXF(200),VYF(200),VXF(200),FORCV(200)
COMMON/DATT/FIMP,H,D1,D2,FM,FI,NTP,IMULT,DELO,S1,S2,TB,NTEE,NT1,TV
XAX,TE,PH1,PH2,P1,P2,D3,GRV,FMU,IPIV
C
C   WITH NEW STATE AT T+DELT, DETERMINE
C
C   WHAT MOD WE ARE IN, USE PREV.
C   MODE TO COMPUTE FORCES
CALL FORCEC,T,XN(3),XN(5),XN(1),H,D1,S1,S2,FT,NT,DEL,DELH)
GO TO (1,2,3,4,5,6,7),MOD
C
C   LOGIC FROM STATE MOD=1 ****
C
1 GO TO 5
C   MOD=1 IMPLIED AT 1
C
C   END LOGIC FROM MOD=1 ****
C
C   START LOGIC FROM MOD=2 ****
C
2 CALL FOR2(FUN1,X,1)
UXCDOT=XN(4)
SG=SG+(UXCDOT)
FV1=FV1(7)
FV2=FV2(9)
IF(FV1.GT.0.0.AND.FV2.GT.0.0)GO TO 80
IF(FV1.LE.0.0.AND.FV2.LE.0.0)GO TO 81
IF(FV1.LE.0.0)GO TO 82
IF(UXCDOT*XP(4).GT.0.0)GO TO 84
IF(SG*FMU*FV1.LT.FT)GO TO 84
GO=4
GO TO 8
80 IF(UXCDOT*XP(4).GT.0.0)GO TO 8
IF(SG*FMU*(FV1+FV2).LT.FT)GO TO 8
MOD=7
GO TO 8
C
C   MOD=2 IMPLIED AT 80
C
81 MOD=1
GO TO 8
82 IF(UXCDOT*XP(4).GT.0.0)GO TO 85
IF(SG*FMU*FV2.LT.FT)GO TO 85
MOD=3
GO TO 8

```



```

85 MOD=5
   GO TO 8
84 MOD=6
   GO TO 8
C
C   END LOGIC FROM MOD=2 *****
C
C   START LOGIC FROM MOD=3 *****
C
3  CALL FUN3(FUNN,XN,T)
   FV2=FUNN(9)
   FH2=FUNN(10)
   IF(FV2.GT.0.0)GO TO 90
   MOD=1
   GO TO 8
90 IF(FH2.GT.-FMU*FV2.AND.FH2.LT.FMU*FV2)
   XGO TO 8
C
C   90 IMPLYS MOD=3
C
C   MOD=5
C   GO TO 8
C
C   END LOGIC FROM MOD= 3****
C
C   START LOGIC FROM MOD=4 *****
C
4  CALL FUN4(FUNN,XN,T)
   FV1=FUNN(7)
   FH1=FUNN(8)
   IF(FV1.GT.0.0)GO TO 92
   MOD=1
   GO TO 8
92 IF(-FMU*FV1.LT.FH1.AND.FH1.LT.FMU*FV1)
   XGO TO 8
C
C   92 IMPLYS MOD=4
C
C   MOD=6
C   GO TO 8
C
C   END LOGIC FROM MOD=4
C
C   START LOGIC FROM MOD=5
C
5  CALL FUN5(FUNN,XN,T)
   FV2=FUNN(9)
   FH2=FUNN(10)
   UXB2DT=FUNN(11)
   SG=SGN(UXB2DT)
   IF(FV2.GT.0.0)GO TO 95
   MOD=1
   GO TO 8
95 IF(XP(11)*UXB2DT.GT.0.0)GO TO 8
   IF(SG*FMU*FV2.LT.FT ) GO TO 8
C
C   95 IMPLYS MOD=5

```




```

C      MOD=3
      GO TO 8
C
C      END LOGIC FROM MOD=5 ****
C
C      START LOGIC FROM MOD=6 ****
C
6 CALL FUN6(FUNN,XN,T)
  FV1=FUNK(7)
  FV2=FUNK(9)
  UB1XDT=FUNK(12)
  SG=SGN(UB1XDT)
  IF(FV1.GT.0.0)GO TO 96
  MOD=1
  GO TO 8
96 IF(XP(12)*UB1XDT.GT.0.0)GO TO 8
  IF(SG*FV2.FV1.LT.FT)GO TO 8
C
C      96 IMPLYS MOD=6
C
C      MOD=4
C      GO TO 8
C
C      END LOGIC FROM MOD=6
C
C      START LOGIC FROM MOD=7
C
7 MOD=7
  GO TO 8
C
C      END LOGIC FROM MOD =7
C
6 CONTINUE
C
C *** COMPUTE DISPLAC, AND VELOCITIES ***
C
C      IF(NL.NE.1)GO TO 9
C
C      LOAD INITIAL VALUES
C
      IF(IPIV.LT.3)GO TO 721
      UYF(1)=0.0
      UXF(1)=S1
      VYF(1)=0.0
      VXF(1)=0.0
      UYT(1)=H
      UXT(1)=S1
      UYB(1)=0.0
      UXB(1)=S1+S2
      UXBL(1)=0.0
      UYBL(1)=0.0
      TB(1)=T0
      VXT(1)=0.0
      VYT(1)=0.0
      GO TO 722
721 UYF(1)=0.0
      UXF(1)=0.0

```



```

VVF(1)=0.0
VXF(1)=0.0
UYT(1)=D1
UXT(1)=S1+S2
UYB(1)=0.0
UXB(1)=S1+S2
LXBL(1)=0.0
UYBL(1)=0.0
TP(1)=TO
VXT(1)=0.0
VYT(1)=0.0

```

```

722 CONTINUE
CALL FORCE(TO,S1,D1,0.0,H,D1,S1,S2,FTTO,HTTO,DELO,DELHO)
FORC(1)=FTTO
FORCV(1)=HTTO
NL=NL+1

```

```

9 CONTINUE
SN=SIN(XN(1))
CN=COS(XN(1))
UB1X=XN(3)-D1*SN-S1*CN
UB2X=XN(3)-D1*SN+S2*CN
UB1Y=XN(5)-D1*CN+S1*SN
UB2Y=XN(5)-D1*CN-S2*SN
UB1XDT=XN(4)-D1*CN*XN(2)+S1*SN*XN(2)
UB1YDT=XN(6)+D1*SN*XN(2)-S2*CN*XN(2)
UB3X=XN(3)+D3*SN
UB3Y=XN(5)+D3*CN
UB3XDT=XN(4)+D3*CN*XN(2)
UB3YDT=XN(6)+D3*SN*XN(2)
UB4X=XN(3)-D1*SN
UB4Y=XN(5)-D1*CN
UB4XDT=XN(4)-D1*CN*XN(2)
UB4YDT=XN(6)+D1*SN*XN(2)
TIM=T
UB5X=XN(3)-S1*CN
UB5Y=XN(5)+S1*SN
UB6X=XN(3)+S2*CN
UB6Y=XN(5)-S2*SN
UB5XDT=XN(4)+S1*SN*XN(2)
UB5YDT=XN(6)+S1*CN*XN(2)
UB6XDT=XN(4)-S2*SN*XN(2)
UB6YDT=XN(6)-S2*CN*XN(2)

```

C
C
C

```

LOAD PRINT VECTOR

```

```

12 CONTINUE
IF(IPIV.LI.3)GO TO 723
UXB(NL)=UB2X
UYB(NL)=UB2Y
UXT(NL)=UB3X
UYT(NL)=UB3Y
VXT(NL)=UB3XDT
VYT(NL)=UB3YDT
UXBL(NL)=UB1X
UYBL(NL)=UB1Y
UXF(NL)=UB4X
UYF(NL)=UB4Y

```



```

VXF(NL)=UB4XDT
VYF(NL)=UB4YDT
TN(NL)=TIM
GO TO 724
723 UX8(NL)=UB2X
UY8(NL)=UB2Y
UXT(NL)=UB6X
UYT(NL)=UB6Y
VXT(NL)=UB6XDT
VYT(NL)=UB6YDT
UX8L(NL)=UB1X
UY8L(NL)=UB1Y
UXF(NL)=UB1X
UYF(NL)=UB1Y
VXF(NL)=UB1XDT
VYF(NL)=UB1YDT
TN(NL)=TIM
724 GO=1 IN=0
MODE(NL)=MODE
CALL FORCE(TIN,XN(3),XN(5),YN(1),H,D1,S1,S2,FTTIM,HTTIM,DELTN,DELTN
XTN)
FORC(NL)=FTTIM
FORCV(NL)=HTTIM
NL=NL+1

```

```

C
C UP DATE PAST VECTOR OF Y
C
DO 421 JX=1,6
421 XP(JX)=YN(JX)
C
C DEFINE PAST VECTOR OF OFF CENTROID VFL. AND FORCES
C
DO 422 JK=7,12
422 XP(JK)=FONN(JK)
C
C ENVELOPE SEARCH
C

```

```

NO=NL-1
IF(UXT(NO),GE,YHMAX) GO TO 91
IF(UXT(NO),LE,YHMIN) GO TO 62
IF(UYT(NO),GE,YHMAX) GO TO 93
IF(UYT(NO),LE,YHMIN) GO TO 94
GO TO 65
91 WRITE(6,70)
70 FORMAT(1X,'***YHMAX EXCEEDED***')
GO TO 101
62 WRITE(6,71)
71 FORMAT(1X,'***YHMIN EXCEEDED***')
GO TO 101
93 WRITE(6,72)
72 FORMAT(1X,'***YHMAX EXCEEDED***')
GO TO 101
94 WRITE(6,73)
73 FORMAT(1X,'***YHMIN EXCEEDED***')
101 ISW=1
NTP=NO
WRITE(6,74)TN(NTP),UXT(NTP),UYT(NTP),VXT(NTP),VYT(NTP)
74 FORMAT(1X,'TIME OF HEAD IMPACT=',E16.8//

```



```

1      1X,'HORIZONTAL HEAD DISPLACEMENT=',E16.8//
1      1X,'VERTICAL HEAD DISPLACEMENT=',E16.8//
1      1X,'HORIZONTAL HEAD VELOCITY=',E16.8//
1      1X,'VERTICAL HEAD VELOCITY=',E16.8//)
      GO TO 65
65 RETURN
      END

```

E.5.6 Subroutine PLOTS Listing

After the solution is completed, the PLOTS subroutine is called by the MAIN program for the purpose of printing and plotting the final results. Upon completion of this routine, the program begins a new problem. All output variables to be plotted are transferred to PLOTS through common block "PRNT." It should be noted that routines PDVICE, PLOGXY, ONEPLT and PLOT3 are special library routines available by the Westinghouse Computer Facilities; these listings are therefore omitted since they are not available to us.

```

SUBROUTINE PLOTS
COMMON/FSBT/IFSBT
COMMON/PAGE/NPAGE
COMMON/NOOV/NOOE(200)
DIMENSION CTTL(15),ATITLE(3),XTITLE(5),YTITLE(5),CTTX(30),
XATITL(3),XTITX(3),YTITX(6)
DATA IPLSK/1/
C
C IPLSK EQ 1 IMPLYS NO SECOND PLOT , NE 2 IMPLYS SECOND PLOT
C DIMENSION X(200,4),Y(200,4),NPNTS(4)
C DATA IXYS/200/
C COMMON /PRNT/UXB(200),UYB(200),UXT(200),UYT(200),VXB(200),VYT(200)
C X,UX(200),UXBL(200),UYBL(200),FORC(200)
C X,UYF(200),UXF(200),UYF(200),VXF(200),FORCV(200)
C COMMON/DAT1/FIMP,H,D1,D2,FM,FI,NTP,IMULT,DELO,S1,S2,TB,NTEE,NTI,IN
C XAX,TE,PH1,PH2,R1,R2,D3,GRV,FMU,PIV
C
C *****
C NSGN=+1 POINTS CONNECTED
C NSGN=-1 POINTS UNCONNECTED
C
C DATA NSGN/-1/,NSGNN/+1/
C *****

```

```

NPAGE=NPAGE+1
IFSET=1
DO '81 JQ=1,NTP
61 TMX=TM(JQ)

```

```

C
C
C      DETERMINE NONDIM. FACTORS FOR PLOTS

```

```

      CALL MAXVEC(OUT,NTP,OUTMAX)
      CALL MAXVEC(OYT,NTP,OYTMAX)
      CALL MAXVEC(VXT,NTP,VXTMAX)
      CALL MAXVEC(VYT,NTP,VYTMAX)
      UMAX=AMAX1(OUTMAX,OYTMAX)
      VMAX=AMAX1(VXTMAX,VYTMAX)
      OUTMAX=UMAX
      OYTMAX=UMAX
      VXTMAX=VMAX
      VYTMAX=VMAX

```



```

      WRITE(6,771)NPAGE,VXTMAX,VYTMAX,OUTMAX,OYTMAX
771  FORMAT(1X,///1X,'***NONDIMENSIONAL VEL. AND DISP. FACTORS FOR
      XCASE',12//1X,///1X,'OUTMAX=',E16.8//
      X          1X,'OYTMAX=',E16.8//
      X          1X,'VXTMAX=',E16.8//
      X          1X,'VYTMAX=',E16.8//)

```

```

      WRITE(6,10)
10  FORMAT(7X'T',DBX'UXF'DBX,'UYF'DBX,'OUT'DBX,'OYT'DBX,'VXT'DBX,'VYT
      X'DBX,'VYF',DBX,'FV1',DBX,'FHZ',6X,'ND'//)
11  FORMAT(1X,10(E16.4,1X),1X,11)
      WRITE(6,11)(TM(M),UXF(M),UYF(M),OUT(M),OYT(M),VXT(M),VYT(M),
      XVYF(M),FORCV(M),FORC(M),MODE(M),M=1,NTP)
      HH=F
      IF(IPIV.NE.3)HH=S1+S2
      NDEL=3

```

```

C
C
C      NDEL RELATES TO THE DENSITY OF THE DISPLACEMENT PLOT TRAJ.

```

```

      NTPX=NTP/NDEL
      DO 30 NX=1,NTPX
      ND=(NX-1)*NDEL
      IF(NX.EQ.1)ND=1
      IF(NX.EQ.NTPX)ND=NTP
      Y(NX,1)=OYT(ND)/HH
      X(NX,1)=OUT(ND)/HH
3  Y(NX,2)=UYF(ND)/HH
      X(NX,2)=UXF(ND)/HH
30  CONTINUE
      NPNTS(1)=NSGN*NTPX
      NPNTS(2)=NSGN*NTPX
      DATA CTTL,'TOP

```

BOTTOM

```

      X  ' ',
      X  NAN'/',XTITLE/'HORZ.DISPLACEMENT'/',YTITLE/'VERT.DISPLACEMENT'/'

```

```

CALL PDVICE(1)
CALL PLOGXY(0,0)
CALL ONEPLT(X,Y,IXYS,2,NPTS,CTTL,12,ATITLE,17,XTITLE,17,YTITLE,NP
XAGE,0)
DO 40 NN=1, NPT
X(NN,1)=TX(NN)
X(NN,2)=TY(NN)
X(NN,3)=TX(NN)
X(NN,4)=TY(NN)
Y(NN,1)=UXT(NN)/UXTMAX
Y(NN,2)=VXT(NN)/VXTMAX
Y(NN,3)=UYT(NN)/UYTMAX
40 Y(NN,4)=VYT(NN)/VYTMAX
DATA CTIX//HORIZONTAL HEAD DISPLACEMENT HORIZONTAL HEAD VELOCITY
X VERTICAL HEAD DISPLACEMENT VERTICAL HEAD VELOCITY
X//
XLOTS'/,YTITX//TIME SEC./,YTITX//NORMALIZED DISP. OR VEL./
NPTS(1)=NPT*10000
NPTS(2)=NPT*10000
NPTS(3)=NPT*10000
NPTS(4)=NPT*10000
IF (IFLSM.NE.1) GO TO 1333
CALL PDVICE(1)
CALL PLOGXY(0,0)
CALL ONEPLT(X,Y,IXYS,4,NPTS,CTIX,10,ATITLX,9,XTITX,23,YTITX,NPAGE
X,0)
1333 CONTINUE
CALL PLOTS
RETURN
END

```



E.5.7 Subroutine MAXVEC Listing

The routine MAXVEC simply searches a vector, Y(I), Y=1,...NE, for its largest value and returns the maximum value YMAX.

E.5.8 Function SGN Listing

The subfunction SGN examines the sign of its argument, XDUM, and returns a +1, 0, -1 depending on the respective sign of XDUM. A zero is returned if YDUM=0.

```
SUBROUTINE MAXVEC(Y,NE,YMAX)
  DIMENSION Y(NE)
  YMAXP=ABS(Y(1))
  DO 1 N=2,NE
    YMAXP=MAX(YMAXP,ABS(Y(N)))
1  CONTINUE
  YMAX=YMAXP
  IF(YMAX.EQ.0.)YMAX=1.0
  RETURN
END
```

```
FUNCTION SGN(XDUM)
  IF(XDUM)1,2,3
1  SGN =-1.
  RETURN
2  SGN =0.
  RETURN
3  SGN =+1.
  RETURN
END
```

REFERENCES

1. Albright, G. H., et al, Evaluation of Buried Corrugated-Steel Arch Structures and Associated Components, WT-1422, Operation Plumbbob, Feb. 1961.
2. Beck, C., Nuclear Weapons Effects Tests of Blast Type Shelters, A Documentary Compendium of Test Reports, Civil Effects Branch, Div. Biology and Medicine, U.S.A.E.C., Washington, D.C., June 1969.
3. Randall, P. A., Damage to Conventional and Special Types of Residences Exposed to Nuclear Effects, WT-1194, Operation Teapot, Feb.-May 1955.
4. Denton, D. R., A Dynamic Ultimate Strength Study of Simply-Supported Two-Way Reinforced Concrete Slabs, TR 1-789, U.S. Army Engineer Waterways Experiment Station, Corps of Engineers, Vicksburg, Miss., July 1967.
5. Design and Testing of Blast-Loaded Reinforced Concrete Slab System, for OCD by U.S. Army Engineer Waterways Experiment Station, Vicksburg, Miss., July 1967.
6. Zaghlool, E.R.F., et al, Tests of Reinforced Concrete Flat Plate Floors, J. Struc. Div. Proc. Am. Soc. Civil Eng., Vol. 96 No. ST3, Mar. 1970.
7. Brode, H. L., Review of Nuclear Weapons Effects, Annual Review of Nuclear Science, Vol. 18, 1968.
8. Buried and Semiburied Structures, Manual Corps of Engineers, EM 1110-345-421, Jan. 1960.
9. Arches and Domes, Manual Corps of Engineers, EM 1110-345-420, Jan. 1960.
10. Air Force Design Manual, Principles and Practices for Design of Hardened Structures, AFSWC-TDR-62-138, Dec. 1962.
11. Przemieniecki, J. S., Theory of Matrix Structural Analysis, McGraw-Hill Book Co., 1968.
12. Rempel, J.R., "Ground Shock and the Survival of the Contents of Personnel Shelters," Contract SRI-MU-4949-431 for the Office of Civil Defense, Nov. 1967.
13. Norris, C. H., et al, Structural Design for Dynamic Loads, McGraw-Hill Book Co., 1959.
14. Longinow, A. and Stepanek, O. J., Civil Defense Shelter Options for Fallout and Blast Protection (Single-Purpose), for OCD, Contract DAHC 20-67-C-0167, Work Unit 1613B, IIT Res. Inst. Proj. J6115, June 1968.

15. Dual-Purpose Blast Resistant School and Community Shelter for 350, 550 and 1100 Persons and a Blast Capacity of 5, 25 and 50 psi, OCD, Protective Struc., Shelter Design Ser. S55-3, Mar. 1963.
16. Dual-Purpose Parking Garage and Community Shelter for 5000 Persons with Blast Resistance Capacity of 5, 25 and 50 psi, OCD Protective Struc. Shelter Design Ser. G35-2, Apr. 1963.
17. Design of Structures to Resist the Effects of Atomic Weapons, Buried and Semiburied Structures, EM 1110-345-421, Manual Corps of Engineers, U. S. Army.
18. Operation Plumbbob, WT-1467, AEC Civil Effects Test Group, June 30, 1959.
19. Design of Structures to Resist the Effects of Atomic Weapons, Structural Elements Subjected to Dynamic Loads, EM1110-345-416, Manual - Corps of Engineers, U. S. Army, Mar. 15, 1957.
20. Building Code Requirements for Reinforced Concrete, ACI 318-63, Am. Concrete Inst., June 1963.
21. Harrenstien, H., et al., Yielding Membrane Elements in Protective Construction, OCD Contract PS-64-217, Eng. Res. Lab., Univ. Ariz., Tucson, Ariz., May 28, 1965.
22. Richard, R. M. and Goldberg, J. E., Analysis of Nonlinear Structures: Force Method, Proc. ASCE, J. Struc. Div., Dec. 1965.
23. Design and Analysis of Underground Reinforced Concrete Arches, Tech. Rep. No. 2-590, U.S. Army Engineer Waterways Experiment Station, Corps of Engineers, June 1962.
24. Salmon, M. A., et al, An Application of the Finite Element Method to Elastic-Plastic Problems of Plane Stress, Air Force Flight Dynamics Lab., Wright-Patterson AFB, Ohio, 1968.
25. "Air Blast Attenuation," Technical Manuscript S-1, Construction Engineering Research Laboratory (CERL), Champaign, Ill., Feb. 1971.
26. White, C. S., Biological Blast Effects, USAEC Tech. Rep., TID-5564, Office of Tech. Ser. Dept. Commerce, Washington, D.C., Sept. 1959.
27. Winslow, C.-E. A., Herrington, L. P., Temperature and Human Life, Princeton Univ. Press, Princeton, N. J., 1949.
28. Webb, P., "Pain Limited Heat Exposures," Temperature, Its Measurement and Control in Science and Industry, Part 3, Vol. 3, Hardy, J. D., Reinhold Publ. Co., 1963.
29. Kaufman, W. C., "Human Tolerance Limits for Some Thermal Environments of Aerospace," Aerospace Medicine, Vol. 34, No. 10, Oct. 1963.

30. Broido, A. and McMasters, A. W., Effects of Mass Fires on Personnel in Shelters, U.S. Dept. Agriculture, Forest Service, Pacific Southwest Forest and Range Experiment Station, Aug. 1960.
31. Moritz, A. R., et al, "The Effects of Inhaled Heat on the Air Passages and Lungs," Amer. J. Path., Vol. 21, pp 311-356, 1945.
32. Buettner, K., "Effects of Extreme Heat on Man," J. Am. Med. Assn., 144, pp 732-738, 1950.
33. Schlichting, H., Boundary Layer Theory, McGraw-Hill Book Co., New York 1960.
34. Par, S., Fluid Dynamics of Jets, D. Van Nostrand Co., Inc., New York, N.Y., 1954.
35. Abramovich, G., The Theory of Turbulent Jets, M.I.T. Press, Cambridge, Mass., 1963.
36. Protective Blast Shelter System Analysis Detroit, Michigan, Bechtel Corp., for OCD, Contract OCD-PS-66-10, 1968.
37. Earp, K. F., Death from Fire in Large-Scale Air Attack with Special Reference to the Hamburg Fire Storm, Home Office, Scientific Advisers' Branch, Whitehall, J.W.1, 1963.
38. Pryor, A. J. and Yuill, C. H., Mass Fire Life Hazard, Southwest Res. Inst. for OCD, Contract N228(62479)68663, 1966.
39. Vodvarka, F., Full-Scale Burns in Urban Area, IIT Res. Inst. for OCD, Contract N00228-69-C-0781, 1969.
40. ASHRAE Guide and Data Book, United Engr. Center, New York, N.Y., 1965 and 1966.
41. By private communication with Portland Cement Assoc. R and D, Skokie, Ill.
42. Ahlers, E. B., Debris Clearance Study, IIT Res. Inst. for OCD, Contract OS-62-202, 1963.
43. Feinstein, D. I., Debris Distribution, IIT Res. Inst. for OCD, Contract OCD-PS-64-50, 1966.
44. Rotz, J., Debris Model Research with Building Damage, Fire Spread and Debris Predictions for Five City Study, Contract B-70924(4949A-20)-US, OCD Five-City Study Rep. 55-11101-3312B-04, 1967.
45. Coulter, G. A., Air Shock Filling of Model Rooms, BRL MR No. 1916, Mar. 1968.

46. Glasstone, S., (editor) "The Effects of Nuclear Weapons," U.S. Government Printing Office, Washington, 25, D.C., 1962.
47. Shock Tube Facility Staff, Information Summary of Blast Patterns in Tunnels and Chambers, Second Edition, BRL MR 1390, Mar. 1962.
48. Hoener, S. F., Fluid Dynamic Drag, Published by the Author, 1965.
49. Prandtl, L. and Tietjens, O. G., Applied Hydro and Aerodynamics, McGraw-Hill Book Co., Inc., New York, N.Y., 1934.
50. Richmond, D. R., Bowen, I. G., and White, C. S., "Tertiary Blast Effects," Aerospace Medicine, Vol. 22, pp 789-805, 1961.
51. Ingberg, S. H.; Dunham, John W.; and Thompson, James P.; Combustible Contents in Buildings, U.S. Dept. Commerce, Natl. Bu. Standards, Bld. Matl. and Struc. Rep. 149, 1957.
52. Allen, F. C., Mechanical Equipment Requirements, Symposium on Survival Shelters, Proc. Am. Soc. Heating, Refrigerating, and Air-Conditioning Engrs., Inc., E. 47th St., New York, N.Y., June 1962.
53. Dual-Purpose School and Community Shelter for 350, 550 and 1100 Persons, OCD Protective Struc. Shelter Design Ser. S55-1, Sept. 1962.
54. Parking Garage and Community Shelter for 5000 Persons, OCD, Protective Struc. Shelter Design Ser. G35-1, Sept. 1962.
55. Private Communication with Mr. G. N. Sisson, Staff Director, Shelter Res. Div., OCD, The Pentagon, Wash., D.C., May 17, 1969.
56. Scarborough, J. B., Numerical Mathematical Analysis, The Johns Hopkins Press, Fourth Edition, 1958.
57. Brode, H. L., A Review of Nuclear Explosion Phenomena Pertinent to Protective Construction, R-425-PR, The Rand Corp., May 1964.
58. Prezmieniecki, J. S. and Berke, L., Digital Computer Program for the Analysis of Aerospace Structures by the Matrix Displacement Method.
59. Biomedical Handbook, National Aeronautics and Space Administration, 1962.

60. Barnett, R. L. and Hermann, P. C., Fragmentation of Reinforced Concrete Slabs, for OCD, Subcontract B-70942(4949-34)-US, OCD Work Unit 3322B, IIT Research Institute Project J6107, Oct. 1968.
61. Childers, M. A., "Protective Capability of the National Fallout Shelter System," Contract DAHC20-67-C-0148, OCD Work Unit 1614C, for the Office of Civil Defense, The Vertex Corporation, Nov. 1968.
62. Gleister, D. H., "The Effects of Acceleration of Short Duration," Chapter 26, p 775 of "Textbook of Aviation Physiology" Pergamon Press, 1965.
63. Longinow, A., "Civil Defense Shelter Options for Fallout and Blast Protection (Dual-Purpose)," Contract OCD-PS-64-50, Subtask 1613B, for Office of Civil Defense, IIT Research Institute, Project M6101, May 1967.
64. Havers, J. A., et al, "An Investigation of Minimal Equipment Needs in Personnel Shelters," IIT Research Institute, Contract OCD-PS-64-50, Subtask 1216-A, June 1965.
65. Travslar, D. A., et al, "Minimum Requirements for Auxiliary Power Systems for Community Shelters," Contract OCD-OS-62-190, Subtask 1411C, Battelle Memorial Institute, July 1969.
66. Behls, H. F., and Libovicz, B. A., "Shelter Package Ventilation Kit K17," OCD Work Unit 1423A, General American Transportation Company, Oct. 1965.
67. WMATA (Washington Metropolitan Area Transit Authority) Specs, Sec B-1, B&O Route; Contract Drawings, Sec B-1, B&O Route, October 1969.
68. Shimizu, B., et al, "Hardness Study of Proposed Washington Metropolitan Area Rapid Transit System," for U.S. Atomic Energy Commission, Contract W-7405-eng-26, Holmes & Narver, Inc., June 1969.
69. Leonards, G. A., (editor) "Foundation Engineering," McGraw-Hill Book Co., Inc., New York, 1962, p 789.
70. Terzaghi, K., and Peck, R. B., "Soil Mechanics in Engineering Practice," John Wiley & Sons Inc., New York, 1948, p 29.
71. Reinforced Concrete Design Handbook - Working Stress Method, ACI Committee 317, American Concrete Institute, Third Edition.
72. Salmon, M. A.; Longinow, A.; Chiapetta, R. L. "Analysis of The Effects of Fire Temperatures on Composite Floor Panels," to be presented at the National ASCE Conference, April 1972.